Masters   Engineering

2004-02-01

Design and Development of a Respiratory Monitoring Device to be Used in Conjuction with MRI Scanners

Aidan McNally
Technological University Dublin

Follow this and additional works at: https://arrow.tudublin.ie/engmas

Part of the Engineering Commons

DESIGN AND DEVELOPMENT OF A RESPIRATORY MONITORING DEVICE TO BE USED IN CONJUNCTION WITH MRI SCANNERS

AIDAN MCNALLY

MPHIL

DUBLIN INSTITUTE OF TECHNOLOGY

SUPERVISOR: DR. GERRY WOODS

SCHOOL OF MANUFACTURING ENGINEERING

FEBRUARY 2004

I certify that this thesis which I now submit for examination for the award of MPhil, is entirely my own work and has not been taken from the work of others save and to the extent that such work has been cited and acknowledged within the text of my work.

This thesis was prepared according to the regulations for postgraduate study by research of the Dublin Institute of Technology and has not been submitted in whole or in part for an award in any other Institute or University.

The Institute has permission to keep, to lend or to copy this thesis in whole or in part, on condition that any such use of the material of the thesis be duly acknowledged.

Signature _Aidan McNally_

Date _1/10/04_

Acknowledgements

Abstract

The aim of this project was to design and manufacture a respiratory monitoring device that operates in conjunction with MRI scanners to produce higher quality images. The resultant quality of many MRI images depends on how well the patient can control their breathing activity. This research has been successful in designing and manufacturing a device that can be used to teach patients how to hold their breath correctly prior to scanning and also provide them with feedback about their breathing activity during the scan.

The project involved research into MRI technology and the materials that can be used in the MRI environment. This heavily influenced the design of the transducer for monitoring breathing and the design of the feedback systems for providing the patient with information about their breathing activity during the scan. The system for breath monitoring is a rubber bladder, which is strapped to the chest of the patient, and is connected to a pressure transducer. This bladder is a low cost design compared to similar transducers already on the market and tests have shown similar performances between all of these. A number of different feedback systems have been designed that can work together or separately as required. These include a visual method where information is transmitted from a bar graph LED display via polymer optical fibres to the patient. Software was also written to generate a graphical display of the breathing activity and to produce a corresponding audio tone.

A requirement of the respiratory monitoring device was for it to be compact and ergonomically designed. Various manufacturing processes were investigated and researched in order to produce a suitable housing for the device. An initial rapid prototype model was made from which new ideas were obtained. It was finally decided to use a vacuum forming process to make the housing from ABS plastic.

The European Union's Medical Devices Directive was consulted and examined and its rules followed to ensure that the device is in compliance with medical standards. The necessary documentation for CE Marking of the finished product has also been prepared. The entire device has been tested within the MRI environment with positive results.

TABLE OF CONTENTS

1

TABLE OF FIGURES

7

dimensions in mm.

1   INTRODUCTON

Magnetic Resonance Imaging (MRI) is a modern and accurate medical aid available to physicians for the sectional imaging of the inner body. This "magnetic view" provides physicians with a host of detailed information on the location, size and composition of the body tissue to be examined. This knowledge may be decisive in helping to establish a fast and accurate diagnosis. These machines are expensive, and a limited number exist in Irish hospitals, thus demand on usage is very high.

The technology gives a high quality output compared to other imaging procedures such as X-ray or Ultrasound, however the quality of the output, and the cycle time is dependent on the ability of the patient to control their breathing cycle during the scanning procedure. As a patient breathes, organs can be displaced in both location and size due to diaphragm movements. If this displacement takes place during the scanning procedure the resultant image will become distorted and output quality effected. Much time is spent teaching the patients how to control their breath during the scanning, thus leading to excessive times on the MRI machine and their operators.

The aim of this project was to design and manufacture a low cost respiratory monitoring device that operates in conjunction with MRI scanners to produce higher quality images. The research has been successful in building a device that can be used to teach patients how to hold their breath correctly prior to scanning and also provide them with feedback about their breathing activity during the scan.

The project required research into the MRI technology and various techniques developed to solve the problem of image distortion due to breathing. These techniques include improving the hardware to speed up the scanning process and using movement compensation techniques as discussed in chapter 2. While these techniques are constantly improving they are still far from perfect. The solution developed through this research may even be used in conjunction with other techniques.

An initial prototype was created for use in the offline situation as discussed in chapter 3. This prototype was contained in a timber housing. Initial tests on the device showed a marked improvement in patient's breath holding ability. The initial prototype was then used to develop the transducer and feedback systems to bring the device online.

Research into the materials that can be used in the MRI environment was also required. With magnetic forces of 1.5 Tesla or greater associated with the scanner standard electrical equipment and magnetic materials could not be used. This heavily influenced the design of the transducer for monitoring breathing and the design of the feedback systems. The system for breath monitoring is a rubber bladder, which is strapped to the chest of the patient, and is connected to a pressure transducer. This bladder is a low cost design compared to similar transducers already on the market and tests have shown similar performances to other types of transducers. The design of the bladder is discussed in chapter 4.

A number of different feedback systems have been designed that can work together or separately as required. These include a visual method where information is transmitted from a bar graph LED display via polymer optical fibres to the patient. The optical fibres are separated into a display within the scanner tunnel. Software has also been used to generate a graphical display of breathing activity. The visual feedback system is discussed in chapter 6. Software is also used to produce a corresponding audio tone as discussed in chapter 5. This tone can be used as an audio feedback to the patient and utilises the sound system already in place in most MRI scanners.

A suitable housing for the electrical components of the device was required. This part of the device must be located outside the MRI room and be as small and ergonomic as possible. A number of manufacturing processes were considered. A rapid prototype model was made from which new design ideas were obtained. It was finally decided to use the vacuum forming process to make the housing from ABS plastic.

The European Union's Medical Devices Directive has been researched and its rules followed to ensure that the device is in compliance with medical standards. This influenced the materials used in the device and the electrical components of the device. The necessary documentation for CE Marking of the finished product has also been prepared.

The field tests for the device were carried out in Waterford Regional Hospital under the supervision of Dr. Ian Kelly, the consultant radiologist involved with the project. The device was tested at various stages of development from an initial prototype through to the final design. The entire device has been tested within the MRI environment with positive results. This included MRI compatibility testing and

the retrieval of clinical images of a patient showing a marked improvement in image quality. The results are discussed in chapter 9.

Finally a costing is presented for the device as discussed with other conclusions in chapter 10.

2   LITERATURE SURVEY

2.1   Introduction

Radiology has been developing since the late 1800's. In that time it has become increasingly important as a medical tool. Many different imaging techniques have been developed and are used in hospitals worldwide. One of the most recent imaging techniques to have been developed is Magnetic Resonance Imaging (MRI) and continuous research and development is ongoing to improve this technology. Of all the imaging techniques MRI is the most suited to examination of the inner organs of the body. There are various problems associated with this technique. The speed of the scanning process is relatively slow. Problems arise, due to the restrictive nature of the scanner itself, for the patient, the radiologist and the design engineer. These problems lead to increases in cost and decreases in image quality. This research looks closely at one particular problem, distortions of the final image due to respiratory motion. In this chapter the origins of radiology, the development of the various imaging techniques and the problem due to respiratory motion are all discussed.

2.2   History of Radiology

In 1869 a German physicist named Wilhelm Conrad Roentgen [1] discovered the previously unknown radiation "X-rays". They were given this name because "X" frequently stands for an unknown quantity in mathematics. His unique discovery changed the world of physics and immediately became a useful tool for medical science.

One of the first imaging improvements was the fluoroscope. It consisted of a tube with a fluorescent screen at one end and an eyepiece at the other. A body part placed between the X-ray tube and the screen produced an image even in a lighted room.

The development of skeletal radiography began with Roentgen's discovery of the X-ray. This started with the human hand; bones and joints were ideal subjects because they absorbed X-rays so well. Within a few months of Roentgen's discovery, the secrets of the skeleton were being revealed. In the late 1890's, equipment was primitive, electricity was not readily available, there was little experience, and no literature existed. Dr. William Morton [2], a pioneer of radiology, created the first single-film full body skeletal radiograph in 1897.

The basic principle of the X-ray tube has not changed significantly since Roentgen's discovery. Current applied to a metal cathode produces free electrons. The X-rays are produced when the rapidly moving electrons are suddenly stopped as they strike the metal target of the tube. Around 1913, William David Coolidge [3] developed a new X-ray tube that, unlike the old gas tube, could provide radiographs with consistent exposure and quality. Coolidge did initial work on improving the filament in light bulbs. His work with tungsten filament played a major role in the development of modern X-ray tubes.

Shortly after Roentgen's discovery, it was noted that a camera could be used to produce a permanent image from the fluoroscopic screen that could record more information than the eye could see on the fluoroscopic screen. In the late 1930s, physicians wanted to screen large populations of people for tuberculosis and other lung diseases. Because mass X-ray screening with conventional equipment was impractical, photofluorographic devices were set up in clinics and hospitals to allow countries around the world to mass screen their populations.

In 1903, Marie [4] and Pierre [5] Curie, and Henri Becquerel [6] received the Nobel Prize in physics for their work on radioactivity. In 1911 Marie Curie received the Nobel Prize again, in recognition of her work in isolating radium in its pure metallic form and developing the first international standard for measuring the substance. During World War I, she worked as an X-ray technician, taught radiological technology, and equipped mobile X-ray vans to assist in the war effort.

The ability to see anatomical structures without the use of ionising radiation proved to be a major advancement in modern medicine. Ultrasound originated in the work of physicists exploring energy propagation by sound waves. Fifteen years before Roentgen's discovery of the X-ray, Pierre and Jacques Curie explained piezoelectricity and developed the principle that led to the development of ultrasonic transducers. In the early 1900s, experimentation took place with high-frequency ultrasound to detect submarines, leading to the development of sonar. It was not however until the 1960s that ultrasound scanning became a recognized medical tool.

An angiogram is performed by injecting contrast media into the blood vessels of the body. In 1954, the first iodinated contrast media was introduced. This is still used for angiograms today.

In 1952 the Nobel Prize in physics was awarded to Felix Bloch [7] and Edward Purcell [8] for their discovery of nuclear magnetic resonance. This discovery laid the

groundwork for one of the most unique inventions in medical imaging since the discovery of the X-ray. Magnetic resonance imaging (MRI) uses a strong magnetic field, radio waves, and computers to look inside the patient's body. This can be done as a non-invasive procedure and without any ionising radiation exposure to the patient.

Since Roentgen's discovery of the X-ray in 1895, much scientific advancement has taken place. Inventors adapted their discoveries to the field, while physicians around the world became specialists and further developed the profession. They were the forerunners of today's radiologists and radiation oncologists.

American Paul C. Lauterbur [9] and Briton Sir Peter Mansfield [10] won the 2003 Nobel Prize for medicine for the work they did in the 1970's that laid the groundwork for making MRI a useful imaging tool. Lauterbur discovered the possibility of creating a two-dimensional picture by producing variations in a magnetic field. He is now at the Biomedical Magnetic Resonance Laboratory at the University of Illinois in Urbana.

Mansfield, showed how the signals the body emits during an MRI exam could be rapidly analysed and transformed into an image. Mansfield also showed how extremely fast imaging could be achievable. This became technically possible within medicine a decade later. He is now at the University of Nottingham in Britain.

2.3   Imaging Modalities

The field of medical imaging has experienced phenomenal growth within the last century. Whereas imaging was initially developed most by the defence and space science areas in the past, with the advent of powerful, less-expensive computers, new and expanded imaging systems have found their way into the medical field. Systems range from those devoted to planar imaging using x-rays to technologies such as virtual reality. Some of the systems such as Ultrasound are relatively inexpensive, while others, such as positron emission tomography (PET) facilities, cost millions of euro for the hardware and the employment of personnel to operate them. Systems that make use of x-rays have been designed to image anatomic structures, while those that make use of radioisotopes provide functional information. The fields of view that can be imaged range from the whole body to images of cellular components using MR microscopy. The medical imaging device field is extremely broad. From the design of transducers for the imaging devices, to the post processing of the data to allow for

easier interpretation of the images by medical personnel, there are many aspects to the medical imaging devices field.

2.3.1 X-Ray

Conventional x-ray radiography produces images of the anatomy that are shadow-images based on x-ray absorption. The x-rays are produced in a region that is nearly a point source and then are directed on the anatomy to be imaged. The x-rays emerging from the anatomy are detected to form a two-dimensional image, where each point in the image has a brightness related to the intensity of the x-rays at that point. Image formation relies on the fact that significant numbers of x-rays penetrate through the anatomy and that different parts of the anatomy absorb different amounts of x-rays.

X-rays are electromagnetic waves. In medical imaging the x-ray energy typically lies between 5 and 150 kiloelectronvolts (keV), with the energy adjusted to the anatomic thickness and the type of study being performed. X-rays striking an object may either pass through unaffected or may undergo an interaction. These interactions usually involve either the photoelectric effect (where the x-ray is absorbed) or scattering (where the x-ray is deflected to the side with a loss of some energy). X-rays that have been scattered may undergo deflection through a small angle and still reach the image detector reducing image contrast and degrading the image. This degradation can be reduced by the use of an air gap between the anatomy and the image receptor or by use of an anti-scatter grid.

Because of health effects, the doses in radiography are kept as low as possible. However, x-ray quantum noise becomes more apparent in the image as the dose is lowered. The quantum noise depends on the average number of x-rays striking the image detector and is the fundamental limit to radiographic image quality.

X-ray radiography continues to be used worldwide as an imaging technique and has been developed further to produce Computed Tomography. However due to the high risks to health and with the development of more advanced imaging techniques it is becoming less and less popular.

2.3.2 Computed Tomography

Computed Tomography (CT) enables physicians to obtain high-quality tomographic (cross-sectional) images of internal structures of the body. Since it was first developed in the early 1970's manufacturers have competed for the world CT market. CT continues to develop, with new capabilities being researched.

CT images are reconstructed from a large number of measurements of x-ray transmission through the patient called projection data. The resulting images are tomographic maps of the x-ray linear attenuation coefficient. These images are reconstructed from the projection data using various mathematical techniques. Projection data are typically acquired in approximately 1 second and the image is reconstructed in 1 to 5 seconds. The fundamental task of CT systems is to make an extremely large number (approximately 500,000) of highly accurate measurements of x-ray transmission through the patient in a precisely controlled geometry.

Projection data is acquired in one of several different possible geometries depending on the scanning configuration, scanning motion, and detector arrangement. These geometries range from the simplest first generation Parallel-Beam Geometry to the newer fifth generation Scanning Electron Beam.

The major limit of CT is the relatively high radiation exposure to patient and physician compared to other imaging modalities such Magnetic Resonance. In particular, radiation exposure to physician's hands during interventional procedures with CT fluoroscopic guidance may be high. To make real-time adjustments in needle trajectory, the physician's hand is in proximity to the scanning plane. Physician hand exposure has been theoretically and empirically determined to be approximately 2 mGy (milligray) per procedure [11]. Kato et al [12] calculated that a physician with continuous hand exposure would be limited to performing only four CT fluoroscopic procedures [13] each year. A number of procedural techniques and shields have been suggested to minimise radiation exposure [14]. Kato et al used needle holders and lead drapes to minimise exposure. Another system that was developed used a robot [15] that could hold, orient, and advance a needle, with fluoroscopic guidance. This robot could be either computer or joystick controlled. Physician radiation exposure was found to be negligible during the CT fluoroscopy-guided procedures.

New techniques such as the temporal subtraction technique are helping to improve CT all the time [16], especially in the area of chest radiography. This technique is a method with which a previous chest radiograph is subtracted from a

current radiograph so that interval changes are enhanced. The purpose of the temporal subtraction technique in the interpretation of a chest radiograph is to alert the radiologist to the location of newly developed abnormalities and to assist radiologists in their final decision. Techniques such as these help to avoid incorrect diagnoses. Such developments continue to promote CT as a leading imaging modality.

2.3.3 Ultrasound [17]

An Ultrasound transducer generates acoustic waves by converting magnetic, thermal or electrical energy into mechanical energy. The most efficient technique for medical ultrasound uses the piezoelectric effect. This is where a stress is applied to a quartz crystal and the electrical potential across opposite faces of the material is detected. The inverse piezoelectric effect is where an applied electrical field across the crystal induces a mechanical deformation. In this manner, a piezoelectric transducer converts an oscillating electric signal into an acoustic wave, and vice versa.

The tissues of the body are inhomogeneous and signals, such as high-frequency sound, sent into these tissues are reflected and scattered by the tissues. Scattering, or redirection of some of an incident energy to other directions is why the beam of a spotlight is visible in smoke or fog. That part of the scattered energy that returns to the transmitter is called backscatter. This is how an ultrasound image is obtained.

Ultrasound is any sound whose frequency is above the limit of human hearing, which is approximately 20kHz. Since frequency and wavelength (and hence resolution) are inversely related, the frequency of sound commonly used is around 1MHz, with a trend toward higher frequencies in order to obtain better resolution. Axial resolution is approximately one wavelength, and at 1MHz, the wavelength is 1.5mm in most soft tissues, so one must go to 1.5MHz to achieve 1mm resolution. Attenuation of ultrasonic signals increases with frequency in soft tissues, and so a trade-off must be made between the depths of penetration that must be achieved for a particular application ant the highest frequency that can be used.

Ultrasonic imaging has many economic advantages over other imaging modalities. The imaging systems are typically much less expensive than those used for other modalities and do not require special preparations of facilities such as shielding of x-rays and the magnetic field in MRI.

2.3.4 Magnetic Resonance Imaging

Magnetic Resonance Imaging (MRI) is a modern and accurate medical aid available to physicians for the sectional imaging of the inner body. This "magnetic view" provides physicians with a host of detailed information on the location, size and composition of the body tissue to be examined. This knowledge may be decisive in helping to establish a fast and accurate diagnosis.

The procedure is based on the magnetic properties of atoms that make up all matter - including the human body. Protons in the body tissue can be viewed as tiny bar magnets. In a strong magnetic field, such as the one produced by the MRI scanner, these protons will align with the magnetic field. If a radio frequency (RF) pulse is sent into the body it will cause the protons to form a magnetic field perpendicular to that of the MRI scanner. These magnetic fields, emitted by the protons in the body tissue, induce electrical signals in a circular antenna surrounding the patient. Signal intensity varies according to tissue type. A computer assigns the signals to the corresponding points on the body areas under examination and transforms them into an image on a screen.

MRI was traditionally a clinically important modality due to its exceptional soft-tissue contrast. MRI research involves fundamental tradeoffs between resolution, imaging time, and signal-to-noise ratio (SNR). It also depends heavily on both gradient and receiver coil hardware innovations. The main advantages of MRI over other imaging modalities are its excellent image resolution and contrast and the fact that there is no risk of radiation exposure as in x-ray imaging and CT. However imaging duration is relatively long. This is the main disadvantage of MRI and leads to various other problems such as distortions due to motion. Other disadvantages of this type of imaging technique are problems with claustrophobic patients using the closed bore magnets, difficulty with MR intervention due to inaccessibility and dB noise levels generated by the scanners that can lead to hearing problems for the radiographer.

2.4 Spin Physics

The body is made up of millions of atoms all containing protons. Protons have a positive electrical charge and spin in a way similar to the earth about its axis. It can be said that protons possess a spin. As the proton spins about its own axis, the positive charge spins with it. A moving electrical charge is called current. By the laws of

physics an electrical current induces a magnetic field i.e. where there is an electrical current there is a magnetic field. Thus, a proton has its own magnetic field and can be thought of as a tiny bar magnet.

In a strong magnetic field (B_0 as seen in figure 2.1), such as that created in the MRI system, the protons, or tiny bar magnets, align themselves with this external magnetic field. They align either parallel or anti-parallel to the direction of the external field, both directions of alignment are on different energy levels. The lower energy state is the parallel state. The preferred energy state is the lower energy state and hence more protons will align parallel to the external magnetic field, producing M_0 as in Fig 1a. Approximately 7 in 10^7 more protons will align parallel than anti-parallel. The longitudinal magnetic field vectors of a proton aligned in parallel will cancel that of a proton aligned in anti-parallel. Hence, there will be a resultant magnetic field vector in parallel, as when all the anti-parallel vectors have cancelled there will still remain a number of parallel vectors.

Protons do not simply lie in parallel or anti-parallel to the external magnetic field, they also move around in much the same way as a spinning top as can be seen in figure 2.2a & 2.2b. This type of movement is called precession. The precession frequency i.e. the rate at which the protons rotate is denoted ω_0.

$$\omega_0 = \gamma * B_0$$

where γ is the gyro magnetic constant and is approximately 42.5 MHz/T for protons. B_0 is the external magnetic field strength.

This precession does not have an effect on the longitudinal resultant - it is still present. Neither does it
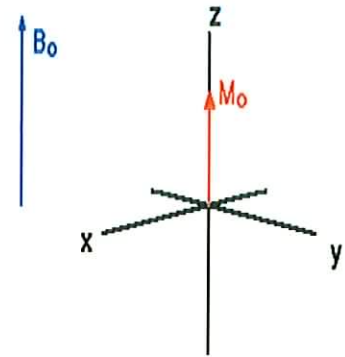
Figure 2.1: M_0 – the resultant created by protons in the body
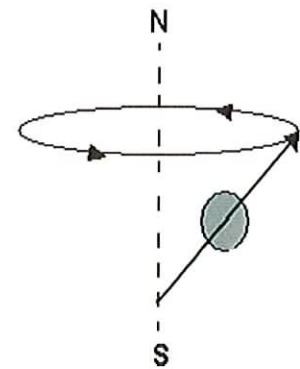
Figure 2.2a: Precession of a proton within the body.
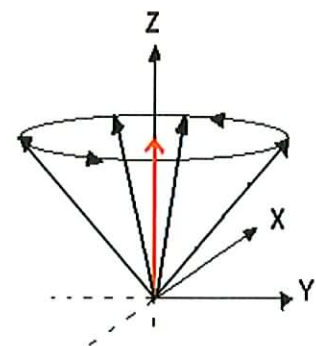
Figure 2.2b: Precession of protons within the body.

22

add a transversal magnetic resultant, as the magnetic vectors in the Y-direction will cancel each other out.

The patient when placed in the MRI unit effectively becomes a magnet himself. That is, the vectors of the protons that don't cancel add up to give an overall magnetic vector. This will be in the longitudinal direction, that is, parallel to the magnetic field created by the MRI unit.

An RF pulse with frequency equal to the precession frequency is then sent into the body. This has two effects on the precessing protons.

Firstly, it causes resonance to occur. That is, as the RF pulse has the same frequency as the precessing protons some of the energy from the pulse is transferred to the protons. This will cause some of the protons previously in the lower energy state (with magnetic vectors parallel to the external magnetic field) to jump to the higher energy state (where the magnetic vector will be anti-parallel to the external magnetic field). This has the effect of decreasing the longitudinal magnetic vector as fewer protons are now facing in that direction. This can be seen in figures 2.3 and 2.4. The longitudinal magnetic vector in figure 2.3 is less in magnitude than in figure 2.4.

Secondly, the RF pulse synchronises the protons so that they all precess together. This creates a magnetic vector in the Y-direction as the protons now add together in this direction instead of cancelling each other out.

This resultant transversal magnetic field vector moves in phase with the precessing protons as shown in figure 2.4. Therefore it has a frequency equal to the precession frequency. This is a moving magnetic field, which by the laws of physics will induce an electrical
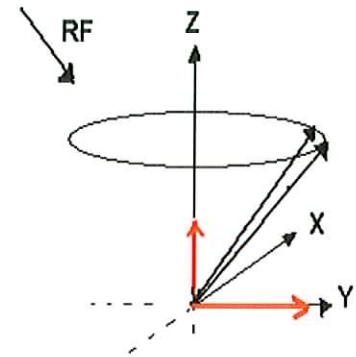
Figure 2.3: Resonance occurs due to RF pulse. M_0 decreases, magnetic vector grows in the Y-direction.
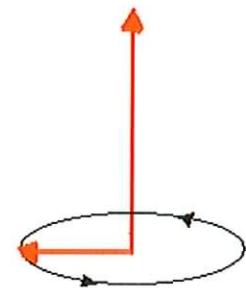
Figure 2.4: Resultant transversal magnetic field vector moves in phase with the precessing protons.

current in a circular antenna surrounding the patient. It is this signal that is used to create the magnetic image of the body tissue under examination. The frequency of the signal received in the antenna also is the precession frequency.

Figure 2.5: plot of the longitudinal magnetic vector strength against time.

When the RF pulse is removed the energy given to the protons by the pulse is removed and the protons that had jumped to the higher energy state begin to drop back to the lower energy state. Hence the longitudinal magnetic vector begins to grow again. A plot of the longitudinal magnetic vector strength against time gives the T1 curve as shown in figure 2.5. That is, the time it takes for the longitudinal magnetisation to go back to its original value is described by the longitudinal relaxation time, denoted T1.

When the RF pulse is removed the precessing protons fall out of synch with each other and hence their Y-components will begin to cancel each other out again. This will cause the transversal magnetic vector to decrease back to zero. A plot of transversal magnetic vector strength against time gives the T2 curve as shown in figure 2.6. Again, the time it takes for the transversal magnetisation to go back to its original value is described by the transversal relaxation time, denoted T2.
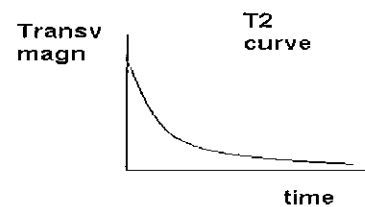
Figure 2.6: plot of transversal magnetic vector strength against time.

It is from these curves, T1 and T2, that the image is formed. Different tissues have different values of T1 and T2. The computer interprets these differences and it gives an image of the tissues. It is really the contrast between tissues that is seen.

2.4.1 What influences T1?

T1 is influenced by tissue composition, structure and surroundings. As the protons, which had jumped to the higher energy state, start to fall back to the lower energy state energy is emitted. This is usually in the form of thermal energy handed

over by the protons to the surrounding lattice. The protons have a magnetic field that is constantly changing at the precessing frequency. The lattice also has its own magnetic fields. If the lattice fields have frequency close to the precessing frequency of the protons then very effective energy transfer can take place.

Hence, tissues such as fat have a short T1 due to the carbon bonds having frequency close to the precessing frequency. It is generally tissues with medium sized molecules that will have a short T1 as the molecules move and have fluctuating magnetic fields near the precessing frequency.

Also, T1 will be longer in stronger external magnetic fields. This is because in stronger magnetic fields the difference between the low and high-energy states is greater. It takes more energy for protons to align themselves anti-parallel to the external magnetic field. When the RF pulse is removed there is more energy to be handed down than if the field was weaker, thus causing a longer T1.

2.4.2 What influences T2?

T2 relaxation comes about when the protons fall out of phase after the RF pulse is removed. This is usually due to inhomogeneities in the external and internal magnetic fields. Water molecules move around very fast so there is no net difference in internal magnetic field from place to place. No large difference in internal magnetic field means that the protons will stay in synch for longer. Tissues with larger molecules have larger variations in local magnetic fields causing a shorter T2.

2.5 Instrumentation and Types of Scanner

Three types of magnetic fields – main fields or static fields (B_0), gradient fields, and radio frequency (RF) fields – are required in MRI scanners. It is also usually necessary to use coils or magnets that produce shimming fields to enhance the spatial uniformity of the static field B_0. Instrumentation capable of human scanning fast became available in the late 1970's [18]. The successful implementation of MRI requires a two-way flow of information between analogue and digital formats. The main magnet, the gradient and RF coils, and the gradient and RF power supplies operate in the analogue domain. The digital domain is centred on a general-purpose computer that is used to provide control information to the gradient and RF amplifiers, to process time-domain MRI signal data returning from the receiver, and

to drive image display and storage systems. The computer also provides control functions, such as allowing the operator to control the position of the patient table.

The main field magnet is required to produce an intense, static magnetic field over the entire region to be imaged. To be useful for imaging purposes, this field must be extremely uniform in space and constant in time. The field strength to scan humans is usually at 1.5 Tesla (1 Tesla equals 10,000 gauss; the earth's magnetic field is 0.6 gauss). However it can be as high 4T. The signal-to-noise ratio (SNR) is the ratio of the MR signal voltage to the ever-present noise voltages that arise within the patient and within the electronic components of the receiving system. The SNR is one of the key parameters that determine the performance capabilities of a scanner. The maximum available SNR increases linearly with field strength. The improvement in SNR as the field strength is increased is the main reason for development of high-field strength magnets for MRI systems [19].

Magnetic fields can be produced by using either electric currents or permanently magnetised materials as sources. In either case, the field strength falls off rapidly away from the source. Consequently, to produce the highly uniform field required for MRI, it is necessary to more or less surround the patient with a magnet. As well as this the main field magnet must meet other stringent performance requirements. Hence, this magnet is the most important determinant of the cost, performance, and appearance of an MRI scanner.

There are many configurations of MRI scanners depending on the type of magnet. Currently, there are three types of magnets: superconducting, resistive, and permanent magnets. The superconducting magnets generate the highest field strengths and require liquid nitrogen to super cool the coiled wire so it will superconduct without resistance. These magnets may contain a long bore or hollow tube where the patient is placed around which the coiled wire and coolant are housed. Many newer high field strength superconducting magnets are now being produced with a much shorter bore for patient comfort. Resistive magnets are air-cooled and therefore, the coiled wire has a certain resistance and a lower magnetic field. These magnets can be designed in open (figure 2.7) or closed (figure 2.8) bore configurations depending on the strength and homogeneity of the magnetic field desired. Permanent magnets are similar to the common bar magnet but much larger. These magnets do not require current to generate the magnetic field and are all low field strength magnets. However, these magnets can be designed in much more open configurations and is the

typical magnet currently used for the popular Open MRI scanners. Current technology has allowed image quality of Open or Low Field Strength magnets to approach and sometimes surpass the High Field Strength magnets. Open magnets typically employ two spaced-apart magnetic assemblies with the space between the assemblies allowing for access by medical personnel for surgery or other medical procedures during MRI imaging. The open space helps the patient overcome feelings of claustrophobia that may be experienced in a cylindrical magnet design.

Figure 2.7: Open bore configuration MRI scanner.
Figure 2.8: Closed bore configuration.

The main disadvantages of these high-field strength magnets, some of which have already been stated, are problems with claustrophobic patients using the closed bore magnets, difficulty with MR intervention due to inaccessibility and dB noise levels generated by the scanners. Sound pressure levels (SPL's) during interventional MRI may create an occupational hazard for the interventional radiologist [20].

2.6 Preparatory Measures

As preparatory measures clothing need not be removed, as is the case in most X-ray examinations, however, patients are asked to remove all objects, which may interfere with the imaging process, especially those containing metal. This includes earrings, brooches, necklaces, wristwatches, but also ballpoint pens and keys. Patients should also take out any removable dental plates and inform the physician if they have any other metallic implants or foreign objects including:

- Earrings, brooches, necklaces, wristwatches, ballpoint pens and keys.
- Heart pace-maker,
- Artificial limb,

- Metal plates or screws,
- Metal splinter or shrapnel.

2.7 Trends and Advances in MRI.

2.7.1 Sports Medicine

Sports medicine is one of the most rapidly growing subspecies in orthopaedics. MRI in sports medicine includes depiction of conditions in almost every joint in the body, but the MR examinations most frequently requested are of the knee and shoulder. Clyde A. Helms at the Duke University believes that the reported high accuracy of MRI in the knee has resulted in MRI being preferred to diagnostic arthroscopy by leading orthopaedic surgeons [21]. For example, the reported accuracy of MRI of the knee for meniscal tears is 90-95%, and for cruciate ligaments the accuracy is as high as 95-100%. With such high accuracy it is understandable why MRI is the preferred choice. Also, in evaluating the shoulder, MRI is becoming the preoperative imaging procedure of choice for many sports medicine surgeons. As the field of sports medicine expands, radiologists will continue to see increased requests for MR imaging, because sports medicine and high-quality imaging are inextricably linked.

2.7.2 Sound Exposure

Sound pressure levels (SPLs) during interventional MRI may create an occupational hazard for the interventional radiologist. That is, there is the potential risk of hearing impairment for the interventional radiologist who works near the magnetic bore. The risk is in the accumulation of noise exposure during long and repetitive interventional MR procedures. Doctors from the Departments of Radiology and Audiophysics at the Erasmus University Medical Centre, Rotterdam have quantified this sound exposure [20]. Previous emphasis about the acoustic noise of MRI has been on patient exposure during MRI. Therefore, measurements usually represent the acoustic noise levels in the isocentre of the magnet bore. The research at Rotterdam focused on the SPLs at the entrance of the magnet bore, which are more relevant to assess the acoustic burden on the interventional radiologist. They also investigated the acoustic levels produced by some of the newer fast imaging

techniques. Most MRI systems use a 1.5T field strength magnet. This is the type of system that the data was collected from. The ambient noise in the MRI suite at rest was found to be quite high, with equivalent-continuous linear SPL of 52.3dB. The SPL values depended on the sequence and ranged from 81.5 to 99.3dB with peak SPLs greater than 100dB for all sequences. Since hearing loss may occur as a result of chronic exposure to noise levels greater than 80dB there is a real risk to the interventional radiologist. Hence, they should use adequate hearing protection such as earplugs and earmuffs. This should also be provided to the patient.

A device has been patented by General Electric (US) [22] for low noise MR imaging of a subject that substantially minimises acoustic noise generated during imaging. The imaging apparatus comprises a magnet assembly, a gradient coil assembly, and an RF coil assembly, wherein at least one of the magnet assembly, the gradient coil assembly and the RF coil assembly are configured to reduce the generation and transmission of acoustic noise in and about the imaging apparatus. Improvements such as these may help to alleviate the problem of noise exposure.

2.7.3 Patented MRI device

An MRI scanner has been patented [23] that has a magnet whose interior working space within the magnet frame is sufficient to accommodate a physician and a patient. Because the physician is positioned inside the magnet frame, the physician has unimpeded access to the patient. Elements of the magnet frame encompass a room, and the magnet frame may be concealed from view of a patient within the room as shown in figure 2.9. The magnet actually forms the shape of a room. The patient can be led to believe that they are in an ordinary room as the bottom, top, and sides of the magnet can be covered in material one might associate with the floor, ceiling, and walls of an ordinary room.

This device is the ultimate open bore configuration MRI scanner. It removes the problem of claustrophobia and will allow even the largest of patients to be scanned. It also allows for interventional radiology with enough room to allow the radiologist easy access to the patient. However, limitations such as the cost effectiveness and the actual image quality are not discussed in this patent. None the less, devices such as these may play a role in MRI of the future.
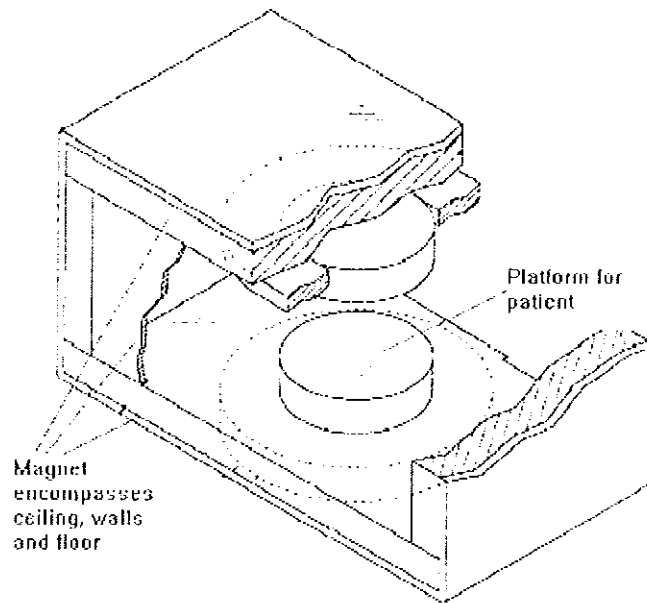
Figure 2.9: MRI Apparatus – variation on scanner design [23].

2.7.4 Whole Body MRI Angiography

A technique for performing whole-body MRI angiography has been developed at the University Hospital Essen, Germany [24]. In this case a self-developed rolling table platform allows the patient to be manoeuvred within the scanner permitting the use of the main surface coil in the scanner. This resulted in high SNR and contrast-to-noise ratios, and was most beneficial in detecting vascular diseases. The whole-body image, as shown in figure 2.10, is created from five slightly overlapping data sets in immediate succession. The five data sets cover the cranial and thoracic regions, the abdomen, the pelvic region, the thighs and finally the calves. The quality of images obtained were excellent and allowed assessment of the entire vascular tree.
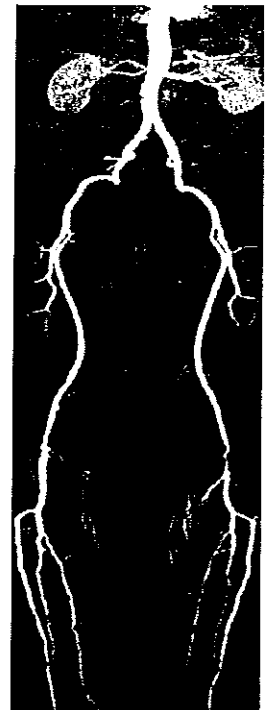
Figure 2.10: Whole body MRI image of the vascular tree

2.8 Image Artifacts

An image artifact is any feature that appears in an image that is not present in the original imaged object. An image artifact is sometimes the result of improper operation of the imager, and other times a consequence of natural processes or properties of the human body. Artifacts are typically classified as to their source. For example:

- RF Quadrature: Failure of the RF detection circuitry
- RF Inhomogeneity: Failure of RF coil
- Flow: Movement of body fluids during the sequence

And

- Motion: Movement of the imaged object during the sequence.

As the name implies, motion artifacts are caused by motion of the imaged object or a part of the imaged object during the imaging sequence. The motion of the entire object during the imaging sequence generally results in a blurring of the entire image. Movement of a small portion of the imaged object results in a blurring of that small portion of the object across the image.

The solution to a motion artifact is to immobilize the patient or imaged object. Often times the heart beating or the patient breathing causes the motion. Both of which cannot legally be eliminated.

During the respiratory cycle it is mainly the movement of the diaphragm inside the body that causes breathing. Hence, as patient's breath, organs can be displaced in both location and size due to diaphragm movements. If this displacement takes place during the scanning procedure the resultant image will become distorted and the output quality effected.

The following are examples of such motion artefacts:
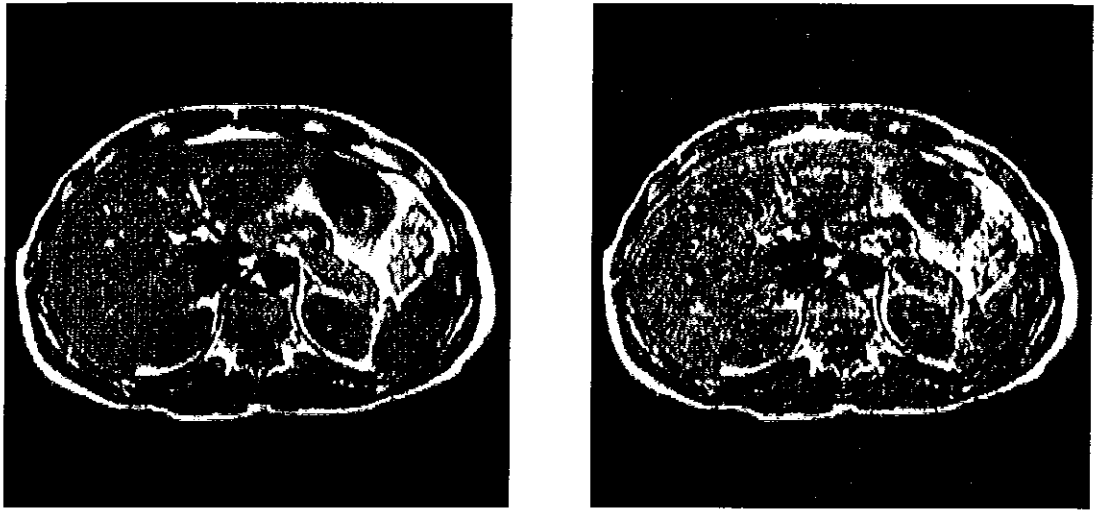
Figure 2.11a: Image of the abdomen.

Figure 2.11b: Image distortion due to respiratory motion of the abdomen [25].

2.9 Solutions

There are various different tried and tested techniques for reducing image artefacts due to breathing. These include speeding up the process to reduce scan time, respiratory triggering of the imaging sequence to the cardiac or respiratory cycle of the patient, and movement compensation techniques. While these techniques are continuously improving they are still far from perfecting the process. Another solution to the problem is to train the patient to hold their breath during the scanning procedure. Much time is spent teaching the patients how to control their breath during the scanning, thus leading to excessive times on the MRI machine. The object of this research was to design a low cost respiratory monitoring system that could be used offline to prepare patients for the procedure, and modified to be used in the MRI environment providing feedback to patient regarding breathing activity during the scanning procedure.

Research into this problem is ongoing throughout the world. There are different societies and organisations that research into the area and produce Journals on the topic. Some examples of these are the Radiology Society of North America (RSNA), the European Journal of Radiology and the Irish Medical Organisation {[16] [20] [21] [24] [26]}. MRI produces images that can lead to fast and accurate diagnoses and is amongst the best of imaging techniques. Therefore, as the technology develops it is becoming more and more popular and the need for more efficient scanning is growing. Traditionally MRI's main advantage was its exceptional soft tissue contrast.

32

As the time to acquire images decreases MRI has grown into other areas such as bone and joint studies. MRI research involves fundamental tradeoffs between resolution, imaging time, and signal-to noise ratio (SNR). It also depends heavily on scanner hardware innovations. In order to solve the problem of respiratory motion artefacts a number of areas are currently being researched and developed.

2.9.1 Speeding up the Process

The main focus of attention is on trying to speed up the scanning process. To speed up the process would cause the movement due to breathing to have less of an effect on the image. If the scanning time is quick enough then the image could be taken before the movement was great enough to have a serious effect. The process is getting faster all the time but it is still far from being fast enough to satisfactorily solve the problem. Although typical imaging studies range from 1 to 10 minutes, new fast imaging techniques acquire images in less than 50 ms. Conventional spin-warp images typically require several minutes to acquire. Fast spin echo techniques can reduce this to the order of 20 seconds. The echo-planar technique requires substantially increased gradient power and receiver bandwidth but can produce images in 40 to 60 ms. Vivian S. Lee and Daniel Resnick from the Department of Radiology – MRI, New York University Medical Centre have used fast imaging techniques for cardiac scanning during a single breath-hold [27]. Their results were comparable to those obtained from conventional scanning techniques. Some of the fast imaging techniques are discussed in a book by Gary P. Zientara [28]. This book describes how non-adaptive fast MRI pulse sequence methods are approaching the limit of temporal resolution, with field-of-view (FOV), signal-to-noise-ratio (SNR), and tissue contrast limitations. The advanced dynamic MRI methods of the future, those yielding high contrast, high spatial resolution 2D MRI at near video rates, are only at the early stages of development. These techniques and other fast magnetic resonance body imaging techniques are discussed in a book by H Hatabu and H Imhof [29].

2.9.2 Respiratory Triggering

Another solution is to gate the imaging sequence to the cardiac or respiratory cycle of the patient. This method uses a bellows to monitor the patients breathing. At the same point in each breath cycle a short scan is taken. Therefore, although the

patient is continually breathing the scan is broken up into many short scans taken when the lungs are in the same position for each. This has proved not to be very effective in practice however. The images are still blurred and the amount of time the patient must spend in the scanner is increased. It is however still an important technique and can produce good results in certain circumstances. In an article in the American Journal of Roentgenology GD Low and A Shimakawa [30] claim that by acquiring data during a period of reduced respiratory motion the respiratory triggered fast spin echo (RTFSE) sequence produced images with sharper anatomic detail, and a measurable improvement in the lesion-liver contrast and contrast to noise ratio (CNR). The respiratory triggering method is currently being improved upon. R Sinkus and P Bornert from the Philips Research Laboratories, Hamburg Germany are working on an automatic real-time respiratory gating algorithm [31]. Two indicators are introduced: first a parameter that registers changes of the motion pattern due to breathing, and second an indicator that expresses the quality of the data set already obtained. Based on these indicators, the gating algorithm decides to change gating parameters during scanning automatically. This new approach has the potential to increase the scan efficiency considerably without the need of operator interaction or significant patient cooperation. P Bornert is also working on a new method, which could reduce the total scan time considerably [32]. The MRI data acquired is only accepted if the motion-induced displacements measured from a reference position are below a chosen gating threshold function. During the scan the scanner analyses respiratory motion, decides in real-time which data can be measured according to the gating threshold function and performs data acquisition. Radiologists from the University of Bonn have shown that pulse triggering, triggering data acquisition to the cardiac cycle, with a single breath-hold reduces respiratory motion in MR imaging of abdominal organs [33]. Developments such as these could cause respiratory triggered scanning to be a successful technique in the future.

2.9.3 Movement Compensation Techniques

There are also various movement compensation techniques. L Hofland, S Scampini and B Savord have patented a device that uses this technique [34]. In this case the motion artefacts can be reduced when the instantaneous position of the moving part is known. This instantaneous position is derived from navigator signals. These are generated separately from the other imaging signals. By deriving a phase

and frequency correction from the navigator signals and applying them to the received imaging signals the problem due to movement can be solved. Other variations on this method are used. Using abdominal slice images and a navigator pulse sequence after initiation of each breath-hold to acquire data enables the slices to be registered retrospectively [35] [36]. This method can be used in conjunction with respiratory-triggered techniques [31].

2.9.4 Other Devices

There are also various devices on the market that may be of use to this research, such as devices that are specially designed for children or for people with learning disabilities. Certain types of visual aid for example could be incorporated into this project. V Gerasimov and W Bender from the MIT have developed a hand held doctor for children [37]. This device uses a cartoon character that visualises three physiological parameters: pulse, breathing, and temperature. This provides an interface with which children are better able to react. There is also the possibility of sharing devices with other imaging technologies such as CT Fluoroscopy [38], [39]. One such apparatus developed by R Castile is for the controlled ventilation of a patient [40]. A pause in the patient's respiratory cycle is induced by inflating the lungs synchronously with natural inspiration to a greater volume than normal tidal inspiration for several closely spaced respiratory cycles. This is done using a mask to introduce pressurised air into the patient's lungs. After a few cycles of full breaths, the breathing rhythm of a patient naturally pauses for a period of several seconds, during which an image can be made. This technique is most often used on infants.

The highest field strength commonly used in MRI scanners is 1.5T. To achieve better SNR's, higher field scanners, operating at fields up to 4T, have been studied experimentally. The need for very high-field scanners has been enhanced by the development of functional brain MRI. This technique utilises magnetisation differences between oxygenated and deoxygenated haemoglobin, and this difference is enhanced at higher field strengths it has now become possible to construct 3 to 4T scanners of the same physical size as the 1.5T systems, and this is resulting in a considerable increase in the use of high-field systems.

2.9.5 Patented breath-hold monitor for MR imaging

A device has been patented [41] that is similar to the design that this research hopes to achieve. However, this system uses the MRI device itself as the breath monitor. That is, instead of using a bellows, this device uses an MR signal to track the position of the diaphragm during the scan and then this navigator signal is used to change the MR image signal accordingly. The advantage of this is that no attachments, such as the bellows, need be placed on the patient during the scan. The disadvantage of this method is that the patient cannot be trained to hold their breath before entering the MRI room. This will lead to greater time being spent in the MRI room, time that is already at a premium in hospitals. The other disadvantage of this method is that a lot of programming of the scanner's computers is required. If a peripheral device is used then the scanner can operate as usual with the peripheral device working alongside it.

Another aspect of interest of this device is the method of feedback to the patient. A visual feedback system is used whereby an array of LED's describes the breathing activity of the patient. This is fed to the patient using a mirror placed within the scanner tunnel. Hence the patient sees a reflection, in the mirror, of the LED's, which are placed a safe distance from the scanner so as not to interfere with the operation of the scanner. This will lead to problems such as trying to align the mirror correctly so that the patient can view the LED array. The mirror must be easily attached to the scanner tunnel so that it can be removed. The scanner tunnel is narrow so there is not a lot of room to manoeuvre the mirror into the required position. Also, the LED array must be far enough away from the scanner so as not to cause interference. This may lead to problems with the ease of visibility of the array.

This is a complicated system that will be difficult to implement into a typical MRI scanner. The feedback system is of interest but may be difficult to perfect.

2.10 Breath Monitoring Devices.

There are numerous breath monitoring devices available on the market. Most of these are for medical purposes, however they can have other uses such as breath-alcohol content measuring required for legal reasons. Some of the different techniques were researched with a view to developing a breath monitor that could be used in the MRI environment for the purposes of monitoring the patient's breath hold.

<u>2.10.1 Breath Content Monitors</u>

There are many applications for breath content monitors. The alcohol level of the breath may be monitored for legal reasons. Oxygen and carbon dioxide levels are measured to ensure that respiration is performing correctly in such cases as infant sleep apnoea. Such a breath content monitoring system was considered for use in this project. By monitoring the oxygen and carbon dioxide levels of the breath it can be determined whether the patient is inhaling or exhaling. With a sensitive system it may even be able to determine when the breath is being held with reasonable accuracy. If the oxygen and carbon dioxide levels remain the same it would suggest that neither inspiration nor expiration are taking place which corresponds to a breath hold.

The Gemini Respiration Monitor [42] from CWE, Inc is capable of measuring breath-by-breath oxygen and carbon dioxide concentrations for accurate respiratory assessment. Respiratory rate can also be calculated by using the normal inspiration/expiration excursion of the carbon dioxide signal. Such devices as this require a mouthpiece through which the patient breathes. These devices are often used to monitor the respiration cycle during surgery when the patient is unconscious. In such cases a tube is passed down to the endotracheal tube of the patient.

It was decided against using such a device for a number of different reasons. Firstly, an MRI scan is already an uncomfortable procedure for the patient. The strict confines of the scanner tunnel are claustrophobic. Using a mouth piece in this already difficult environment for the patient may have the undesirable effect of causing irregular breathing making it more difficult to provide an accurate breath hold. Secondly, while respiratory rate can be monitored with reasonable accuracy it is more difficult to determine if a correct breath hold is taking place in real time using such a device. Subtle changes are more difficult to determine. Finally, it is the movement of the diaphragm that causes the imaging problems. Thus it is the diaphragm movement that must be stopped. Just because there is no flow of air from the patients mouth does not mean that there is no movement of the diaphragm. Breathing is usually abdominal and thoracic. This means that when breathing the chest and abdomen expand to allow the lungs to expand and the diaphragm move. Although there is no airflow from the mouth the patient may relax from a thoracic expansion to an abdominal expansion, which can result in a movement of the diaphragm. Such a movement will not register on a breath content monitoring device, as there is no resultant flow of air from the mouth. For these reasons it was decided that such a device would not be used.

37

2.10.2 Spirometer

Spirometers are mainly used to measure the tidal volume of patient's lungs. The tidal volume is the total volume of air that the lungs can hold. A simple schematic of a spirometer can be seen in figure 2.12 below. The patient is asked to inhale to full extent and then, after placing the mouthpiece in their mouth they are asked to exhale to full extent. The inverted bell will rise by an amount proportional to the volume of air that was released from the patient's lungs.
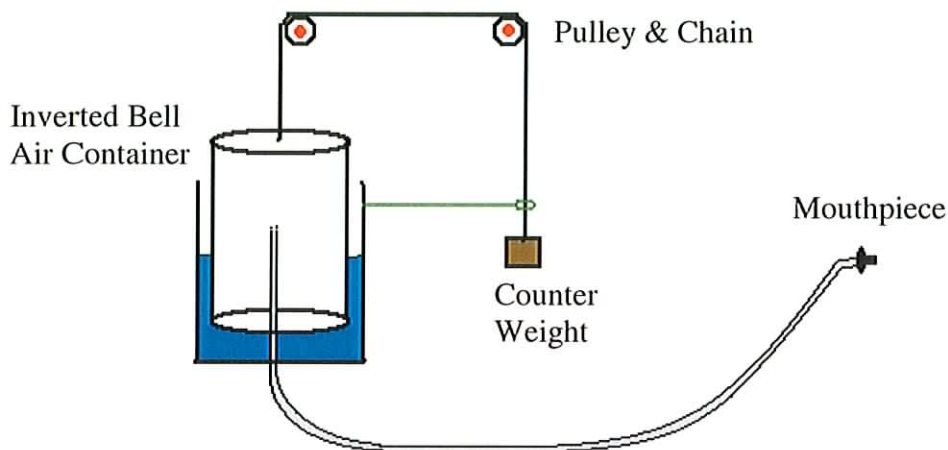
Figure 2.12: Schematic of a simple Spirometer

Such a system could be used to test for a breath hold. In this case the patient would be told when to blow into the mouthpiece and would then be asked to hold their breath. The air chamber would rise as they blow into the mouthpiece and then should remain in the same position as they hold their breath.

As with the breath content monitors this device would require a mouthpiece. This is an undesirable trait as already discussed. This device would also only measure airflow and hence would not necessarily register all diaphragmatic movements. Therefore it was decided that such a device would not be used.

2.10.3 Pressure Sensors

Another option available was to use very sensitive pressure sensors. These could be used in a variety of ways to monitor breathing. There are also different types of pressure sensors that work off various different principles.

One option is to use a strain gauge that measures movement in the rib cage or the abdomen. Another is to measure thoracic impedance. In this case a current is

applied to the thorax, which serves as an electrical conductor. The total impedance decreases as the volume of the conductor increases and vice versa. Another possibility was to use an air pouch with a small piezoelectric pressure sensor attached. This set up is used to monitor infants with respiratory problems [43].

Piezoresistive pads can also be used to measure breathing [44]. These consist of a silicon diaphragm, which is ideal for receiving the applied force. Silicon is a perfect crystal and does not become permanently stretched. After being strained, it returns to the original shape. The sensing element of a solid-state pressure or force sensor consists of four nearly identical piezoresistors buried in the surface of a thin circular silicon diaphragm. A pressure or force causes the thin diaphragm to flex, inducing a stress or strain in the diaphragm and also in the buried resistors. The resistor values will change depending on the amount of strain they undergo, which depends on the amount of pressure or force applied to the diaphragm. Therefore, a change in pressure is converted to a change in resistance (electrical output). The resistors can be connected in either a half-bridge or a full Wheatstone bridge arrangement. For a pressure or force applied to the diaphragm using a full bridge arrangement, the resistors can be theoretically approximated as shown in figure 2.13 (non-amplified units). $R \pm \Delta R$ and $R - \Delta R$ represent the actual resistor values at the applied pressure or force. R represents the resistor value for the undeflected diaphragm where all four resistors are nearly equal in value. ΔR represents the change in resistance due to an applied pressure or force. All four resistors will change by approximately the same value. Note that two resistors increase and two decrease depending on their orientation with respect to the crystalline direction of the silicon material. The signal voltage generated by the full bridge arrangement is proportional to the amount of supply voltage (Vcc) and the amount of pressure or force applied which generates the resistance change.

V_{CC} = SUPPLY VOLTAGE

$R-\Delta R$ $R+\Delta R$

V_1 V_2

$R+\Delta R$ $R-\Delta R$

GND
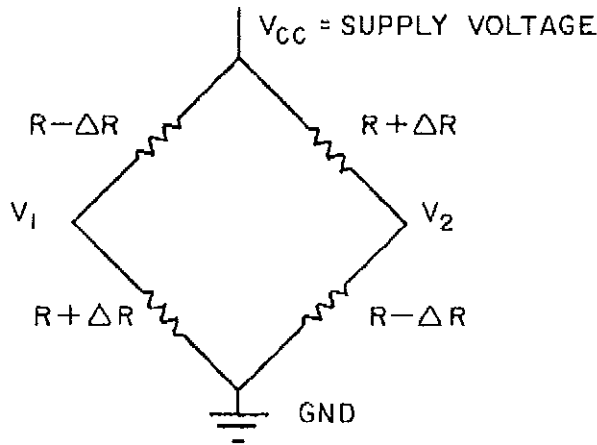
Figure 2.13: Full Wheatstone Bridge arrangment for piezoresistors on a silicon pressure diaphragm.

These pressure sensors were an attractive option to use, as they do not all require the use of a mouthpiece. The small pads would cause minimal discomfort to the patient. While these sensors could be used in the offline case they do have one major disadvantage. The large magnetic forces associated with the MRI magnet will cause problems with the use of electrical wires. A magnet will induce a current in a wire and similarly a current in a wire will induce a magnetic field around the wire. Thus the scanner will have an adverse affect on these sensors and what is worse, the sensors may distort the image signal of the scanner, which is based on magnetism. Therefore it was decided to try and find a method that did not include any electrical components.

2.10.4 Air Mattress System

Another option is an inflated air mattress on which the patient lies. Changes in pressure due to respiratory movement can be recorded. A mechanical filter is usually employed with such a system to protect the transducer from large changes in pressure due to movement of the body. One particularly interesting device [45] uses a multiple compartment air mattress as shown in figure 2.14. This allows distinguishing and monitoring of both thoracic and abdominal movements due to respiration. It is this movement that is most relevant to breath holding. Movement in one or other of these areas indicates diaphragmatic movement. In this device each of four compartments are connected to pressure transducers via 3m polyurethane tubes. Two of the

compartments are for thoracic measurements and two are for abdominal measurements.

The mattress is 850mm * 1900mm * 40mm in size. This is too large for use within an MRI closed bore scanner whose inner tunnel radius is usually about 600mm. Even without the mattress, there is little room for the patient. The tunnel ceiling is usually within approximately 200mm of the patients face so even a 40mm thick mattress will take up a significant amount of space.

Another problem with such a mattress is that the respiratory movements are very small compared with a movement of the body. Any such movement could cause the transducers to saturate. To combat this solenoid release valves are used. These valves could not be used in the MRI environment.
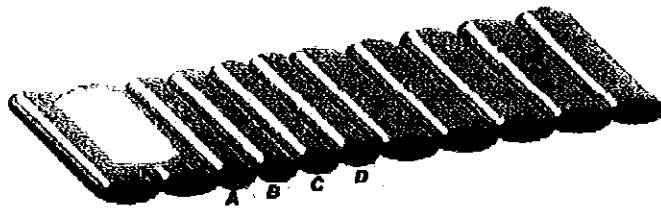
Figure 2.14: Four Compartment Air Mattress System for Respiratory Monitoring.

2.11 Conclusion

The object of this research is to design a low cost respiratory monitoring system that could be used offline to prepare patients for the procedure, and modified to be used in the MRI environment providing feedback to patient regarding breathing activity during the scanning procedure. Through discussions with the consultant radiologist involved with the project it was believed that this method, if perfected could lead to improvements in abdominal scanning. The research carried out for this literature review provided further evidence that such a device could lead to impovements. This method could be used along with other methods such as movement compensation techniques. Even though the scanning process is gradually speeding up the need remains for the patient to hold their breath. Having researched various methods of breath monitoring it was also decided to attempt to develop a cheap transducer that could carry out this function within the MRI environment. This device should measure chest movements as opposed to air flow so that diaphragm movements are noted.

3   INITIAL PROTOTYPE

3.1   Introduction

A number of different breath monitoring technologies were initially considered. Having chosen a technology, which would be compatible with the MRI environment, the task was then to build and test an initial prototype. Further work was then required to develop the feedback systems and to commercialise the final product. For the purpose of carrying out preliminary tests an initial prototype was built and housed in a wooden housing. This would eventually be replaced by an improved version that can be used online in the MRI environment and should be close to a marketable product.

3.2   Breath Monitoring Options

There are numerous devices available on the market for breath monitoring as discussed in chapter 2. These range from breath content measuring devices to breath volume measuring devices. These are used in many different industries but are most commonly used in the medical industry. A number of key factors determined what type of breath monitor would be most suited to the requirements of this project. Firstly, the main requirement is that the patient receives feedback about breathing activity. Chest movements, or airflow from the mouth or both could be used to determine breathing activity. Secondly, the MRI environment itself will rule out any magnetic component within the MRI room. Finally, it was hoped that the device would be non-invasive to avoid placing further stress on the patient in the already claustrophobic atmosphere of the scanner tunnel. This would also make it easier to obtain the CE Mark for the device, as rules are less strict for non-invasive devices.

3.2.1 Flow Meter

A simple mechanical flow meter as shown in figure 3.1 was initially considered. This operates on the principle of a very sensitive propeller, which is activated by the slightest movement of air in or out of a narrow orifice. The mouthpiece tapers down into a small orifice, in which this device would be placed. As the person breathes, this would cause the sensitive propeller to rotate and a paper drum would be marked simultaneously, indicating that air movement occurred.

This was a simple idea but it would have been difficult to bring to a stage where it could be brought online to provide the patient and the radiologist with feedback

about the breathing activity. It also has two main disadvantages as some of the previous devices discussed in chapter 2. The mouthpiece is undesirable and flow rate does not necessarily register all diaphragmatic movement. Hence it was decided that this device would be unsuitable.

Air movement either way causes propeller to rotate

Air channel sectioned

Propeller mounted in airway

Ink marker, to highlights movement on paper roll

White paper Roll, which is marked if propeller rotates
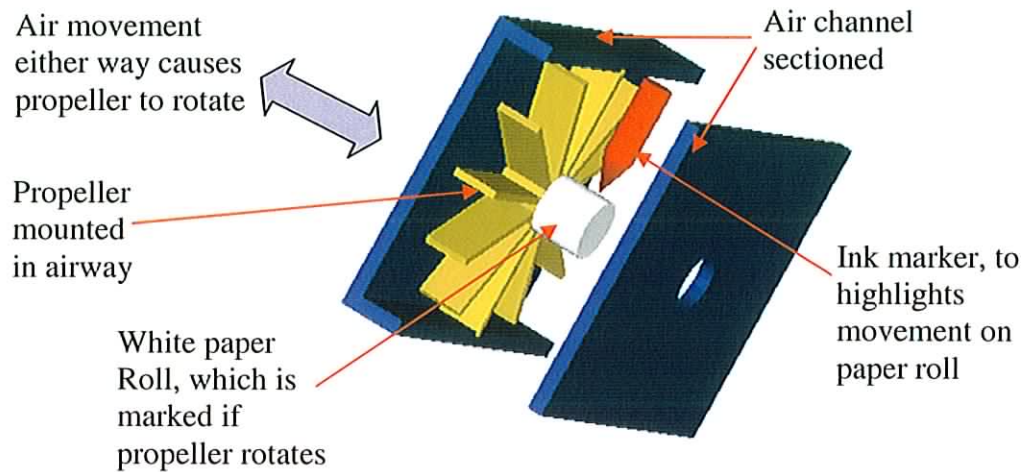
Figure 3.1: Sketch of a proposed flow meter design.

3.2.2 Pressure Coil

A pressure coil is already employed in some MRI units for use in respiratory-triggered MR sequences as discussed in Chapter 2. The pressure coil is a small accordion like tube 200mm in length with a diameter of 20mm. A polyurethane tube connects the coil to a pressure transducer imbedded in the MRI table. The coil is strapped around the patients lower thoracic region. The strap is attached at either end of the coil with a Velcro fastener that is fastened behind the patients back. A photograph of the pressure coil can be seen in figure 3.2 below.

Figure 3.2: Pressure Coil used in the Initial Prototype.

The operator must first do a trial run to ensure that the patient's diaphragm movements do not exceed the pressure ranges set on the transducer. This can be dealt with by either adjusting the tightness of the bladder on the patient or by resetting the pressure range on the transducer. This coil works off negative pressure. As the patient breathes in the chest expands and the coil is extended. This extension causes an increase in volume within the coil and hence the pressure drops below atmospheric pressure. As the patient exhales the coil relaxes back to its original position and the pressure increases again. These changes in pressure are registered on the transducer and are used in the respiratory-triggering sequence to help improve the scan. In a similar way the coil can be used to test for breath holding.

This was a coil that had been previously used in the MRI suite for respiratory triggering. It was well suited for use in the initial prototype and provided a basis from which initial tests could be carried out. This type of breath monitor measures chest movements as opposed to airflow. Thus movement of the chest when there is no airflow is still noted. This ensures that all diaphragm movements are registered leading to an improved breath hold. However, these coils are prone to leaks due to their complex shape. These leaks tend to occur due to perforations along the seams in the coils as shown in figure 3.3. They are also extremely expensive. Because of this it was decided to design and manufacture a bladder that would suit the purposes of this project and be relatively cheap and easy to make. A rubber bladder was designed and manufactured that operates from positive pressure but provides similar results. This new design is discussed in chapter 4.

44

Grooves between the coils stretch and compress. Small perforations begin to appear.
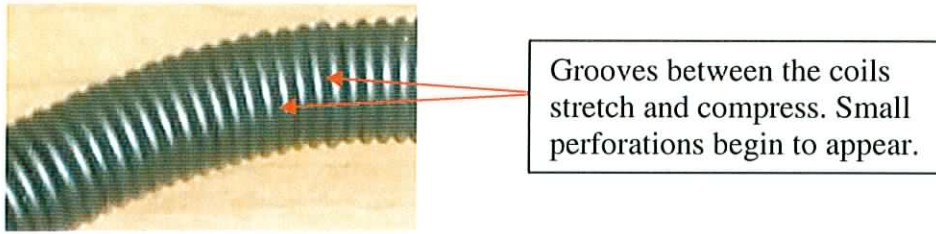
Figure 3.3: Section of the Pressure Coil showing where perforations occur.

3.3 Pressure Transducer

A pressure transducer was needed to convert the pressure changes into a corresponding electrical signal in order to be compatible with a computer. This electrical signal could then be recorded and processed by computer or displayed using LED's. There are many pressure transducers on the market and they vary in numerous ways. The main distinguishing factor is the pressure range in which they can accurately operate. They vary from ultra low-pressure transducers, which operate up to a few kilopascals (kPa), to ultra high-pressure transducers that can operate at pressure levels of over 10^6kPa. The pressure coil operates at pressures of approximately -10kPa to 0kPa. Therefore a relatively low-pressure transducer was required. To allow for experimentation with pressure ranges it was desirable that the pressure transducer could be easily calibrated. This would enable the best pressure range for the coil to be found and would also allow new pressure coils or bladders to be tested. As the pressure coil operates in a negative pressure range it was necessary that the transducer could operate in this range. It was thought that at a later stage a positive pressure bladder might be tested also so this required the transducer to have a range encompassing positive and negative values.

The pressure transducer chosen was the Model FCO332 differential pressure transmitter from Furness Controls [46]. This transducer has an operating range of 20kPa above and below atmospheric pressure, which is adequate for its required use in this case. The transducer has one port connected to the bladder and the other is left open to atmosphere as the reference. A feature of the transducer is the 4.5" LCD display. This provides a digital indication of pressure in units of kPa. This output can also be directed through a computer interface that allows for a larger on screen numerical as well as graphical display. The pressure cell within the transmitter that reads the pressure is based on a unique reliable capacitive sensor. A microprocessor is used to control all functions of stability such as temperature correction and linearity.

The pressure range can be adjusted by a 10:1 ratio while maintaining accuracy. This pressure transducer would later be used in the final device.

There are three configuration options with the model FC0332. The configuration must be chosen when ordering the product. The configuration options include:

- 2-Wire 4 to 20mA Current output.
- 3-Wire Voltage output.
  - 0 to 1V, 0 to 2V, 0 to 5V, 0 to 10V, 0.2 to 1V, 0.4 to 2V, 1 to 5V, 2 to 10V
- 4-Wire Voltage output,
  - 0 to 1V, 0 to 2V, 0 to 5V, 0 to 10V, +/-1V, +/-2V, +/-5V, +/-10V

The second configuration was chosen with a 3-wire 0-10Volts dc output. This was chosen as the LED bargraph display that is also used in the respiratory monitor accepts a 0-10Volts dc input. Therefore the two devices can be directly linked together. The output voltage on the pressure transducer varies between 0-10Volts dc as the return pressure varies. This output is fed to the bargraph display, which gives a simple visual indication of breathing activity.

The transducer has a pressure range of 20kPa above and below atmospheric pressure. There are two pneumatic outputs, one for positive pressure and the other for negative pressure. During the course of the research and development of the device different types of bladders and pressure coils were used to monitor breathing. Some of these work off negative pressure and others work off positive pressure. It is necessary to configure the pressure transmitter for operation with the various devices. The pressure range also varies from device to device. For a very sensitive bladder or coil a small pressure range may be set (e.g. 0 – 2 kPa), with the range increasing as the sensitivity decreases. For breath monitoring it was decided that the pressure range should encompass the whole breathing cycle. Therefore, when using positive pressure, if the patient breathes in the pressure should be at the top of its range and when the patient breaths out the pressure should drop to the bottom of its range. This will provide a full-scale output of 0-10V and will provide better results on the LED display.

The software that comes with the pressure transmitter is used to calibrate it for the required pressure range. The transmitter is connected to the computer using a USB connection. The USB port on the transmitter is found under the front cover. Figure 3.4 shows a typical example of how to use the software for calibrating the device. In this case the differential pressure is set between 1kPa above atmospheric pressure and 5kPa above atmospheric pressure. These are the settings used for the final bladder design for the respiratory monitoring device. For the initial prototype a negative pressure coil was used with the differential pressure set between -3kPa and -7kPa below atmospheric pressure.
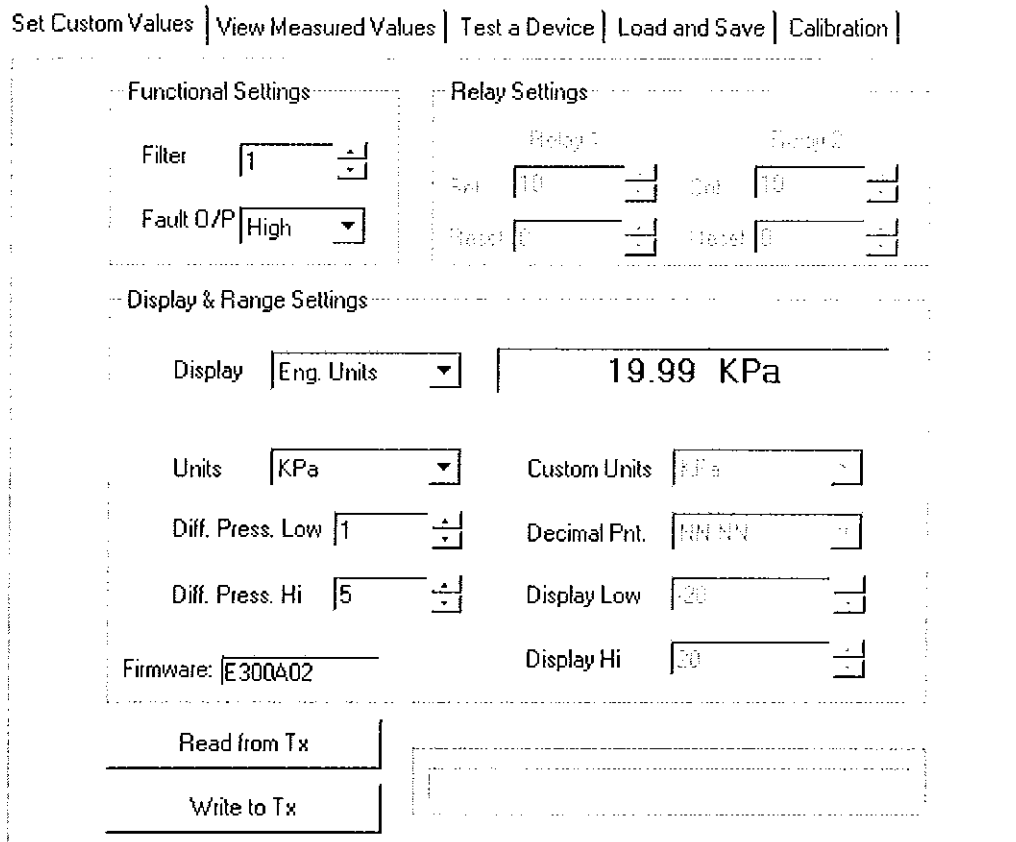
Figure 3.4: FC Software interface for configuring the FC0332 Pressure Transmitter.

The pressure transducer is enclosed in a polycarbonate casing as shown in figure 3.5. The dimensions of this casing are 120x * 80y * 58z (all dimensions in mm). There is also a 36mm electrical output in the y direction.

The pneumatic connections are for 4mm inner diameter push on tubing. The tubing chosen has a 6mm outer diameter. The tubing is approximately 10m long so that it can reach from inside an MRI scanner, where it is attached to the bladder, out to the control room, where it is attached to the pressure transducer.
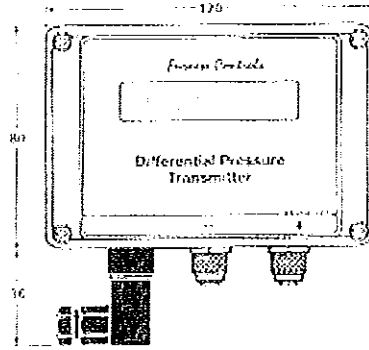
Figure 3.5: FC0332 Pressure Transmitter from Furness Controls.

The electrical socket on the transmitter accepts a number of different wiring set-ups depending on the configuration. This device was configured for a 3-wire set-up. This caters for a single input, single output set up where the ground is common to both. Figure 3.6 shows how to wire the socket. The positive input from the power supply feeding the transmitter is connected to Pin 2. These pins are clearly labelled on the socket. The ground from the power supply is connected to Pin 4. This pin is also used for the ground output. Pin 3 is for the positive output. Pin 1 is left unconnected.

PIN	Voltage O/P		Current O/P
	3-Wire	4-Wire	4 to 20mA
1	n.c	-ve	-ve
2	-ve	+ve	+ve
3	O/P	O/P	n.c
4	GND	GND	n.c.

Figure 3.6: Wiring instructions for the 3-wire set up.

This pressure transducer was the only part of the initial prototype that was used in the final design. This was due to a number of factors including its sensitivity and the ease with which it may be configured. The LCD display which gives a pressure readout is also an attractive feature. This display allows the device to be tested quickly without any feedback system.

3.4 Bargraph Display

A visual display was required to show the readings from the pressure coil and pressure transducer. The FCO332 has an LCD display, which displays the pressure readings within the coil. However from this digital display alone it would be difficult

48

to obtain any comprehensive information about a patient's breathing activity. An easily legible design that showed clearly the extent of inspiration and expiration was required. A bargraph display was used to convey this simple clear feedback to patients about their breathing activity.

The large Model PRO-BAR [47] from London Electronics as shown in figure 3.7 was used in the initial prototype. This can be horizontally mounted and contains 50 segment displays of bright wide angle LED'S. The 250mm scale length provides good legibility from long distances. The analogue input to this unit is 0-10Volts dc, which allows a direct connection with the pressure transducer. It also has own power requirements of 240Volts ac.
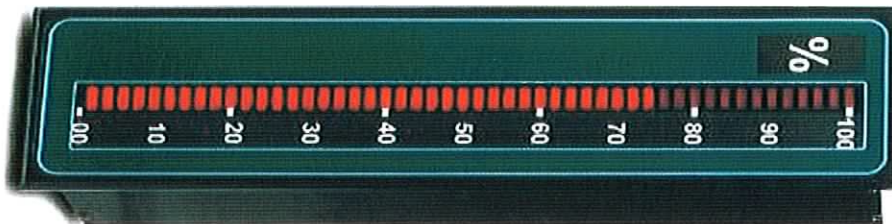
Figure 3.7: PRO-BAR LED from London Electronics. When operating with the device the LEDs give a bargraph display that increases and decreases as the patient breaths in and out.

The bargraph display input comes from the pressure transmitter output. This is a 0-10V dc signal. For a 0V input the display will register no lights. As the input voltage increases the lights start to turn on until at 10V all 50 segments will be lit. When the patient breathes in, the pressure in the bladder increases, leading to an increase in voltage from the pressure transmitter which in turn leads to an increase in the number of LED's that are lit in the display. This has the effect that as the patient breathes in and out the LED's come on and off giving a varying bargraph display. When the patient holds their breath the same number of LED's are continuously displayed.

This LED display was used in the initial prototype, as it was large and easy to use for initial device assessment. In the final breath-monitoring device a smaller LED display was used. This was the Model BAR-X from London Electronics as shown in figure 3.8. This model has a 75mm scale length with 30 red LED display segments. The analogue input to this unit is 0-10Volts dc. Therefore this bargraph display is also

compatible with the pressure transmitter configuration. It also has own power requirements of 240Volts ac.

The BAR-X has a number of extra functions that the PRO-BAR does not have. It has an alarm system that allows limits to be set on the display which, when exceeded, set off the alarm. There is a also cheaper version of this model without alarms. It also has a screw mounting to the rear of the panel allowing the device to be easily mounted. Both models have detachable coded screw terminals and are simple to install. They also have a high immunity to noise which helps in the high magnetic radiation environment of the MRI suite.

Figure 3.8: Model BAR-X bargraph display from London Electronics.

However it is the rear screw mount and smaller size of the BAR-X that made it most attractive for use in the final design. Indeed, it was even hoped to develop a customised LED display but it would have been an extremely expensive process. Some of the device specifications of both models are shown in figure 3.9.

	Pro Bar	Bar – X
Display Segments	50	30
Scale Length	250	75
Analogue Input	0 – 10V dc	0 – 10V dc
Power Supply	240V ac	240V ac
Display Bezel Dimension	288mm*72mm*12mm	96mm*48mm*12mm
Panel Cut-out	273mm*64mm	92mm*45mm
Depth behind panel	105mm	125mm
Weight	0.95Kg	0.3Kg
Case Material	Black powder coated heavy	UL Rated Noryl

Figure 3.9: Device specifications for the LED displays.

3.5 LabVIEW

As well as having the bargraph display it was necessary that the signal could be sent to the computer for processing. Computer software was necessary to carry out this function. Some of the key requirements of the software would be to provide a visual display as well as record the data collected from the 0-10Vdc signal from the pressure transducer. Further manipulation would also be required at a later stage. It was decided to use Laboratory Virtual Instrument Engineering Workbench (LabVIEW). This is a development environment based on graphical programming. It relies on graphical symbols rather than textual language to describe programming actions. It is integrated fully for communication with hardware such as a General Purpose Interface Bus (GPIB) and plug-in data acquisition boards.

LabVIEW has been used in this project for a number of different applications. It was chosen for the ease with which complex test and measurement applications can be set up. A number of programs were written with varying functions. These include recording and viewing the breathing information of the patient. The programs were written in such a way that the information can be displayed as a waveform on screen and can simultaneously be stored as an Excel file. The waveform display is a valuable visual aid that can be used to teach patients the concept of holding their breath correctly. It is a clear and simple view of the breathing activity even for those who are not technically minded. The information stored to file can later be analysed and the results from a number of patients can be used to form statistical analyses. The initial programs were later amalgamated into one program that is to be used with the final device.

LabVIEW can also be used as a testing rig for the pressure coil. The same program that was used to monitor the patient's breathing can be used to check for leaks. If the bladder is held under constant pressure then any leak will result in the LabVIEW programme showing a decreasing waveform. Small leaks can be detected by viewing the Excel files of data recorded over long periods of time.

Traditional measurement and automation systems consist of expensive, closed instruments designed for specific tasks. Typically, one is forced to design a traditional system from the ground up and have an extensive knowledge of computer programming. In these traditional systems, the hardware defines the system. LabVIEW's graphical programming language provides an easy means for non-programmers to quickly design and implement complex test and measurement and

51

automation applications. With LabVIEW, the software defines the system, saving both valuable development time and resources.

A data acquisition card was required for connecting the signal from the pressure transducer. The card supplied by National Instruments was the PCI – 6023E. This is an input only card.

3.5.1 How To Program in LabVIEW

In order to understand how LabVIEW works it essential to know some of its basic concepts. The basic files created in LabVIEW are called Virtual Instruments, or VIs. Each VI consists of two main parts – the front panel and the block diagram, and a third part – the icon and connector.

The front panel contains the user interface of the VI. The image in figure 3.10 is an example of a front panel window.
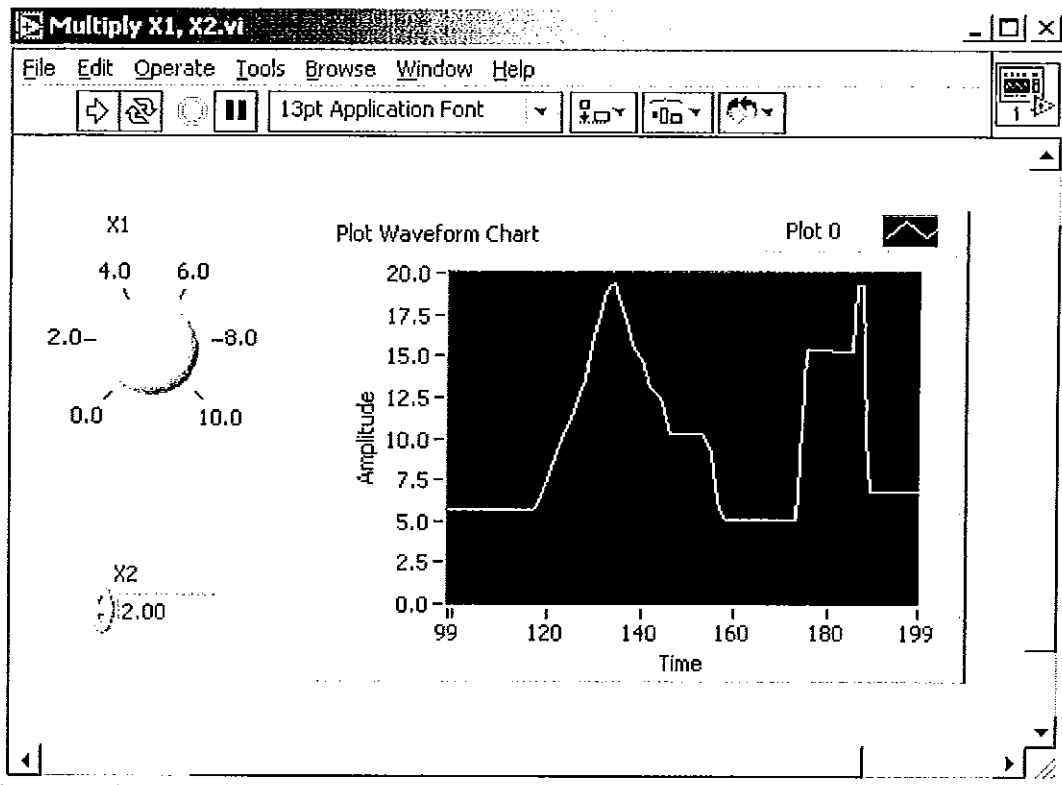
Figure 3.10: Typical Front Panel of a LabVIEW program or VI.

The block diagram contains the graphical code for the VI. The image in figure 3.11 is an example of a block diagram window. In this case the values assigned to X1 & X2 are multiplied every 400ms and plotted on a waveform chart. This happens N amount of times.

52
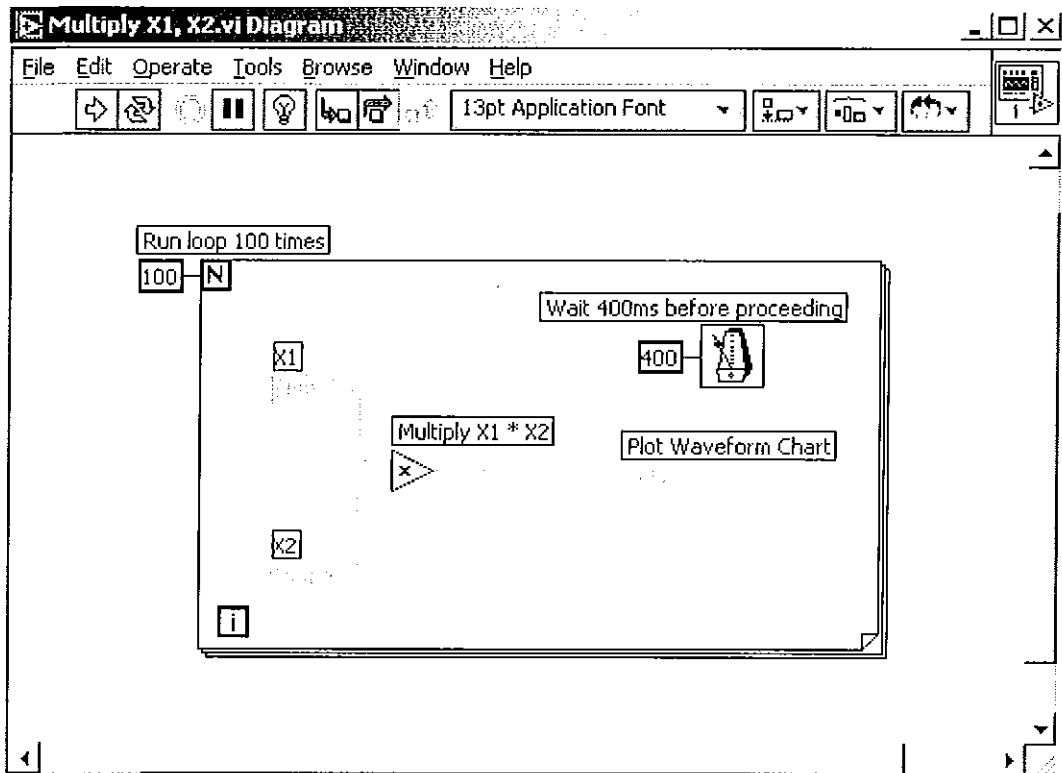
Figure 3.11: Typical Block Diagram of a LabVIEW program or VI.

The icon and connector of a VI are located in the upper-right corner of the front panel and block diagram window. The icon is what you see on the block diagram when you use a VI as a subVI.

Controls Palette: A front panel is built by placing controls and indicators from the controls palette. The controls palette can be seen along with the functions palette and tools palette in figure 3.12. Each palette icon represents a sub palette, which contains controls that can be placed on the front panel. A control is a front panel object that the user manipulates to interact with the VI. Simple examples of controls are buttons, slides, dials, and text boxes. An indicator is a front panel object that displays data to the user. Examples of indicators are graphs, thermometers, and gauges. When a control or indicator is placed on the front panel, a corresponding terminal is placed on the block diagram.

Functions Palette: A block diagram is built using the terminals from the front panel controls and indicators and the VIs, functions, and structures from the Functions

palette. Each palette icon represents a sub palette, which contains VIs and functions placed on the block diagram. The structures, functions, and VIs collectively known as nodes, on the Functions palette provide the functionality of the VI. As nodes are added to the block diagram, they are wired to each other and to the terminals from the front panel objects using the Wiring tool, found on the Tools palette. A complete block diagram appears similar to a flowchart.
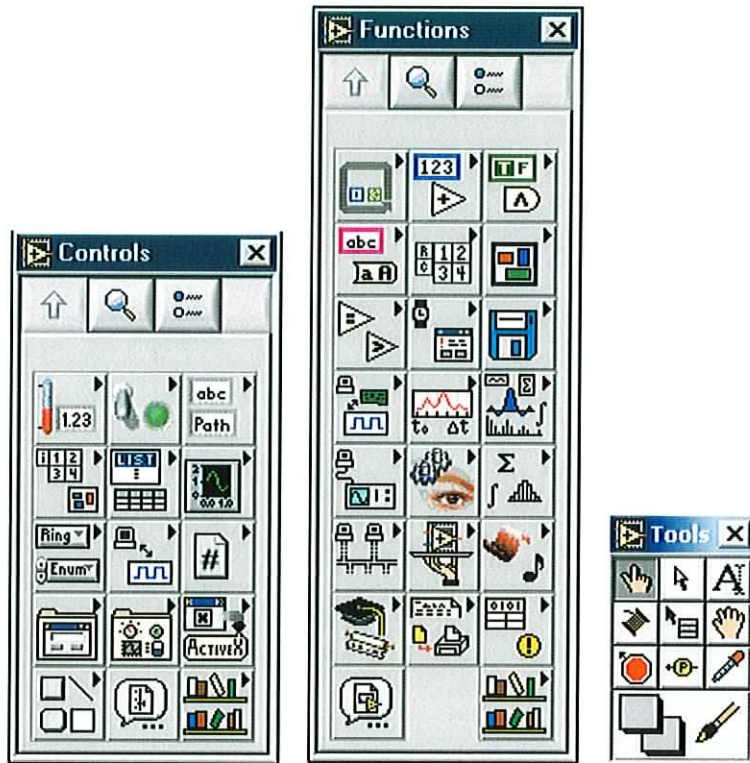
Figure 3.12: The Controls, Functions & Tools Palettes used in LabVIEW programming.

Traditional text-based programming, such as C++, relies on top-down design, where you must write lines of code that execute line by line. LabVIEW is based on graphical programming. You do not need an extensive knowledge of programming languages or programming techniques to create virtual instruments. Instead of top-down execution, LabVIEW operates on the concept of data flow.

3.5.2 Initial LabVIEW program

The first LabVIEW VI used was Breathing Waveform.vi. This VI shows the breathing activity of the patient as a waveform. As the patient breaths the breathing waveform is generated and displayed simultaneously. Therefore the patient can be

shown the waveform of their breathing activity as they breathe. Figure 3.13 shows the front panel of this program. The block diagrams for the VI's and their descriptions can be found in the appendices of this thesis. The waveform is varying initially according to how the person is breathing. A peak represents inhaling and a trough represents exhaling. When the patient holds their breath the wave should stay at the same level – horizontal. The breathing activity information is also stored as a text file: DATA.txt. This information can later be viewed and analysed.
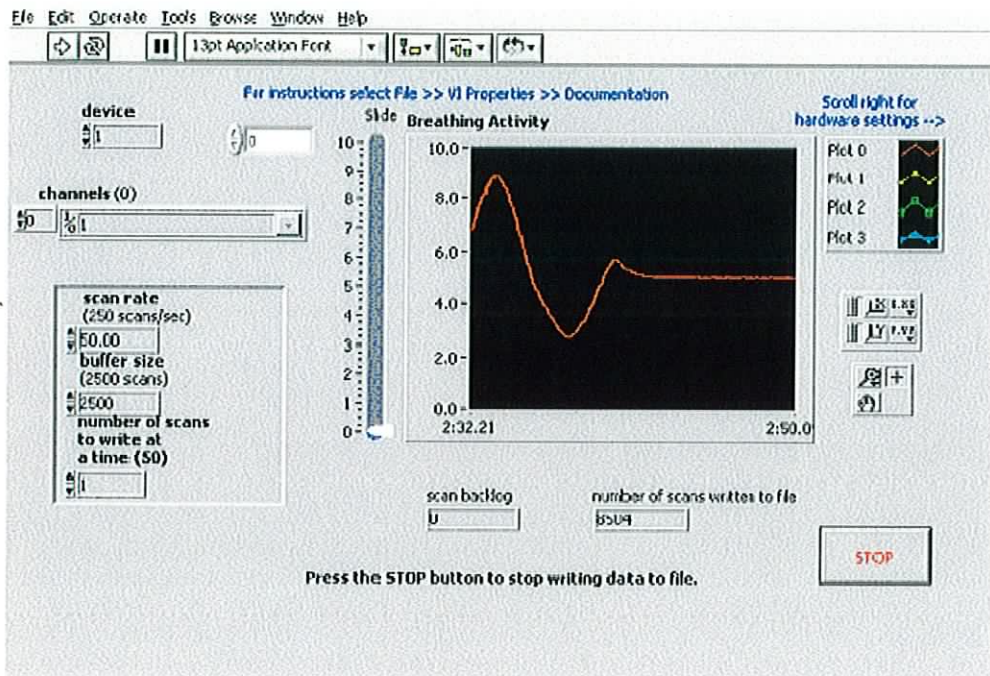
Figure 3.13: Front panel of the Breathing Waveform.vi program.

3.6 Overall Description of the Initial Prototype

The device uses a bladder or pressure coil, which is attached to the patient's waist and reflects the breathing cycle by monitoring changes in pressure inside the coil as the person inhales and exhales. A sensitive differential pressure transducer monitors these changes in pressure. The transducer has one port connected to the bladder and the other is left open to atmosphere, which is used as the reference. The transducer has an LCD display which gives a numerical display of pressure changes. This output can also be directed through a computer interface that allows for a larger on screen numerical as well as graphical display. The variable output voltage from the transducer is a 0-10Volts dc signal. This is directed to a bargraph display unit, to give a more visual display to the patient. It is also fed to the PC where computer software

(LabVIEW) translates the 0-10Volts into a waveform on the screen for an alternative form of display. Figure 3.14 shows the components used with the device.
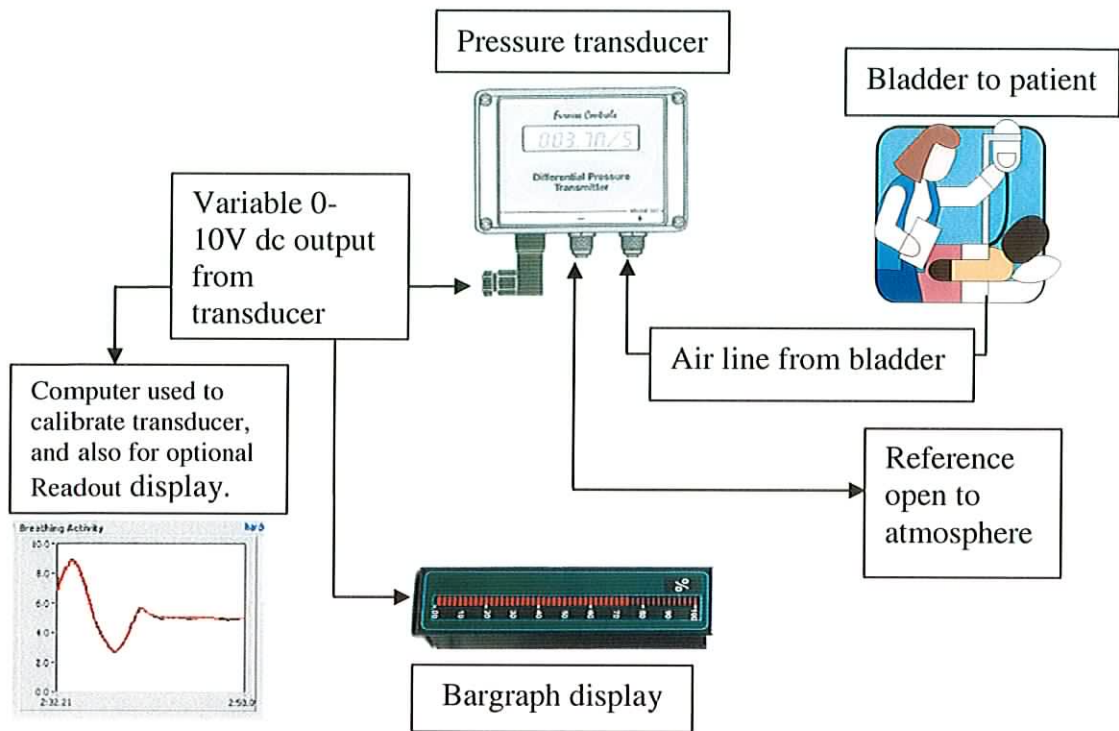
Figure 3.14: Device Schematic.

These components were housed in a simple wooden housing as shown in figure 3.15 and 3.16. This housing allowed easy access to the pressure transducer and the LED display. It also provided a mounting for the electrical and pneumatic connections to the device. A circuit diagram for the prototype can be seen in figure 3.17.
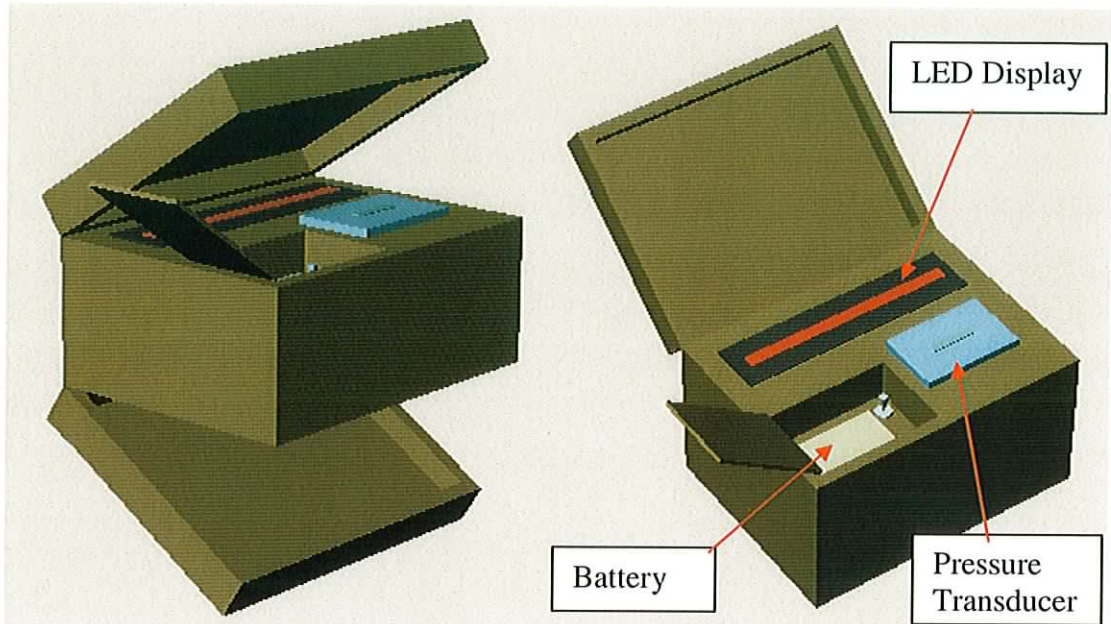
Figure 3.15: Sketch of the Initial Prototype – wooden box holds the electrical components of the device.
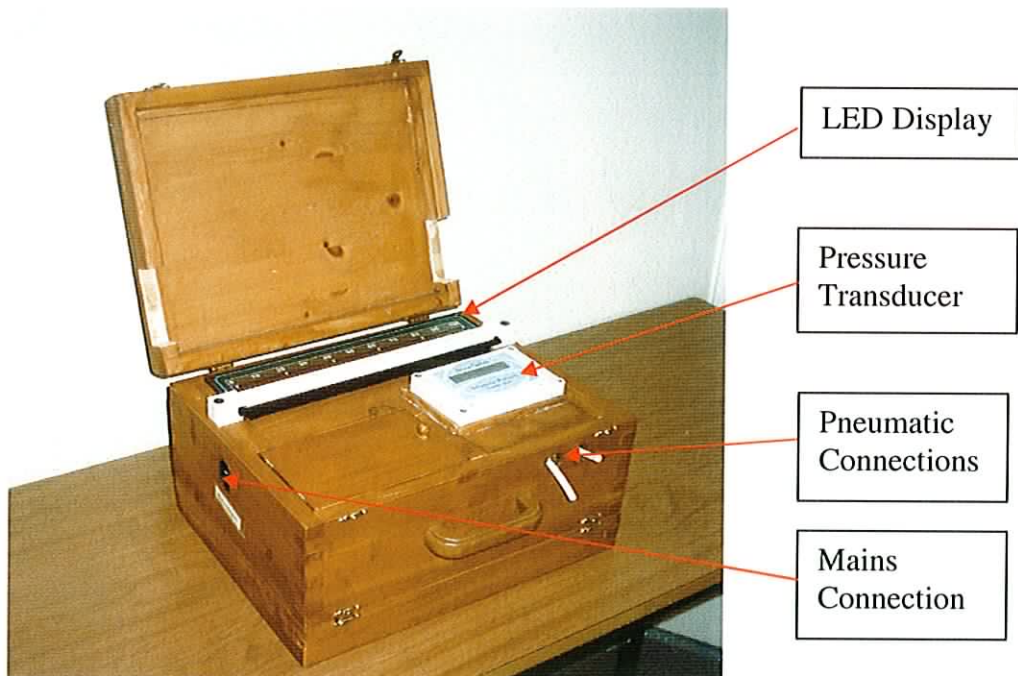
Figure 3.16: Photograph of the Initial prototype. Dimensions: 340x * 270y * 185z.
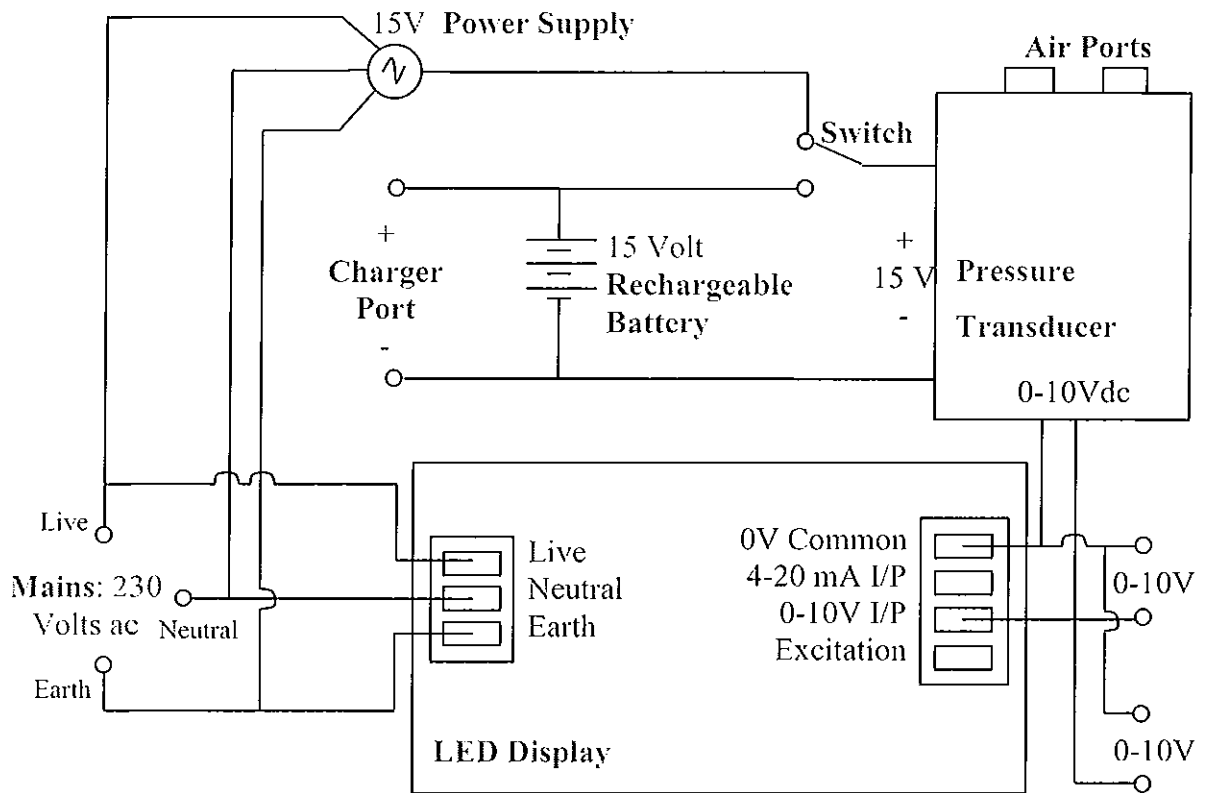
Figure 3.17: Wiring Diagram for the Initial Prototype.

3.7 Prototype Assessment

The initial prototype is a basic, working, offline version of a breath-monitoring device. With this basic prototype it was possible to develop the peripheral parts of the device such as the bladder and the feedback systems. However, in order to provide full justification for the research it was necessary to assess the prototype before progressing further. The testing of the prototype is described in detail in Chapter 9. The results from these tests proved that the prototype works and hence development of the mark 2 version and the feedback systems could commence.

3.8 Conclusion

This initial prototype, while crude, carried out the basic functions of breath monitoring. The same basic idea would be used in the final device. The wooden box was relatively cheap and simple to make but a more ergonomic design would be necessary to make the device marketable. From this basic working model it was established that breath monitoring with visual feedback did in fact improve a person's

ability to hold their breath. Using this prototype the feedback systems needed for use in the MRI environment were then developed while other designs were being manufactured. The feedback systems and the initial prototype were the basis for a paper written and presented at the International Manufacturing Conference in Queens University Belfast in August 2002 [48].

4   BLADDER DESIGN

4.1   Introduction

The initial prototype respiratory monitor used a pressure coil and pressure transducer to obtain the breathing information from the patient as described in Chapter 3. These types of pressure coils are already used in some MRI units for respiratory-triggering. They are however expensive devices and are prone to leaks due to their complex shape. The transducer with which they are designed to work is embedded within the scanner tunnel. The object of this research was to build a low-cost respiratory monitoring device that would work along side the MRI scanner. Therefore it was decided to create a less expensive bladder, better suited for breath holding and that was in no way connected to the scanner itself.

Development of the bladder has consisted of a number of different stages. Firstly the initial negative-pressure coil was used for the initial tests on the device. This was followed by a crude inflated positive pressure rubber design. Finally the no-inflated positive pressure bladder was developed. This was the bladder used in the final design and the field tests. Testing of the bladder and the connections for leaks was necessary at each stage. Because of the problems associated with the strong magnetic field in an MRI environment, it was decided to use solely rubber and plastic parts.

4.2   Initial Positive Pressure Design

The pressure coil used in the initial prototype worked on the basis of negative pressure. The transducer used in this device can work off positive or negative pressure so the option of a positive pressure bladder was available. The negative pressure coil works by extension of the coil in the longitudinal direction in a similar way to a bellows. This increases the volume inside the coil, decreasing the pressure. The coil is at atmospheric pressure when it is at rest and it then drops below this during extension, hence the term negative pressure. If a simple rubber tube is used instead of a coil then by squeezing the tube laterally the volume inside the tube decreases, increasing the pressure. In this case the pressure increases above atmospheric pressure, hence the term positive pressure.

As an initial positive pressure test a portion of a rubber bicycle tube was used as shown in figure 4.1. This was sealed at both ends using rubber bungs. The rubber

bungs had a diameter of 37mm compared with the tube rubber tube relaxed diameter of 30mm. Thus the tube was stretched over the bung and glued into place. This sealed the ends of the tube. A 5mm diameter hole was drilled through the centre of one of the bungs. A plastic reducer with an outer diameter of 8mm was then pressed and glued into this bung. A pipe was fed from the plastic reducer to the pressure transducer. The pipe used was a 6mm/4mm outer/inner diameter tube. The nozzle present on the bicycle tube can be used to inflate the tube to an increased pressure if required.
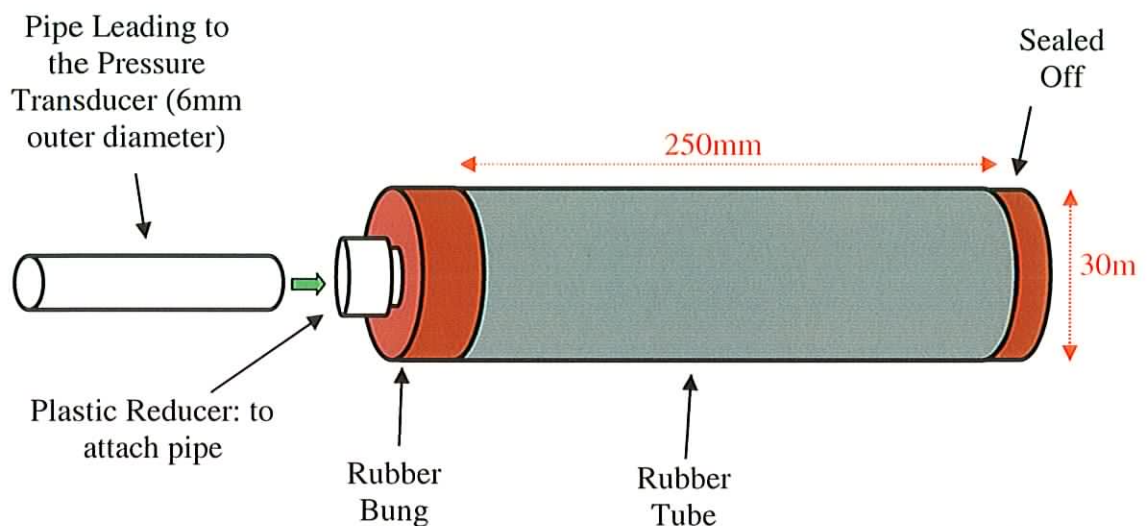
Figure 4.1: Crude initial design for the positive pressure bladder. Consists of a portion of bicycle tube with rubber bungs at either end.

The negative pressure coil was tied around the chest and was hence extended as the patient breathed. This positive pressure device cannot work in the same way. Instead a strap or plate is needed to compress the bladder. The compression leads to an increase in pressure. Thus a strap was made with a plastic plate as shown in figure 4.2. This strap is tied around the chest and the rubber bladder is placed underneath it. As the patient breathes in the gap between their chest and the plate decreases and the bladder becomes compressed. Thus a pressure change is registered on the pressure transducer and the patients breathing activity can be recorded.
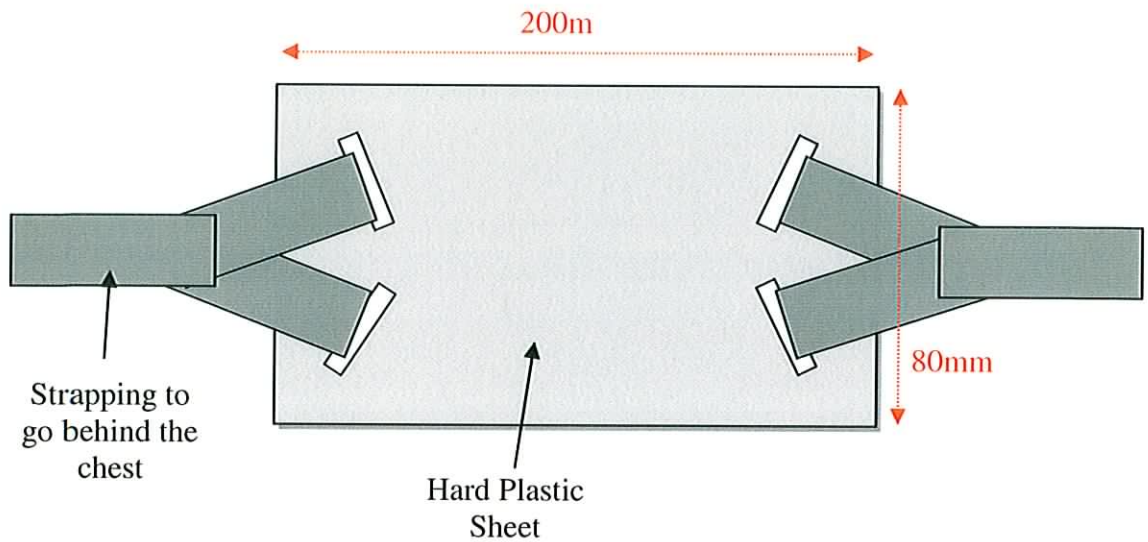
Figure 4.2: Nylon Strap and Perspex Plastic Back Plate for the crude initial design for the positive pressure bladder.

This was a crude design but it showed that the basic idea of the positive pressure bladder should work. Figure 4.3 shows the data from a series of nine breaths taken over approximately 30 seconds. The inspiration rate is approximately 1.3seconds with expiration at 2.0seconds. This is the breathing signal of a conscious patient in a state of relaxation. It is usual for the inspiration time to be about two thirds that of the expiration.
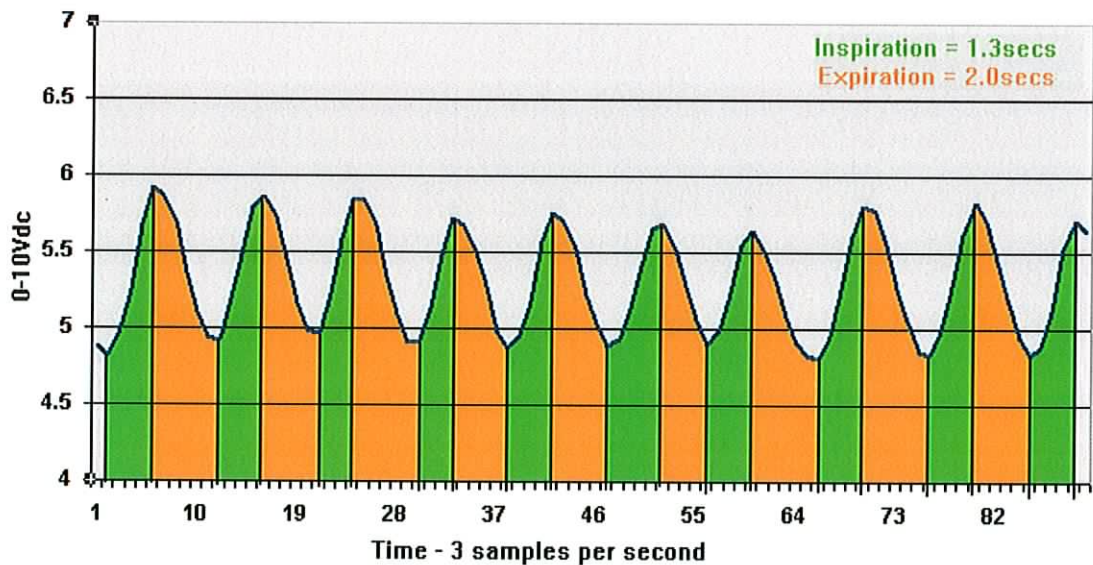
Figure 4.3: Normal breathing for 30seconds (9 breaths) using the initial positive pressure bladder. Voltage(0-10Vdc) versus time(data collected at 3 samples per sec).

Figure 4.4 shows the data from a typical breath hold. The region shaded yellow denotes the actual breath hold which lasts for 20seconds – 60samples at 3 samples per second. The large peak after the breath hold denotes a large inhalation after the breath hold.
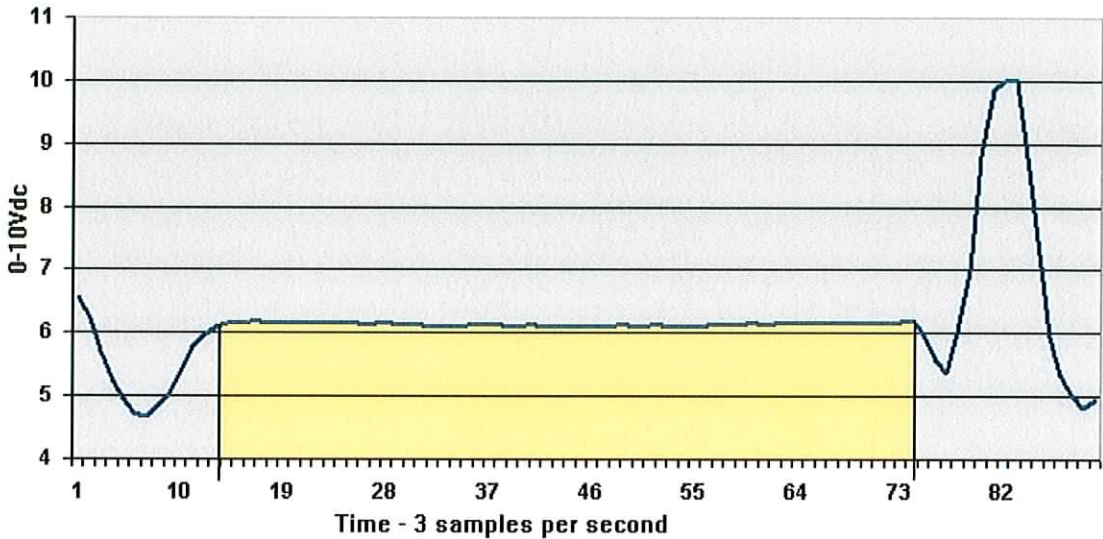
Figure 4.4: 20 second breath hold using the initial positive pressure bladder. Voltage(0-10Vdc) versus time(data collected at 3 samples per sec).

Figure 4.6 shows the same breath hold data as figure 4.4 except in more detail. The small fluctuations that can be seen are due to the beating of the heart. These are not of concern and cannot be seen on the larger scale waveform that the patient sees. The bargraph display acts as low-pass filter as such small fluctuations in the signal are not registered on the display. These fluctuations could be completely removed if necessary using electronic low-pass filters.

This does suggest a further possible use for this device however. If the sensitivity of the transducer is increased the device could also be used as a heart rate monitor. Figure 4.5 shows the results obtained when the sensitivity was increased. Each cycle shows a beating of the heart. The data shown was recorded at 10 samples per second. As there are 150 samples showing this is equivalent to a 15 second segment. Approximately 18 heart beats can be seen within this segment suggesting a heart rate of 4*18 = 72 heart beats per minute which is normal for a healthy adult at rest. A high pass filter could be used to block any undulation due to breathing to provide a smoother graph.
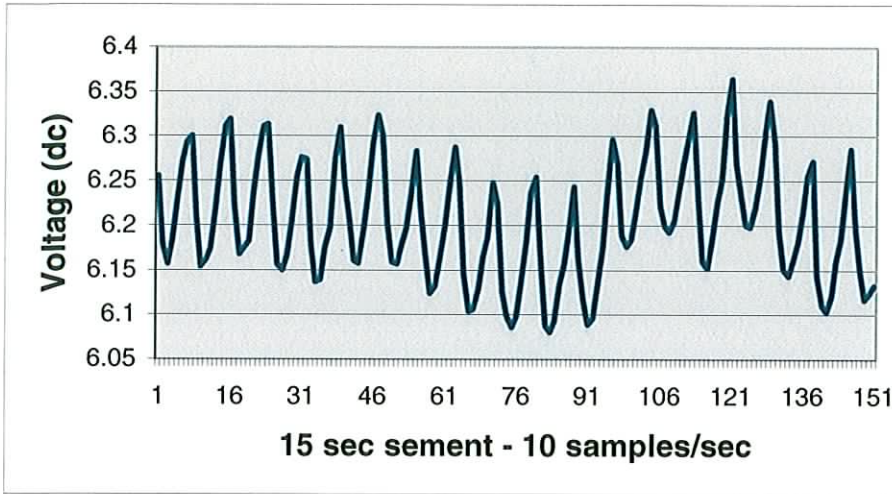
Figure 4.5: 15 second segment showing heart rate. Voltage (0-10Vdc) versus time. Heart rate is calculated as 18heart beats in 15 seconds = 72beats/min.

The signal shown in figure 4.6 shows fluctuations due to the heart beating but it fluctuates more slowly also. It does so over a region of approximately 0.1Vdc from 6.09V to 6.19V. With the system set up to show a full lung tidal volume over the 0-10Vdc this means that the patient has registered 1% of their possible movement due to breathing. The smaller this percentage is the better the breath hold is. Hence this system provides a way of monitoring a breath hold and thus it was decided to use this type of design.
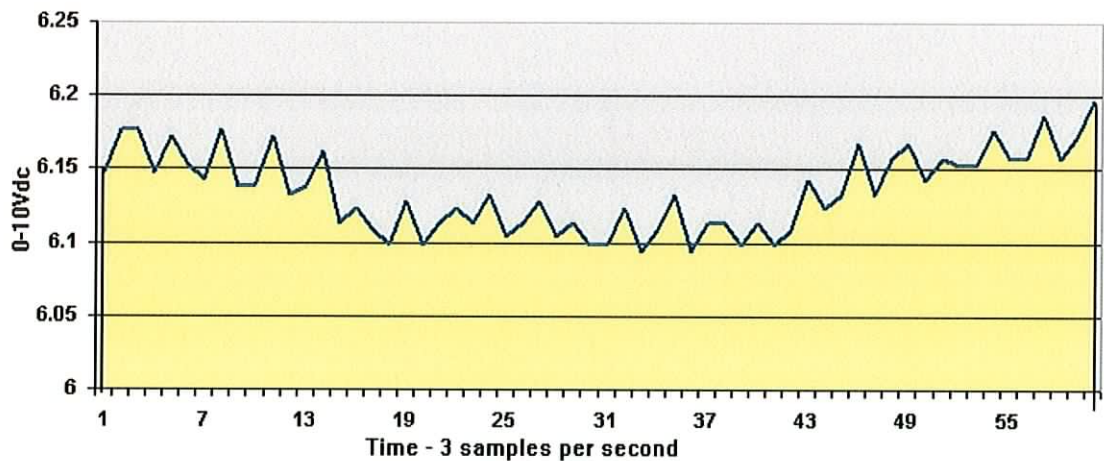
Figure 4.6: 20 second breath hold using the initial positive pressure bladder. Voltage(0-10Vdc) versus time(data collected at 3 samples per sec).

These results were compared with similar results from the negative pressure coil used in the initial prototype. The results from the coil can be seen in figure 4.7 and

4.8. From these figures it can be seen that a leak developed in the coil. The small fluctuations due to the beating of the heart are not as pronounced in this case as the coil extends as opposed to the rubber bladder that is compressed. With the bladder placed close to the position of the heart the beating from the heart is more pronounced. This should have little effect on the performance of the bladder however as these fluctuations are so small that they do not register on the LED display.
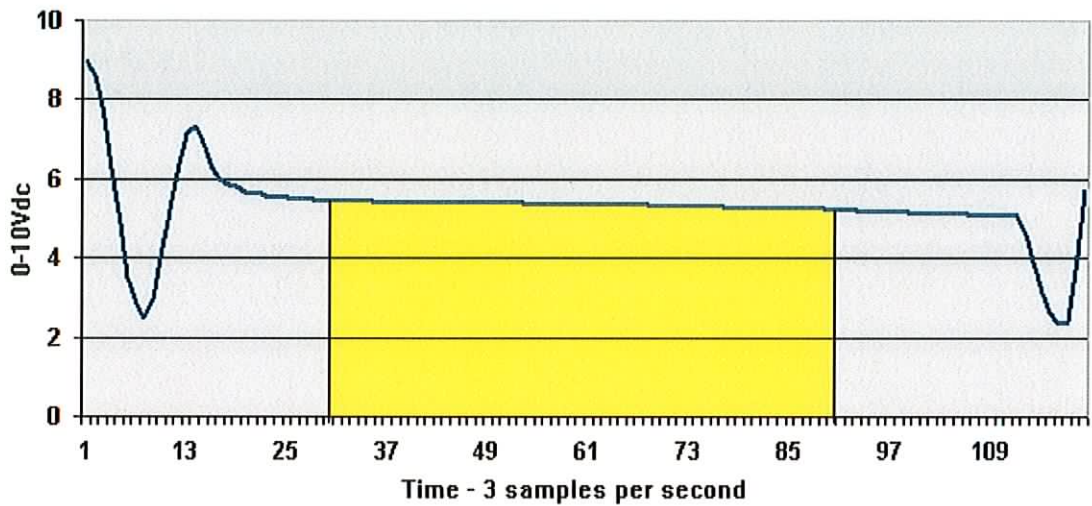
Figure 4.7: 20 second breath hold using the negative pressure coil. Voltage (0-10Vdc) versus time (data collected at 3 samples per sec).
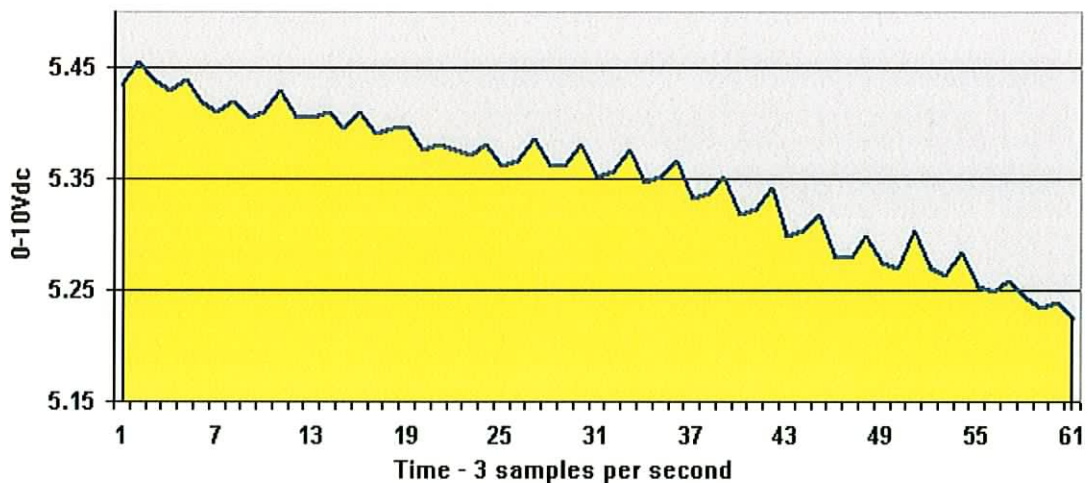
Figure 4.8: Magnified data from 20 second breath hold using the negative pressure coil.

While the bicycle tube design provided good results it was still a crude design that needed to be improved upon. The rigid back plate was prone to rocking and slipping. This was unacceptable as it could distort the results. The rubber bungs at either end of the tube were clumsy and did not allow the base plate to be placed over the entire device, as they were too large. This design was also made from a piece of bicycle tube that would not be acceptable in the professional environment of a hospital. Thus an improved design that was more user-friendly was required.

4.3   Improved Positive Pressure Design

To avoid the need for the bungs it was decided to glue the ends of the device and incorporate a length of tube from the bladder so that the whole bladder was one piece. This design was built by a company called Viking Extrusions based in the UK [48]. It was also decided to use a modified strap to hold the bladder and provide the platform against which pressure could be applied to it. This consisted of a broad nylon strap with a cotton holder for the bladder. The cotton holder situated between the nylon strap and the patient's chest holds the bladder in place. The strap itself, instead of the plastic back plate, provides the necessary pressure to register the breathing movements. A photograph of the bladder, strap and cotton holder can be seen in figure 4.9.

The nylon strap was used, as this is the same type of strap that is already used in MRI units to hold receiver coils around the patient during scanning. Cotton was chosen as the material for the holder as it is hypoallergenic meaning it doesn't irritate sensitive skin or cause allergies. Cotton is a natural product and does not contain any chemicals. Finally the bladder is made from medical grade silicone. These are the only parts of the device that come in contact with the patient; hence it was necessary to ensure that the materials used would not adversely affect the patient as well as the scanner.
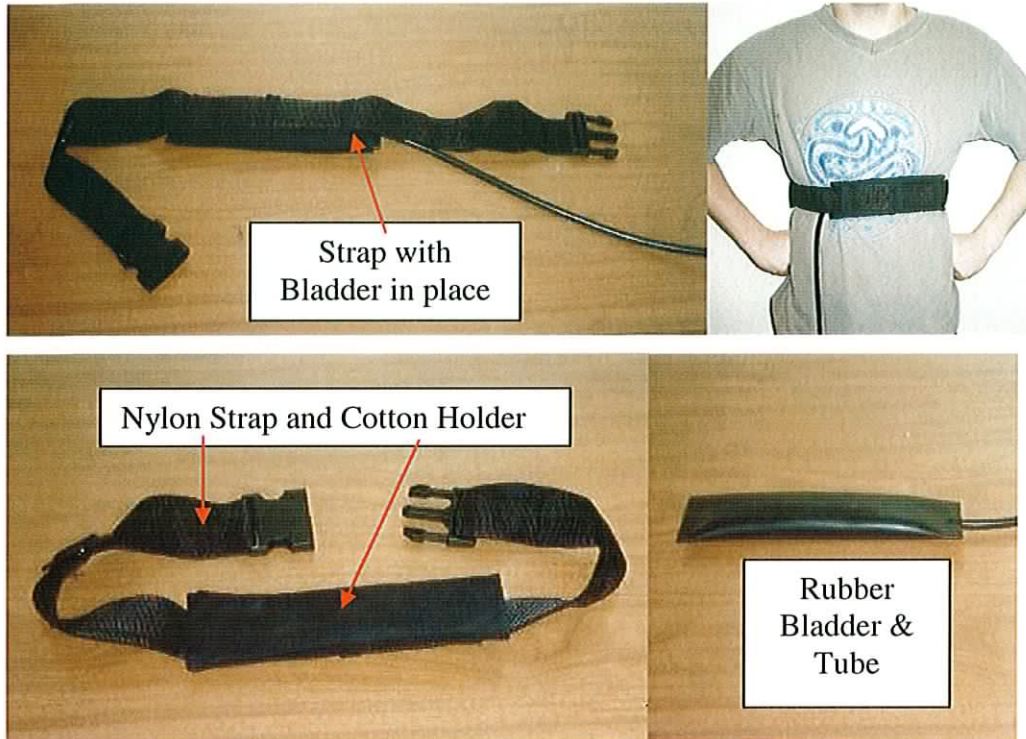
Figure 4.9: The Pressure Belt – This consists of the silicone bladder and the nylon strap and cotton holder. The strap is attached around the thoracic region and the bladder is held in place with the cotton holder.

The length of the strap can be easily adjusted to provide the correct pressure for each individual patient. When tied around the lower thoracic region the device should register the full tidal volume of the patient's lung over the 0-10Vdc range. Therefore the pressure transducer should read 10V (5kPa) at full inhalation and 0V (1kPa) at full exhalation. Figure 4.10 shows a 60second segment of breathing activity with a full inhalation and exhalation in the shaded area. There are 9 breath cycles in total during this period with expiration time slightly longer than inspiration.
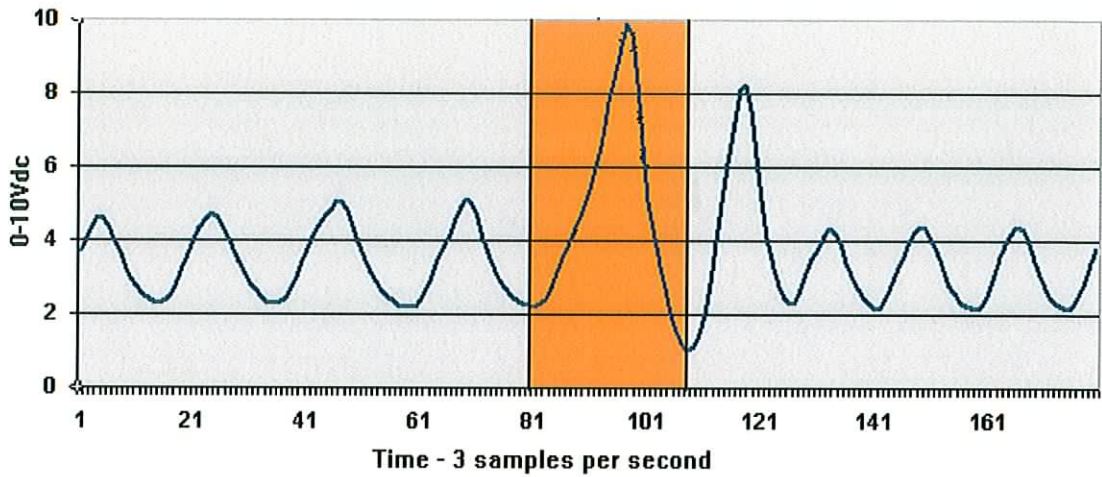
Figure 4.10: 60 second segment of breathing activity with a full inhalation and exhalation shown in the shaded area.

Figure 4.11 is similar to figure 4.4 except that this is a breath hold as recorded by the new bladder design. Again the breath hold is for 20 seconds (60samples at 3samples/sec) and is marked by the area shaded in yellow.
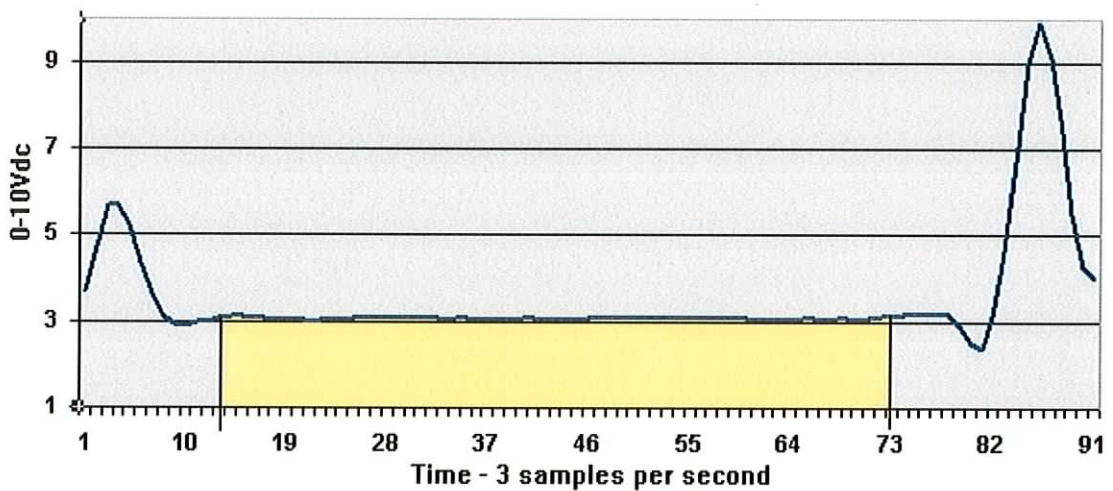
Figure 4.11: 20 second breath hold using the new positive pressure bladder design.

Figure 4.12 shows the same breath hold data as figure 4.11 except in more detail. Again the small fluctuations in the signal are due to the beating of the heart, which is filtered out when using the bargraph LED to display the data. The larger fluctuations, those that are spread over a longer period of time, are due to movement of the chest. These movements are over a range of approximately 1.3% of the total movement of the chest due to breathing. The peak during this period is 3.14V and the lowest point is 3.01V. Hence there is a fluctuation of 0.13V out of a possible 10V.

68
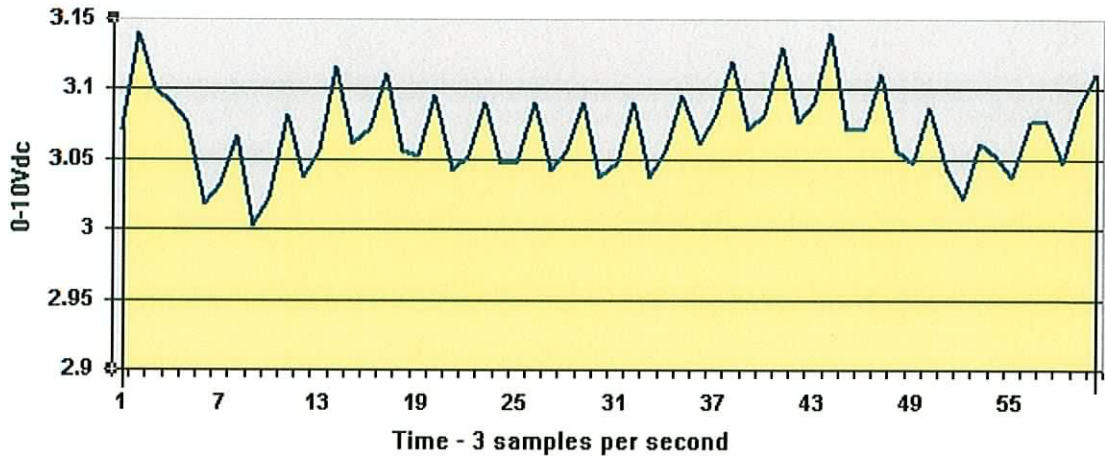
Figure 4.12: Magnified data from the 20 second breath hold using the new positive pressure bladder design.

4.4   Conclusion

The positive pressure bladder is a cheaper alternative to the pressure coil. The performances of both are very similar. However, the positive pressure bladder is less susceptible to perforation as there are no coils. It provides enough information about breathing activity to assess a breath hold thoroughly. The device has been tested in the MRI environment as discussed in the field tests in chapter 8. The materials used are all MRI compatible and are in line with the Medical Devices Directive (90/385/EEC) as discussed in chapter 7.

5   Audio Feedback

5.1   Introduction

Audio feedback is a method by which an audio signal is transmitted back to the patient to inform them of their breathing performance. By varying a property of an audio signal the patient can distinguish where in the breathing cycle they are and if they are holding their breath correctly. With this information available to them they should be able to perform the breath-hold techniques used in MRI scanning to better effect. There are a number of factors that are important in determining how best to relate the information to the patient. These include how to transmit the signal to the patient and what property of the signal to vary.

Most MRI scanners come with their own sound system. This consists of a radio/compact-disc player and microphone, which are stationed outside the MRI room and a system for transporting the music/commands into the room to the patient. This system uses air tubes down which the sound travels to a headpiece attached to the scanner. The plastic air tubes do not affect the scanning procedure, as they are invisible to magnetic radiation. There is also a loud speaker in place in the room, which can be used when it is impossible to use the headphones. As this system for transporting sound to the patient is already in place, it was considered for development to provide an audio feedback for this breath-monitoring device. A number of possibilities were explored. One method was to vary the volume or voltage of a signal or tone relative to the 0-10Volts dc provided by the pressure transducer. Another method is to vary the frequency of a tone relative to the 0-10Volts dc. So, as the patient breathes in, they will hear an increase in volume/frequency of the tone and, as they breathe out, they will hear a decrease in volume/frequency of the tone. When they hold their breath they will hear a tone with constant volume/frequency.

5.2   Volume Control

In order to test the volume theory a personal stereo was used. The volume control used in most stereos is simply a variable resistor. This variable resistor provides a voltage, which determines the volume of the output. If the resistor is bypassed and the 0-10Volts is used as the voltage controlling the volume of the output then the breathing information can be passed onto the patient. The system is summarised in figure 5.1.

70

The voltage supplied by the resistor to the audio output in this case is between 0 and 1.5Volts supplied by a 1.5Volt battery. However a sufficient audio range is provided by 0 – 0.5Volts. Hence a simple voltage divider was used to transform the 0 – 10Volts signal into a 0 – 0.5Volts signal. The divider was constructed from a simple two-resistor circuit as shown in figure 5.1. The resistor values chosen to provide the required potential drop were R_1=22kΩ and R_2=1.2kΩ. Hence as the stereo plays a tone of constant frequency the volume of the tone will increase and decrease as the patient breathes in and out.

Voltage Transducer | Potential Divider | Volume control | Sound System | Audio Output

R_1 R_2
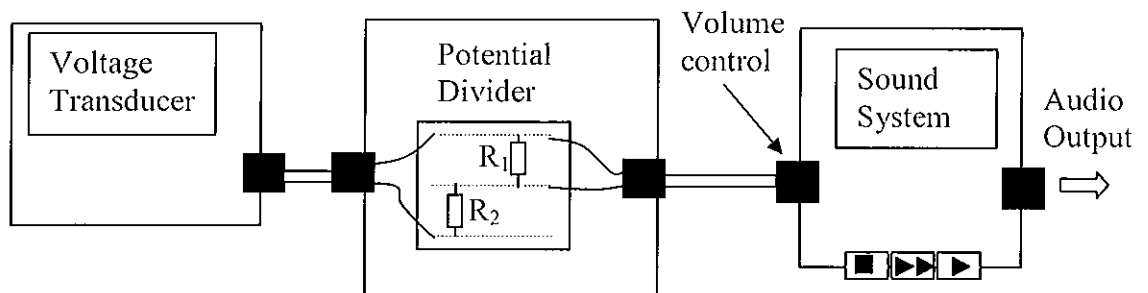
Figure 5.1: The Sound System used to convey the 0-10Volts to the patient.

While this is a novel idea that could work under the right circumstances it is not very suitable for use in the MRI environment. The MRI scanner produces high levels of audio noise. The noise to the patient can peak at 100dBa with the most powerful gradient type and the most rigorous sequences. Typical values would be 88dBa. Because of these high levels of noise the volume control feedback method is not the most desirable. The difference in noise levels between the area where the patient is trained and the MRI room itself will cause difficulties for the patient. Volume is relative by nature and the volume of a tone in a room with no noise may seem higher than in a room with such high levels of noise as the MRI room. The noise within the scanner can vary also. The scanners tend to make a banging noise as the gradient is switched on and off. Trying to hold a tone at constant volume under such circumstances is practically impossible. Although attempts are being made at reducing the noise levels of the scanner it is thought that this type of audio feedback will not be used.

5.3 Frequency Control

The second form of audio feedback varies the frequency of a tone relative to the 0 –10Volts dc output from the transducer. The patient hears a change in pitch as they breath in and out. Frequency/Pitch has the benefit of being unaffected by noise levels. Two methods of feedback have been used to vary the frequency – through hardware and software.

5.3.1 Software Frequency Control

As the LabVIEW Software was already being used to display the breathing activity as a waveform it was decided to use this software to vary the pitch of a tone also. The program used to produce the breathing activity waveform was extended to incorporate this function in the Breathing & Sine Waveforms.vi. The front panel of this vi can be seen in figure 5.2. The diagram for the vi is contained in the appendices of this thesis. The tone is produced by the software and passed to the sound card of the computer. It can then be heard via speakers or headphones. This tone can then be transmitted to the patient through the audio system already in place in the MRI room.

The tone that is created is basically a sine wave whose frequency varies according to the information received. The sine wave produced by this method is a clear tone. It has excellent timbre as its shape is smooth and sinusoidal and the frequency transition is smooth and constant. This will allow the patient to detect the correct frequencies with greater accuracy.

As the frequency of this sine wave increases the pitch of the tone increases. The 0 – 10Volt dc output from the transducer controls the frequency. The frequency can also be scaled up or down by scaling the 0 – 10Volts dc. The sine wave is plotted as a waveform so that the change in frequency can be viewed also. Figure 5.3 shows the sine waveform for a number of different voltages. The frequency increases with the voltage.

Upper and lower limits can be placed on the system so that if the patient fails to hold their breath correctly a warning light can be seen. A warning buzzer can also be added. This would be distinguishable from the audio feedback tone as it is a buzzing sound as opposed to a smooth tone of varying frequency. The front panel of the program that has been developed can be seen in figure 5.2. This is what the radiologist in the online situation and both the patient and the radiologist in the offline situation view.

72
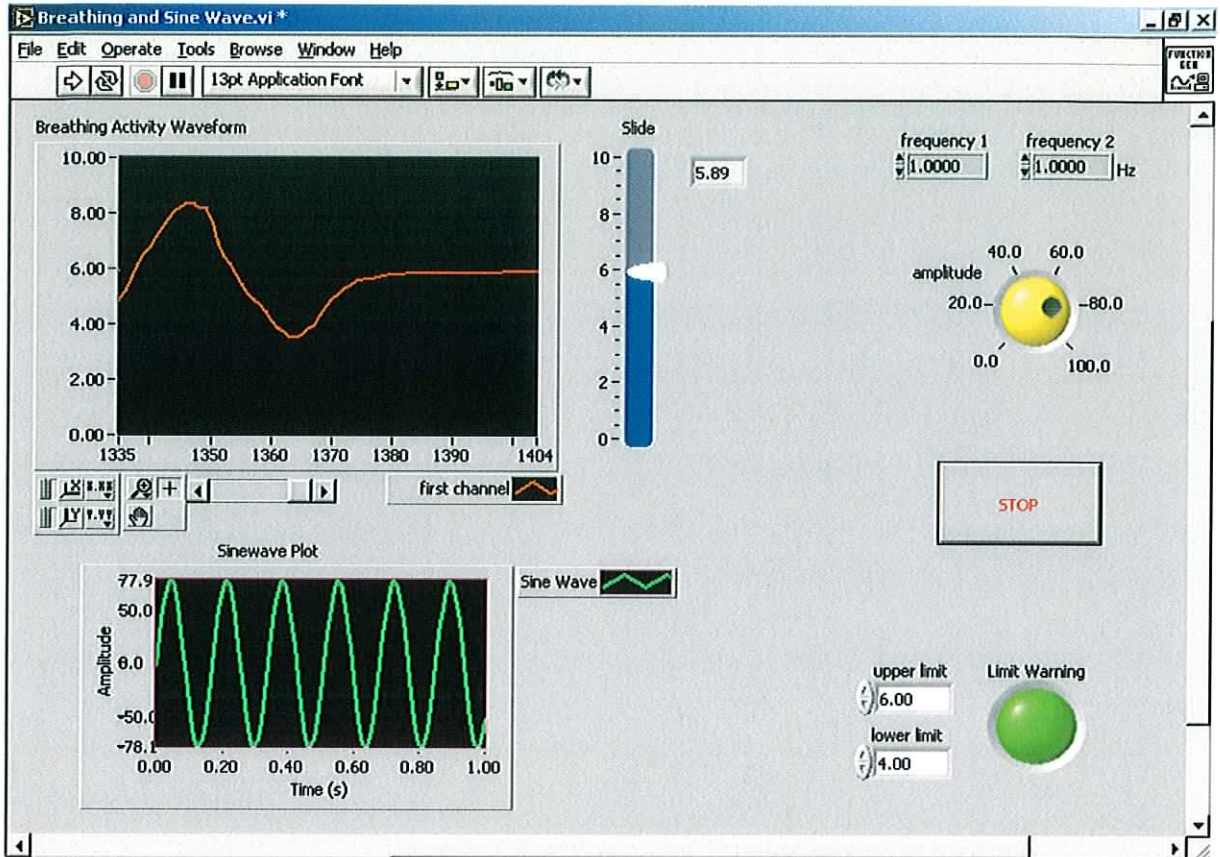
Figure 5.2: Front Panel of LabVIEW Program showing Breathing Activity and Sine Waveform Graphs. The Breathing Activity Waveform shows Voltage (0-10Volts) versus time (secs).

The input voltage from the pressure transducer determines the frequency of the tone. The voltage value is read in by the LabVIEW vi and Normalised for a value of 100Hz. This value is then used as the input to the Sine Wave.vi, which creates the sine wave. This vi uses equation {5.1} to produce the sine wave.

$$y_i = a * \sin(phase[i]) \quad \text{for i} = 0,1,\ldots\ldots\ldots\ldots\ldots\ldots.n\text{-}1. \qquad \{5.1\}$$

where

$$phase[i] = \text{initial phase} + f * 360 * i \qquad \{5.2\}$$

initial phase is set to 0 on the front panel

a = amplitude, set on the front panel

$$f = \text{normalised frequency} = \frac{InputVoltage}{100Hz}$$

Figure 5.3a, 5.3b, and 5.3c show the normalised frequency for input voltages of 1V, 4V and 8V consecutively. The amplitude in each case was set to 78.2. This is only a scaling factor.
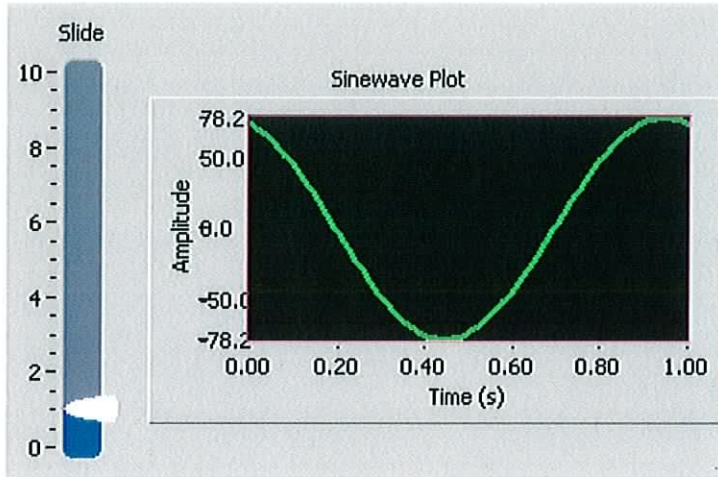
Figure 5.3a: Sine Waveform as shown on the Front Panel. The waveform is plotted over a one second interval for normalised frequency. This corresponds to a 1Vdc input from the pressure transducer and creates a signal of frequency 441Hz.
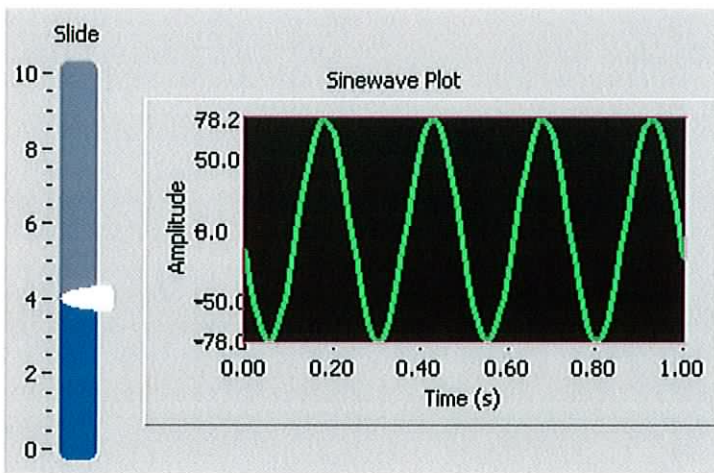
Figure 5.3b: Sine Waveform as shown on the Front Panel. This corresponds to a 4Vdc input from the pressure transducer and creates a signal of frequency 1764Hz.
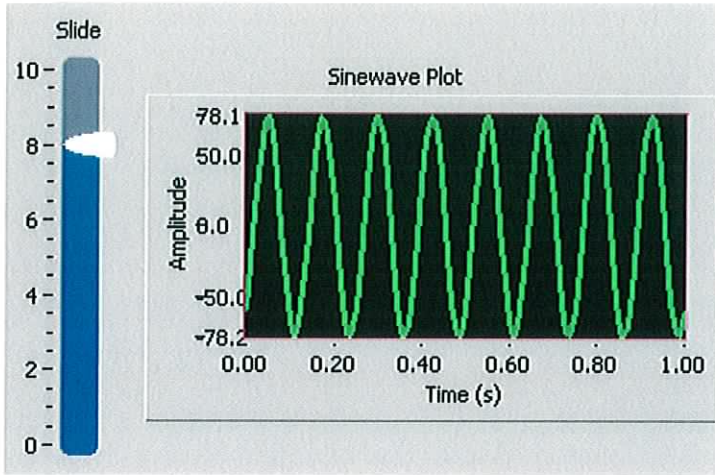
Figure 5.3c: Sine Waveform as shown on the Front Panel. This corresponds to a 4Vdc input from the pressure transducer and creates a signal of frequency 3528Hz.

The number of samples outputted by Sine Wave.vi is set to 4410 on the front panel. This figure was chosen, as it is a scaled down value of the playing rate used in the sound format that the sound card uses to play the tone. The number of cycles per 4410 samples can be calculated. The sine waveform generated by Sine Wave.vi is then sent to Sound Write.vi. As the sound format for the sound card is set at a rate of 44100 (10 times greater than the amount of samples used in Sine Wave.vi) the number of cycles per second (output frequency) will be 10 times the number of cycles per 4410 samples. The calculations are shown in Table 5.1.

Input Voltage (Vdc)	Normalised Freq (Cycles/Sample)	Cycles/4410samples	Output Frequency
1	0.01	44.1	441
2	0.02	88.2	882
3	0.03	132.3	1323
4	0.04	176.4	1764
5	0.05	220.5	2205
6	0.06	264.6	2646
7	0.07	308.7	3087
8	0.08	352.8	3528
9	0.09	396.9	3969
10	0.1	441	4410

Table 5.1: Conversion of the input voltage to the output frequency.

Table 5.2 compares these values to those of some well-known frequencies. The scale of the output frequency in this case is very similar to that of a piano. This was chosen as it provides a broad range with which to distinguish between frequencies and is well within the limits of human hearing.

Source	Lowest Frequency (Hz)	Highest Frequency (Hz)
Software signals	0	4,410
Hardware signals	0	4,000
Piano	27.5	4,186
Female speech	140	500
Male speech	80	240
Compact disc	0	22,050
Human hearing	20	20,000

Table 5.2: Software signal frequencies compared with some well-known frequencies.

5.3.2 Hardware Frequency Control

This method is based on the same principle as the software frequency control method but done through hardware. The 0 – 10 Volt dc output from the pressure transducer is sent to circuit that operates as a voltage-to-frequency converter using an LM331N chip. A company called National Semiconductor supplies this chip. The chip itself is an amplifier specific to voltage-to-frequency conversion. The datasheets accompanying the chip provide schematics of typical applications including a stand alone voltage-to-frequency converter. The schematic for this was altered to provide a circuit that would produce the frequency required.

The chip was placed on a small piece of circuit board to which the resistors and capacitors were then also soldered. A circuit diagram for the board can be seen in figure 5.6. A 9 Volt battery powers the board. The battery and the circuit board are encased in an electronic black box. A dc plug socket was inserted into the box to provide a port for the input from the pressure transducer. A second socket was also placed in the box for the output. This is for a stereo plug that can either be used to connect earphones directly to the box or alternatively it can be connected to the computer. An on/off switch was also attached to the box, which cuts off the power so

as not to waste the battery. A sketch of the plastic box to house the circuit board can be seen in figure 5.4. A photograph of the box showing the circuit can be seen in figure 5.5.
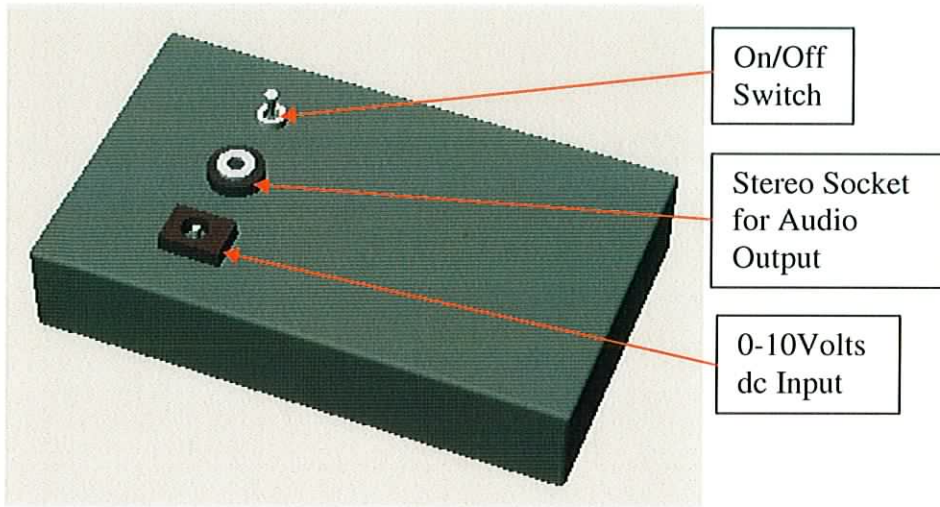
Figure 5.4: Plastic box for housing the hardware feedback system circuit board.
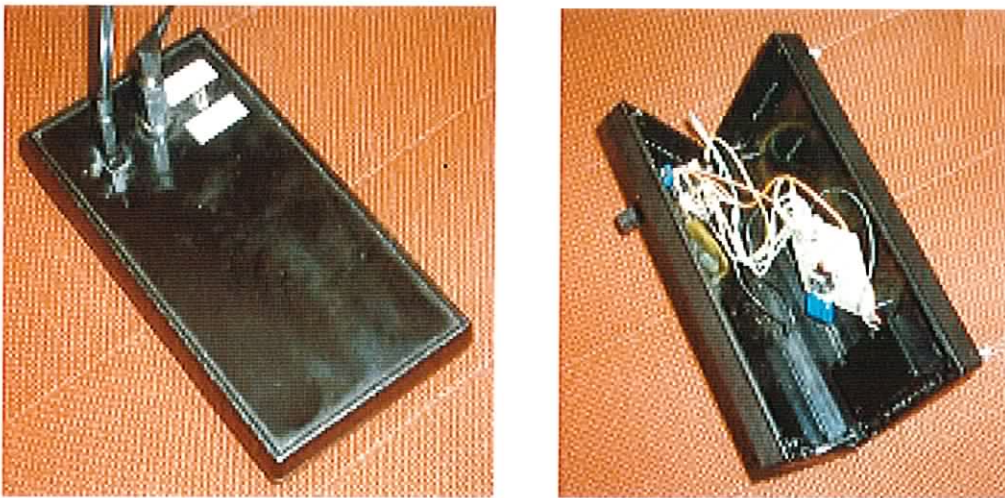
Figure 5.5: Photograph of the plastic box showing the circuit board.

The output signal is an approximate square wave. As in the software case, as the voltage level from the transducer increases/decreases the frequency of the output tone increases/decreases.

R_{IN}=100kΩ, C_{IN}=0.1μF, R_t=6.8kΩ, C_t=0.01μF, R_L=500kΩ, C_L=1μF, R_X=47kΩ, R_S=28kΩ.
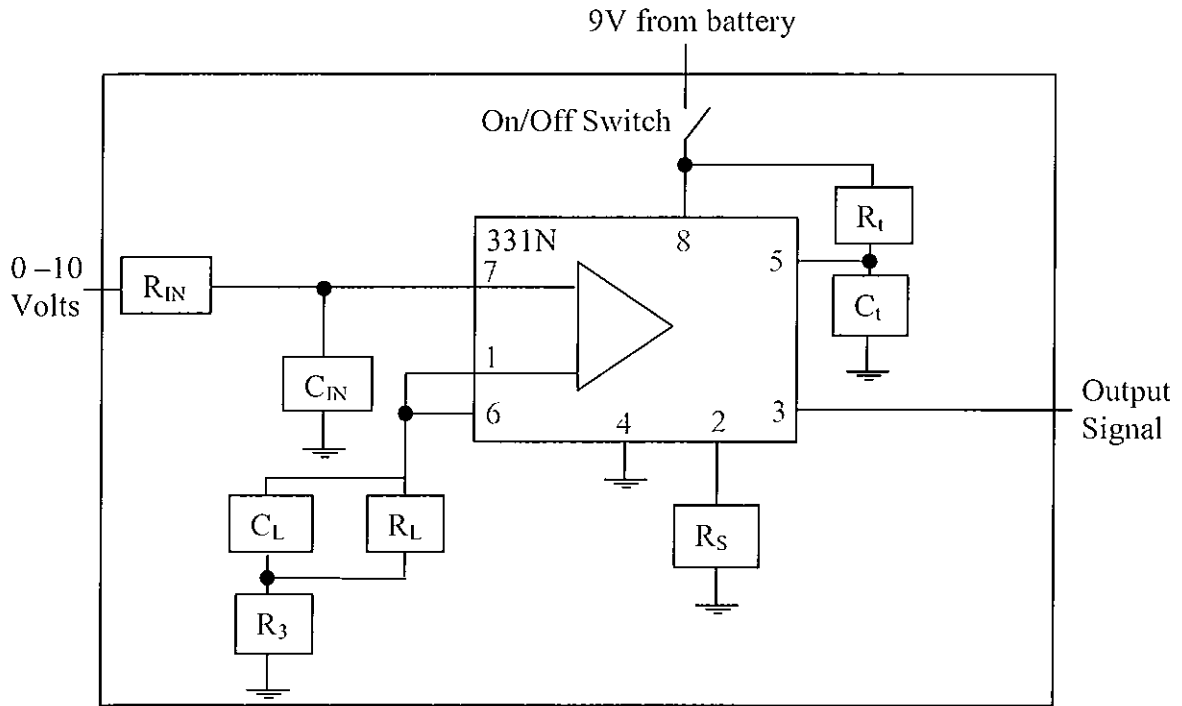
Figure 5.6: Voltage to Frequency converter circuit.

The original circuit, by National Semiconductor, from which this was created, accepted a 0-10Vdc input and provided a 10kHz full-scale output. Equation {5.1} is the equation given by National Semiconductor to calculate the output frequency.

$$f_{OUT} = \frac{V_{IN}}{2.09V} \times \frac{R_S}{R_L} \times \frac{1}{R_t C_t}$$
{5.1}

where, V_{IN} = 0-10Vdc

The same resistor and capacitor values were used in both circuits except for the source resistance, R_S, and the load resistance, R_L. By changing these values it was possible to vary the output frequency values. The values used in the National Semiconductor example were R_S=14kΩ and R_L=100kΩ. Using these values provided a full-scale frequency of 10kHz. It was decided that an output frequency of 4kHz was appropriate for this application as this is within an easily audible range for the human while allowing enough variation for distinguishing between frequencies. To obtain a full-scale frequency of 4kHz these values were changed to R_S=28kΩ and R_L=500kΩ. This effectively changes the initial equation by a factor of 0.4. There were other

78

effects of changing these values. The current discharged through the load resistance R_L affects the triggering of the circuit. By increasing R_L the triggering of the circuit will be slowed. R_S alters the gain of the amplifier. This effectively alters the volume of the output. Changing the values did not alter the operation of the device in an adverse way. It did however produce the required 0 - 4kHz output tone required.

5.3.3 Comparing of the Hardware and Software Methods

With two methods of providing the audio signal for audio feedback it is necessary to carry out a comparison to determine which of the methods produces the best signal. Both methods should produce signals of similar frequency but the quality of the signal may vary. This may be a determining factor as to which method may be used in the online environment. The better the quality of the signal produced the easier it will be for the patient to distinguish between frequencies, hence improving the overall operation. Other factors such as which method is easiest to produce may also be of consideration. For example, in the offline situation there may be no access to a computer, which is necessary to produce the software signal. Therefore in this case the hardware method would be the preferred method.

In order to carry out some comparisons between the tones produced by the hardware and software methods it is necessary to understand a number of simple properties of tones. A tone can be described using three different properties; amplitude, frequency and timbre.

The amplitude determines the volume of the tone. It is determined by the distance of the sound wave above and below its own centreline. The centreline is the horizontal line in figure 5.7 below. The vertical arrows denote amplitude. Simply stated, the larger the distance above and below the line the louder the sound.
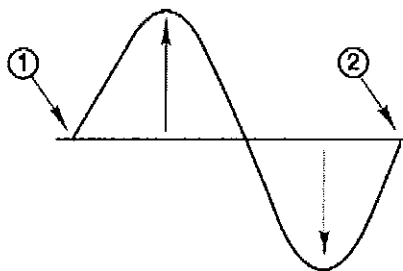
Figure 5.7: Sinewave showing Amplitude (arrows) and Period (time between point 1 and 2.

The second property is frequency. This is measured in Hertz, which is calculated as how many cycles per second the wave goes through. One cycle is the part of the wave shown between numbers 1 and 2 in the figure 5.7. This measurement can be taken anywhere in the wave as long as the measurements are taken at the stage in the wave cycle. The number of times this happens in one second is the frequency of the wave. The more cycles per second the higher the sound. So frequency is related to pitch. Every musical note, for instance, has a related hertz value.

Timbre is the quality of sound that makes different signals sound different even if they have the same period and volume. Timbre is related to the shape of the cycle. Although there are infinitely many different timbres (since there are infinitely many shapes for the cycles), timbre can be described using words such as "purer" or more "complex." Pure is a sound close to a pure tone, which has a cycle shaped like a sine wave. Complex is having oscillations with many other frequencies present.

In order to compare them the signals from both methods were first recorded at constant frequency using a LabVIEW program. This program takes in the sound signal through the computers sound card and then shows the time waveform and power spectrum of the signal. It also outputs the frequency, phase and amplitude of the signal to an excel file. The signals used were taken in steps of 1V from 0 – 10Vdc from the pressure transmitter using both the hardware and software methods.

At 0V no identifiable signal was found. This is because no signal is being produced. As the frequencies were increased from 0V a signal began to appear. Both methods produced signals of similar frequency but the shape of the signals was quite different, particularly in the lower frequency range. In figure 5.8a and 5.8b the signals from the hardware and the software methods can be seen for a voltage of 4Vdc. It is clear immediately that the timbre of the hardware signal is less pure than that of the software signal. That is, the software signal is close to a perfect sine waveform but the hardware signal is closer to a square wave. This means that the software signal will sound better, or more pure, than the hardware signal. Essentially the hardware signal will sound more broken, or less smooth than the software signal. The rippling effect on the maxima of the hardware signal is most likely due to transients in the circuit. These may have been exaggerated by changing the values of the R_S and R_L resistors. From figure 5.8 it can also be seen that the frequency of both methods are approximately the same.
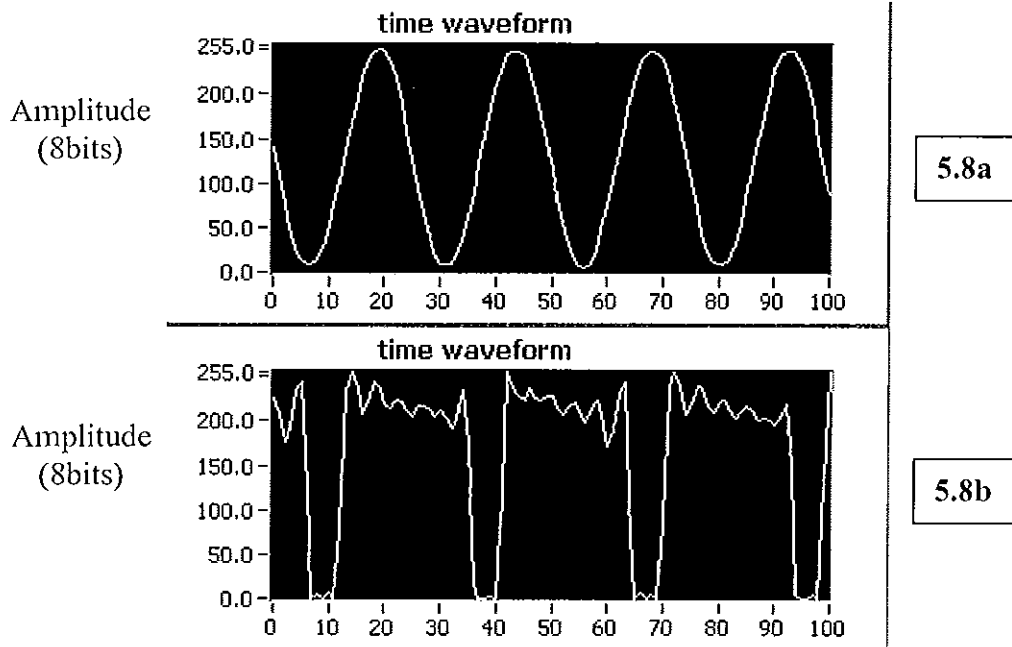
Figure 5.8a, 5.8b: The software (5.8a) and hardware (5.8b) signals produced at 4V from the pressure transmitter. Software Frequency ≃ 1760Hz. Hardware Frequency ≃ 1500Hz. The y-axis shows the normalised frequency of each signal.

Figure's 5.9a and 5.9b show the hardware signal at 4V (1500kHz) and 10V (4000Hz) respectively. From this it can be seen that at higher frequencies the hardware signal begins to form a more sinusoidal type of signal. The maxima and minima are of similar duration at higher frequencies. This will cause the hardware signal at higher frequencies to sound smoother than that at lower frequencies.
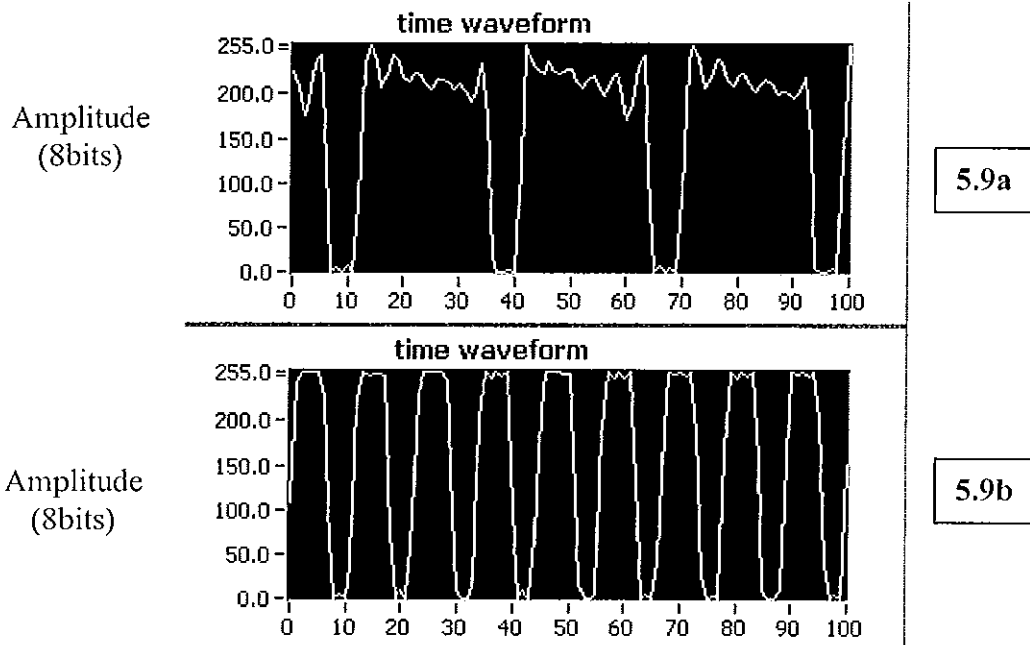
Figure 5.9a, 5.9b: The hardware signals produced at 4V (1500Hz) and 10V (4kHz) consecutively from the pressure transmitter. The y-axis shows 100 samples of each signal (approx 2.27msec).

Figure 5.10 shows the frequency versus voltage plots for both methods. The frequencies produced by both methods are similar. Both are operating within the same frequency range, which is well within the limits of human hearing capabilities. Both methods produce close to a straight-line graph, as the frequency increases uniformly with voltage. The frequencies produced by the software method are slightly higher than those produced by the hardware method.
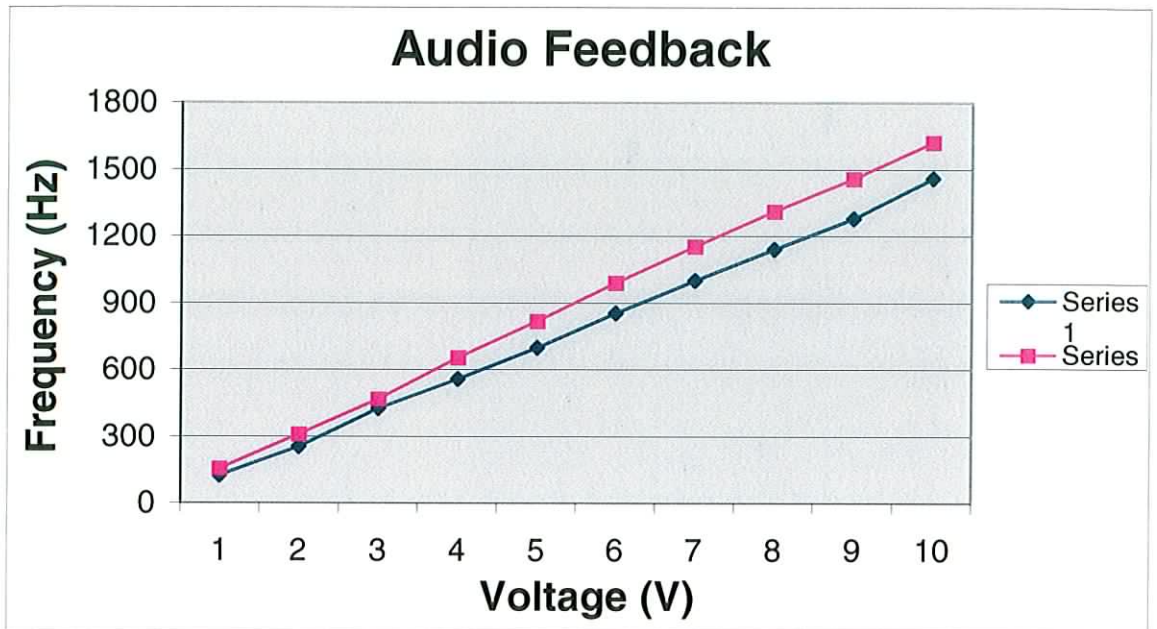
Figure 5.10: Frequency vs. Voltage graph for the Hardware (Series1) and Software (Series2) methods of audio feedback.

5.4 Conclusion

As a result of this analysis it is intended that the software frequency control shall be the method used for audio feedback especially in the online situation. The software method produces a smoother and hence clearer tone. The hardware frequency control method can be used for the offline situation if a computer is not available. The hardware that produces the signal is contained in a separate housing to the rest of the main device. This could be incorporated into the main housing if necessary.

While the audio feedback method will be beneficial to those with visual impairments it is thought however that a visual form of feedback will provide the patient with a more simple and clear understanding of their breathing activity.

6   VISUAL FEEDBACK

6.1   Introduction

The main objective of this research is to design and develop a device which can be used to teach patients how to hold their breath and also to provide them with feedback about their breathing activity during the scan with a view to improving the scan image. For the offline situation the bargraph display and LabVIEW waveform on the computer provide an effective visual feedback to the patient showing them their breathing activity. However an LED or electrical display cannot be used in proximity to the scanner due to the electromagnetic restrictions of the scanners. It was therefore necessary to develop a feedback system that provided the patient with a visual display but that contained no electrical or ferrous material. This feedback system must provide an easily legible display within the confines of the scanner tunnel. It should not affect the scanner's performance or damage it in any way.

A visual form of feedback would be preferred to an audio form of feedback for a number of different reasons. The human eye is better suited for reading information than the ear under MRI operating conditions. The MRI scanner produces a high level of noise so variation in tone or volume of an audio signal will be difficult even for a trained ear to distinguish. A visual feedback will not be affected in the same way by the level of noise in the scanner tunnel. Visual feedback can include light from a number of sources, relieving the need to distinguish between certain signal properties from a single source. The audio signal would be an alternative for use with visually impaired people. However, as more information can be represented accurately on a visual display it is the preferred feedback media.

Polymer optical fibres are practically invisible to magnetic radiation. They do not conduct any electrical current and do not contain any ferrous material. Hence a system was devised where the information is transferred from outside the MRI room into the patient via optical fibres. These can be relatively easily coupled to an LED. The light from the LED can then be transferred from one end of the fibre to the other. Thus fibre optics technology was used to replicate the bargraph display within the MRI room as shown in Figure 6.1.
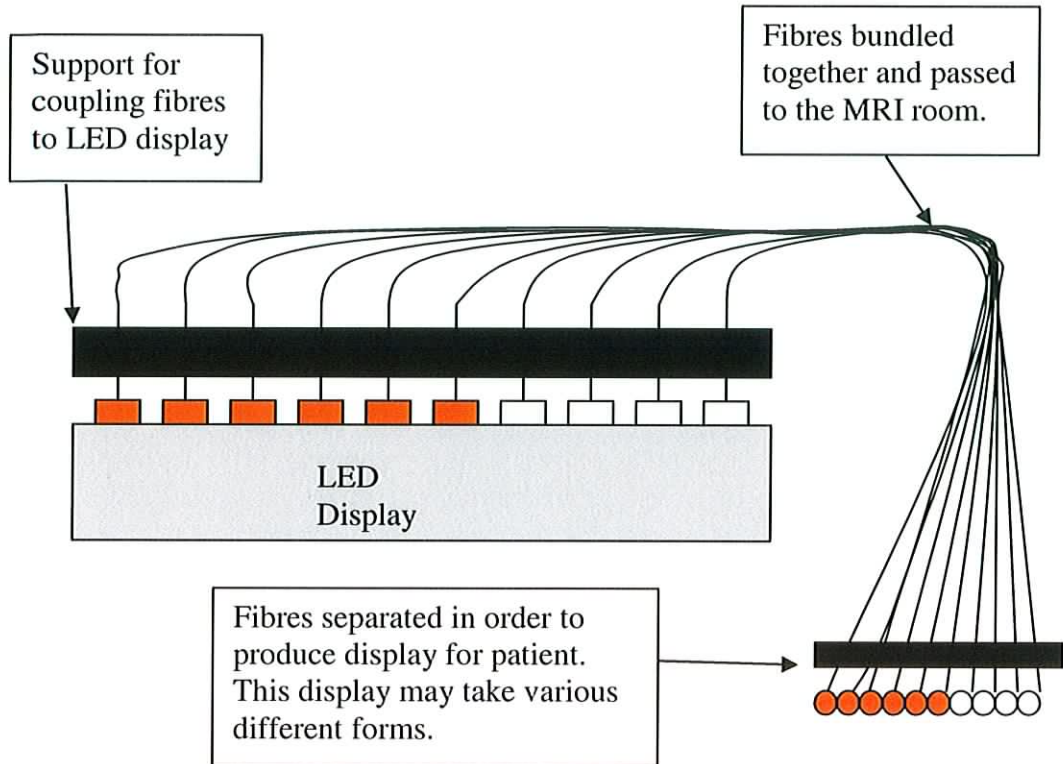
Figure 6.1: Visual feedback System used to convey the 0-10Volts to the patient.

6.2 Fibre Optics

The fibre optic used is acrylic optical cable sheathed with special fluorine containing polymer. These are made and distributed in 20m sections by Farnell Ltd. These were later cut to a length of ten metres using a special blade. Ten metres provide enough length to transfer the light from the LED display in the main part of the device, located outside the MRI room, into the fibre optic display located in the scanner in the MRI room. Figure 6.2 shows what a small segment of these fibres looks like.

Figure 6.2: Small section of the polymer fibre optic.

6.2.1 Verification of the Use of Polymer Fibre Optics

In order to predict if a fibre optic feedback system would work it was necessary to obtain a proper understanding of how the fibres work. Firstly it was necessary to predict whether the light beam would be lost over the required length of cable. An

insight into the operation of fibre optics would also be necessary to set up this type of feedback system correctly.

The LED's in the display used as the light source for the fibres are red. They have a wavelength of approximately 650nm. The chart in figure 6.3 shows the attenuation in the fibres for various wavelengths. It can be seen that for red light (650nm) the attenuation is about 150-300dB/Km. The length of the fibres in this case is 10m. Therefore there should be a 1.5 - 3dB attenuation over the entire length of the fibre. This means that 0.71 - 0.5 of the signal that enters the fibre will leave the fibre. Therefore, with the high brightness LED's used for this device, these fibres should be more than adequate for these purposes.
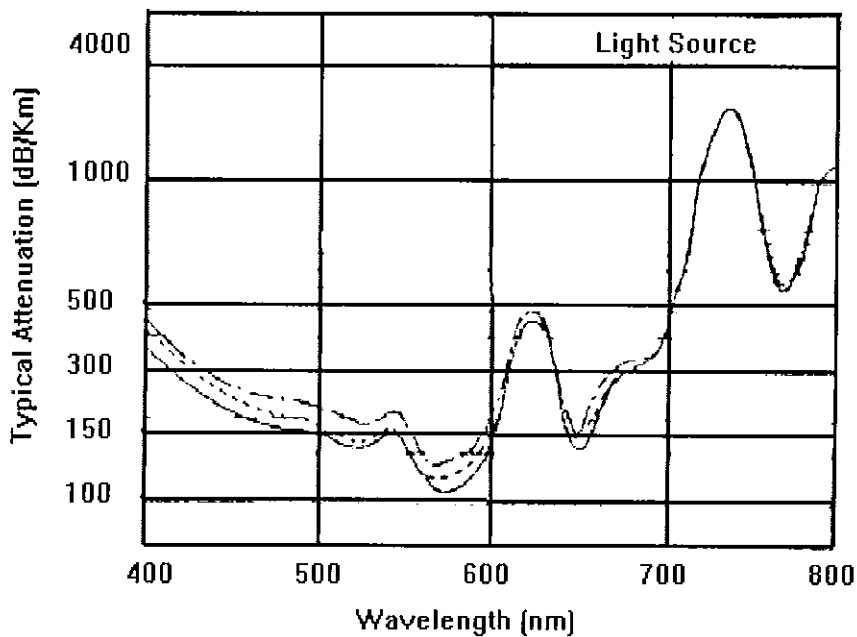
Figure 6.3: Typical attenuation against wavelength for the polymer fibre.

Fibre optics work on the principle of total internal reflection. This phenomenon occurs when light tries to pass from a material with a high refractive index to a material with a low refractive index. Any light that is transmitted into the second material usually changes direction. This bending of light is called refraction and hence each material has its own refractive index.
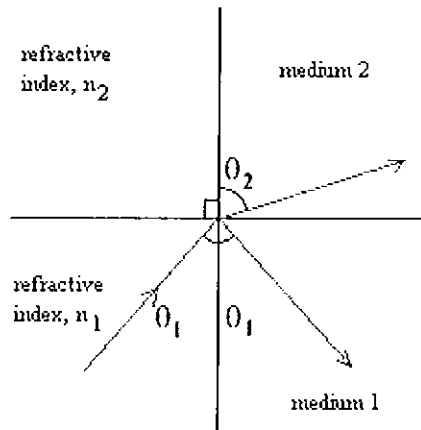
Figure 6.4: Refraction.

So the light passes out of the first medium and into the second medium. There is also some light reflected back into the first medium. As the angle with which the light strikes the surface, θ_1, increases the angle of refraction, θ_2, approaches 90degrees. When θ_1 equals the critical angle θ_c, then θ_2 equals 90degrees. From this point on total internal reflection occurs. The light is completely reflected inside the first medium with none of the light escaping to the outer medium. This is shown in figure 6.4 and 6.5.

In the case of this fibre the inner filament has a higher refractive index than the outer cladding. θ_c in this case is 23degrees. Hence, as long as θ_1 is greater than θ_c the phenomenon of total internal reflection continues to happen allowing the light to propagate along the fibre as shown in figure 6.5.
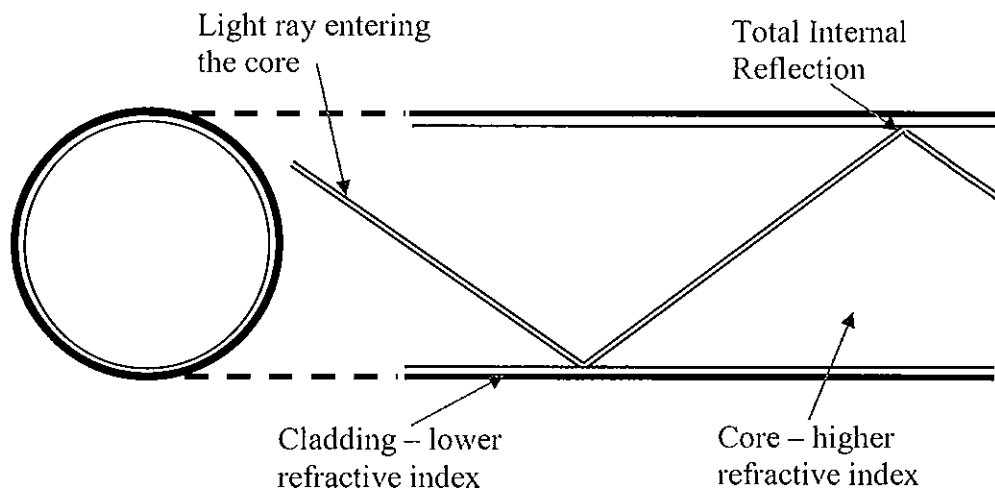
Figure 6.5: Structure of the Optical Fibre and Diagram of Light Transmission.

The refractive index for a material can be calculated as follows:

$$n = \frac{C}{V}$$

{6.1}

where

n is the refractive index,

C is the speed of light in a vacuum,

V is the speed of light in the material.

In this case the optical fibre has the following refractive indexes:

Core refractive index (n_1): 1.492

Clad refractive index (n_2): 1.417

Numerical Aperture: $N.A = \sqrt{(n_1)^2 - (n_2)^2}$

{6.2}

$$= 0.46709$$

Acceptance angle: $\sin^{-1}(N.A) = 56 \text{degrees}$

The acceptance angle is twice the critical angle, therefore $\theta_c = 23\text{degrees}$. This is the angle at which the light must reach the entrance to the fibre if it is to enter and propagate through it. This is very important when dealing with a collimated light source. An LED can be viewed as many smaller light sources however and hence the angle is not as important. This was still taken into account however and hence the fibre is held normal to the LED to provide the largest angle possible. It is because of this that the fibre must be cleanly cut also. If the fibre was cut an angle then it could cause problems due to the acceptance angle as shown in figure 6.6. The angle can also lead to light reflection and dispersion.
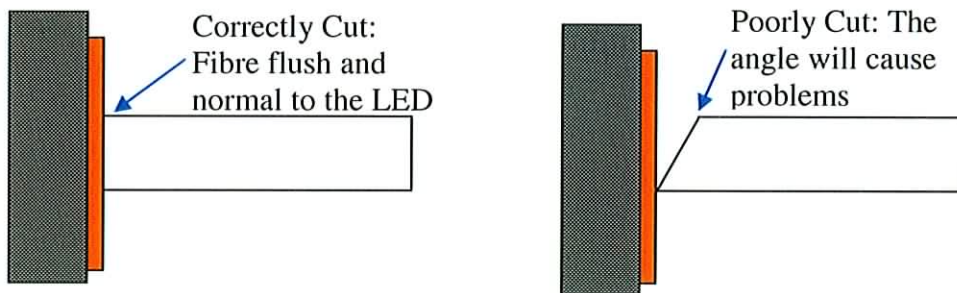
Figure 6.6: If the cable is not properly cut then less light will enter the fibre due to light dispersion and reflection.

6.3 Fibre Optic Plug

For this system to work it is necessary to be able to couple the fibre optic cables to the LED's. A special plug was needed that would carry out this function. The optical fibres used have a relatively large diameter which made it easy to attach them to the LED's. It is sufficient to hold the fibres normal and flush to the surface of the LED's as shown in figure 6.6. A plug and socket were constructed from polyacetalhomopolymer (POM-H) plastic. This is a food grade plastic that is also used in the electrical housing for the device as discussed in Chapter 7. Therefore this material was chosen, as it was readily available and suitable for handling. The plug and socket are shown in figure 6.7 and 6.8. The plug was drilled with 2.5mm holes to hold the fibres. The fibres are then glued into place within the plug so that they are just flush with the edge of the plug. The plug and the fibres are held firmly against the LED's when attached properly. Figure 6.7 shows an exploded view of the plug and the fibres. There is also a screw that is used to hold the plug in place once it is inserted. This is screwed through the housing of the main part of the device into a metal insert in the socket that can be seen in figure 6.9.
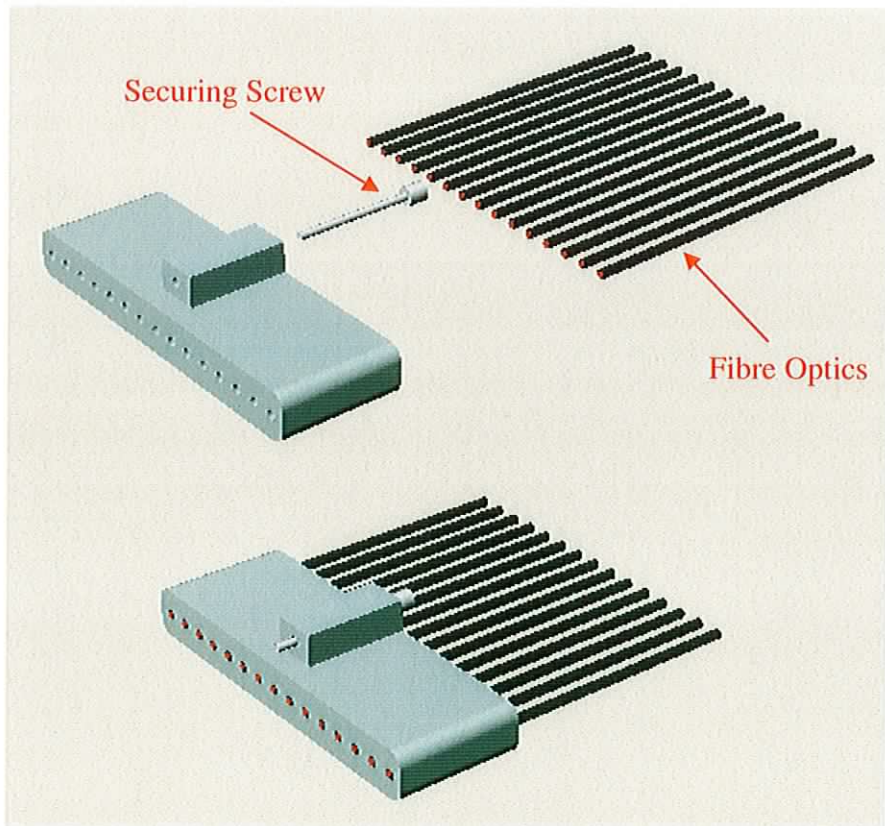
Figure 6.7: Fibre optic plug for attaching the fibres to the LED's.

The socket that is used to guide the plug is glued to the front of the LED display. The socket is designed to fit inside the outer grove of the display bezel on the LED display. This is used to ensure that the socket is accurately and securely positioned. This is important as it is the socket that aligns the plug and hence the fibres to the individual LED's inside. The fibres must fall directly on the LED's to obtain maximum light intensity. The plug and socket are shown in figure 6.8. The brass insert for the securing screw can be seen on the socket. It is important to have a securing mechanism to ensure that the plug and fibres stay flush with the LED's at all times. Any movement would cause degradation in light intensity. A photograph of the main part of the breath-monitoring device can be seen in figure 6.9. This photograph shows how the plug looks when plugged into the device.
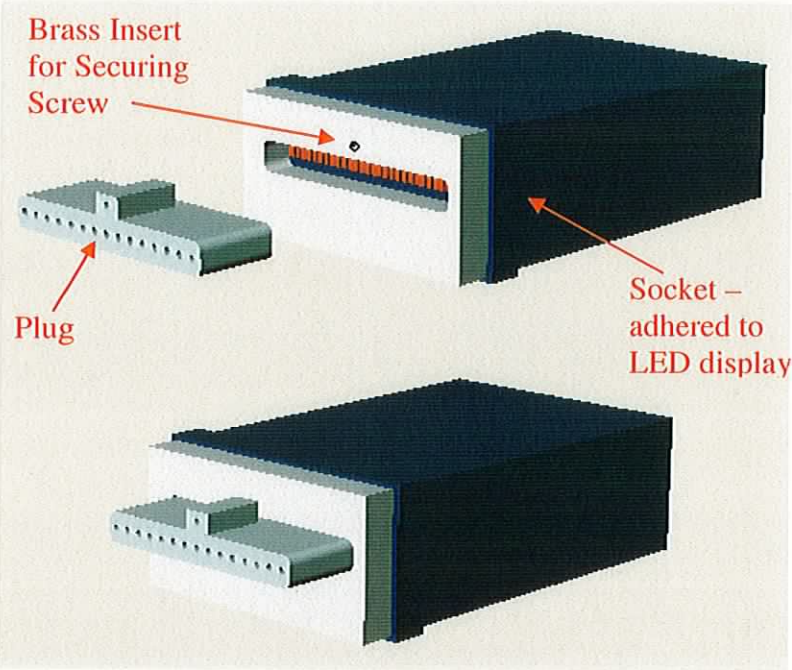
Figure 6.8: Fibre optic plug and socket for attaching the fibres to the LED's.
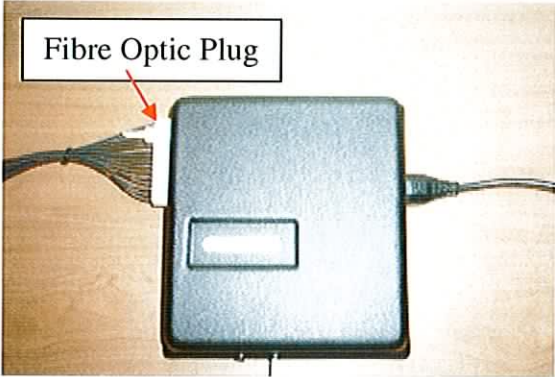
Figure 6.9: Fibre optic plug when attached to the main part of the device.

The dimensions of the plug are shown in figure 6.10 below. This is a relatively simple part to manufacture. It is made from a 10mm thick piece of POM H plastic cut to have dimensions 77.5mm * 26mm. The corners are sanded down to have an approximate 3mm radius as shown. The 15 holes for the fibres are drilled with a 2.5mm drill bit. The fibres are 2.3mm in diameter allowing relatively simple insertion into the plug where they are glued in place.
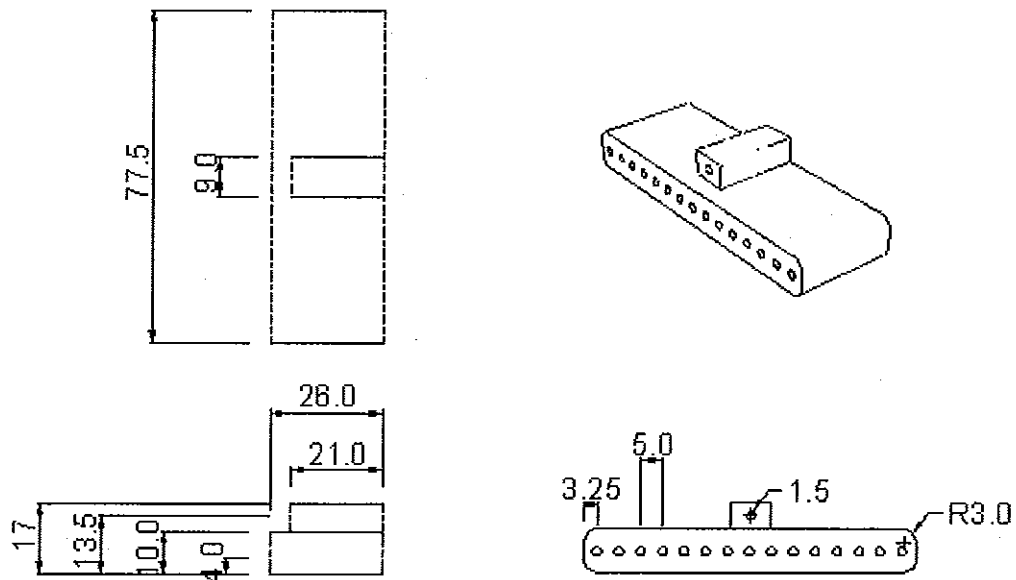
Figure 6.10: Dimensions in mm for the fibre optic plug.

When compared with the dimensions for the plug the socket should be a snug fit. The socket provides support in two directions for the plug with the screw providing support in the third direction. Hence there should be no movement of the plug when it is screwed into the socket. The socket dimensions are shown in figure 6.11.
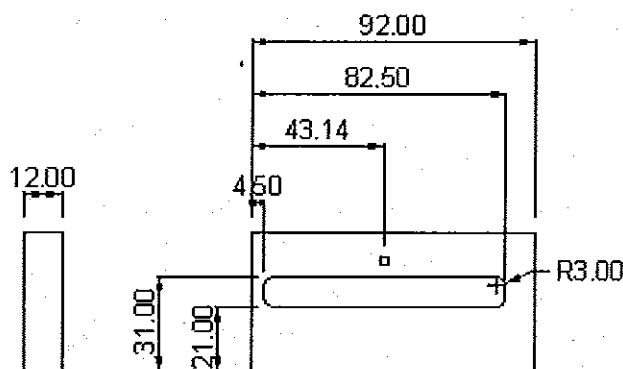
Figure 6.11: Dimensions in mm for the fibre optic socket.

91

6.4   Fibre Optic Display

Once the bundle of optical fibres are fed into the MRI room they must be separated and displayed to the patient. Therefore a display was needed that would provide a clear visual feedback for the patient within the restrictive confines of the scanner tunnel. The display and the bundle of fibres leading to it cannot disrupt the movement of the table that moves the patient into the tunnel. The display should also have no sharp edges which might injure a patient or damage the scanner in any way. The confined space in the scanner obviously requires that the part be small and that it uses the most of the space that is available. The claustrophobic nature of the tunnel requires that the display is simple and does not add any further discomfort to the patient in an already stressful environment.

The tunnel within the scanner, where the patient lies, is typically 60cms in diameter. The table upon which the patient lies is approximately 48cms from the top of the tunnel. The patient is usually provided with a head cushion for added comfort so the face is even closer to the roof than the rest of the body. This leaves a maximum of about 20cm from the roof of the tunnel to the patients face in which to place the display. Therefore there is very little room for the display. Figure 6.12 shows a sketch of the tunnel dimensions and an approximate area within which the display can be placed shaded in green.
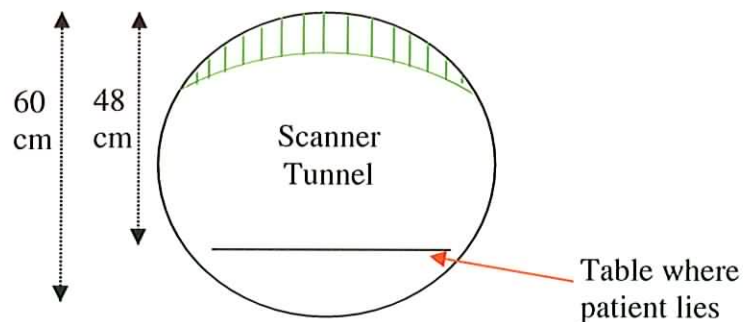
Figure 6.12: Dimensions of the scanner tunnel showing the available region within which the display can be placed (shaded in green).

6.4.1 Ergonomics of Display

The angle at which the patient will most comfortably view the fibres and how far around the circumference of the tunnel the fibres can be spread are also issues. The field of view of the human eye is approximately a 120degrees cone as shown in figure

6.13 below. This is the maximum angle through which one can see but this is with the eye fully extended.
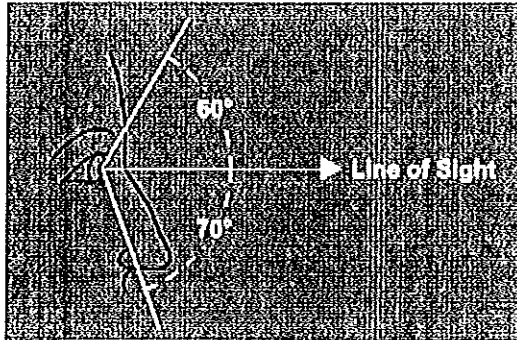
Figure 6.13: Field of view of the human eye.

When looking directly forward the clearest objects are those directly in front of the eye with objects in the peripheral vision becoming increasingly blurred as they spread out from the direct line of sight. Therefore it was decided to restrict the angle from the eye so that the display would both be more easily viewed and be more clear. The patient should be able to at least view the whole display without having to turn their head. To calculate how large a display can be to keep it within a certain cone of sight formula {6.3} is used as shown in figure 6.14. For the field of view of the human eye then the length of the display should be no more than s = θ*r. Therefore, with θ = 120degrees = 2.094radians, then s = 2.094*200 ≈ 420mm.

$$s = \frac{\theta}{r} \qquad \{6.3\}$$

θ is the angle of sight required to view the display in radians,

r is the distance from the patient's eyes to the display,

s is the curved length of the display.
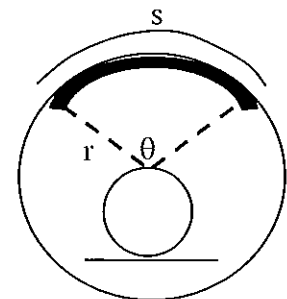
Figure 6.14: To calculate the angle of sight required for a given display.

The angle at which the head is inclined is also important. With the head cushion in place the head will be inclined slightly. It is also more comfortable to look at a slightly downward angle. Therefore it was decided to place the display down the tunnel slightly instead of directly above the eyes and have the fibres showing at an

angle as in figure 6.15 below. This also means that the display is slightly further away allowing it be slightly larger. The angle chosen for the final display design was 45degrees. Due to the large field of view of the eye the position of the display in this direction is not critical as the display will be narrow in this direction leaving some room to play with.
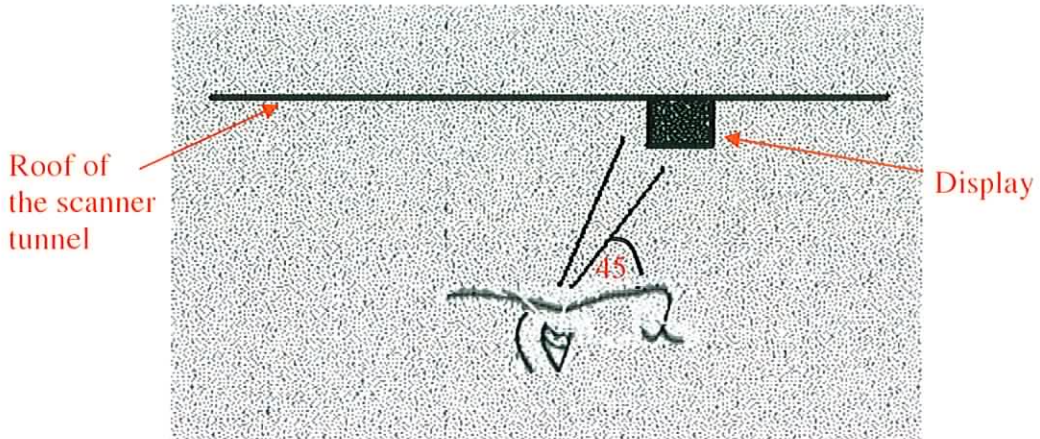
Figure 6.15: Position of the display relative to the patient.

6.4.2 Self-Clamping Fibre Optic Display

A cheap prototype display was first built. This display uses a firm plastic mount made from black nylon plastic which holds the fibres at a 17 degree angle to the horizontal as shown in Figure 6.16. 30 holes 2.5mm in diameter were drilled to hold the fibres. This mount (approximately 100cm) is slightly greater in length than half the circumference of the tunnel (approxiamtely 94cm). Once it is bent into the tunnel it clamps itself against it as it tries to straighten back to its original shape. Velcro can also be used to help secure the mount.
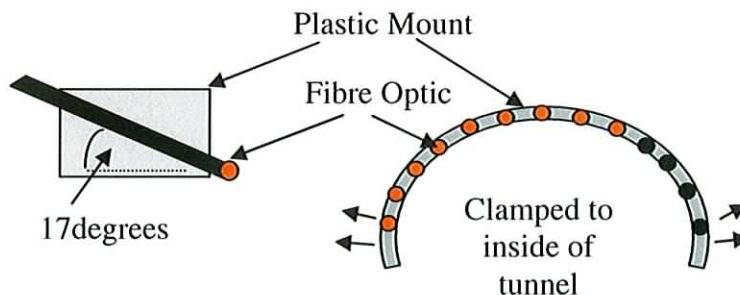
Figure 6.16: The initial plastic mount for the optical fibres.

This display follows the curve of the scanner tunnel and hence takes up very little space. A photograph of the display showing the lit fibres can be seen in figure

6.17. 13 of the 30 fibres used in this case are lit. The fibres in this case are hidden behind a screen to enhance the image.
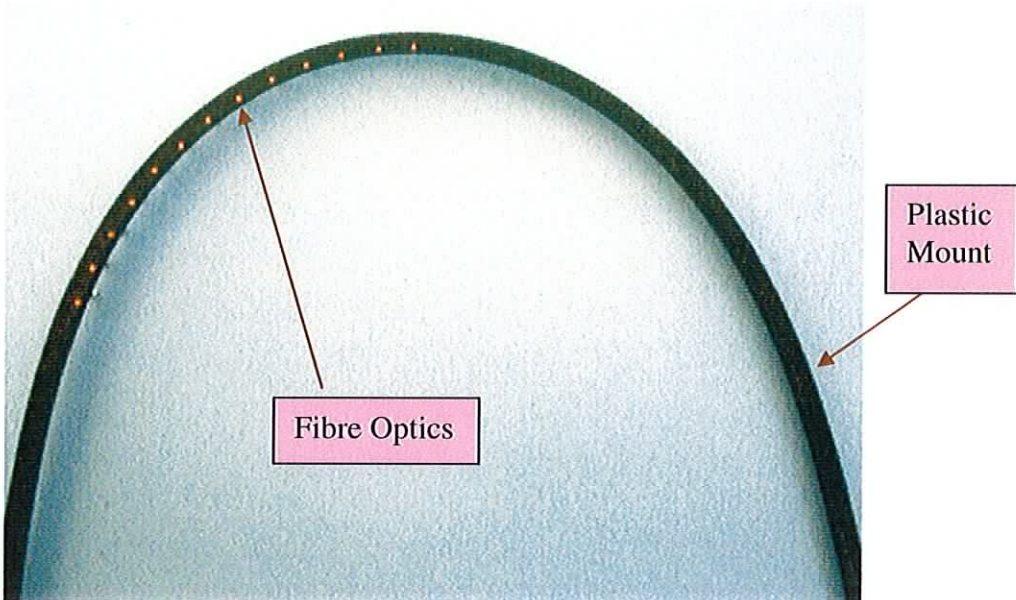
Figure 6.17: The initial self-clamping fibre optic display.

The light from the fibres is magnified by a small lens that fits over the end of the fibres. With these lenses the angle at which the light from the fibre can be viewed also increases. A sketch of these lenses can be seen in figure 6.18 below. The plastic lens surround is designed to grip the fibre once it is pressed into it. This helps to hold the fibres in place in the display. The lens also protects the head of the fibre. The fibres are alligned as they are in the plug that connects them to the LED's. This means that the lenses will light up one after the other from the left hand side as the patient breathes in. They will then start to go off from the right hand side when the patient breathes out. Finally, the same amount of lenses should be lit when the patient is holding their breath.
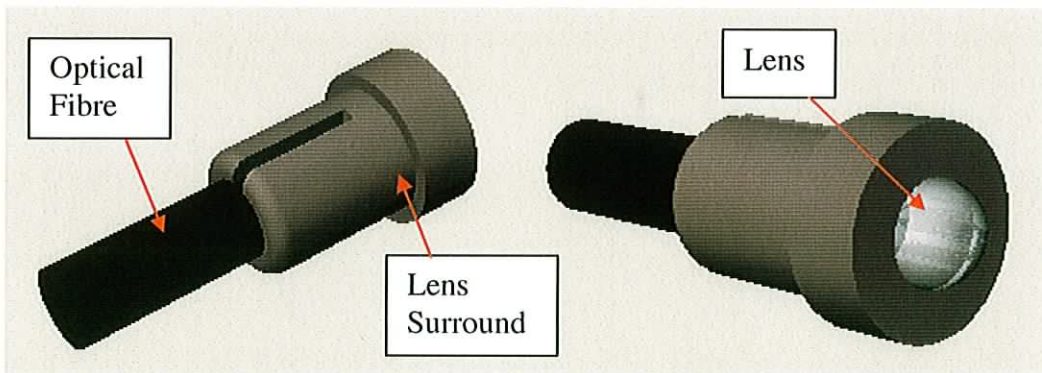
Figure 6.18: Lens used to magnify the light from the fibres.

This initial display was self-clamping. Once placed inside the tunnel the natural tendency of the plastic to straighten caused it to form the shape of the tunnel and effectively clamp itself against it. This has the advantage that it can be placed anywhere in the length of the tunnel. Hence during testing the position of the display could be manoeuvred. It also meant that there was no need for a permanent attachment in the tunnel to hold the display. With the huge cost of MRI scanners and the huge demand on them it was not possible to tamper with the scanner itself in anyway.

This display however was very crude and was really only used for an initial field test to gain more ideas for a final display design which would be more professional and aesthetically pleasing. While the self-clamping system has its advantages it was found to have one major flaw during the field-testing. When the patient was being slid into the tunnel on the scanner table invariably either the head cushion for the patient or the patient's elbow would catch the display and sometimes knock it out of place. This was because of the length of the display. As can be seen in figure 6.19 the display extends a few centimetres beyond half the circumference of the tunnel. As discussed earlier the main space available for the display is toward the roof of the tunnel. It was the lower regions of the display that caused the problems while the patient was slid into the tunnel.
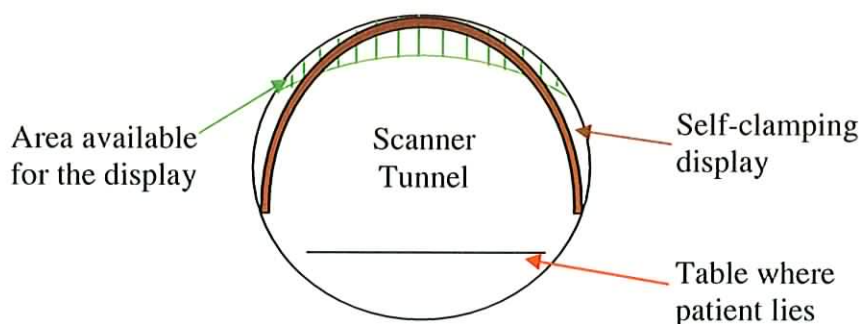
Figure 6.19: The initial self-clamping fibre optic display.

Another disadvantage of this display was that although the plastic mount formed the general shape of the tunnel it did not form a perfect semi circle as is also shown in figure 6.19 above. This effectively increased the area needed for the display and contributed to the problems encountered when sliding into the tunnel. This problem

could be rectified to a degree by using a Velcro strap to help secure the mount against the tunnel perimeter. This would both help keep the mount flush with the perimeter and prevent any movement if knocked while the patient was being inserted. However using Velcro would nullify the main advantage of this display as it would no longer be solely a self-clamping device.

From the initial field test it was concluded that a much smaller display would be necessary. The angle at which the fibres point toward the patient could be increased to make viewing easier also.

6.4.3 Vacuum Formed Fibre Optic Display

A new more aesthetically pleasing fibre optic display was required that would be smaller in size and more stable than the original self-clamping display. Having already used the process of vacuum forming to create the housing for the device (as discussed in chapter 7) it was decided that this would be an appropriate method of manufacture for a new display design.

In the initial self-clamping design the bundle of fibres is separated before entering the plastic mount. This means that the individual fibres can be seen stretching out to their consecutive holes. This creates an untidy appearance. Hence for the new design it was decided that the bundle of fibres would enter as a bundle into a housing where they would then be seperated and displayed. It was also decided to have the bundle of fibres enter from the side so that the patient has as little view of these as possible.

To utilise the space to maximum effect it was decided to permanently form the display into the shape of the tunnel. This was part of the reason for choosing vacuum forming as the manufacturing technique for this design as opposed to a part that was manually constructed. Once the correct radii are placed on the mould many parts can be easily made. A 45degrees angle (as shown in figure 6.15) was also placed on the edge where the fibres protrude from. The holes that hold the fibres are drilled normal to this surface so that the fibres point in toward the patient. The new display design can be seen in figure 6.20. This is the view similar to what the patient would have in the tunnel.
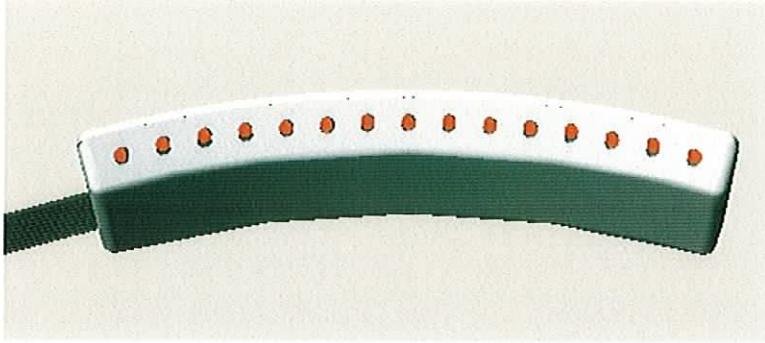
Figure 6.20: The vacuum formed fibre optic display with fibres.

The vacuum-formed part requires a back that is screwed to it using plastic screws. A sketch of the vacuum-formed part itself can be seen in figure 6.21 below. The slot where the bundle of fibres enters can be seen on one side. The side of the part where the holes are that hold the lenses in place is at a 45degrees angle. The holes are drilled normal to this curved surface.
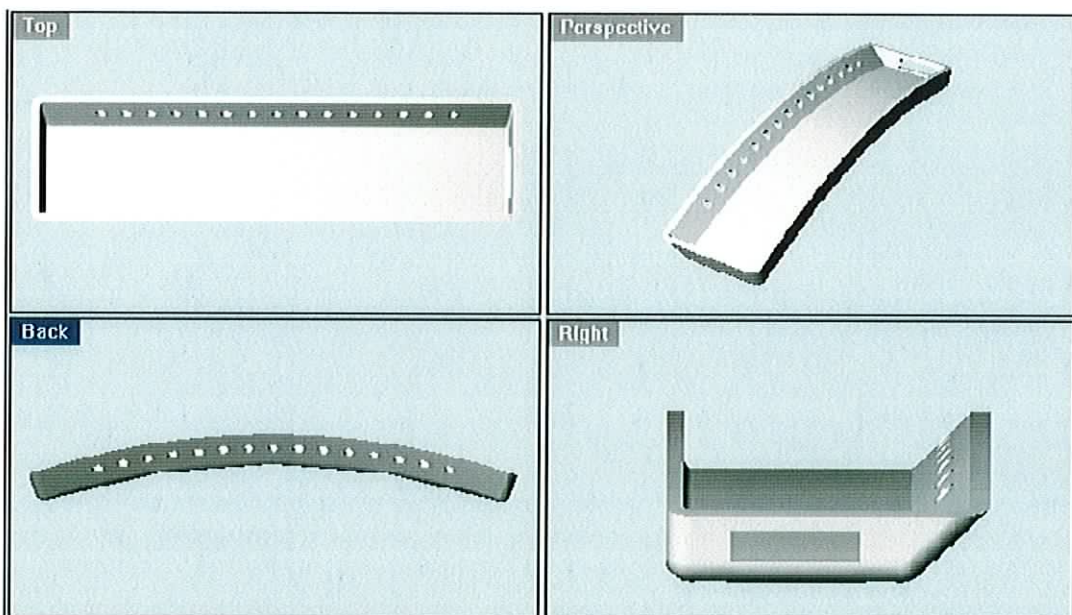
Figure 6.21: The vacuum formed fibre optic display.

The dimensions of the vacuum formed display can be seen in figure 6.22a below. The part is much smaller in length than the previous design that had a total length of 1000mm and had its fibres separated over a distance of 500mm. The angle of sight required for the self-clamping device was too large. This was calculated for a distance of 200mm from the patients eye to the display as shown in figure 6.14. For the self-clamping display the angle was calculated using formula {6.3} to be;

$$\frac{500mm}{200mm} = 2.5radians \approx 145\,degrees$$

This is greater than 120degrees which is the field of view of the human eye. Thus movement of the patient's head would be required to view all the lenses. In the vacuum-formed display however the angle is calculated as;

$$\frac{200mm}{200mm} = 1radian \approx 57\,degrees$$

which is well within the field of view of the human eye. The individual fibres are seperated by 10mm in this case. There are 15 fibres creating a display that is less than 200mm long. In the previous design there were 30 fibres placed at 18mm apart and this was later changed to 15 fibres at 36mm apart. The number of fibres was decreased for a number of reasons. Firstly, the cables are expensive and by halving the number of cables the cost of the device is considerably decreased. Obviously with fewer fibres the bundle entering the MRI room and scanner is smaller and lighter. Less weight is placed on the display, which is important if the display is being held with Velcro. It is also easier to display a smaller number of fibres in the confined space available. By choosing to use only every second LED the fibres were easier to couple to the LED's as there was more space between them. It was also determined that 15 increments of the breath cycle are enough to provide sufficient information to the patient and to keep movement due to breathing to an acceptably small level. The results obtained using 15 fibres were as acurate as those obtained using 30 fibres. The dimensions of the vacuum-formed display is shown in figure 6.22a. The dimensions of the mould used to create the display are shown in figure 6.22b.
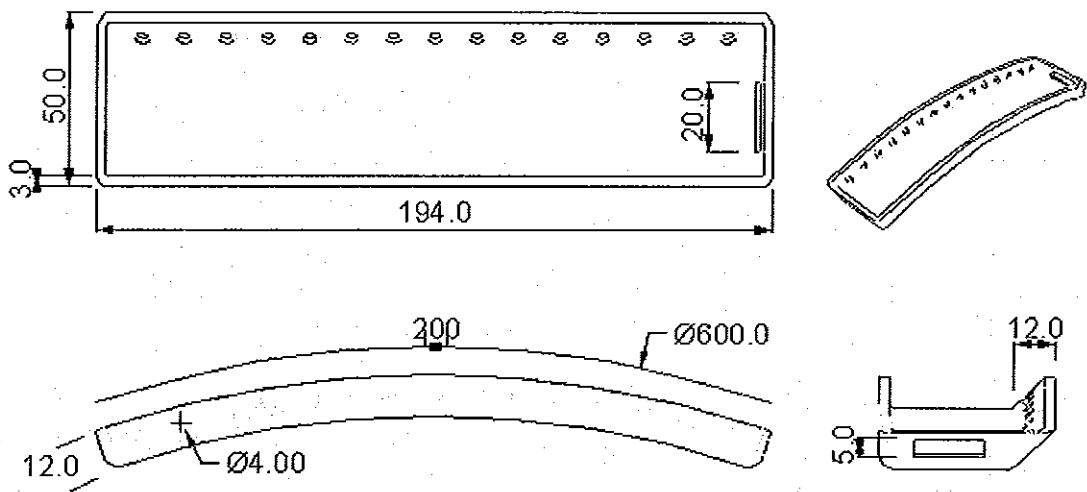
Figure 6.22a: Dimensions of the vacuum formed fibre optic display.
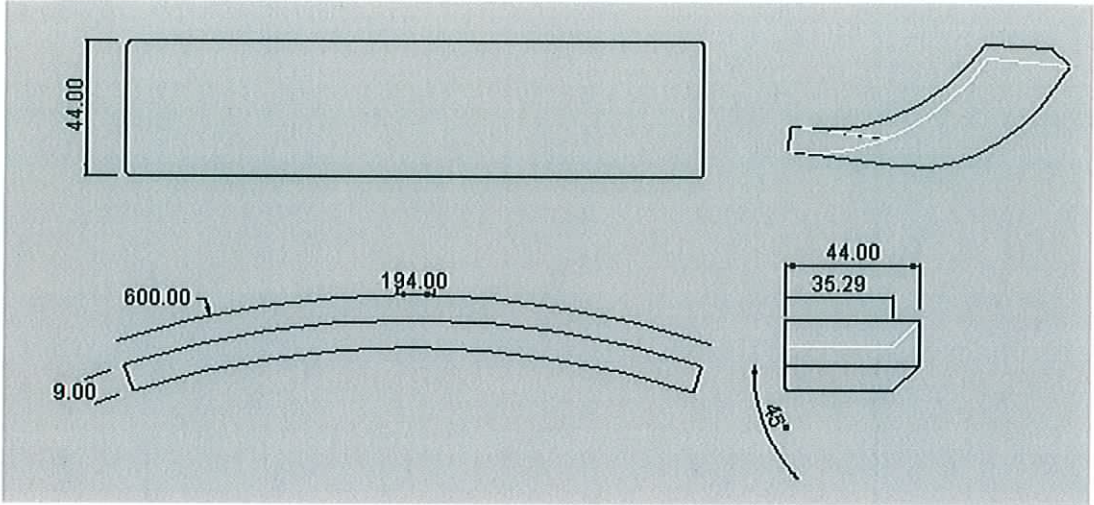
Figure 6.22b: Dimensions of the mould used to create the vacuum formed display.

A sketch of the wooden mould showing the location of the air vents (in red) for the vacuum forming process can be seen in figure 6.23. The significance of these holes and the vacuum forming process are discussed in chapter 7. A photograph of the display showing the spreading of the fibres can be seen in figure 6.23.
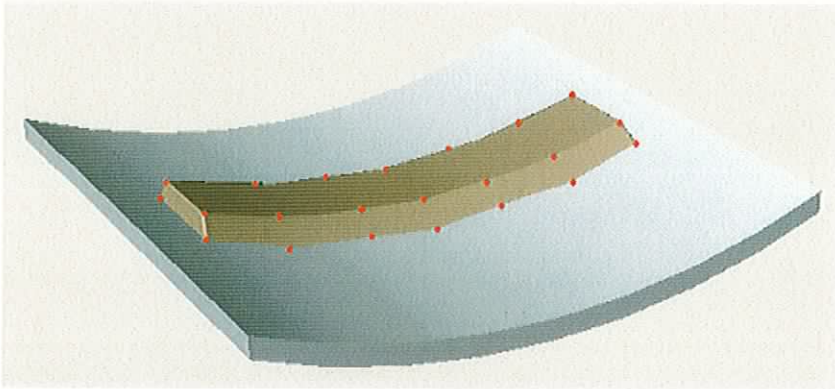
Figure 6.23: Sketch of mould used to create the vacuum formed fibre optic display.

Back is attached with plastic screws to ensure MRI compatibility
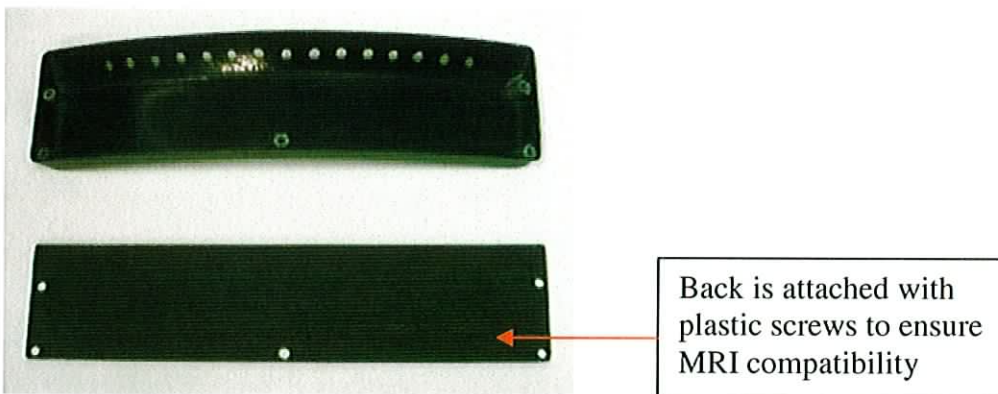
Figure 6.24: Photograph of the vacuum formed fibre optic display.

100

6.4.2 Other Possible Fibre Optic Displays

Other types of display could be used such as a single fibre coupled to a varying intensity LED or a varying colour LED. However the human eye can only distinguish between certain changes in colours and intensities and so this form of feedback may not be able to supply enough information.

A device has been patented [50] that uses mirrors to reflect the information into the patient as discussed in chapter 1. The mirrors reflect the information from an LED display outside the scanner into the patient. However such a system requires a mount for the mirror inside the tunnel. The mirror must be small due to the confines of the tunnel and must be aligned perfectly to reflect the LED display. With the distance required between the mirror and the LED display visibility is a problem.

A system could also be constructed where a display such as the vacuum formed display is attached to an arm that can reach into the tunnel from a stand beside the scanner. This would take away the need for Velcro and make the display completley stand alone. This system is viewed as possible future work on the project.

Another potential type of display would clamp itself to the scanner table. This would slide into the tunnel with the patient on the table. However with the lack of space and the need for a clamp on this heavily utilised table such a design would be difficult to implement.

6.5   Conclusion

The initial self-clamping display operated well and showed that the use of fibre optics was viable. It provided a good platform for testing the device in initial field tests. It also provided critical information on the design of the final display unit. It was decided that the new display unit needed to be smaller and more suitable for use with patients. This was then used in the final field tests and proved much superior.

7 HOUSING DESIGN

7.1 Introduction

The main part of the device containing the power supply, the LED display and the pressure transducer required some form of housing. There were a number of factors determining the design for this housing. It must provide a safe holding for the components that allows the device to function correctly and provide a sufficient level of safety to the patient. It must also be aesthetically pleasing and be cheap to manufacture. It must be robust enough to be moved around without damaging the internal workings of the device. On top of this it must pass the medical device standards.

There are also some restrictions on the size and shape of the housing. The size and shape of the components to be placed within the housing and the electrical connections between them will affect this. This main part of the device is to be situated outside the MRI room so there is no restriction on the materials used with respect to magnetic radiation. However the device should be capable of either being placed on a desktop, in a cabinet, wall mounted or be capable of a number of these functions. There are various connections to the device, such as the electrical inputs/outputs, the air tubes from the bladder and the fibre optic display connection that the housing must allow. These must be easily accessible and simple for the user to connect. The housing should allow easy access to the device components should maintenance be required.

Three main stages of development have gone into the design of the housing. Firstly three-dimensional (3-D) CAD models of various designs were drawn up using Rhinoceros. Then a Rapid Prototype was made. Finally two different designs were made up using two different methods. The first design used Reaction Injection Moulding to build the housing. The second used a method called Vacuum Forming. Each method has their advantages and disadvantages. The vacuum formed part was the part used in the final design.

There are numerous manufacturing techniques available for the building of such a housing. A number of these techniques were utilised. This part of the project was used as the bases for a final year project for two manufacturing engineering students studying in DIT [51]. The research carried out by these students resulted in an alternative design and manufacturing process being assessed. They used Reaction

102

Injection Moulding (RIM) to build their versions of the housing. They also had rapid prototypes built during the course of their work. Neither design was used in the end but they were a valuable addition to the project and highlighted some of the advantages and disadvantages of RIM compared with other manufacturing techniques.

A number of alternative solid models of the housing were created using CAD. These went under preliminary assessment by the consultant radiologist. Rapid prototypes were used to help in this process and valuable lessons were learned from these. One of these designs was chosen to which some modifications were made. Vacuum Forming was the process used to create the final housing. This type of manufacturing technique, along with the final design used, proved to be the least expensive and also proved to be more aesthetically pleasing and modern than designs created using RIM. This final design consists of a plastic base plate that holds the components and a vacuum formed housing to cover them. The vacuum formed housing is made from medical grade ABS plastic in order to help the device pass the European medical standards as discussed in Chapter 8.

7.2   3-D Modelling

The various housing designs were drawn up using Computer-Aided Design (CAD). Various 3-D models were drawn up and compared at each stage. The visualisation of the housing was important for its development and also for documentation of the design. This allowed the design to be changed and improved as time went on. By using 3-D models various restrictions on size and shape could be taken into account at the design stage and the best fit could be established early on.

The Software used to develop the various housing designs was Rhinoceros. Rhinoceros is a modelling program for Windows. It provides a flexible, accurate, and fast working environment where objects can be modelled and rendered. The learning curve for designing with Rhinoceros is faster than other software packages, which made it attractive for the design of the housing for this project. It is also capable of exporting designs to programs for stereolithography and manufacturing which would later be used to create a rapid prototype of the housing. It uses 3-D NURBS (non-uniform rational B-splines) geometry to form mathematical representation that can accurately define any shape from a simple line to a complex 3-D free-form surface or solid. It can then create polygon mesh objects that approximate the NURBS objects

for exporting to programs for stereolithography. Therefore Rhinoceros was chosen as the modelling program for the design of the housing of the device.

7.3   General Design Considerations

There were many restrictions placed on the design of the housing. These ranged from the assembly arrangement of the components to the ease and cost of manufacture. From discussions with the Radiologist and to keep costs to a minimum it was decided to keep the size of the housing as small as possible. The environment in which the device is to be placed and the components that it is intended to house obviously affect the design of the housing. The size and positioning of the components also influences this. The design also influences the type of manufacturing technique used to create it. In injection moulding the raw materials, such as aluminium, for the moulds are extremely expensive and hence the smaller the design the cheaper it will be to manufacture.

A major design consideration is how the components will be mounted within the housing taking into account the electrical connections between the components themselves and between the components and the input/output connections of the device. The components should be accessible in case maintenance is required. Therefore if the housing is made of two separate parts it is better if all the components and electrical connections are attached to one part so that the other can be removed providing the required accessibility. The components must also be securely mounted so that they are not displaced when the device is moved.

Other considerations such as what displays need to be visible and what type of connection plugs are to be used affect the design of the housing. The electrical connections, the fibre optic display connection and the air-tube connections must either be connected to the housing or through the housing to components within. Decisions must also be made on whether or not digital displays and bar graph displays on the components should be made visible through the housing.

For manufacturing techniques such as Injection Moulding and Vacuum Forming there is also the question of a taper in the wall of the housing. This is necessary for removing the part from the mould. Figure 7.1 shows how to calculate the taper angle for a given wall length and taper. The recommended taper angle for manufacturing processes is usually about 1.5 degrees. Therefore for a part that has a wall length of 30mm long the taper should be at least 0.75mm. Without this taper the part would

harden around the mould and be impossible to remove without damaging either the mould or the part. The tapers in all the designs discussed in this chapter are at least 1.5 degrees.
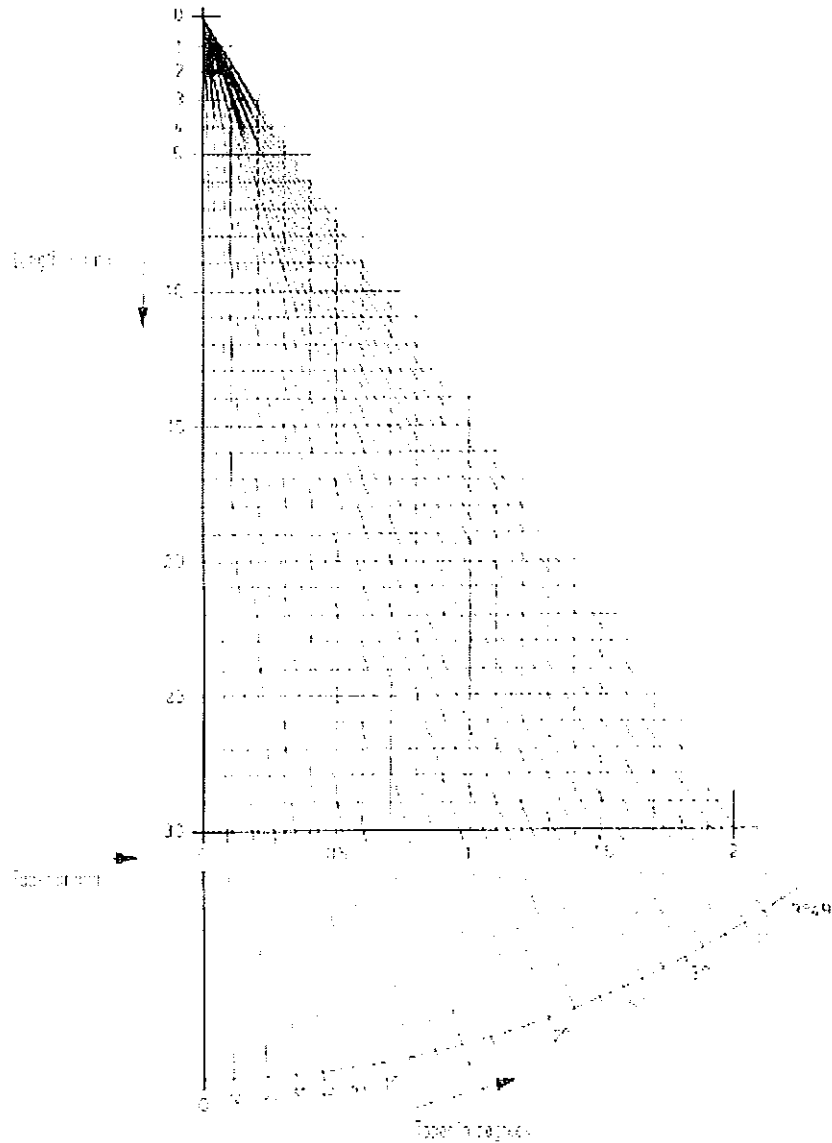
Figure 7.1: Taper chart – Taper in mm against Wall Length in mm.

For each of the manufacturing techniques used during the course of the research slightly different designs were used. These design considerations for each individual case are explained.

7.4 Rapid Prototyping

In manufacturing, productivity is achieved by bringing a product from concept to market quickly and inexpensively. Rapid prototyping technology aids this process. It allows the design to be created as a physical object from a 3-D CAD model. This physical model conveys more complete information about the product earlier in the development cycle. The turnaround time for a typical rapid prototype part can take a few days. Conventional prototyping may take weeks or even months, depending on the method used. Rapid prototyping can be a quicker, more cost-effective means of building prototypes as opposed to conventional methods. Due to the limited time and funding available to the project it was convenient to build a rapid prototype for the device.

Stereolithography [52], or 3-D printing, is a layer-additive process that enables the generation of physical objects directly from CAD data. The software, in this case Rhinoceros, first generates what is called a tessellated object description known as an STL, or stereolithography, file. This a connected array of triangles formed from the boundary surfaces of the CAD 3-D model. These triangles can be as large or as small as desired. Smaller triangles result in finer resolution of curved surfaces and improved accuracy, while larger triangles minimise the file size at the expense of accuracy. Once the STL file is generated it is sliced into closely spaced horizontal planes. The physical model is then built up in these horizontal planes, one on top of the next. This can be achieved in a number of different ways using a diverse range of disciplines from laser physics and photopolymer chemistry to viscous fluid dynamics. Some of the main methods of creating the physical model are Stereolithography, Laminated Object Manufacturing, Selective Laser Sintering, Fused Deposition Modelling, and Solid Ground Curing. Stereolithography (SL) and Selective Laser Sintering (SLS) use lasers to manipulate liquid polymer resins and powders in their layer-additive procedure for building the physical model. Laminated Object Manufacturing (LOM) also builds objects in thin layers but in this case laminated sheet material is used. Consecutive layers are joined using a temperature and pressure sensitive adhesive. Solid Ground Curing (SGC) like SL uses photopolymer resins but does not use lasers. In this case electrical charge distribution is used to form a powder mask over which the resin is distributed. Finally there is Fused Deposition Modelling (FDM) which was the technique used to build the rapid prototype of the housing for this device.

7.4.1 Fused Deposition Modelling

This technique uses spools of thermoplastic filament as the basic material for building the physical model. The material is heated just beyond melting point in a delivery head and is then extruded through a nozzle in the form of a ribbon. It is then deposited in computer-controlled locations forming the shape of the model. As is the case with other rapid prototyping techniques FDM builds up the model layer by layer. This process is shown in figure 7.2.
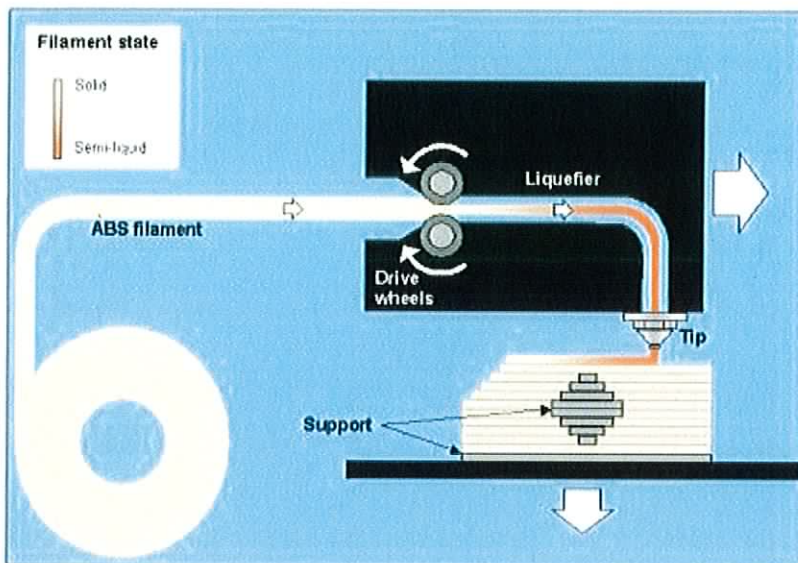
Figure 7.2: Fused Deposition Modelling (FDM).

One of the major advantages of the FDM system is that it can operate in an office environment. There are no high-powered lasers used as in some other rapid prototype systems and the materials are provided in a convenient spool format that does not require any special handling and presents no environmental concerns.

Mr Ray Walsh in the department of Mechanical and Manufacturing Engineering, Trinity College made the Fused Deposition Modelling (FDM) rapid prototype using their FDM machine. This was a Prodigy Plus FDM machine made by Stratasys Inc [53] who is the original developer of the FDM process. Figure 7.3 shows a photograph of the Prodigy Plus FDM machine. In this picture the feed for the two spools can be seen at the bottom of the machine below the main door. The FDM machine is capable of building parts with dimensions up to 203x * 203y * 305z mm.
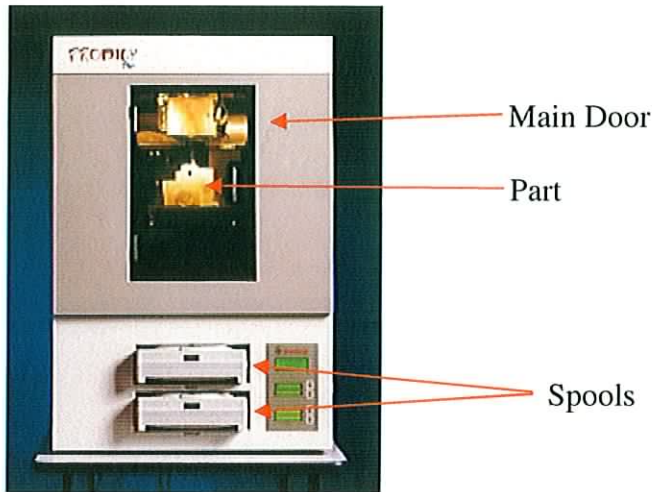
Figure 7.3: Prodigy Plus FDM Machine.

<u>7.4.2 Rapid Prototype Design</u>

- The main design consideration with respect to the rapid prototype was the size of the components that were to be placed within it. The size of the device was to be kept to a minimum while providing enough space for the components. The components must be placed in such a way as to allow them to be connected to each other.

- In order to make the part cheaper to manufacture it was decided to have only a single piece that would be placed as a lid over a simple rectangular base plate. The components are attached to the base plate and the rapid prototype housing is simply placed over it and screwed into place.

- In order for the LED system and the pressure transducer to be visible openings were left in the housing. These would also provide support for the components that would protrude from them.

- As the FDM process builds the part up layer-by-layer there are certain restrictions placed on the design. Each layer supports the next so it is impossible to build downwards. Hence the design must allow for the process.

- As this is only a prototype there is also a taper in the walls. This is because the prototype must be designed with a view to building the design using an alternate manufacturing process in the future.

Figure 7.4a shows what the rapid prototype looks like with the components present. The pressure transducer stands out from the top. This allows its LCD display

108

to be viewed and it also allows easy access to its USB connection, which is used to configure the device. The LED display protrudes from the front of the housing. The display bezel is larger than the rest of the LED display. A lip in the housing is designed to hold the bezel in place with further support provided by two brackets at the rear of the LED display and another to its side. The housing sits flush with the base plate and is attached with screws from beneath.
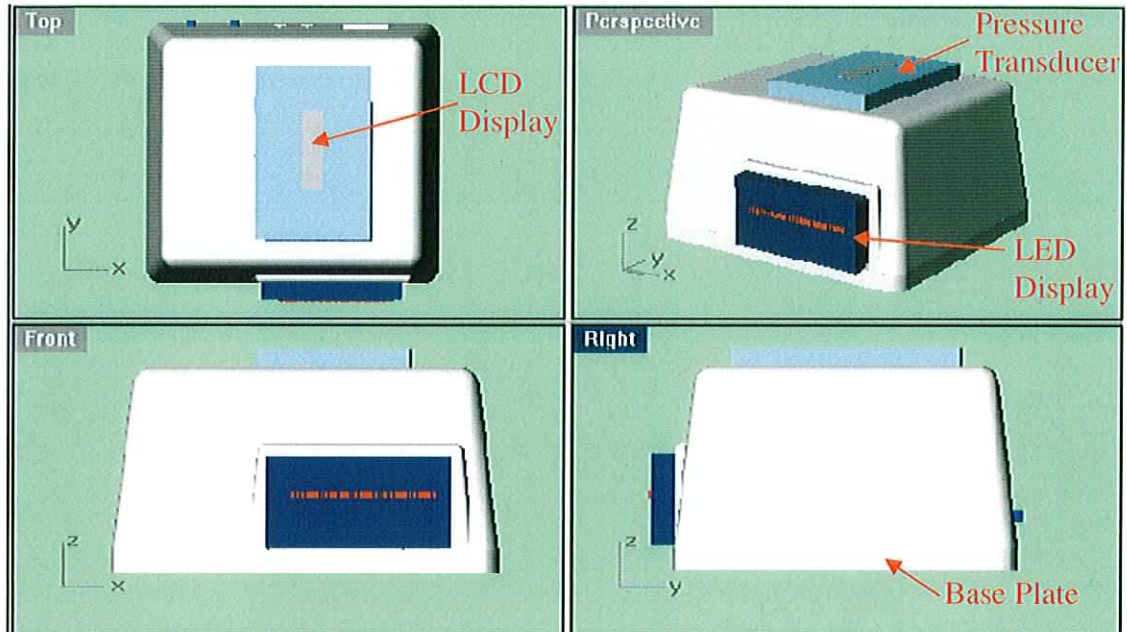
Figure 7.4a: Top, Perspective, Front and Right views of the Rapid Prototype with the components in place.

Figure 7.4b simply shows the Rapid Prototype without the components present. When this is compared to figures 7.4a and 7.4b it can be seen how the part fits over the components and onto the base plate.
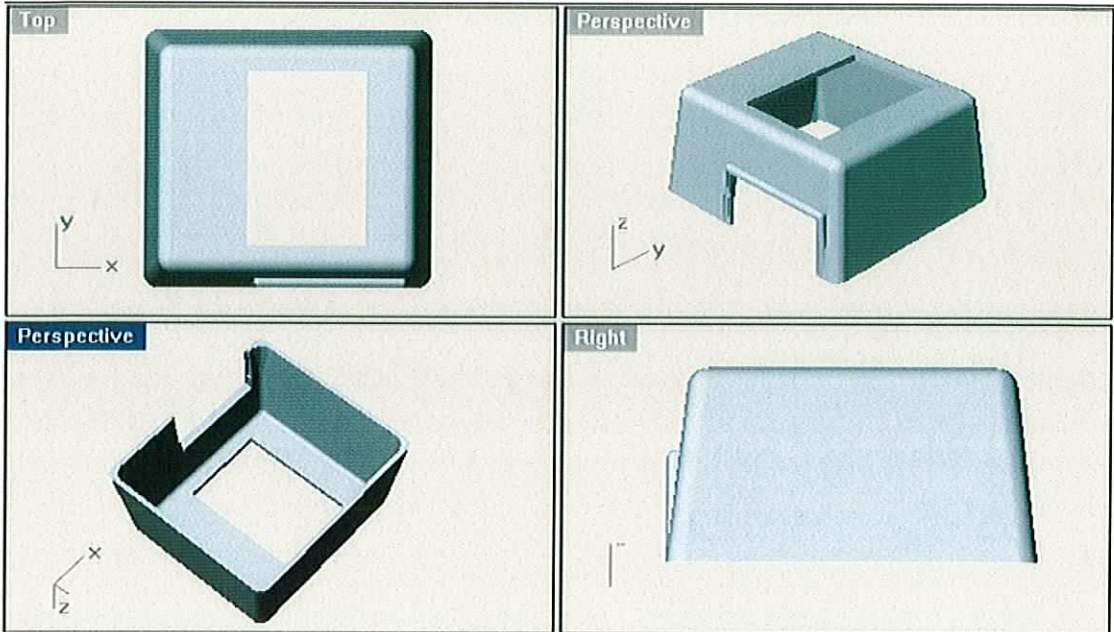
Figure 7.4b: Top, Perspective, and Right views of the Rapid Prototype.

Figure 7.4c shows how the components are placed within the rapid prototype housing. All the components are attached to the base plate so that the housing can be easily removed. The pressure transducer is elevated above the LED display and is attached to the base plate with 50mm long, 3mm diameter screws. The cutout in the housing through which it protrudes provides extra support for it. The LED display is held in place by two rear brackets and a single side bracket. This is also given extra support by the housing once it is in place. The power supply is held in place by its own custom built bracket. The electrical input/output connections can also be seen. These too are attached to the base plate. The air tube connections from the pressure transducer can be seen also.
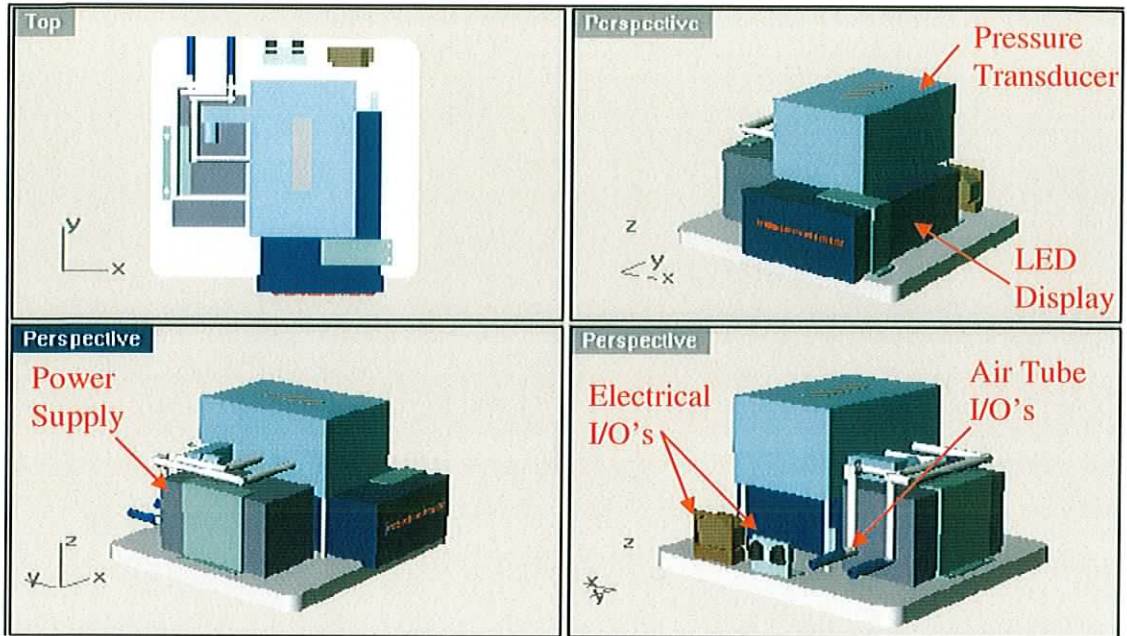
Figure 7.4c: Top and Perspective views with the Rapid Prototype housing removed.

Figure 7.5 shows the dimensions of the rapid prototype housing. These dimensions (200x * 180y * 95z mm) are within the limits of the Prodigy Plus FDM Machine used to build the part.
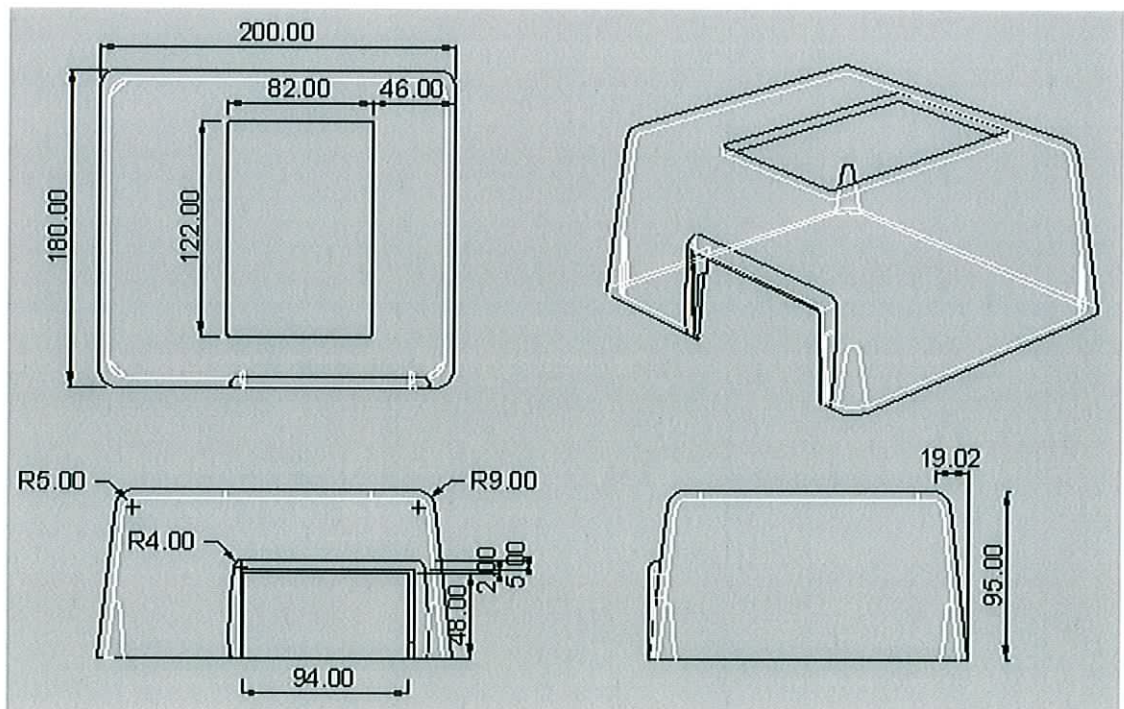
Figure 7.5: Top, Perspective, Front and Right views of the Rapid Prototype showing dimensions. Wall taper = 8.2 degrees.

7.4.3 Advantages of building the Rapid Prototype

The purpose of building the rapid prototype was to convey more complete information about the housing earlier in the development cycle. Sometimes it is difficult to determine how the part will appear and if the components will fit correctly from the 3-D model alone. To build a prototype using techniques such as injection moulding can be expensive and time consuming. By using this comparatively cheap method any dimension mistakes can be corrected early on and any design modifications can be made.

In the case of this rapid prototype there were some major design alterations made as a result of getting the rapid prototype made. The main consideration was that upon viewing the physical model it was decided that while the design was sufficient as a basic housing for the components it was not aesthetically pleasing enough. Due to the size restrictions placed upon it by the machine the design was made taller than wished. The rapid prototype had been designed with a view to eventually making the design by the injection moulding process. Hence it was necessary to have a taper in the walls. This, along with the height of the housing, deteriorated the appearance of the rapid prototype. It was decided that a flatter design would help to improve the appearance.

The housing, in the case of the rapid prototype sits on top of the base plate. Screws from beneath the base plate attach them. This is not the most suitable way of attaching the two objects as if the housing and not the base plate is lifted up a tensile force is applied to the screw. The threads of the screws in turn place a shear force on the small area of plastic between them creating a weak connection. Hence with this design the device may not be strong or durable enough. If the housing came down over the side of the base plate and the screws entered from the side then the connection would be better able to handle the shear force that is applied. This led to a design modification, which can be seen in the vacuum formed part, which has a lip that comes down over the sides of the base plate.

Another negative aspect of the shape of the rapid prototype was that it would require a very large mould for the injection moulding process. As the materials used to build these moulds, such as aluminium, are very expensive the cost of manufacture will increase dramatically due to the design. Therefore, with respect to the injection moulding process this design was not suitable.

Another benefit of having created a rapid prototype was gaining experience of tolerances. The tolerances given to the holes through which some of the components protrude were too generous. This design flaw was due to inexperience and was rectified for further designs.

Building the rapid prototype was a valuable exercise and led to improved future designs. Some of the lessons learned were invaluable and the time and cost of building the final housing was greatly reduced as a result.

7.5 Injection Moulding

Injection moulding is the process that moulds plastic through heat and pressure, by injecting molten plastic polymer into the desired mould. It is the most commonly used process for moulding plastics because it gives a good surface finish and can be used for very complex mouldings. Injection moulding, although being a relatively expensive process, becomes very economically viable in mass production and gives a very low unit production cost. Injection moulded plastics are invariably thermoplastics because thermosetting plastics assume their final shape through heat and so cannot be moulded with this process. Familiar products manufactured by injection moulding include: computer enclosures, milk crates, CD cases and mobile phones.

The plastics that are used in injection moulding include: polythene, low-density polyethylene (LDPE), high-density polyethylene (HDPE), polystyrene (PS), polypropylene (PP) and acrylonitrilebutadienestyrene (ABS). Further information on injection moulding can be found in *How to make Injection Molds* [54].

7.5.1 Reaction Injection Moulding

This is a low-pressure injection moulding technique where low viscosity (liquid) monomers are mixed as they enter the mould. Mould pressures are typically very low for this technique. This is a relatively new injection moulding technique that is still being developed [55]. RIM differs from conventional thermoplastic injection moulding because it uses polymerisation in the mould rather than cooling to form a solid polymer. In RIM the pressure and temperature are low but the impingement mixing activates the reaction.
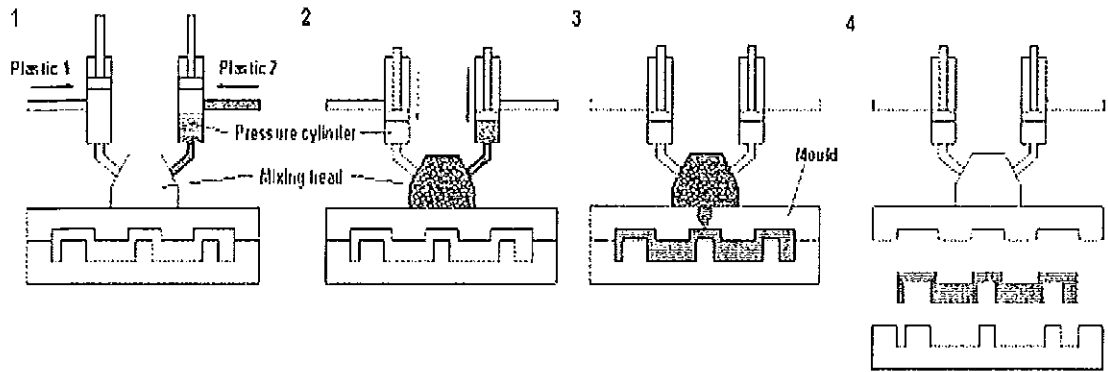
Figure 7.6: Four stages of the RIM process.

There are four main stages to in the RIM moulding process as shown in figure 7.6.

• Stage1: Two or more liquid reactants are stored in separate pressure cylinders. The most commonly used materials are polyurethanes. In the pressure cylinders the same hydraulic arm is used to fill the cylinders by suction as is used to empty them in stage 2. The cylinders also ensure that the correct amount of each reactant is used and are usually computer controlled.

• Stage2: The reactants are then pumped at pressures ranging typically from 1500 to 3000psi into a mixing chamber. Here they impinge at high velocity and begin to form the polymer

• Stage3: As the mixture begins to polymerise they flow into the mould cavity. The mixture is at a lower temperature compared to that of the mould and as the viscosity is initially low only low pressure is needed to fill the mould. This is contrary to other moulding techniques where polymer melt that is much hotter than the mould is injected into the mould at high pressure.

• Stage4: Once it cures, polymerises and solidifies sufficiently it can be de-moulded. Due to the low temperature of the mixture entering the mould this can be done quicker than in other injection moulding processes.

There are a number of benefits of using RIM over other injection moulding techniques. Some of the main advantages arise from the fact that the mould is filled with low viscosity liquid at low pressure. This means that larger and more complex shapes can be made. The low pressure also means that mould clamps can be smaller and are cheaper to make. The lighter weight and lower cost of moulds means that

production time is shortened to the extent that RIM can in some cases be used for prototype applications. It was for this reason that this process was chosen for the purpose of building the housing for this device.

There are also disadvantages of RIM that arise due to its low viscosity. Low viscosity liquids can penetrate mould surfaces leading to mould release difficulties especially at high viscosity. Another problem is that gas bubbles can become trapped during filling. This is a problem that was experienced in the production of the housing for this device. Numerous indentations formed by bubbles in the liquid mixture appear in the final housing part. In RIM nitrogen is added to one of the reactants. In the metering cylinders the gas is compressed, bubbles collapse and dissolve. In the mixhead the pressure drops and the bubbles grow again as they flow into the mould. Any bubbles still in the mould when the liquid gels are trapped. Addition of a liquid elastomer can be used to control the formation of these bubbles. Mould temperature also affects the size of the bubbles and can be used to control the damage done by such bubbles. Further information on RIM can be found in *Fundamentals of RIM* by Christopher W.Macosko [56].

A final year student as his final year project conducted this part of the project. On completion of his design it was decided that he get it made using RIM by a company called FF-Polymers in Drogheda. This design was then to be compared to another design made using the vacuum forming method. The two designs vary greatly in both shape and cost of manufacture. These factors, along with how the parts looked when assembled, would influence which design would be proposed for use as the finished product.

Figure 7.7a and 7.7b show what the RIM housing looks like when fully assembled. The housing is made in two molded parts from a material called NYRIM. Nyrim is a specially developed plastic for the RIM process. It is a rubber toughened recyclable nylon thermoplastic. Varying the ratio of raw materials in the formulation can vary the amount of rubber in Nyrim from 10% to 40%. A typical formulation is NYRIM1500, which contains 15% elastomer. Reinforcement fillers and other additives can also be included in the formulation to obtain the required material properties. Metal inserts and glass or carbon fiber can also be moulded into or encapsulated in Nyrim to optimize part properties.

Benefits of Nyrim

- High strength to weight ratio material.
- Exceptional toughness.
- Excellent impact properties.
- Good dynamic properties.
- Working temperature range -40C to 120C.
- High abrasion resistance.
- Corrosion resistant.
- Good chemical resistance.
- Cost effective tooling for low volume production.
- Large complex components can be produced.
- Various material colours available.
- At FF Polymers Ltd. the maximum part weight mouldable is 20Kg.
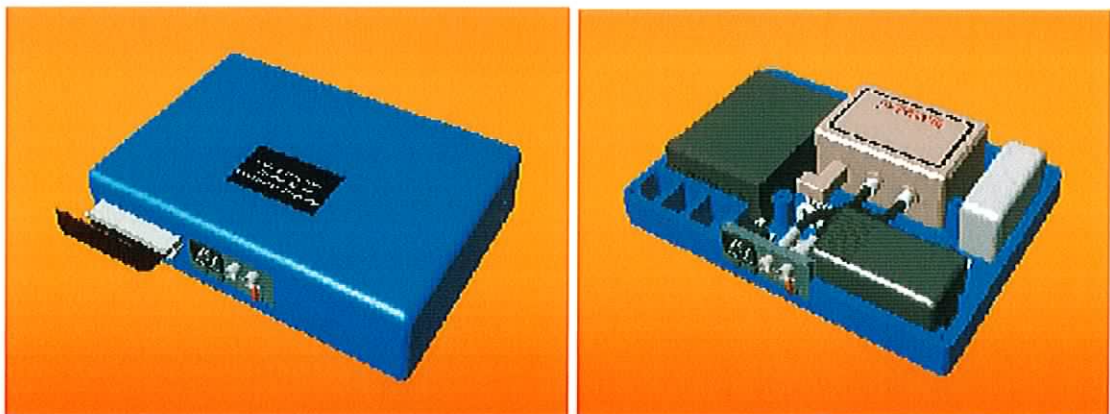
Figure 7.7a: Sketch of finished Nyrim housing.

7.7b: Sketch of bottom part of Nyrim housing holding device components.

Figures 7.8 and 7.9 show the moulded parts and the mould itself. In figure 7.8 it can be seen where the screws are placed that hold the part together. Some of the supports for holding the components in place within the device can also be seen. Figure 7.9 shows how both the top and bottom part are made simultaneously from the same mould. The top half of the mould creates the outer sides of the parts while the bottom half of the mould creates the inner parts of the mould. Figure 7.10 shows how the mould looks when the top and bottom halves are placed together.
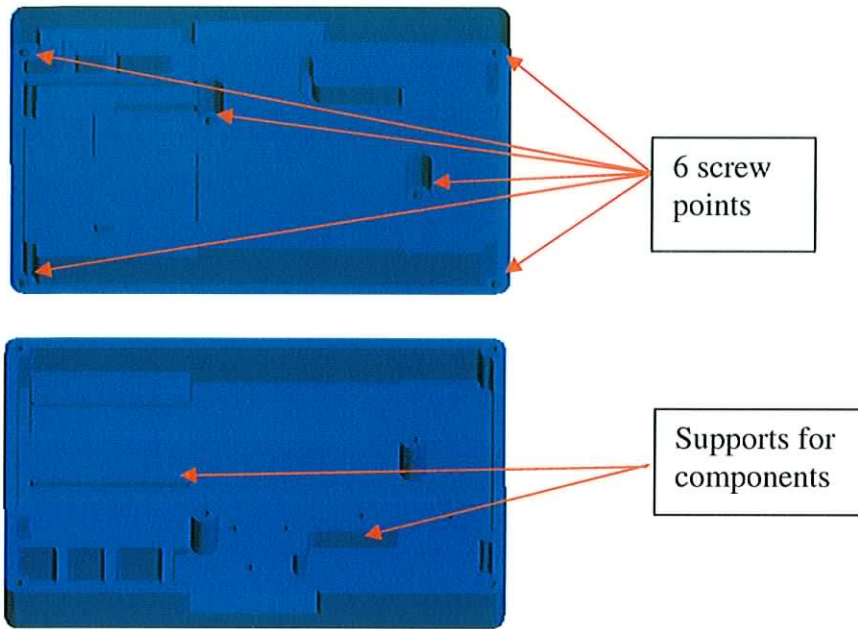
Figure 7.8: The Moulded NYRIM parts. The top part fits onto the bottom and they are held in place by screws.
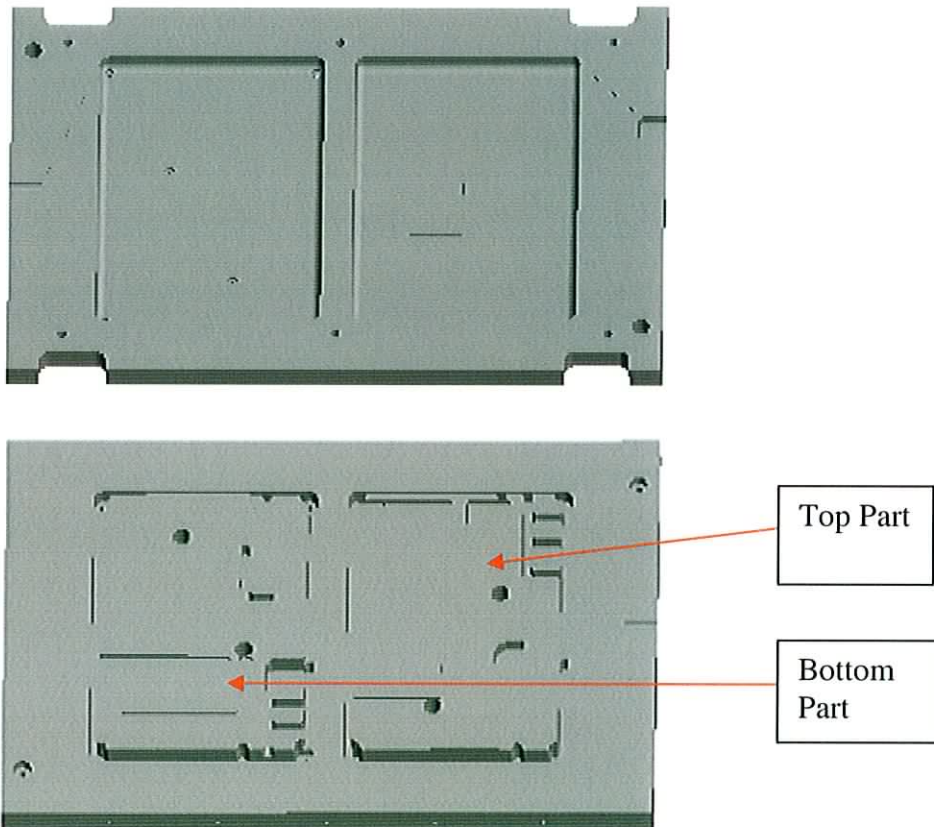
Figure 7.9: The Machined Aluminium Mould. The top piece moulds the outside of the top and bottom parts of the housing while the bottom piece moulds the inside.
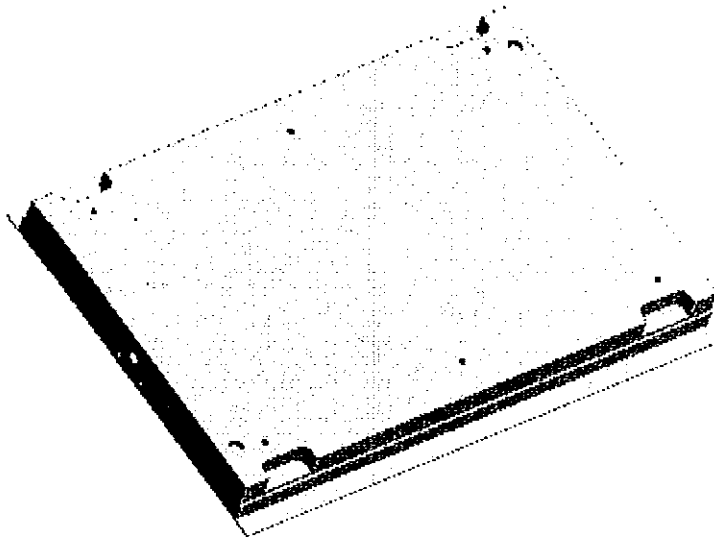
Figure 7.10: The Aluminum Mould.

While this design provides a secure housing for the components there are a number of design flaws. These create the undesirable effects of complicating manufacture and increasing cost.

One of the main problems with the design is that it consists of two parts that must be moulded. Because of this the size of the mould is almost doubled from that of a single part design. Figure 7.9 shows a sketch of the mould design used. It can be seen that on the top and bottom parts of the mould there are two cavities, one for the top part of the housing and the second for the bottom part of the housing. This increase in size will greatly increase the cost of manufacture due to the high costs of the raw materials, machined aluminum, for the mould.

Problems also arise from the fact that the two parts must also fit together. However the design does not include a lip to provide support or lock the two pieces together as is described in figure 7.11a. Instead, the two parts are simply held together by screws. Slight variations in the wall heights due to the shrinking properties of the Nyrim cause the two pieces not to sit perfectly flush with one another as shown in figure 7.11b.

118
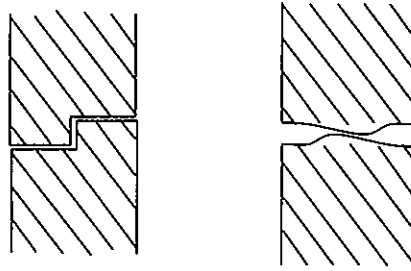
Figure 7.11a: Sketch of how the walls of the housing might join for better support.
7.11b: Sketch of how the walls actually join, providing little or no support.

Another problem with this design is that it requires a number of smaller parts as well as the two main moulded parts. These include a front panel where the electrical and pneumatic input and output connections are held in place. There is also an internal electrical adapter for connecting the electrical components. These pieces must be specially constructed to fit the housing.

As discussed earlier the indentations formed by the nitrogen bubbles deteriorate the finished surface of the housing. Adding a liquid polymer and varying the temperature can rectify this but it may take some trial and error to get the surface finish perfect. This adds further cost and creates a further headache for manufacturing. For this reason and the reasons mentioned above it was decided that this method would not be continued but that the vacuum forming method would be used instead.

7.6   Vacuum Forming

Vacuum forming [57] is a process in which a thermoplastic sheet is heated to a pliable state and then placed over a mould and drawn into the mould to the desired shape of the finished part through vacuum suction. Recent engineering advancements in thermoplastic materials have greatly contributed to the production of parts and prototypes by vacuum forming techniques. Since small volumes do not justify using conventional tooling methods vacuum forming allows a manufacturer to penetrate a small volume market effectively. For this reason, this method of production was the final method chosen for this project.

The first step in making a vacuum formed part is creating a master pattern to produce the mould. The pattern is positioned as needed and a framework is constructed to shape the outside of the mould. Once the mould has set, it is then mounted on a back plate and vacuum holes are drilled through the mould and around

119

the periphery of each pattern. This allows the heated plastic sheet to be pulled completely over the mould to ensure an accurate finished part.

After preparations of the mould have been completed, it is ready to perform the vacuum forming process. The plastic sheet is placed over the mould and clamped into place. A vacuum is then applied from beneath the mould and the heated plastic drawn down into the cavity. After the plastic has been allowed to cool, the clamps are taken off and the formed sheets are removed from the mould, then the individual moulded parts are cut out.

Vacuum forming is used in a variety of different industries. The automotive industry uses vacuum forming to produce automotive trim as well as some interior components. The consumer products industry can make products ranging from plastic glasses to food containers by using the vacuum forming process. On a larger scale, vacuum forming is used to produce many of the signs for service stations and convenience stores. Vacuum forming is also used in a variety of applications in the aerospace and medical industries and is a widely used packaging technique.

Vacuum forming is a very cost effective method for producing small or large quantities of moulded plastic parts. By incorporating rapid prototypes into the vacuum forming process, parts can be produced on a high quantity basis for a relatively low cost, thus saving both time and money.

With the limited funds available to this project and with the injection moulding method already tried this method was the most sensible choice. Consort Case Company Ltd in Co. Kilkenny agreed to make the moulds and parts. A new design was developed that took advantage of certain aspects of the vacuum forming method. The ease with which certain shapes and designs can be made by vacuum forming had some effect in the final design of the housing.

7.6.1 Design considerations:

In a similar way to the rapid prototype the vacuum forming design consists of a single formed part that covers a base plate that holds the components of the device. This type of design has the major advantage of being less expensive to manufacture than a multiple part design. The majority of the support for the device comes from the sturdy base plate so the wall thickness of the formed part can be slightly less allowing a further decrease in cost.

Having learnt some valuable lessons from the rapid prototype it was decided to make the vacuum formed part less tall and a lip was also incorporated in to provide extra support at the base plate and provide an improved platform for screwing the two parts together. This lip can be seen in figures 7.12 and 7.13. The lip allows screws to be placed through the housing from the side into the base plate as opposed to the case in the rapid prototype where the screws were attached through the base plate into the housing from below, providing less strength. The lip also provides more structural strength along the lower edge of the housing than would be the case with just a straight side. The bend in the ABS plastic creates a stiffer shape than a simple flat piece of the same material.
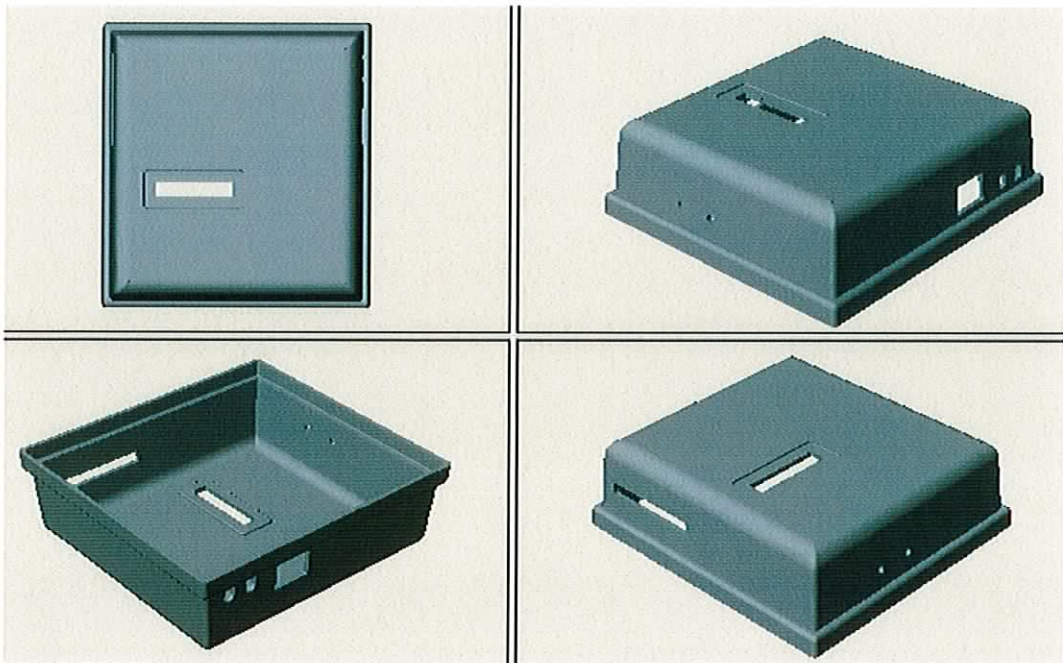
Figure 7.12: Sketch of the ABS vacuum formed part.
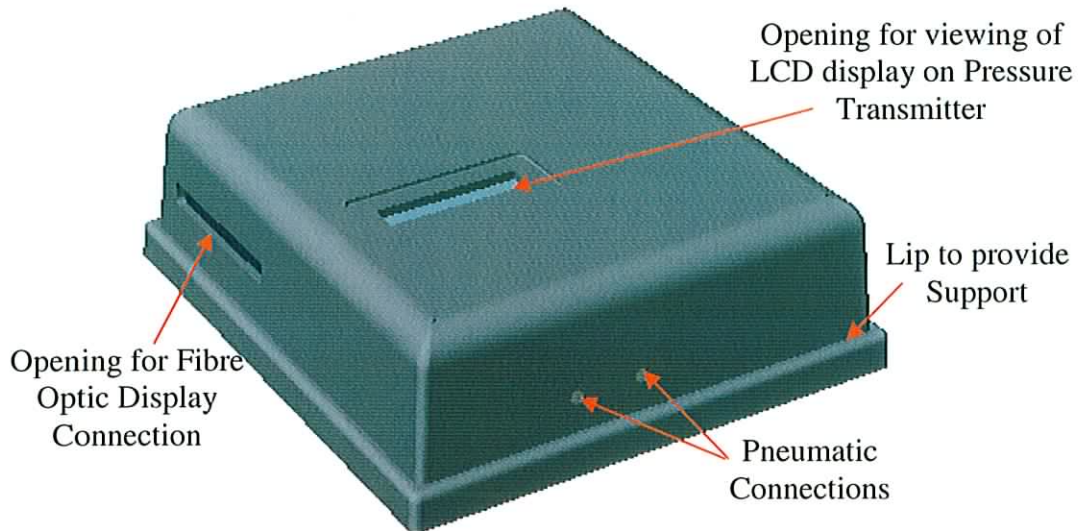
Figure 7.13a: Sketch of the Final Vacuum Formed Housing.

Figure 7.13b: Photo of the Final Vacuum Formed Housing.

A wooden mould was used for the vacuum forming process. Wood has the advantage of being a cheap material and is simple to machine. The lip and the other edge radii are relatively easy to produce on the wooden mould and can then be formed without difficulty using vacuum forming. This allows for an aesthetically pleasing part to be made. As well as providing support the lip also adds to the aesthetic value of the housing.

The wooden mould was made from two separate parts. First there is the simple rectangular base piece that forms the lip. On top of this is attached the more detailed piece which determines the edge radii and the indentation at the top of the device where the cutout for viewing the pressure transmitter LCD display is located. These two pieces were simply glued together. Such moulds will produce in the region of 50 – 100 parts in their lifetime. If required a metal mould can be made and used in the

vacuum forming process for large-scale production. Figure 7.14 shows a photograph of the mould mounted on its back plate. The back plate holds the mould in place during the vacuum forming process. The vacuum-forming machine can be seen in figure 7.15.

Two separate parts glued together.
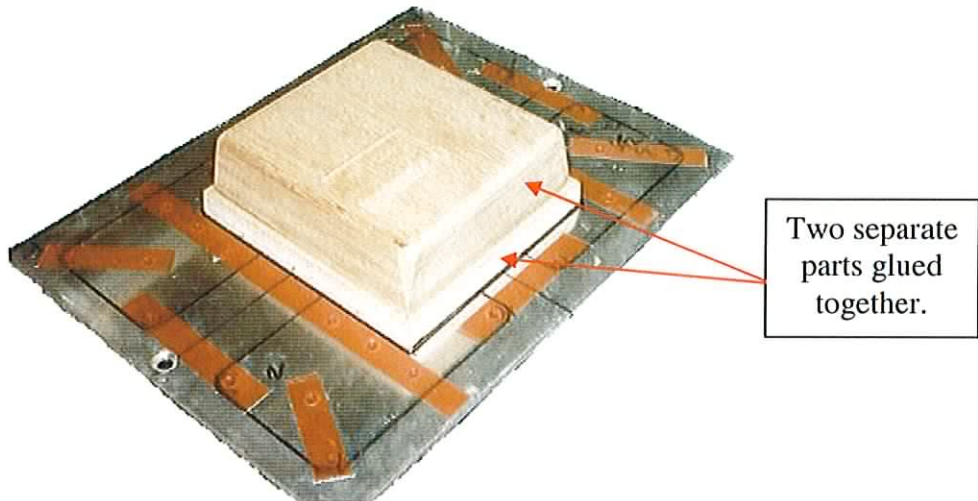
Figure 7.14: Wooden Mould and Mount For Vacuum Forming.

Back Plate is positioned here.
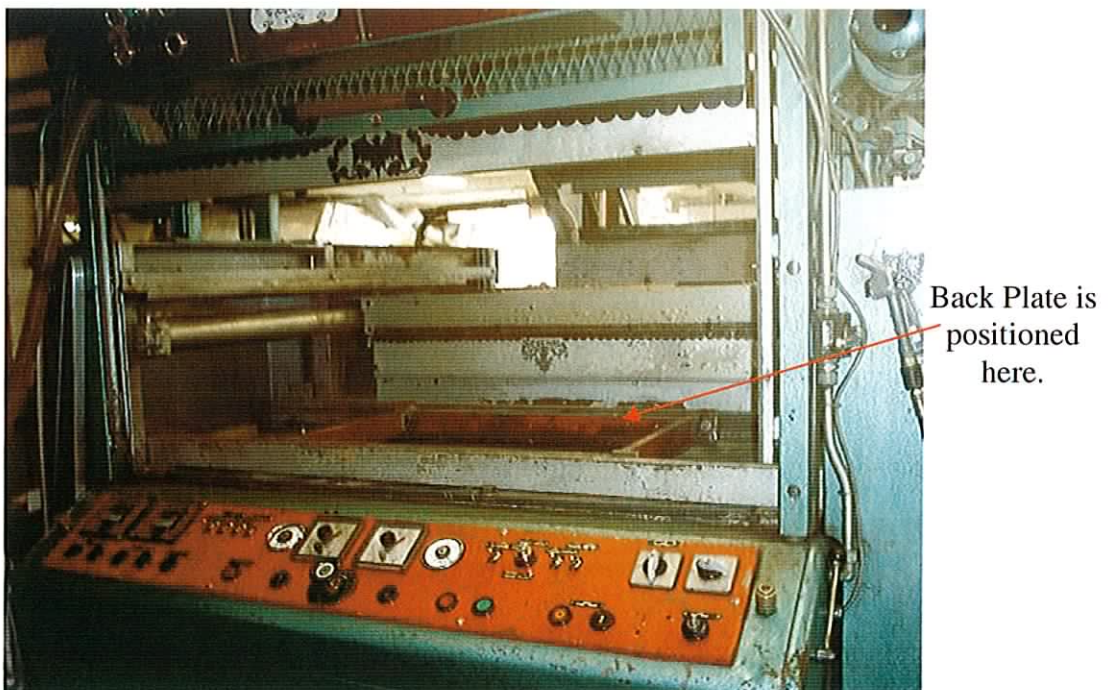
Figure 7.15: Vacuum Forming Machine in Consort Case Company Ltd.

In order for the vacuum forming to work air vents must be placed at regular intervals in the mould to allow the suction of the plastic onto the mould. These air

vents are tiny holes ranging from 0.2mm to 1.0mm in diameter. The diameter varies according to the amount of suction required to form a particular section of the part. Holes are required at corners and along edges and are usually spaced approximately 50mm apart depending again on the intricacy of the section they are needed to form. Figure 7.16 shows the dimensions of the wooden mould and the red spots indicate the location of the air vents through the mould. The most difficult part to form is the indent that forms the lip. This is why the holes are densely spaced around this edge. For a better finish the two pieces of the wooden mould could be attached but held at approximately 0.5mm apart. This is the equivalent to having a single large air vent around the entire inner edge of the lip.
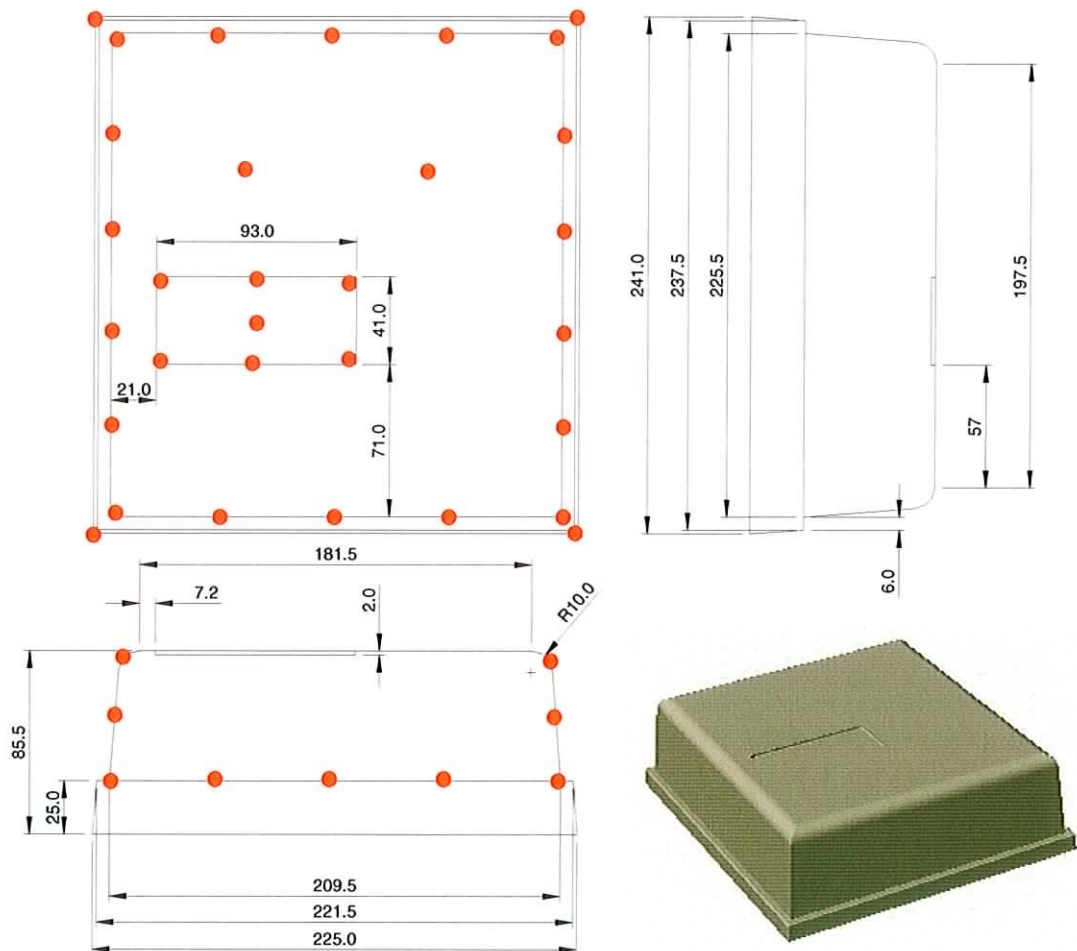
Figure 7.16: Wooden Mould Dimensions and Air Vent Location.

Both male and female moulds can be used if required. A mixture of vacuum and pressure forming can be used to form more intricate shapes. In this case it is a male mould that is used to control the inside of the part; wall thickness variations are to the

outside. Pre-textured ABS plastic was used to give an attractive outside appearance. As it is a male mould the outside radii on the surface of the material are larger as wall thickness stretches around the mould's features.

Figure 7.17 shows the dimensions of the part itself once formed.

- The dimensions of the housing are 228x * 244y * 77z mm.

- The base plate dimensions are 220x * 236y * 12z mm.

- Wall thickness is 4mm.

The cut outs for the fibre optic, electrical and pneumatic connections were carried out post forming. These cutouts were done by hand in this case because of the small number of parts required. However this may be done by machine in the case of larger scale production.
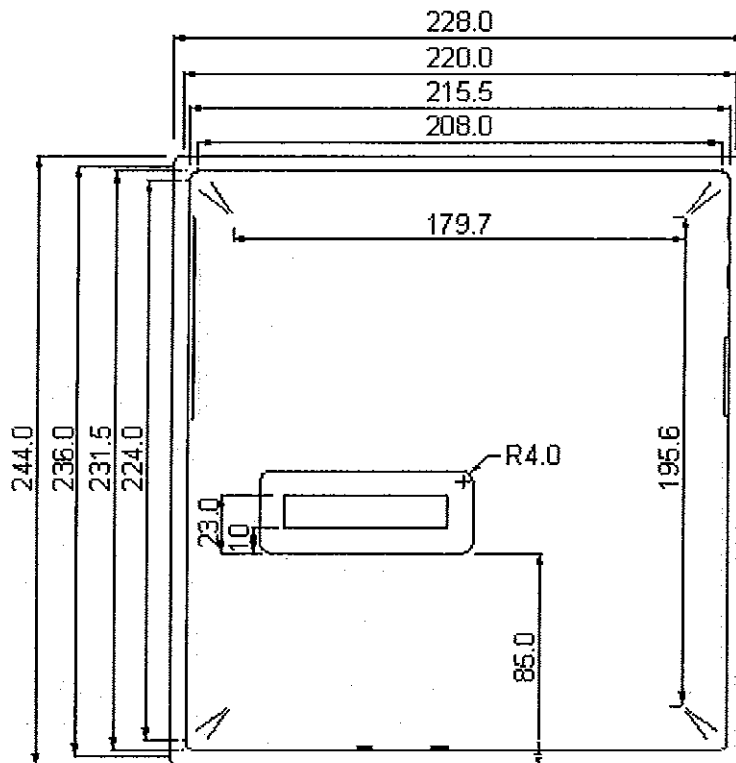
Figure 7.17a: Top view of the Vacuum Formed housing showing dimensions in mm.
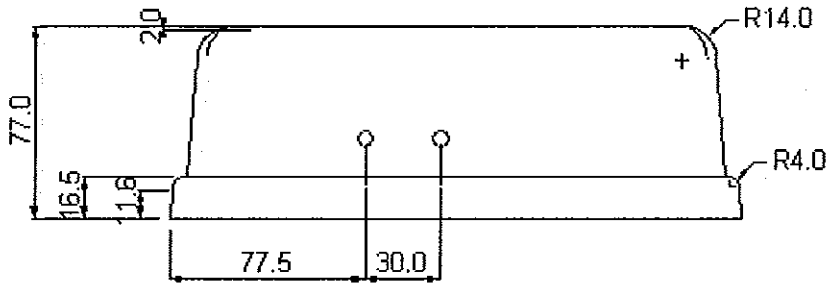
Figure 7.17b: Front view of the Vacuum Formed housing showing dimensions in mm. Wall taper = 5 degrees.
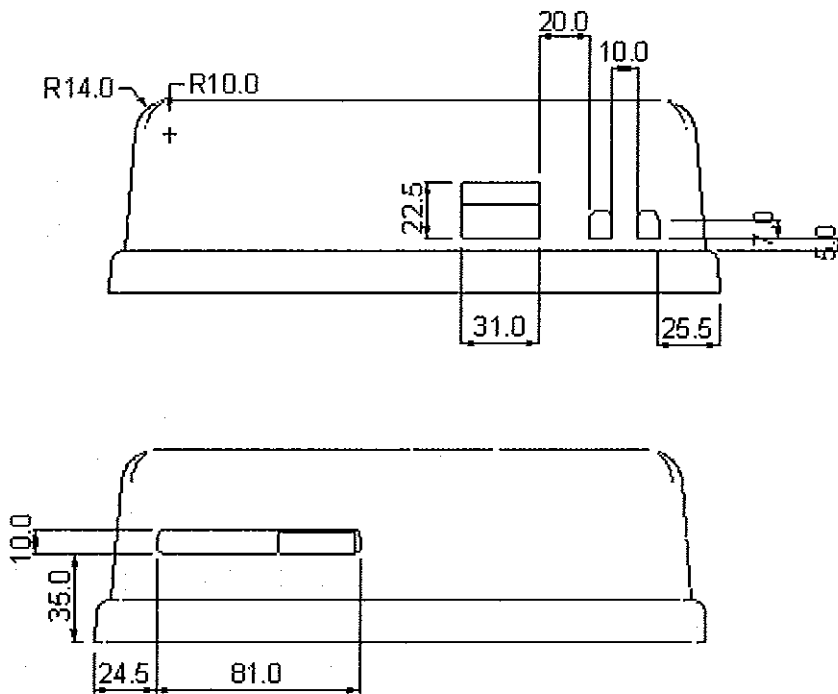
Figure 7.17c: Right and Left views of the Vacuum Formed housing showing dimensions in mm.

The design was made as small as possible while still leaving room to hold the components. However this means that the location of the cut outs must be accurate as there is very little room to manoeuvre the components within the device. Figure 7.18 shows the location of the components within the housing. From this it can be seen how the housing fits over the components to reveal only the required displays and out ports.
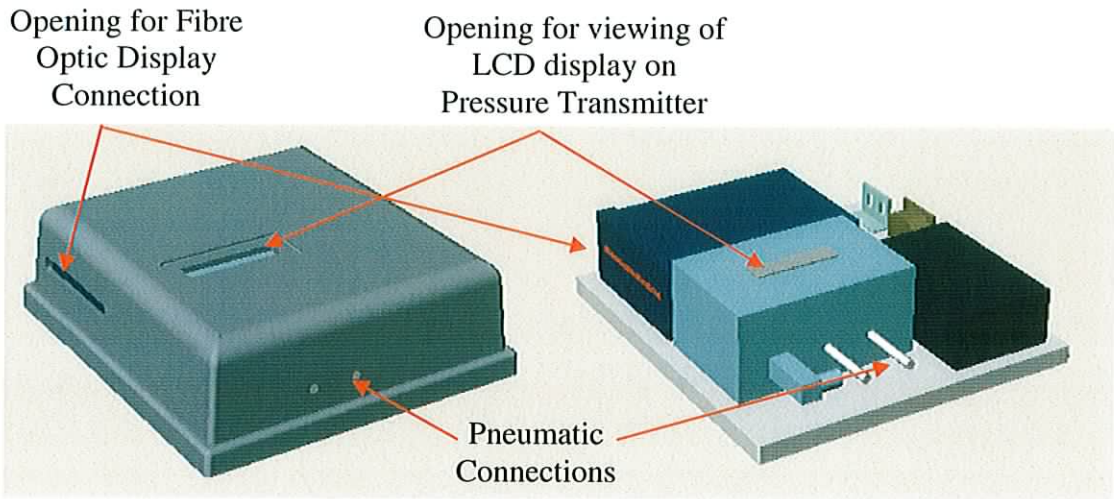
Figure 7.18: Location of the components within the housing.

Figure 7.19 shows the location of the holes for the brass inserts that hold the components in place on the base plate. Also shown (in yellow) are the holes for the feet. These are on the underside of the base plate. All holes are 5.6mm diameter and 8mm in depth. These are designed to hold a TR4 brass insert for 4mm diameter screws. The brass inserts provide a secure thread for the screws that hold the components in place.
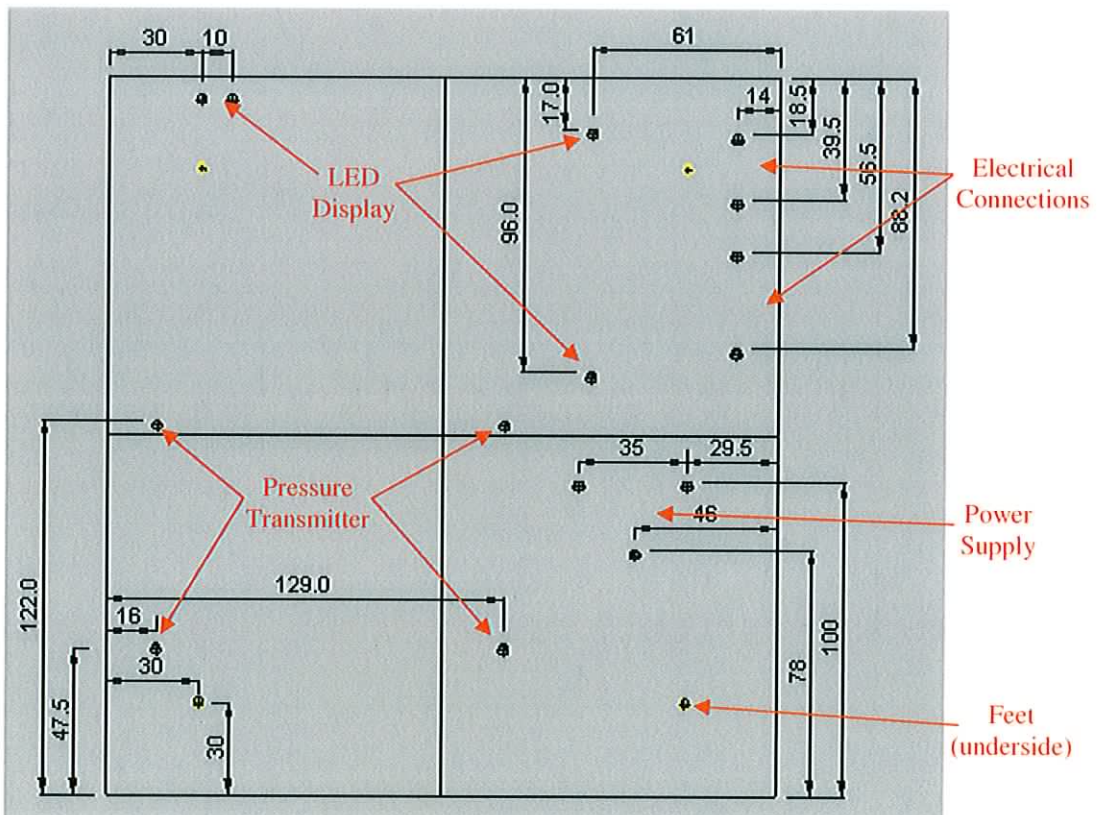
Figure 7.19: The location of the holes for the brass inserts on the base plate.

7.7 Conclusion

The housing for the device is one of its most important parts. It not only provides protection for the components within it but also provides protection to the user against electrical shocks. It must be aesthetically pleasing as it is the housing that is seen by the user. Through research, design and prototyping it is thought that a suitable design has now been made. Different manufacturing techniques were tested but it was decided that the vacuum formed part was the superior and least expensive design. This is a cost effective and modern looking design that caters for the requirements of the device.

8 CE MARKING & MEDICAL DIRECTIVES

8.1 Introduction

The respiratory monitor that has been developed during the course of this research is a medical device. In order to place such a product on the market within the European Union (EU) it must first conform to a set of requirements that allows the manufacturer to place the CE Marking upon it. As part of the research and design of the device these requirements were taken into account so that once completed the CE marking could be applied to the device. This chapter discusses some of the reasons for the CE marking and how it is acquired for medical devices with particular focus on the medical devices directives (90/385/EEC) and (93/42/EEC) and how the requirements affect this respiratory monitoring device.

8.2 Medical Devices Directive (93/42/EEC)

The main purpose of directives is to bring about the completion of the single market by introducing harmonized controls to regulate the safety and marketing of products throughout the EU. The Medical Devices Directives set out essential requirements to ensure that a medical device will not compromise the health and safety of the patient, user or any other person, and that any risks associated with the device are still compatible with patient health and protection. Devices that conform to these requirements are entitled to apply the CE Marking, which allows the product to be freely placed on the market within the EU. There are three medical device directives, the Active Implantible Medical Devices Directive (90/385/EEC), the Medical Devices Directive (93/42/EEC) and the In Vitro Diagnostic Devices Directive (98/79/EEC) (IVDMDD). The device developed in the course of this research is neither an active implantible nor an in vitro diagnostic device; therefore it is subject to the Medical Devices Directive (93/42/EEC).

A Medical Device is defined in Directive (93/42/EEC) as; any instrument, apparatus, appliance, material or other article, whether used alone or in combination, including the software necessary for the proper application, intended by the manufacturer to be used for human beings for the purpose of:

- diagnosis, prevention, monitoring, treatment or alleviation of a disease, an injury or a handicap.

- investigation, replacement or modification of the anatomy or of a physiological process.
- control of conception.

Therefore, as the device developed in this research is a respiratory monitoring device it follows that this is a medical device under the first point. The Directive gives additional definitions of relevant devices and terms.

Under the terms of the Medical Device Directive a competent authority is nominated by the Government of each member state to monitor and ensure compliance with its provisions. The Competent Authority is responsible for:

- designating Notified Bodies to carry out conformity assessment procedures.
- handling applications for clinical investigations.
- ensuring adverse incidents are reported within appropriate time scales and evaluated.
- the withdrawal of unsafe devices from the market.
- effecting the Directives into law through statutory instruments.
- ensuring only those devices bearing the CE marking are allowed onto the market.

Medical devices, bearing the CE marking, are presumed to conform to the appropriate essential requirements, unless there is reason to believe otherwise. Should this be the case, the Competent Authority will take appropriate measures, which may include withdrawal from the market. The Competent Authority must inform the European Commission of any enforcement action taken. The Department of Health [58] is the Competent Authority in Ireland for the Medical Device Directive.

The National Standards Authority of Ireland (N.S.A.I.) [59] is the EU Notified Body designated for the purposes of the Medical Devices Directive (93/42/EEC) on 4th August 1994. It is a certification organisation, which the Competent Authority, of a Member State designates to carry out one or more of the conformity assessment procedures described in the annexes of the Directives. Therefore it is through the NSAI that one seeks to obtain the CE Mark. However it is not necessary to go through the NSAI for the lowest class of medical device, Class I, as is discussed later.

8.3   Purpose and Philosophy of Medical Device Classification

The conformity assessment procedures are the routes available under the Medical Devices Directives, for manufacturers to demonstrate that their devices meet the essential requirements, thus enabling the CE marking to be affixed to the device. Having classified the device according to its properties, function and intended purpose, devices are assigned to one of 4 Classes:

Class 1   -   low risk devices

Class II(a) and Class II(b)   -   medium risk devices

Class III   -   high risk devices

It is not feasible economically nor justifiable in practice to subject all medical devices to the most rigorous conformity assessment procedures available. A graduated system of control is more appropriate. In such a system, the level of control corresponds to the level of potential hazard inherent in the type of device concerned. A medical device classification system is therefore needed, in order to channel medical devices into the proper conformity assessment route. The main purpose is to allow the strictest controls to be applied only to those devices that present the greatest risk to health or safety.

A simple set of classification rules based on technical features of medical devices is impossible, because of the vast number and the changing nature of variables involved. The human body, however, is a relatively unchanging element of the equation. Therefore a classification concept was established, which uses a small set of criteria that can be combined in various ways: duration of contact with the body, degree of invasiveness and local versus systemic effect. These criteria form the bases of the Class system shown above.

It is recognized that although the existing rules will adequately classify the vast majority of existing devices, a small number of difficult cases may arise. Such cases may in particular include the determination of the borderline between two classes. In such cases the manufacturer must request clarification from the notified body.

8.4 Guide to CE Marking

The following guide is as laid out by the NSAI for achieving the CE Mark. Firstly the product must be classified and then the conformity assessment route must be decided. The procedures to follow are detailed in the Directive.

Generally a Class I device, which it will be shown, is what this device turns out to be, requires just internal control of production and compilation of a technical file. The technical file then has to be held in case of a request by a competent authority. The final step is self-certification and registration with a competent authority. These steps are carefully laid out by the NSAI as the Notified Body in Ireland. However, no matter what class, the following three steps are always followed as a rule.

Step 1 Classify the products according to Annex IX of Directive.

Step 2 Decide on the conformity assessment route (Annexes). The following options are open to the manufacturer.

Class I	Technical file and self declaration
Class I Sterile / Measuring	Annex VII + Annex V for Sterile / Measuring aspects
Class II a	Annex II Annex VII + V Annex VII + VI
Class II b	Annex II Annex III + V Annex III + VI
Class III	Annex II Annex III + V

Table 8.1: Conformity Assessment Route (Annexes) for the various Classes of Device.

Step 3 Follow the procedures detailed for the selected Annexes.

These steps have been followed for the respiratory monitoring device of this research. The following is the result:

8.4.1 *Step 1:*

This step requires that the product be classified according to Annex IX of the Directive. Within this Annex there are three classification criteria: Definitions, Implementing Rules, and Classification.

The definitions for the classification rules for the device developed during this research are as follows:

- Duration: This device is of Transient Duration, as it is normally needed for continuous use for less than 60 minutes. Short term (no more than 30 days) and long term (more than 30 days) do not apply here.

- Non-Invasive Device: The device is non-invasive as it does not in whole or in part penetrate inside the body.

- Non-surgical instrument: The device is non-surgical as it is not intended for surgical use by cutting, drilling etc.

- Active Medical Device: The device is an active medical device as it does depend on an external source of electrical energy. The power supply and LED both are fed by the electrical mains supply.

- Active Device for Diagnosis: The device does detect and monitor physiological conditions and therefore is an active device for diagnosis.

- The device is not however an Active Therapeutical Device, it does not deal with the Central Circulatory System and it does not deal with the Central Nervous System.

Hence the device can be defined as an Active Device for Diagnosis and is of Transient Duration.

The implementing rules for the device are as follows:

- The intended purpose of the device is to monitor a patient's breathing during an MRI scan with a view to improving the scan. It is this intended purpose that shall govern the application of the implementing rules.

- The device is to be used with an MRI scanner but the implementing rules shall apply separately to both. This is because the operations of both devices do not depend on each other.
- The software used with the device shall fall automatically into the same class. In this case the software used is Labview.
- The device is to come in contact with the patient solely in the upper abdominal and thoracic regions of the body. Therefore it shall be classified on the basis of its use in this region.
- If several rules apply to the device the strictest rules resulting in the higher classification shall apply.

These implementing rules are then used to help classify the device.

The Classification of the device is determined as follows:
- Rule 1 states that all non-invasive devices are in Class I, unless one of the later rules applies. Therefore as this device is non-invasive it will be in Class I unless a later rule applies to it.
- Rule 10 states that any active devices intended for diagnosis are in Class IIa if they are intended to allow direct diagnosis or monitoring of vital physiological processes. While this device does monitor the breathing cycle, the monitoring of the breathing cycle is not considered in this case to be vital, but simply an aid to improve the image of the MRI scan. Hence Rule 10 does not apply.
- Rule 12 states that all other active devices than those mentioned in Rule 11 are in Class I. Rule 11 states that any active medical device intended to administer and/or remove substances to or from the body are in Class IIa. As this device is not intended for such use Rule 11 does not apply. Therefore Rule 12 applies.
- No other rules apply to this particular device

Therefore, Rule 1 and Rule 12 deem that the device developed in the course of this research shall be classified as a Class I device. This classification is shown in flowchart format in Figure 4.1.

8.4.2 *Step 2*

This step requires that the conformity assessment route be decided. From Table 8.1 above it can be seen that Annex VII and Annex V are the relevant Annexes to Class I devices. However Annex V only refers to Medical Devices with a sterile or measuring function. This device does not have a measuring function as it does not fulfil criterion c) of MedDev 2.1/5 (Definition of Medical Devices with a Measuring Function)[60]. This criterion states that the intended purpose of the device must be sufficiently accurate where the accuracy of the device could result in a significant adverse effect on the patient's health and safety. There is no such risk involved in this device and hence Annex V is not relevant.
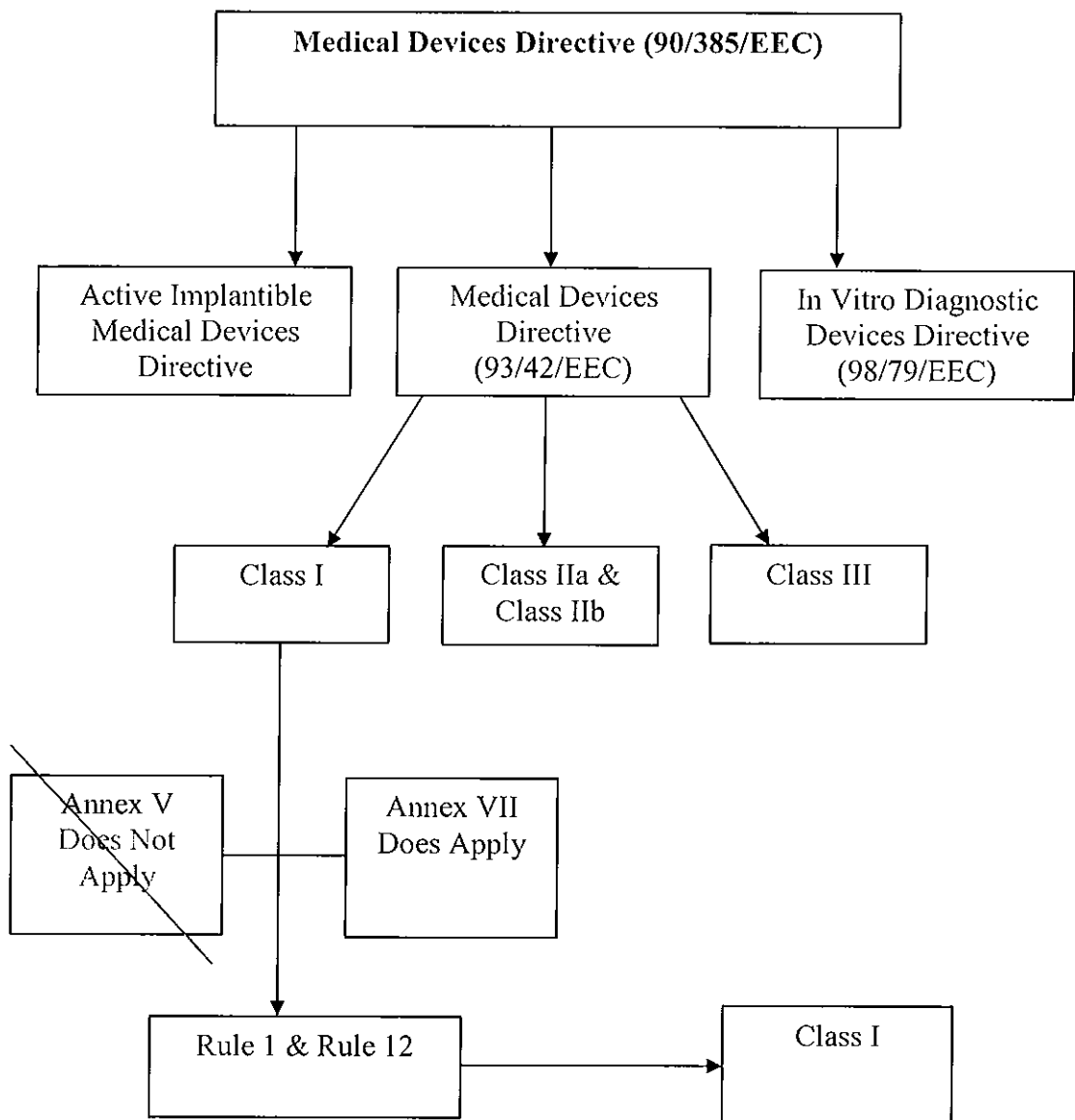
Figure 8.1: Flow Chart for the Classification of the Device.

135

8.4.3 _Step 3_

This step requires that the procedures detailed for the selected Annexes be followed.

Declaration of Conformity

Annex VII is the EC declaration of conformity. This is the procedure whereby it must be ensured and declared that the products concerned meet the provisions of this Directive that apply to them. A technical documentation that allows assessment of the conformity of the product with the requirements of the Directive must then be prepared. It must include in particular:

1. a general description of the product, including any variants planned,

2. design drawings, methods of manufacture envisaged and diagrams of components, sub-assemblies, circuits, etc.,

3. the descriptions and explanations necessary to understand the abovementioned drawings and diagrams and the operations of the product,

4. the results of the design calculations and of the inspections carried out, etc.; if the device is to be connected to other device(s) in order to operate as intended, proof must be provided that it conforms to the essential requirements when connected to any such device(s) having the characteristics specified by the manufacturer,

5. the test reports and, where appropriate, clinical data,

6. the label and instructions for use.

The technical document for this device can be found in the appendices of this thesis.

Annex I deals with the essential requirements for any medical device and the relevant requirements were followed and met. These requirements include the general requirements, which are a general guideline for manufacturing, and they also include the design and construction requirements, which are more specific.

General Requirements

The Directive lays down some general requirements. These are simply a general guideline to follow for basic, good practice in the field of manufacturing with a view to medical devices. They are:

- The device should be designed and manufactured in such a way that when used under the conditions and purposes intended, they do not compromise the clinical condition or safety of the patients or users.

- The design and construction of the device should conform to safety principles.

- The safety characteristics should not be adversely affected by stresses, which can occur during normal conditions of use.

- The device characteristics should not be adversely affected by transport and storage.

Requirements Regarding Design And Construction

- Chemical, physical and biological properties

    The choice of materials used, particularly with regard to toxicity, guarantee the characteristics stated in the general requirements above. The only part of the device that may come in contact with the skin is the bladder and the chest-strap. The device is to be used only on unbroken skin. Therefore the materials used were chosen so as to not irritate the surface of the skin. The bladder and the tube leading from it are made from medical grade silicon rubber. The strap is made from polypropylene nylon and cotton. The nylon strap is the same as straps already used in MRI units to hold the radio frequency coils around the patient. Cotton is hypoallergenic meaning it doesn't irritate sensitive skin or cause allergies. Cotton is a natural product and does not contain any chemicals. This part of the device is the only part that may come in contact with the patient. The patient wears a gown during the scanning process so it is unlikely that even this part of the device will come in contact with the patient's skin. These parts can be detached and packaged separately and can be easily replaced in the case of a contamination. The design and manufacture of the device minimises the risk posed by contaminants and residues to the persons involved in the use of the device. The device has been designed with respect to the nature of the environment in which it is to be used. Within the MRI environment there are no ferrous or electrical components. All the materials used are invisible to magnetic radiation as discussed in the declaration of conformity above.

- Construction and Environmental Properties

The device is to be used with an MRI scanner. The system, including the connection system, is safe and does not impair the specified performances of the devices with which it is used. This is discussed in the technical file for the Declaration of Conformity.

The risks connected to physical features and foreseeable environmental conditions are minimum. The device should not pose any physical danger to the patient or user. There are no sharp edges on any part of the design that could cause harm. The design is lightweight and should not pose any direct threat to those who use it.

The manufacturing method for creating the housing for the electrical part of the device and the fibre optic display was vacuum forming as described in chapter 7. This method uses suction to form a heated plastic sheet over a wooden mould. The part is then cooled before sections are cut out according to the design.

The risk of toxic materials coming in contact with the surface is minimised as the plastic sheets are taken from their packaging and placed on the vacuum-forming machine. After the forming process the parts are stored before the cut out stage and then finally packaged. The parts will be packaged in cardboard boxes filled with foam pellets. In the case of materials such as machine oil coming in contact with the part the ABS plastic used can be easily cleaned. The ABS housing is located outside the MRI room in the control room and does not come in contact with the patient at any time.

The fibre optics used are acrylic optical cables sheathed with special fluorine containing polymer. These are made and distributed in 20m sections by Farnell Ltd. They are later cut to a length of ten metres using a special blade. The fibre optic plug is made from a piece of polyacetalhomopolymer (POM-H). This is drilled with 2.3mm diameter holes into which the fibre optic cables are glued. The plug is attached to the core of the device with a screw mechanism. Once assembled the parts can then be cleaned. The fibre optics, the display case and the plug do not come in contact with the patient at any time.

The bladder and its connecting tube are made from medical grade silicone. The belt in which the bladder is held consists of a nylon strap and a cotton case for the bladder. The nylon strap is similar to straps already used on the MRI table to hold the receiver coils over the patient. The belt is attached over the gown of the patient around the thoracic area.

- Protection against Electrical and Mechanical Risks

  The device has been designed and manufactured in such a way as to avoid the risk of accidental shocks during normal use and in single fault condition. The terminals and connectors to the electricity supplies, which the user has to handle, have been designed to minimise all possible risks.

  The central unit of the device is stored outside the MRI room. It can be placed on the desktop, in a drawer or hung from a wall mount. This is the main part of the device and contains three main electrical components:

  o   Power Supply – Mascot Model 9922

  o   Pressure Transducer – Furness Controls Model FCO332

  o   LED System – London Electronics Model Bar-X

  These components all have the CE Marking and are connected according to the manufacturer's instructions. The Power Supply is an EN 60601-1 compliant power supply – it is medically approved guaranteeing electrical safety. Electrical protective earthing is also in place. The components are also EN 50081 and EN 50082 compliant providing further EMC protection. These standards for emission and immunity requirements apply to electrical and electronic apparatus intended for use in the industrial environment for which no dedicated product emission or immunity standards exist.

  The components and the electrical connections are securely fastened to a 12mm thick Ertacetal plastic plate. An ABS plastic housing then covers this. Once the housing is in place all electrical connections are covered providing further protection from electrical shock. The base plate sits on rubber feet lifting the device 5mm from the surface on which it sits. This provides electrical safety should a case arise where this surface is wet.

  This part of the device does not come in contact with the patient and does not require handling except for turning on/off by means of an isolator switch located on the mains cable. The bladder that is connected to the patient is connected to this part of the device by a pneumatic connector and silicone tube. There is absolutely no electrical connection between the electrical part of the device and the components that come into contact with the patient during the device's intended use. The fibre optic display is connected to the main part of the device by 10m polymer fibres and an Ertacetal Plastic connector providing no electrical connection.

139

Having classified the device and produced a declaration of conformity the DSF-8-01-01/11 form was completed and sent to the Irish Medicines Board (IMB). The IMB have agreed that the device is a Class I device by formal note which can be found in the appendices of this thesis. Following a further meeting with Ms. Maria Carleton in the IMB on the 11th February '03 the following recommendations are to be attached to this thesis for a future manufacturer of the project:

- For best practice – ISO 14971:2000 Medical Devices Application of Risk & Essential Requirement Checklist should be completed.

- Batch Testing – a large number of devices should be manufactured and tested before supply.

- A manufacturer review file should be drawn up to complete the declaration of conformity.

- Apply to the IMB for Registration.

- CE Marked product can then be placed on the EU market.

8.5 CE Marking of Conformity (Annex XII)

Should this device be taken further, to the production stage, the person responsible for marketing it must notify their address and the devices concerned to the IMB or to whatever Competent Authority applies to the location where they have their registered place of business.

The CE conformity marking consists of the initials 'CE' and takes the form shown in Figure 1:
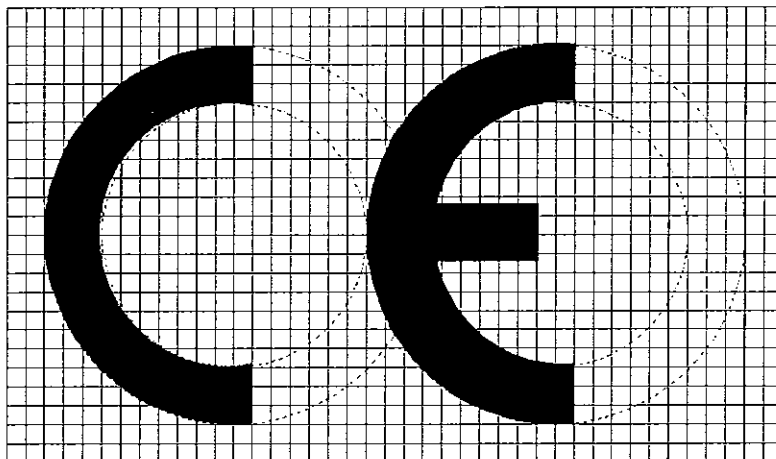
Figure 8.2: How to make the correct CE Mark symbol.

If the marking is reduced or enlarged the proportions given in the above graduated drawing must be respected. The various components of the CE marking must have substantially the same vertical dimension, which may not be less than 5 mm. This minimum dimension may be waived for small-scale devices

8.6 Conclusion

The CE Marking can now be applied to this device. However, should the device move onto the production stage there are a few further simple requirements that must be met as set out in the recommendations by the IMB. During the design and manufacture of the device the guidelines laid out by the Medical Devices Directive (93/42/EEC) have been followed. It has been determined that this is a Class I device and hence requires only internal control of production and a technical file. This file has been written up and must be held in case of request by a competent authority.

9 FIELD TESTS

9.1 Introduction

This device is for use with MRI scanners so it was necessary to carry out the field tests with such a scanner. The tests were carried out in the MRI suite in Waterford Regional Hospital under the supervision of Dr. Ian Kelly. A number of visits were made to the hospital during the course of the research. It was necessary to view the scanner in person so that measurements could be taken and ideas formulated. The final field test consisted of testing the operation of the device with the scanner to produce clinical data. The MRI suite is in high demand and it requires a number of staff to operate the scanner. In order to carry out the field tests the suite was opened after hours with some members of staff remaining behind to assist.

9.2 Initial Field Tests

To ensure that the results of all tests were accurate the equipment used was tested to ensure that there were no leaks. The pressure transmitter guarantees accuracy within 0.5% of the reading. The bladder was held under constant pressure for prolonged periods of time over which the signal did not deteriorate. With the device functioning correctly tests could then begin.

The initial prototype was given to the consultant radiologist involved with the project to carry out the offline tests on patients in the Waterford Regional Hospital as described in chapter 3. This consisted of testing the breath holding abilities of 10 patients before and after being taught with the device how to hold their breath correctly. The data collected was then retrieved from the consultant radiologist and the statistical analysis was carried out. This work was the basis for a paper co-written by the consultant radiologist and presented by him to the RSNA's international conference in Chicago in November '02. The abstract of this paper can be found in the appendix D.

The bladder was placed around the patient's chest and the patient was asked to hold their breath for 20 seconds without looking at the bargraph display or computer monitor. 20 seconds was chosen, as most patients are comfortable with holding their breath for this period. This is also the period of time that is required for most of the breath holding scanning sequences. The data was recorded at 3 samples per second giving a list of 60 data points. If the patients were to hold their breath perfectly there

should be a horizontal straight-line graph as the pressure in the bladder and hence the output voltage would remain the same.

Breath Holding - Pre

Breath Holding - Post
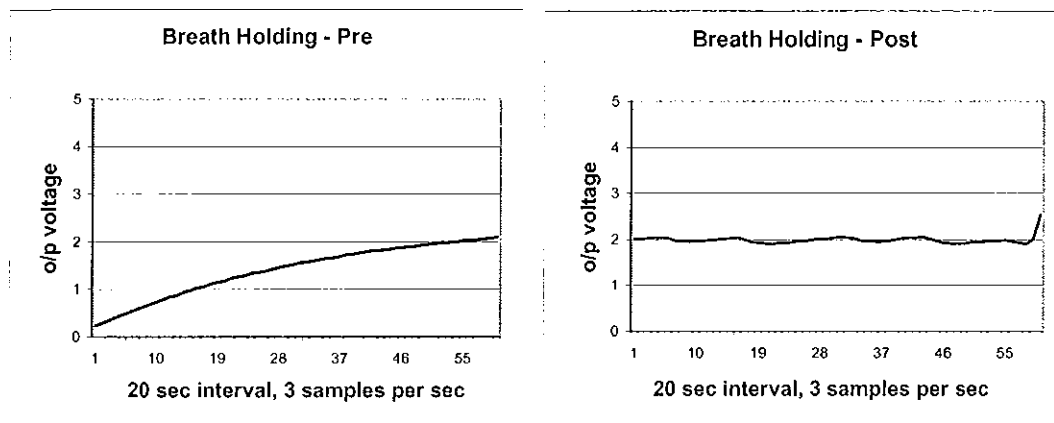
Figure 9.1a: Pre-experiment Data from 1 of the 10 patients.

Figure 9.1b: Post-experiment Data from the same patient.

Both holding breath for 20 seconds – 60 samples at 3 samples per second.

9.2.1 Statistical Analysis

A statistical analysis of the data recorded was then carried out to determine the difference between the pre and post experiment data. The following tables show the average and the standard deviation of the 60 data points collected from each of the 10 patients before using the device and after. The average was simply calculated using the following equation:

$$\text{Average} = \frac{\sum x}{n}$$ {9.1}

The standard deviation was calculated using the following equation:

$$\text{Standard Deviation} = \sqrt{\frac{n\sum x^2 - \left(\sum x\right)^2}{n(n-1)}}$$ {9.2}

Where n = number of elements (60),

and   x = elements from 1 to 60

2.110	1.884	1.024	1.759	1.376	1.786	2.328	1.270	2.236	1.749	Row1
0.210	0.269	0.388	0.343	0.457	0.515	0.064	0.509	0.291	0.380	Row2

Table 9.1: Average (row1) and standard deviation (row2) of the 60 data points for each patient before using the device. Units = Output Voltage, Volts.

| 2.552 | 2.181 | 3.095 | 2.580 | 2.406 | 3.014 | 2.390 | 1.989 | 2.664 | 2.237 | Row1 |
| 0.045 | 0.123 | 0.204 | 0.077 | 0.237 | 0.142 | 0.048 | 0.082 | 0.339 | 0.090 | Row2 |

Table 9.2: Average (row1) and standard deviation (row2) of the 60 data points for each patient after using the device. Units = Output Voltage, Volts

The data showed that the patients were not fully holding their breath. Figure 9.1.a shows the results of one of the 10 patients holding their breath before they were allowed to look at the displays. The voltage rises as they are not holding their breath correctly. There was a standard deviation of up to 0.52Volts from the mean across all 10 patients. If the patients were holding their breath perfectly the pressure and hence voltage reading would not deviate at all. From this it can be assumed that although a patient may think that they are holding their breath correctly it is not the case. Therefore some pre scanning training is necessary.

The patients were then asked to look at the bargraph and LabVIEW waveform while the bladder monitored their breathing. They were again asked to hold their breaths while watching the displays and through trial and error they learn to improve their breath-holding technique. It was noted that the patients responded quicker to the LabVIEW waveform that the bargraph display. Thus the LabVIEW waveform was used to teach the patients to hold their breath correctly. It was also noted that the optimum part of the breathing cycle [42] at which to begin the breath hold was after a small exhalation. This is because there is less relaxation movement in the chest than after an inhalation. Finally they were asked to hold their breaths again for another 20 seconds (Figure 9.1b). This data was also recorded. The standard deviation in this case was only up to 0.15Volts from the mean suggesting an improvement in breath holding. This decrease in variation from the mean is due to less movement from breathing. This means that the inner organs of interest, such as the liver, will be moved less leading to improved clearer images.

9.2.2 Paired t Test

A statistical test was then needed to verify the significance of these results. The paired t-test [62] is a standard statistical test used to compare two sets of results such as pre-experiment and post-experiment results. This test produces a probability (P_{value}) value that states what the probability is that two sets of results are the same. Therefore in this case it was hoped that the P_{value} would be small so that it could be ascertained that the two sets of values are in fact different.

The 60 data points from each person for the pre-experiment case were plotted against time as in figure 9.1. The slope of each line was obtained using Excel which returns the slope of the linear regression line through the given data points. If the patients were holding their breath perfectly then the slope of the line for a given patient would be zero. The same was done for the post-experiment data. The results can be seen in table 9.3.

The difference of the two sets of results is then calculated. It would be wrong to calculate the mean for the pre-experiment data and the mean for the post-experiment data since the variations between patients will swamp any difference there may be between the pre and post data. From these the following results were obtained:

0.049	0.066	0.147	0.062	0.079	0.136	0.053	0.0903	0.104	0.066	Row1
0.008	-0.01	-0.005	0.011	-0.003	-0.012	0.008	0.0005	0.025	0.015	Row2
0.041	0.076	0.151	0.052	0.083	0.147	0.046	0.0898	0.079	0.051	Row3

Table 9.3: Row 1 – slopes (no units) of the lines for the 10 people in the pre-case

Row 2 – slopes (no units) of the lines for the 10 people in the post-case

Row 3 – difference (no units) in slope for each pair

Average of the difference in slope of each pair, $\overline{d}$ = 0.081565

Standard deviation of the difference in slope of each pair, s_d = 0.039522

$n = 10$, the number of points

$v = n - 1 = 9$ degrees of freedom

$$t_{statistic} = \frac{\overline{d}}{\sqrt{\dfrac{s^2}{n}}} = 6.526 \tag{9.3}$$

145

Once the t value and the number of degrees of freedom are known the P value can then be calculated from the t Distribution Tables as shown in Table 9.4. The smallest P value possible is 0.0005

df\p	0.40	0.25	0.10	0.05	0.025	0.01	0.005	0.0005
1	0.324920	1.000000	3.077684	6.313752	12.70620	31.82052	63.65674	636.6192
2	0.288675	0.816497	1.885618	2.919986	4.30265	6.96456	9.92484	31.5991
3	0.276671	0.764892	1.637744	2.353363	3.18245	4.54070	5.84091	12.9240
4	0.270722	0.740697	1.533206	2.131847	2.77645	3.74695	4.60409	8.6103
5	0.267181	0.726687	1.475884	2.015048	2.57058	3.36493	4.03214	6.8688
6	0.264835	0.717558	1.439756	1.943180	2.44691	3.14267	3.70743	5.9588
7	0.263167	0.711142	1.414924	1.894579	2.36462	2.99795	3.49948	5.4079
8	0.261921	0.706387	1.396815	1.859548	2.30600	2.89646	3.35539	5.0413
9	0.260955	0.702722	1.383029	1.833113	2.26216	2.82144	3.24984	4.7809
10	0.260185	0.699812	1.372184	1.812461	2.22814	2.76377	3.16927	4.5869

Table 9.4: t Distribution Tables. For t = 6.526 and with 9 degrees of freedom the corresponding P value is less than 0.0005.

Two tailed P_{value} < 0.0005   (calculated from the t Distribution Tables)

Therefore there is a less than 0.0005 % chance that there is no difference in the two sets of data. Hence there is a very significant difference in the two data sets. This shows mathematically that the patient's breath holding improved after being trained to hold their breath correctly. This gave a basis upon which the research could be validated and continued. This information also provided the consultant radiologist involved with the project the necessary data to publish and present a paper at the Radiology Society of North America's (RSNA) annual conference in November 2002. This paper was can be viewed in the appendices of this thesis.

9.2.3 Feedback Systems

Further visits to the hospital were required for tests on the first version of the visual feedback display as discussed in chapter 6. From these field tests some valuable information was obtained for the development of the final visual feedback display. It was decided that the display needed to be smaller for ease of viewing and also to provide more room for patient comfort. It was also necessary for the display to be

more professional and aesthetically pleasing. A new display has now been made which fulfils these requirements.

9.3 MRI Compatibility Tests

It was necessary to carry out some tests on the visual feedback display, the bladder and the strap, which are all present in the scanner tunnel during testing to ensure that they did not degrade the signal in any way. If they were to degrade the signal by an unacceptable amount then the benefits of the device would have been negated. These tests were done with the help of one of the radiology physicists in Waterford Regional Hospital, Mr. Gregory Holden.

Test objects are used by the physicists to monitor the performance of the MRI equipment. Specific sequences are run using these test objects. The results obtained are compared to data sheets for the equipment to ensure that the scanner is performing to standard. Two of the main tests are the signal-to-noise ratio (SNR) tests and the geometric distortion tests. To obtain some evidence that the bladder and visual feedback display were not affecting the operation of the scanner these same tests were carried out. First the tests were done on the test objects alone. Then the same tests were carried out with the bladder and visual feedback display around the test object. The results from both sets of tests could then be compared to check for any degradation in the signal. The methods of testing and the equations used in these field tests are as outlined in the Institute of Physics and Engineering in Medicine's (IPEM) report for quality control in MRI [63]. The results from the two tests are as follows.

9.3.1 SNR Flood Field Test

SNR is the single most important measurement relating to image quality in MRI systems. However, although it is a sensitive indicator of problems it is not very specific to the cause as it may be as a result of any one of a number of factors. Poor results can be caused by increased noise or a reduction in signal. The factors influencing the SNR of a system include:

- Increased noise from the environment
- Main magnetic Field Strength B_0
- Design of radiofrequency (RF) receive and transmit systems
- Selection of scan sequence parameters

147

- Inhomogeneity of the magnetic and RF fields
- Loading of the RF coil (i.e. the patient)

The physicists in the hospital recommended the test object and sequence to use for the testing. These were recommended as they are regularly used and so any unwanted results could be easily spotted. The SNR flood field test object used is constructed from Perspex and is part of the MagNET Quality Assurance test object set. It is filled with a paramagnetic solution (1.66g $NiCl_2$ / L distilled water, pH 4) and is customised for the Siemens Magnetom Symphony 1.5Tesla Magnet used [64]. The scanning parameters used for the SNR tests were as follows:

Spin Echo Sequence; Transverse Planes;

Time to Echo (TE) = 30ms;

Repetition Time (TR) = 1000ms,

Number of Signal Averages (NSA) = 1;

Field Of View = 250mm;

Matix (Phase Encoded (PE) * Frequecny Encoded (FE)) = 256*256;

Slice width= 5mm,

Scan time = 4min20sec.

An MR image of one of the test objects can be seen in figure 9.2. This image was then used to measure the SNR values at the highlighted regions. The mean or average of these results is taken as shown in table 9.1.
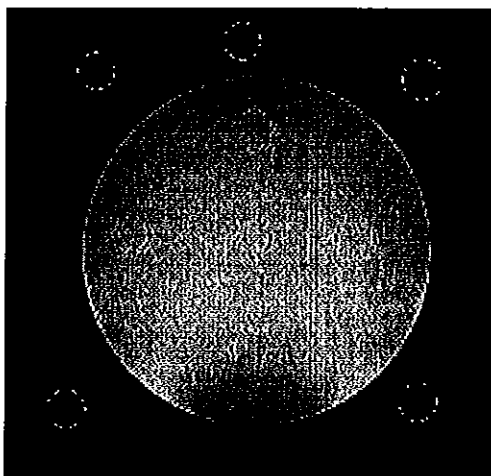
Figure 9.2: Image of the test object showing the regions of interest for the SNR measurements.

NSNR is the SNR per unit volume (cubic cm) per square root unit scan time. It allows comparison of SNR's acquired with different slice widths, numbers of signal averages and pixel sizes. This allows the performance of scanners with different parameters to be compared. Formula {9.4} used to calculate the NSNR values from the SNR values.

$$NSNR = \frac{\left(SNR * Q * \left(\frac{BW}{NBW} \right)^2 \right)}{\left(\left(\frac{FOV^2 * SW}{PE * FE} \right) * (TR * PE * NSA)^2 \right)}$$ {9.4}

where,

Q = Quality Factor = 1 for head coil   (Q head = 63.6, Q unloaded = 63.6)

Normalised BW = 30kHz

BW = Hz/pixel x readout encoding pixel value,

FE = 89Hz/pixel x 256pixels = 22.784 kHz

FOV = Field of View = 250mm (25cm)

SW = 0.5cm

PE, FE = 256

TR = 1000ms (1s)

NSA = 1

The following results are the SNR results measured with the head coil. This coil is not the coil that would be used with the breath monitoring device, however this is the coil with the most test data related to it. Hence tests were carried out with this coil, as any problems were likely to be observed. The SNR results for the head coil are as shown in table 9.1. The transverse plane is the cross section viewed from the feet towards the head. This means that all results are in the geometric x and y directions only. This was thought sufficient for detecting any problems that may have occurred however and reduced the scanner time taken to obtain the results.

Pre Device Insertion   **Post Device Insertion**

Transverse SNR   Transverse SNR

Mean signal	1536.5
Mean noise	10.4
SNR	147.6
NSNR	1685.6

Mean signal	1549.0
Mean noise	10.2
SNR	152.3
NSNR	1740.1

Table 9.1: The Pre & Post Insertion Results using the Head Coil. The signal and signal noise are both measured in decibels (dB).

From these results the percentage difference can be calculated as in equation {9.5}. The SNR or the NSNR values can be used but the choice must be consistent.

$$\frac{SNR_{PRE} - SNR_{POST}}{SNR_{PRE}} = 3.2\% \qquad \{9.5\}$$

The physicist explained that the acceptable difference is 10%, thus suggesting that the device does not cause any notable signal degradation. As this difference is smaller than 10% the difficult process of determining what factor in the SNR test was affected is avoided.

The Phased Array Body Coil was the next coil used for SNR testing. This is the coil of most interest as it this coil that is used to image the abdomen with the use of the breath-monitor. Table 9.2 shows the results obtained with this coil.

PRE DEVICE INSERTION   **POST DEVICE INSERTION**

Transverse SNR   Transverse SNR

Mean signal	43.4
Mean noise	5.6
SNR	7.7
NSNR	88.3

Mean signal	43.9
Mean noise	5.5
SNR	8.0
NSNR	91.2

Table 9.2: The Pre & Post Insertion Results using the Phased Array Body Coil. The signal and signal noise are both measured in decibels (dB).

The percentage difference in this case was calculated to be 3.3% using equation {9.5}. Again, the physicist explained that the acceptable difference is 10% suggesting that the device does not pose any threat to the operation of the scanner.

9.3.2 Geometric Linearity and Distortion Test

Linearity is concerned with whether the image possesses the correct linear dimensions or not. Distortion is where points in the image are in their true spatial location e.g. straight lines appear curved or apparent rotation of the object may occur. The Linearity is simply just the difference between the measured and actual distances of the rods in the test object as shown in figure 9.2. Distortion is given by the variation in the errors between measured and actual distances.
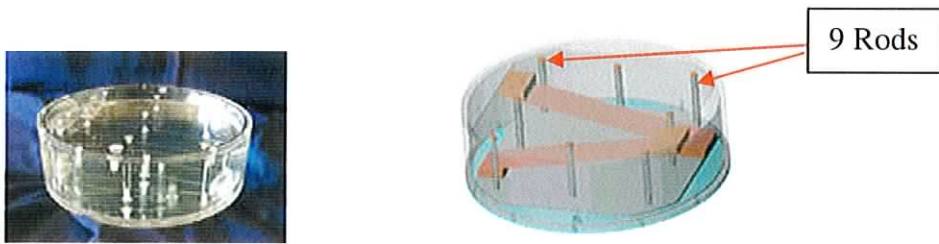
Figure 9.3: Image of the test object for the Linearity & Distortion measurements showing the location of the 9 rods [65].

The causes of linearity problems and distortion include:
- Magnetic Field inhomogeneity
- Gradient maladjustment
- Sampling irregularity

The Geometric Linearity and Distortion test object used is constructed from Perspex and is part of the MagNET Quality Assurance test object set. It is filled with a paramagnetic solution (0.7 g $CuSO_4$ / L distilled water, pH 2) and combines geometric tests with slice width measurements. The scanning parameters were:

Spin Echo Sequence;

Transverse Plane;

Time to Echo (TE) = 30ms;

Repetition Time (TR) = 1000ms;

No. of Signal Averages (NSA) = 1;

Field Of View = 256mm;

Matix (PExFE) = 256x256;

Slice width= 5mm;

Scan time = 4min20sec.

The % coefficient of variation (%CV) in the transverse plane and each gradient direction for this plane (X-Gradient, Y-Gradient) was calculated. Gz is slice selection, Gx is the phase encoding direction and Gy is the readout or Frequency encoded direction. CV is used to characterise the displacement measurements and is defined as

$$CV = \frac{\text{Standard Deviation}}{\text{Mean}} *100\%$$
{9.6}

Table 9.3 shows the results of the linearity test. The actual distance (120mm) is the distance between the rods in the test object. The measured distance is the distance between the rods as determined by the scanner. The linearity error is the difference between the actual and the measured values.

Plane	Gadient Direction	Actual Distance (mm)	Measured Distance (mm)	Linearity Error
Pre Device Insertion				
Transverse	X	120.00	120.10	0.10
		120.00	120.10	0.10
		120.00	120.10	0.10
Transverse	Y	120.00	121.10	1.10
		120.00	121.00	1.00
		120.00	120.40	0.40
Post Device Insertion				
Transverse	X	120.00	121.00	1.00
		120.00	121.00	1.00
		120.00	120.70	0.70
Transverse	Y	120.00	121.50	1.50
		120.00	121.10	1.10
		120.00	120.60	0.60

Table 9.3: The results of the linearity test.

152

From these measurements the %CV in the transverse plane (figure 9.5) and the transverse gradient direction (figure 9.6) were calculated using equation {9.6}. The acceptable %CV is less than a value of 1. As all results were well below this value it can be assumed that this device should not adversely affect the performance the scanner with respect to linearity and geometric distortion.

	Mean of Linearity	SD of Linearity	Mean of Plane	SD	Plane %CV
Pre Device Insertion					
Transverse X	120.10	1.91E-06	120.47	0.47	0.39
Transverse Y	120.83	3.79E-01			
Post Device Insertion					
Transverse X	120.90	0.17	120.98	0.32	0.26
Transverse Y	121.07	0.45			

Table 9.4: Calculations made from the results of the linearity test.

	Mean of Gradient Direction	SD	Gradient %CV
Pre Device Insertion			
Transverse X	120.10	0.00	0.00
Transverse Y	120.83	0.38	0.31
Post Device Insertion			
Transverse X	120.90	0.17	0.14
Transverse Y	121.07	0.45	0.37

Table 9.5: The gradient results of the linearity test.

9.4   Clinical Images

The final field test was to obtain MR images of a dummy patient. Before seeing the breath-hold monitor the healthy patient was first scanned. A breath hold was requested during the scan with no preparation. Two sequences were performed – a

Transverse T1 FLASH Breath Hold sequence and a Coronal T2 HASTE Thin Slice Breath Hold sequence. One image from both of these sequences can be seen in figures 9.4 and 9.6. The transverse image is a view of the cross section looking from the patient's feet towards the head. The coronal image is a view of the cross section looking from the anterior to the posterior. The blurring in these images is known as internal motion artifact as a result of breathing.

The patient was then shown the breath-hold monitor and allowed to practice holding their breath correctly. Finally the second set of sequences was preformed as before. One image from both of the sequences can be seen in figures 9.5 and 9.7. When the image from figure 9.4 is compared to that of figure 9.5 and the image of 9.6 is compared to that of 9.7 there is a marked improvement in image quality. In particular the areas marked in red are significantly clearer showing increased detail.

Further testing would be required within the MRI environment to obtain a more conclusive outcome. However, testing of patients with the initial prototype showed that the device was likely to be of benefit and the final field test has further shown this to be the case.

Area in red marks part of the liver. The detail is greatly enhanced in figure 9.5 compared to figure 9.4.

Figure 9.4: Transverse T1 FLASH Breath Hold sequence image for the Pre-Experiment Scan.

Figure 9.5: Transverse T1 FLASH Breath Hold sequence image with a correct Breath Hold.

Figure 9.6: Coronal T2 HASTE Thin Slice Breath Hold sequence image for the Pre-Experiment Scan.
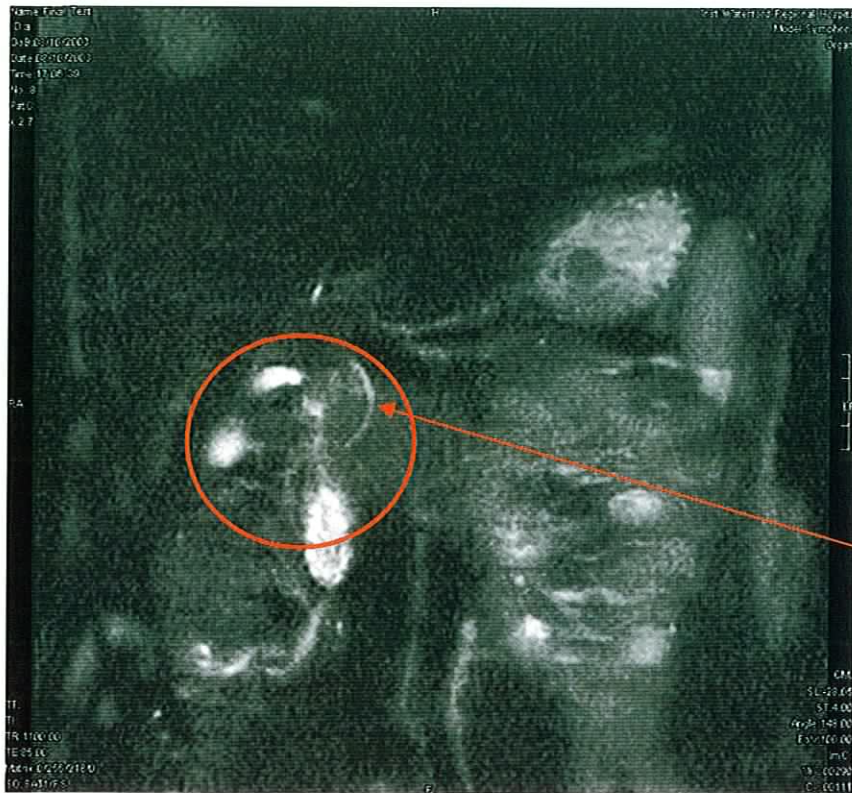
The detail in the area marked in red is greatly enhanced in figure 9.7 compared to figure 9.6. Note the location of the bile duct in figure 9.7 that cannot be distinguished in figure 9.6.

Figure 9.7: Coronal T2 HASTE Thin Slice Breath Hold sequence image with a Breath Hold.

9.4 Conclusion

The initial field tests proved that the device helps patients to control their breathing correctly. These results led to the further development the device. The final field tests proved that this device can be used with an MRI scanner without causing any unacceptable problems. The materials used do not adversely affect the operation of the scanner. The clinical results obtained showed a visible improvement in image quality as was hoped. If this system were to be set up permanently in the hospital further statistical analysis could be carried out.

10   CONCLUSIONS

10.1   Introduction

The aim of this research work was to design and manufacture a low cost respiratory monitoring device that operates in conjunction with MRI scanners to produce higher quality images. The main objectives of this research were to:

i)   Design and develop a device to monitor breathing in the MRI environment.

ii)   To include a design feature that would provide feedback to the patient about their breathing activity during the scan.

iii)   Develop a housing for the electrical components.

iv)   Consult and implement the EU Medical Devices Directive and produce the relevant documentation for obtaining the CE Mark.

v)   Carry out MRI compatibility tests.

vi)   Undertake clinical testing.

All of these objectives have been successfully completed. A positive pressure bladder and strap were used to monitor the patient's breathing in the MRI environment. These components have undergone MRI compatibility testing and are the only components that come in contact with the patient. Thus the materials chosen for this part of the device were chosen carefully with respect to the Medical Devices Directive. The change in pressure in the bladder is registered on the pressure transmitter located outside of the MRI room. The transmitter produces a 0-10Vdc signal that can be sent to the computer and a bargraph LED display. LabVIEW software on the computer was used to create a program that displays the breathing activity of the patient as a waveform. It also stores the breathing activity data and creates a tone whose frequency varies with the input from the transmitter. This is then sent to the patient through the audio system already in place within the MRI room providing feedback to the patient. A bargraph LED also displays the breathing activity of the patient. A fibre optic plug can be attached to this display. The light from the LED's is then replicated in the tunnel with the use of optical fibres. Lenses are used to magnify the light from the fibres. This provides the visual form of feedback to the patient. All the electrical components are stored outside the MRI room and are housed

157

inside a medical grade ABS plastic housing. This housing is a small and ergonomic design and was manufactured using a vacuum forming process.

10.2 CE Marking

The device is a Class 1 medical device as confirmed by the Irish Medicines Board (IMB) on the 10th December 2003. The main advantage of it being declared a Class 1 device is that the manufacturer of the product may apply the CE Mark themselves. The technical file has been written up and is included in the appendices of this thesis. The CE Mark can now be applied to this product. Following a meeting with the IMB on the 11th December '03 the following recommendations are to be attached to this thesis for a future manufacturer of the project should the device go into production:

- For best practice – ISO 14971:2000 Medical Devices Application of Risk & Essential Requirement Checklist should be completed.
- Batch Testing – a large number of devices should be manufactured and tested before supply.
- A manufacturer review file should be drawn up to complete the declaration of conformity.
- Apply to the IMB for Registration.

The CE Marked product can then be placed on the EU market

10.3 Field Testing

The field-testing of the device was carried out in Waterford Regional Hospital. Offline tests on the initial prototype showed that the device improved the breathing control of patients. The bladder and feedback components that enter the MRI room were tested for MRI compatibility. Any image degradation caused by these components is well within acceptable limits. Finally clinical images of a patient were taken before and after using the device. A marked improvement in the image quality can be clearly seen. The consultant radiologist provided a professional opinion and agreed that the image was greatly improved and showed superior detail when compared to typical breath hold images.

10.4 Cost Analysis

One objective of the project stated that this should be a low cost device. This was taken into account in the design of the device. Table 10.1 shows a cost list for the manufacture of the device.

Vacuum Forming	
Wooden mould for housing	300
Wooden mould for fibre optic display	200
ABS plastic vacuum formed housing	30
ABS plastic vacuum formed fibre optic display	30
Electrical Components	
Pressure transmitter	297.00
Power Supply	65.00
LED display	221.00
Wiring & sockets	17.79
Others	
Polymer fibre optic - 160 meters	279.15
15 Lenses	18.72
Plastic base plate, fibre optic plug & socket	46.00
Bladder & Strap	185.71
Pneumatic connectors, tubing	56.75
Screws and metal inserts	8.90
Total	**1756.00**

Table 10.1: Cost list for the Device.

A number of steps were taken to reduce the cost of the device. Vacuum forming was chosen as the method of manufacture of the housing for the device and the fibre optic display. This is much less expensive than other methods such as RIM moulding. The mould is the most expensive part of the process but this can be reused so the cost of producing further devices is decreased. The housing was designed as a single part requiring only one mould, further reducing costs. With the moulds in place the cost of

reproducing the device would be €1250. This cost could further be reduced as prices for components may reduce when bought in larger numbers.

The coil used in the initial prototype for breath monitoring was sourced at over €800. The positive pressure bladder and strap that replaced this coil was manufactured for €187.15. This also created a significant reduction in the cost of the device.

10.5 Recommendations for Future Work

The fibre optic display is attached to the inside of the scanner tunnel using a velcro strip. A display that does not require velcro may be desirable. Such a display could be mounted on a stand that could pivot into the tunnel when required. There is room at the rear of the scanner for such a stand. The stand could also be used to hold the bundle of fibres.

A separate fibre optic display could be created for the offline case. The device could then be used without the aid of a computer. This would enable patients to be taught how to control their breathing correctly before scanning in any room. The device could be mobile on a trolley unit.

This type of breath monitor was designed to be MRI compatible. However, the device could be customised for use in numerous other breath holding procedures such as Ultrasound.

This type of breath monitoring technology could also be used to improve the performance of inhalers and nebulisers. These devices often require medication to be released and inhaled at a specific part of the respiratory cycle. The breath monitor could be used to trigger the release of the medication at the required moment.

The device also has the potential for further development as a heart rate monitor. While examining the breathing activity information gathered with the device it was discovered that the heart rate could also be monitored with the same device. The sensitivity of the pressure transducer must be increased to monitor the small pressure changes due to the pumping action of the heart. A high pass filter could then be used to subtract the larger movements due to breathing.

References

[1] Wilhelm Conrad Röntgen – Biography. Nobel Lecturers in Physics, 1901 – 1921, Elsevier publishing company.

[2] William J. Morton, M.D. "The X Ray, or Photography of the Invisible, and Its Value in Surgery." American Technical Book Company, 1896. 220 pp. Illustrated.

[3] Michael Wolff. "William Coolidge: shirt-sleeves manager." IEEE *Spectrum*, May 1984.

[4] Marie Curie – Biography. Nobel Lecturers in Physics, 1901 – 1921, Elsevier publishing company.

[5] Pierre Curie – Biography. Nobel Lecturers in Physics, 1901 – 1921, Elsevier publishing company.

[6] Henri Becquerel – Biography. Nobel Lecturers in Physics, 1901 – 1921, Elsevier publishing company.

[7] Felix Bloch – Biography. Nobel Lecturers in Physics, 1901 – 1921, Elsevier publishing company.

[8] Edward Purcell – Biography. Nobel Lecturers in Physics, 1901 – 1921, Elsevier publishing company.

[9] Paul C. Lauterbur – Biography. Nobel Lecturers in Physics, 1901 – 1921, Elsevier publishing company.

[10] Sir Peter Mansfield – Biography. Nobel Lecturers in Physics, 1901 – 1921, Elsevier publishing company.

[11] Nawfel RD, Judy PF, Silverman SG, Hooton S, Tuncali K, Adams DF. "Patient and personnel exposure during CT flour copy-guided interventional procedures." Radiology 2000;216:180-184

[12] Kato R, Katada K, Anno H, Suzuki S, Ida Y, Koga S. "Radiation dosimetry at CT fluoroscopy: physicians hand dose and development of needle holders." Radiology 1996;201:576-578.

[13] Irie T, Kajitani M, Matsueda K, Arai Y, Inaba Y, Kujiraoka Y, Itai Y. "Biopsy of Lung Nodules with Use of I-I Device Under Intermittent CT Fluoroscopic Guidance." Journal of Vascular interventional Radiology 2001; 12:215-219.

[14] Nickoloff EL, Khandji A, Dutta A. "Radiation doses during CT fluoroscopy." Health Phys 2000, 70:675-681.

[15] Solomon SB, Patriciu A, Bohlman ME, Kavoussi LR, Stoianovici D. Robotially "Driven interventions: A Method of Using CT Fluoroscopy without Radiation Exposure to the Physician." Radiology 2002; 225:277-282.

[16] Kakeda S, Nakamura K, Kamada K, Watanabe H, Nakata H, Katasuragawa S, Doi K. "Improved Detection of Lung Nodules by Using a Temporal Subtraction Technique." Radiology 2002, 224:145-151.

[17] Matthias Hofer. "Teaching Manual of Color Duplex Sonography: A Workbook on Color Duplex Ultrasound and Echocardiography." Thieme Medical Publishers, 1 April, 2001.

[18] Cohen MS, Weisskoff RM. "Ultra-fast imaging." MRI 1991 9:1.

[19] Sorensen A G. "Advancements in MRI Scanner Technology Lead to Improved Functional Imaging." Electromedia 68 (2000) no.2.

[20] Moelker A, Maas RA, Lethimonnier F, Pattynama PMT. "Interventional MRI at 1.5T: Quantification of Sound Exposure." Radiology. 2002 Sep;224(3):889-95.

[21] Clyde A Helms. "The Impact of MRI in Sports Medicine." Radiology 2002; 224:631-635.

[22] Ackermann RA, Dean DE, Hedeen RA, Mallozzi RP, Miller ML, Purgil DA, Thompson PS, Vavrek RM; General Electric (US). Patent Number US 6437568.

[23] Linardos J, Damadian J, Danby G; Fonar Corp. MRI apparatus. Patent Number: US6445186.

[24] Goyen M, Quick H, Debatin J, Ladd M, Barkhausen J. "Whole-Body Three-Dimensional MR Angiography with a Rolling Table Platform: Initial Clinical Experience." Radiology. 2002 Jul;224(1):270-7.

[25] http://www1.stpaulshosp.bc.ca/stpaulsstuff/MRart/abdon.html

[26] International Society for Magnetic Resonance in Medicine. http://www.ismrm.org/

[27] VS Lee, D Resnick, JM Bundy, OP Simonetti, P Lee, and JC Weinreb. "Cardiac function: MR evaluation in one breath hold with real-time true fast imaging with steady-state precession." RSNA 2002 222: 835

[28] Gary P. Zientara, Ph.D. "Fast Imaging Techniques for Interventional MRI." Ch. 2, pp25-52 in Interventional MR. SPL Technical Report #65, April 1998.

[29] Hiroto Hatabu and Herwig Imhof. "Fast Magnetic Resonance Body Imaging." ISBN 0-444-50516-4, New York, NY, Elsevier, 2000.

[30] Low, GD Alzate, and A Shimakawa. "Motion suppression in MR imaging of the liver: comparison of respiratory-triggered and nontriggered fast spin-echo sequences." AJR 1997 168: 225

[31] R Sinkus and P Börnert. "Motion Pattern Adapted Real-Time Respiratory Gating." Magn Res Med 1999 41: 148

[32] M Weiger, P Börnert, and R Proksa. "Motion-Adapted Gating Based on k-space Weighting for Reduction of Respiratory Motion Artifacts." Magn Res Med 1997 38: 322

[33] Murtz P, Flacke S, Traber F, Van den Brink JS, Gieseke J, Schild H. "Abdomen: Diffusion-weighted MR Imaging with Pulse-triggered Single-Shot Sequences." Radiology 2002; 224:258-264.

[34] Hand-held Doctor for Children, Vadim Gerasimov, Walter Bender. MIT, MA 02139 USA. http://vadim.www.media.mit.edu/hhd/HHD.pdf

[35] Toshiyuki Irie, Motonao Kajitani. "Biopsy of Lung nodules with the use of I-I Device under Intermittent CT Fluoroscopy Guidance." Interv Radiol 2001; 12:215-219.

[36] http://www.pjbpubs.com/clinica : Breathing Aid Vest.

[37] R G Castile. Apparatus for Controlled Ventilation of a Patient. Patent No WO0022985.

[38] L Hofland, S A Scampini, B J Savord. Method of and Device for MRI. Patent No EP0740797.

[39] G Tan, C F Maier. Slice Ordering Method for Breath-hold Abdominal MR Imaging. Patent No EP1139114.

[40] Y Machida. MRI for a Plurality of Selective Regions set to Object Continuously Moved. Patent No US2002115929.

[41] Riederer S, Liu Yu L, Ehman R; Mayo Foundation. Breath-hold monitor for MR imaging. Patent Number: US5363844.

[42]: Gemini Respiratory Monitor. CWE Inc, 25 St. Paul's Road, Ardmore, PA 19003 U.S.A. www.cwe-inc.com

[43]: Kelly Bott, Dr. Jerry J. Cupal. "Non-Invasive Infant Respiration and Temperature Monitor." Electrical and Computer Engineering Department, University of Wyoming, Laramie, WY 82071.

[44]: Brian Wirth. "Micro Machined Pressure Sensors." Medical Device and Diagnostic Industry Magazine, June 1998.

[45]: Patrick Chow, Gangadharan Nagendra, John Abisheganden and Y T Wang. "Respiratory Monitoring Using an Air-Mattress System." Physiol. Meas, 21(suppl. 1A): A1-A6.

[46]: Model FCO332 Differential Pressure Transducer from Furness Controls. http://www.furness-controls.com/diff/fco332.html

[47]: Model PRO-BAR LED Display by London Electronics http://www.london-electronics.com/probar.htm

[48]: A McNally, G Woods. "Respiratory Monitoring Devices to be used in Conjunction with MRI scanners." IMC 19.

[49]: Viking Extrusions, 4 Ivy Arch Road, Worthing BN148BX, West Sussex. www.vikingextrusion.co.uk

[50]: Riederer S, Liu Yu L, Ehman R; Mayo Foundation. "Breath-hold monitor for MR imaging." Patent Number: US5363844.

[51]: Gareth Murray, Brian Cronly. "Design & Manufacture of Housing for Medical Device – Final Year Report." DIT Bolton Street Library.

[52]: Carl Machover, "The CAD/CAM Handbook." McGraw-Hill.

[53]: http://www.stratasys.com/Global/index.html

[54]: Menges, Michaeli, Mohren. "How to make injection Moulds." Hanser Publishers.

[55]: N. J. Teh, P. P. Conway and P. J. Palmer. "Statistical Optimisation of the Thermoplastic Injection Moulding Process for the Encapsulation of Electionic Subassembly." Journal of Electronics Manufacturing, Vol. 10, No. 3 (2000) 171-179. http://www.worldscinet.com/jem/10/1003/S0960313100000150.html

[56]: Christopher W Macosko, "Fundamentals of Reaction Injection Moulding." Hanser Publishers.

[57]: http://www.plastech.org/vacuum.htm

[58]: Department of Health and Children, Hawkins House, Hawkins Street, Dublin 2, Ireland. http://www.doh.ie/.

[59]: NSAI, Dublin, Glasnevin, Dublin 9, Ireland. http://www.nsai.ie/Standards/Contacts/Standards_Contacts.html

[60]: MEDDEV 2.1/5 – Medical Devices Guidance Document for Medical Devices with a Measuring Function.

[61]: "Anatomy and Mechanics of Respiration: Chest Wall." JB Pierce Laboratory Publications, September 29, 1999 (Chap. 13, pp. 418-433).

[62]: Robert F. Woolson. "Statistical methods for the analysis of biomedical data." Published by Wiley, c1987.

[63] IPEM Report No.80: Quality Control in MRI.

[64] Medical Devices Agency, MDA Evaluation Report 01014, April 2001

[65] www.MagNet-mri.org

Appendix A: Component Data Sheets

Included in this section are the component data sheets for the main electrical components. These include:

- FCO332 Pressure Transmitter from Furness Controls
- Mascot 9922 Power Supply
- Bar-X Bargraph LED from London Electronics

Differential Pressure

DESCRIPTION:

The FCO332 is a general purpose differential pressure transmitter available in 2, 3 or 4 wire configuration to suit a wide range of Input and Output requirements.

The transducer is based on the proven and unique Furness Controls capacitive design.
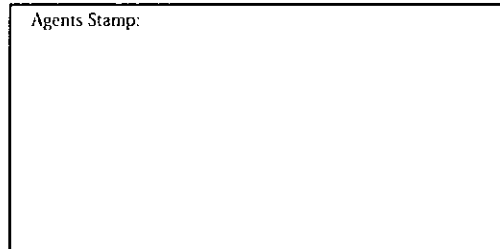
Output can be scaled as linear to differential pressure or as a square root function (cost option) for flow applications. The FCO332 is housed in a compact, robust, polycarbonate enclosure rated to IP54 and has secure pneumatic connections for flexible polymer 6 x 4 mm tubing. A 4 digit LCD (cost option) is available to display output in a variety of engineering units.

Furness Controls

003.7M/5

Differential Pressure Transmitter

— Model 332 —
−   +

All dimensions in millimetres

SPECIFICATIONS

FEATURES AND FUNCTIONS:

- 6 available Models from ±50 Pa to ±20 kPa. Each Model programmable by PC or Keypad to any precise range and/or any equivalent engineering units required, over a 10:1 span.
- Output options:
  - 2-wire current 4 - 20mA
  - 3-wire voltage 0-1, 0-2, 0-5, 0-10, 0.2-1, 1-5, 2-10 vdc
  - 4-wire voltage 0-1, 0-2, 0-5, 0-10, ±1, ±2, ±5, ±10 vdc
- Available pressure units (LCD) - Pa, kPa, mmH2O, mbar, mmHg, "H2O, "Hg, psi
- Available volume flow units (LCD) - l/s, l/min, l/hr, cf/s, cf/min, cf/hr, m3/s, m3/min, m3/hr
- Available mass flow units (LCD) - lb/s, lb/min, lb/hr, kg/s, kg/min, kg/hr
- Available velocity units (LCD) - m/s, ft/s, mph, ft/min, km/hr
- Available misc. units (LCD) - mA, %, none
- Adjustable signal damping 0.1 - 60.0 secs
- Internal error indication output - high 21.0 mA or low 3.0 mA
- Pneumatic connection - barbs with locknut for 6mm OD x 4 mm ID polymer tubing 1/4" BSP female tapped for suitable fitting/adaptor
- 2 Adjustable Trip Levels (Relays) rated 3 amp 50vac/30vdc (Chargeable option)
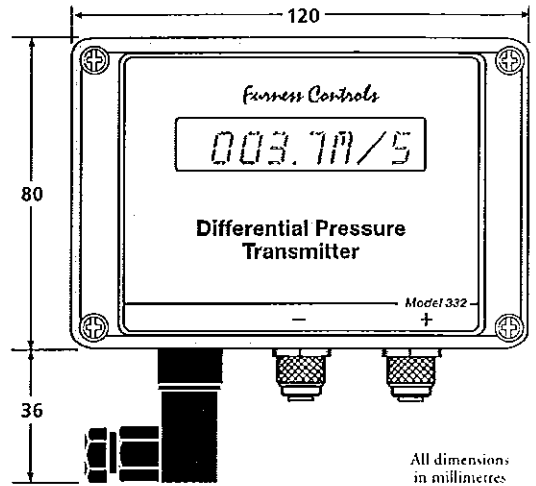
Agents Stamp:

PERFORMANCE:

Accuracy	<0.5% of reading
Span adjustment	10-100% range
Transducer zero range	±10% of factory setting
Linearity	< ±0.4% of reading
Hysteresis	< 0.1% of reading
Temperature coefficient (zero)	<±0.1% FSD/°C
Temperature coefficient (span)	<±0.2%/°C
Temperature compensation	-10 to 60°C
Temperature working limits	-10 to 60°C
Temperature storage limits	-10 to 70°C
Static working pressure	0 to 2 Bar absolute
Overpressure rating	20 x DP range

CONSTRUCTION:

- Polycarbonate IP54 rated enclosure
- Materials in media contact: copper, brass, nickel, mica, PVC
- Media compatibility - non-corrosive gases, max 95% humidity non-condensing
- Dimensions: 120 x 80 x 58 mm (w x h x d) excl. cable gland and pneumatic fittings 116mm (h) incl. electrical connection
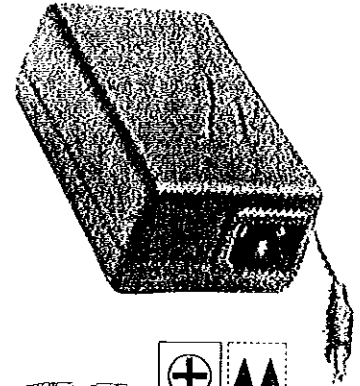- Weight: 0.5 kg

ACCESSORIES:

- UKAS traceable calibration
- FCO301 PC utility software for programming and calibrating
- FCO302 Keypad for programming and calibrating

Furness Controls Limited

NIIH
ISO 9002

UKAS

BS EN ISO 9002
ELECTRICAL EQUIPMENT CERTIFICATION SERVICE

tech spec

9920-9921-9922 | Max. 40 W |

AC/DC SWITCH MODE POWER SUPPLIES

9920 - 3 pins IEC 320
9921 - 2 pins IEC 320
9922 - Fast nettledning / Fixed mains cord

* Universal inngangsspenning (90-264 VAC)
* Medisinsk godkjent (EN 60601)
* UL godkjent (UL-2601-1)
* Kan leveres med festebrakett
* Nettledning ikke inkludert
* Utskiftbare plugger
* Vanntett (IP67) versjon kan leveres

* Universal input voltage (90-264 VAC)
* Medical approved (EN 60601)
* UL approved (UL-2601-1)
* Mounting bracket available
* Mains cord not included
* Exchangeable output plugs
* Waterproof (IP67) version available

Exch. plugs | MEDICAL | IP67
9922

Tekniske data	Technical specifications	
Inngangsspenning	Input voltage	90-264 VAC
Frekvensområde	Line frequency	47-63 Hz
Min. laststrøm	Min. output current	0A
Lastregulering	Load regulation	< 1%
Linjeregulering	Mains regulation	< 0,5%
Svitsjefrekvens ca.	Switch frequency approx.	40 kHz
Oversving (90-10% lastvariasjon)	Overshoot (90-10% load variation)	< 300 mV
Undersving (10-90% lastvariasjon)	Undershoot (10-90% load variation)	< 300 mV
Hold up time	Hold up time	> 20 ms
Temperaturområde	Temperature range	
• Drift	• Operating	-20 - +40°C (-40 - +40°C IP67 vers.)
• Med derating	• With derating	+60°C
• Lagring	• Storage	-25 - +85°C
Derating	Derating	1W/°C over 40°C
Derating UL-versjon	Derating UL-version	TA from 30 to 40°C : 32W
Rippel	Ripple	50 mV p-p
Virkningsgrad (ved 100% last, 230 V)	Efficiency (at 100% load, 230 V)	ca 85 %
Strømbegrensning:	Current limiting:	Ja / Yes
Isolasjonsklasse	Insulation class	Class I
Isolasjonsspenning	Insulation voltage	
• Primær - sekundær	• Primary - secondary	4000 VAC / 5640 VDC
Sikkerhet	Safety	EN 60601-1, EN 60950, UL 2601-1
EMC standarder	EMC standards	
• Medisinsk	• Medical	EN 60601-1-2
• Emisjon	• Emission	EN 50081-1
• Immunitet	• Immunity	EN 50082-1
Utgangsterminaler	Output terminal	Cable with / without plug
Ytre mål (LxBxH)	Dimensions (LxWxH)	107 x 67 x 36,5mm
Vekt	Weight	250g (450g IP67 vers.)

Visse tekniske data kan variere for de forskjellige modeller og spenningsversjoner.
Some technical specifications may differ for other models and voltage versions.

Spenningsversjoner • *Voltage versions*

Utgang *Output* (V)	Maks. strøm *Max. current* (A)	Maks. utgangseffekt *Max. output power* (W)
5 *	3,5	17,5
9 *	3	30
13,2	3	40
16	2,5	40
24	1,6	40
48	0,8	40

* Avventer UL godkjenning / *UL approved pending*

31102003

London Electronics Limited

Warren Court, Chicksands, Shefford, SG17 5QB England

Tel +44 (0)1462 850967   Fax +44 (0)1462 850968

e mail: easy4u a london-electronics com
web   http.//www london-electronics.com

BAR-A and BAR-X
1/8 DIN Process Bargraph Displays
and Controllers

An ideal 1/8 DIN bargraph / ribbon indicator for 4-20mA, 0-10V and other process signals. Fully scalable through a simple no-menu routine.
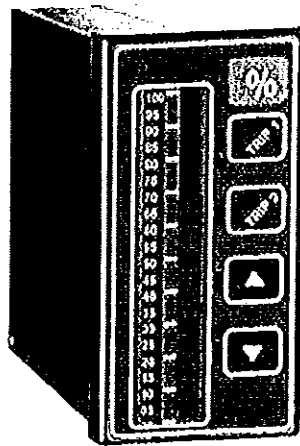
Bezel size 48mm x 96mm. Case depth 125mm. Scale length 75mm.

Choice of 95-265 VAC power or 11-30 VDC power.

Connections and rear switches

Use screened cable for the input signal and connect the screen to power earth at the meter end of the cable only. Keep the signal cable away from the power and alarm cables, because these could carry electrical noise which may interfere with your measurements. Case depth is 125mm. The cables don't add any extra depth.
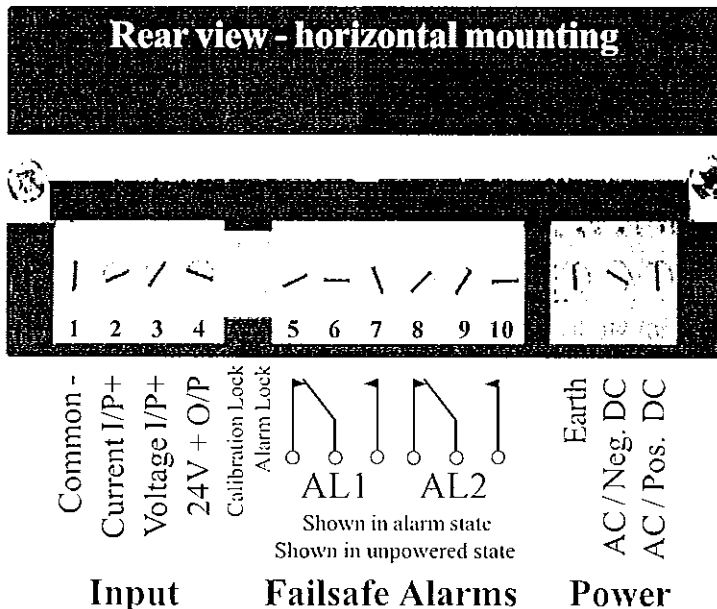
Rear view
horizontal mounting
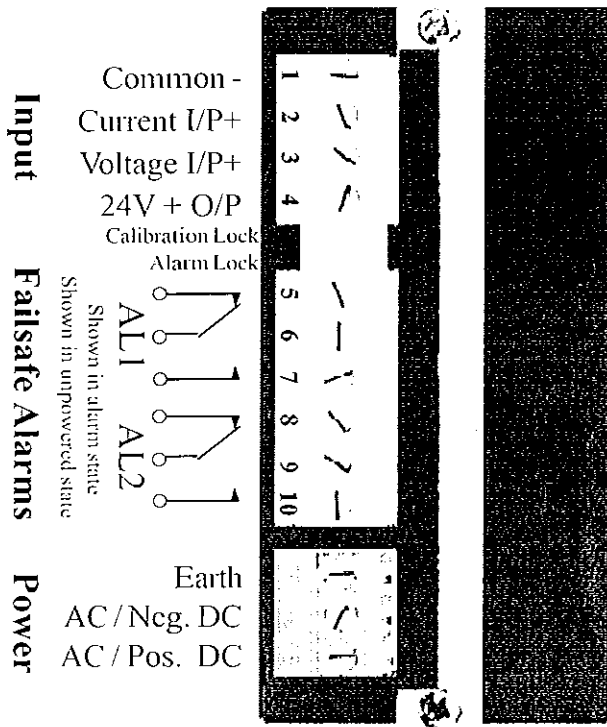
Detachable screw terminal connectors allow rapid installation and servicing.

Use multistrand insulated wire, with ferrules to DIN46228/1.

You can use stripped wire with cross sectional area from 0.5 to 2.5mm^2.

Strip back the insulation 7mm.

You'll find the terminal numbers on the rating label, not on the connectors.

Input

Common -
Current I/P+
Voltage I/P+
24V + O/P
Calibration Lock
Alarm Lock

Failsafe Alarms

AL1 AL2
Shown in alarm state
Shown in unpowered state

Power

Earth
AC / Neg. DC
AC / Pos. DC

Rear view - horizontal mounting

1 2 3 4   5 6 7 8 9 10

Common -
Current I/P+
Voltage I/P+
24V + O/P
Calibration Lock
Alarm Lock

AL1   AL2
Shown in alarm state
Shown in unpowered state

Earth
AC / Neg. DC
AC / Pos. DC

Input   **Failsafe Alarms**   **Power**

Declaration of Conformity

Declaration Reference : BAR-X
Issue Date   : 2 January 2003
Products Covered   : BAR-A and BAR-X
Title   : Bargraph display with alarm option

This certificate confirms that we designed and manufactured this product to meet the following limits :

EN55011:1998 Conducted Emissions: Class B
EN55011:1998 Radiated Emissions : Class B
IEC50082-1:1992 Electro-Static Discharge Immunity: 8kV Air
IEC50082-1:1992 Radiated ElectroMagnetic field Immunity: 3V/m
IEC50082-1:1992 Fast Transient Immunity : AC 1kV, cable 500V

The product was designed and built to conform with the applicable sections of the following standards:

EN 61010-1:1995

and meets the requirements of Council Directive 89/336/EEC for Electro-Magnetic Compatibility.

Conditions

This product is allowed a worst-case error of 1% of its range during electro-magnetic disturbance. It must recover automatically when the disturbance stops, without the need for human intervention, such as resetting, power-down etc.

The product must be installed according to these conditions :-

Signal cabling must be routed separate from power carrying cables(including relay output wiring)
All signal cabling must be screened. The screen must be connected to the power earth terminal near the meter. The screen must not be connected to earth anywhere else.

Certified as true and correct, for and on behalf of London Electronics Ltd.
Warren Court, Chicksands, Shefford, Bedfordshire SG17 5QB, U.K.   J.R.Lees - Director

24

Appendix B: Declaration of Conformity

Annex VII is the EC declaration of conformity. This is the procedure whereby it must be ensured and declared that the products concerned meet the provisions of this Directive that apply to them. A technical documentation that allows assessment of the conformity of the product with the requirements of the Directive must then be prepared. It must include in particular:

1. a general description of the product, including any variants planned,

2. design drawings, methods of manufacture envisaged and diagrams of components, sub-assemblies, circuits, etc.,

3. the descriptions and explanations necessary to understand the abovementioned drawings and diagrams and the operations of the product,

4. the results of the design calculations and of the inspections carried out, etc.; if the device is to be connected to other device(s) in order to operate as intended, proof must be provided that it conforms to the essential requirements when connected to any such device(s) having the characteristics specified by the manufacturer,

5. the test reports and, where appropriate, clinical data,

6. the label and instructions for use.

1. General description of the Product

MRI technology produces high quality images of the inner body. As a patient breathes, organs can be displaced in both location and size due to diaphragm movements. If this displacement takes place during the scanning procedure the resultant image will become distorted and output quality effected. As a result patients are required to hold their breath during scanning. Under normal conditions it is difficult for the patient to hold their breath correctly and this is exaggerated in the claustrophobic environment of the MRI scanner tunnel.

Much time is spent teaching the patients how to hold their breath correctly. This leads to excessive times on the MRI machine. This design is a low cost respiratory monitoring system, which can be, used offline to prepare patients for the procedure, and modified to be used in the MRI environment providing feedback to the patient regarding breathing activity during the scanning procedure. The device monitors the

172

patients breathing to help them improve the images obtained. It is not intended to monitor breathing as a vital physiological process.

The device operates by monitoring the changes in pressure inside a bladder, which is attached to the patient. These changes are displayed both graphically and numerically to provide visual feedback to the patient and radiologist about their breathing activity.

Bladder:

The bladder is a silicone rubber tube. This is strapped to the patient's thoracic region with a nylon strap. A cotton pouch attached to the strap holds the bladder in place. This is shown in figure E. As the patient inhales the pressure increases in the bladder and when the patient exhales the pressure decreases in the bladder.

Pressure Transducer:

The bladder is attached to a pressure transducer that translates the pressure reading to an electrical reading. The transducer has an output of 0 – 10Volts dc depending on the pressure in the bladder. At maximum expiration the pressure in the bladder is at a minimum and the pressure transducer will output a signal of 0Volts dc. As the patient breathes in the pressure in the bladder increases and the transducer output will increase accordingly. At maximum inspiration the pressure transducer will output a signal of 10Volts dc. If the patient holds their breath the output should remain the same.

LED display:

The 0 – 10Volts dc output signal from the transducer is sent to an LED display. This consists of a set of 30 LED's in a row. As the signal increases from 0Volts the LED's start to turn on until at 10Volts all the LED's are on. This provides a bargraph type display. As the patients breathes in the LED's come on and as the patient breaths out the LED's turn off as shown in figure A below. When the patient holds their breath the same number of LED's should stay on. Hence the patient can view their breathing activity and can tell when they hold their breath correctly.
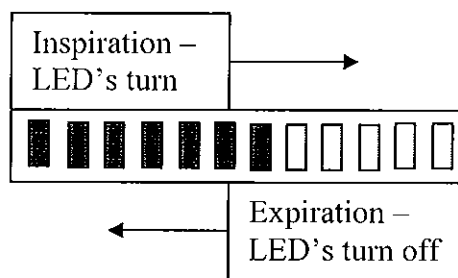
Figure A: Sketch of the fibre optic display.

173

Fibre Optic Display:

Due to the nature of the MRI scanners no electrical equipment can be used in proximity to them. This is due to the high magnetic forces involved. Thus the LED display cannot be brought into the patient while they are in the scanner. Therefore a fibre optic system was set up that transmits the light from the LED display to the patient. The fibres are plastic and are invisible to magnetic radiation. A fibre is attached to each LED and then the bundle of fibres is sent into the patient in the scanner where they provide a display similar to that of the LED display. The system is shown in the sketch in figure B below. A sketch of the actual fibre optic display can be seen in figure F.
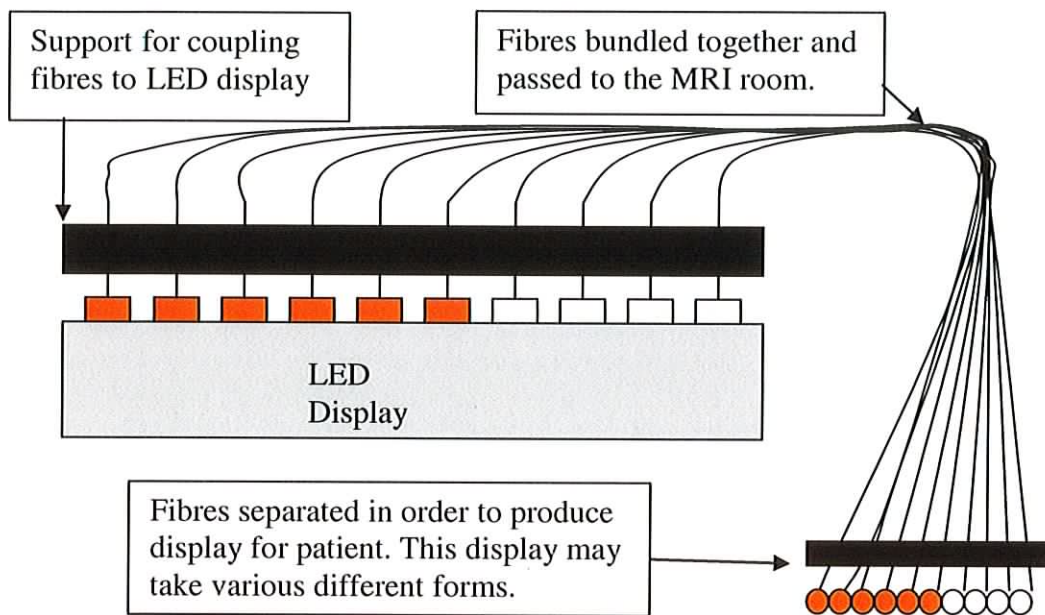
Figure B: Fibre Optic Display System

Inside/Outside the MRI Room:

Hence it is intended that the electrical part of this device shall be kept outside the MRI room. The bladder is located inside the MRI room and is attached to the electrical part of the device by 10m plastic tubing. The fibre optic display is also inside the MRI room and is attached to the electrical part of the device by the 10m polymer fibres. The main components and how they are connected can be seen in figure C below.

Main part of the device: holds the electrical components.

0-10Vdc o/p

Mains Connection

MRI Room

Fibre Optic Display
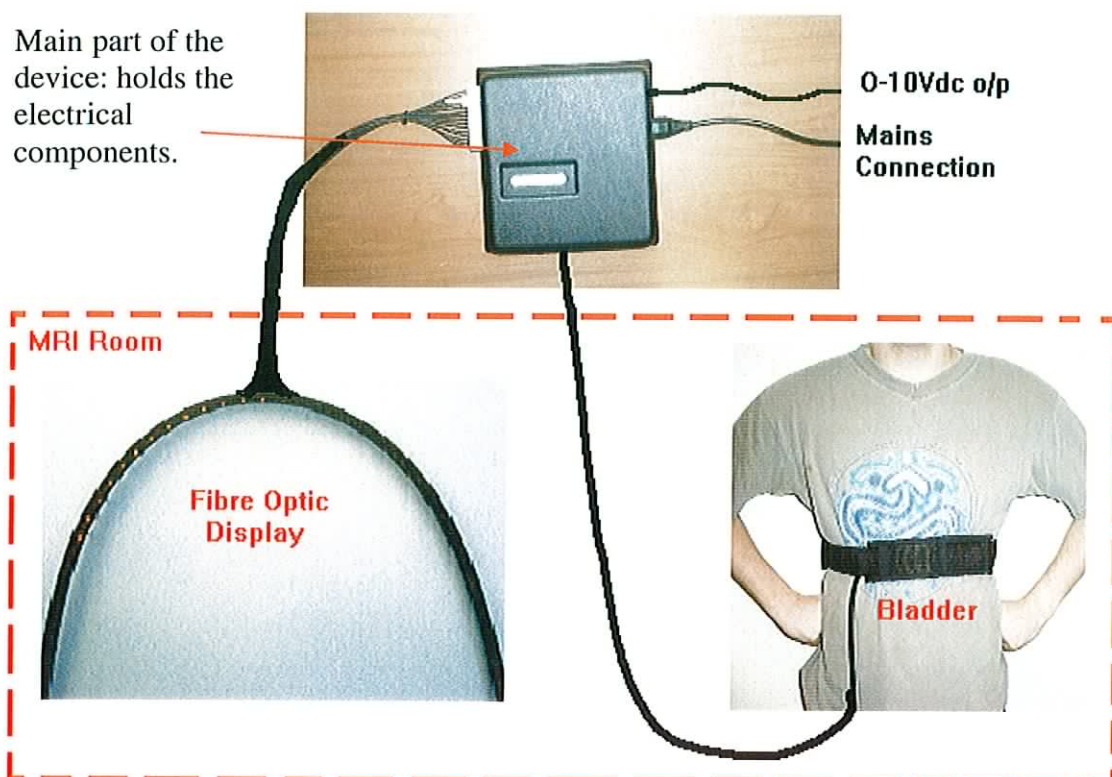
Bladder

Figure C: The main components and how they are connected in and outside the MRI room.

Contact with the Patient:

The only part of the device that comes into contact with the patient is the bladder and strap. The bladder is made from silicone rubber and the pouch is cotton. The strap is a nylon strap with plastic buckle similar to those already used in the MRI room. These components have no electrical connection but are connected to the pressure transducer in the main part of the device by 10m of plastic tubing.

The fibre optic display is made from ABS plastic. This is located in the scanner tunnel with the patient during scanning but there should be minimal contact with the patient if any.

Intended use of the Device:

The radiologist can use this device to teach the patient before scanning and to ensure that the patients hold their breath correctly during scanning. The device's main purpose is to improve the image quality. It is not intended to provide physiological data to the radiologist for any other purpose.

2,3. Design Drawings, Methods of Manufacture, Descriptions of Components, Sub Assemblies and Circuit Diagrams

This section includes sketches, photographs and descriptions of the various components. Firstly the main parts, those that are seen by the user, are described. The methods of manufacture are also discussed followed by detailed design drawings and diagrams. There is also a brief description of how to use the Labview software.

<u>Design Drawings</u>

Figure D: The Core – this is the main part of the device where the electrical components are housed and the peripheral parts of the device are attached.
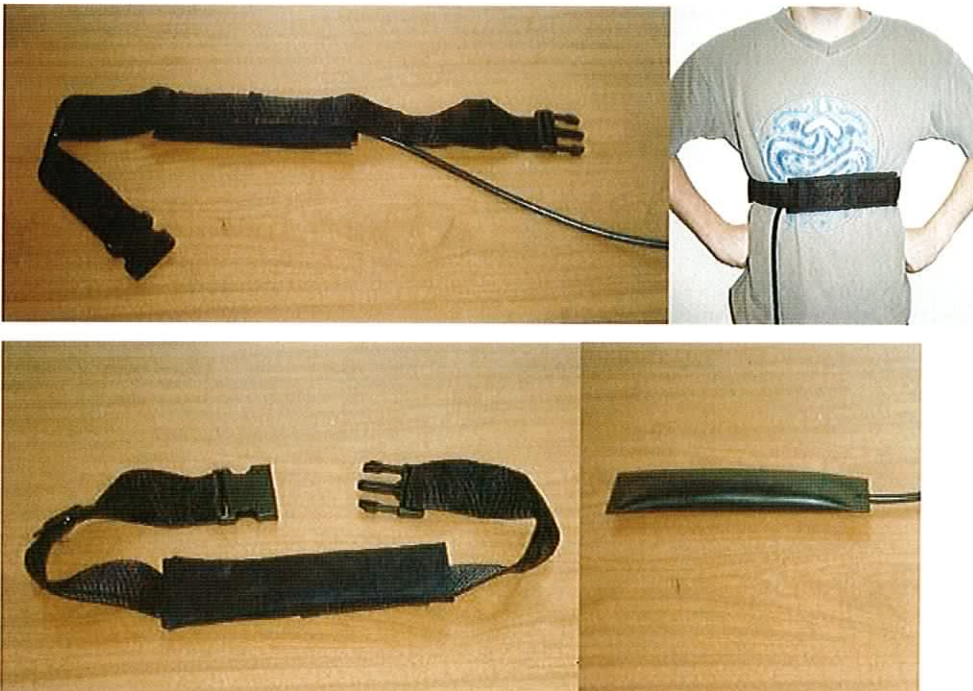
Figure E: The Pressure Belt – This consists of the silicone bladder and the nylon strap and cotton holder. The strap is attached around the thoracic region and the bladder is held in place with the cotton holder.
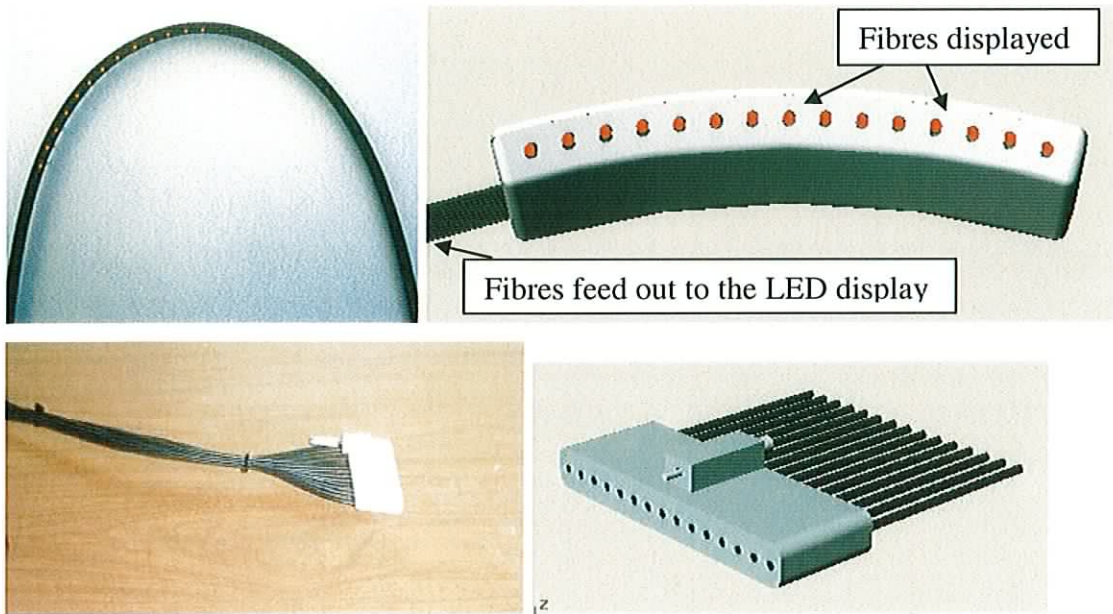
Figure F: Fibre Optic Display – There are two forms of display. The first is a self-clamping device that assumes the shape of the tunnel. The second is a specially made device that is formed to follow the contour of the tunnel and is held in place by Velcro. Also shown is the fibre optic plug at the other end of the bundle of fibre optic cables.

Manufacturing Method

- The manufacturing method for creating the housing for the core and the fibre optic display was vacuum forming. This is a process in which a thermoplastic sheet is heated to a pliable state and then placed over a mould and drawn into the mould to the desired shape of the finished part through vacuum suction.

The first step in making a vacuum formed part is creating a master pattern to produce the mould. The mould is then mounted on a back plate and vacuum holes are drilled through the mould and around the periphery of each pattern. This allows the heated plastic sheet to be pulled completely over the mould to ensure an accurate finished part.

After preparations of the mould have been completed, it is ready to perform the vacuum forming process. The plastic sheet is placed over the mould and clamped into place. A vacuum is then applied from beneath the mould and the heated plastic drawn down into the cavity. After the plastic has been allowed to cool, the clamps are taken

off and the formed sheets are removed from the mould, then the individual moulded parts are cut out.

The risk of toxic materials coming in contact with the surface is minimised as the plastic sheets are taken from their packaging and placed on the vacuum-forming machine. After the forming process the parts are stored before the cut out stage and then finally packaged. The parts will be packaged in cardboard boxes filled with foam pellets. In the case of materials such as machine oil coming in contact with the part the ABS plastic used can be easily cleaned. The ABS housing is located outside the MRI room in the control room and does not come in contact with the patient at any time.


- The fibre optic used is acrylic optical cable sheathed with special fluorine containing polymer. These are made and distributed in 20m sections by Farnell Ltd. They are later cut to a length of ten metres using a special blade. The fibre optic plug is made from a piece of polyacetalhomopolymer (POM-H). This is drilled with 2.3mm diameter holes into which the fibre optic cables are glued. The plug is attached to the core of the device with a screw mechanism. The parts are then cleaned. The fibre optics, the display case and the plug do not come in contact with the patient at any time.

The bladder and its connecting tube are made from medical grade silicone. The belt in which the bladder is held consists of a nylon strap and a cotton case for the bladder. The nylon strap is similar to straps already used on the MRI table to hold the receiver coils over the patient. The belt is attached over the gown of the patient around the thoracic area.

The following are the design drawings for the device. These include drawings of the mould and the housing, the assembly of the components and dimensions. There is also a circuit diagram to show how the devices should be connected.
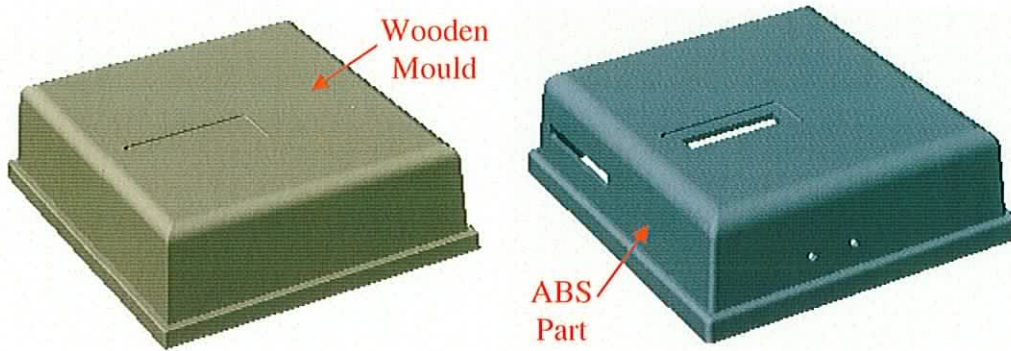
Figure G: From the wooden mould the housing of the device is formed and slots are cut out for the device connections. The housing is made from medical grade ABS plastic.
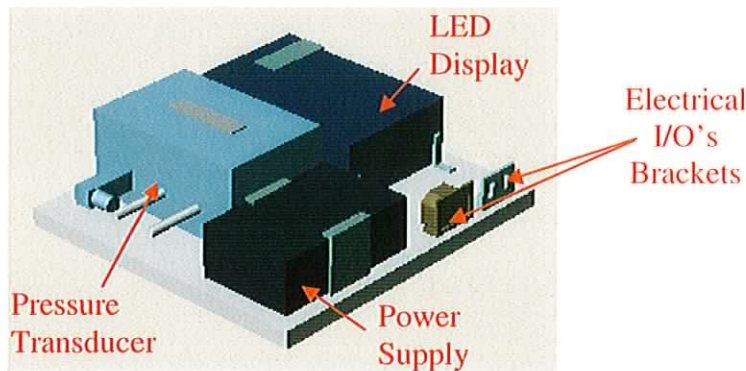
Figure H: The housing then is placed over the base plate, which holds the components. Feet are also attached under the base plate. The dimensions of the base plate and the positioning of the components can be seen in Figure L. Once in place the components must be wired together. A circuit diagram for this is shown in Figure M.
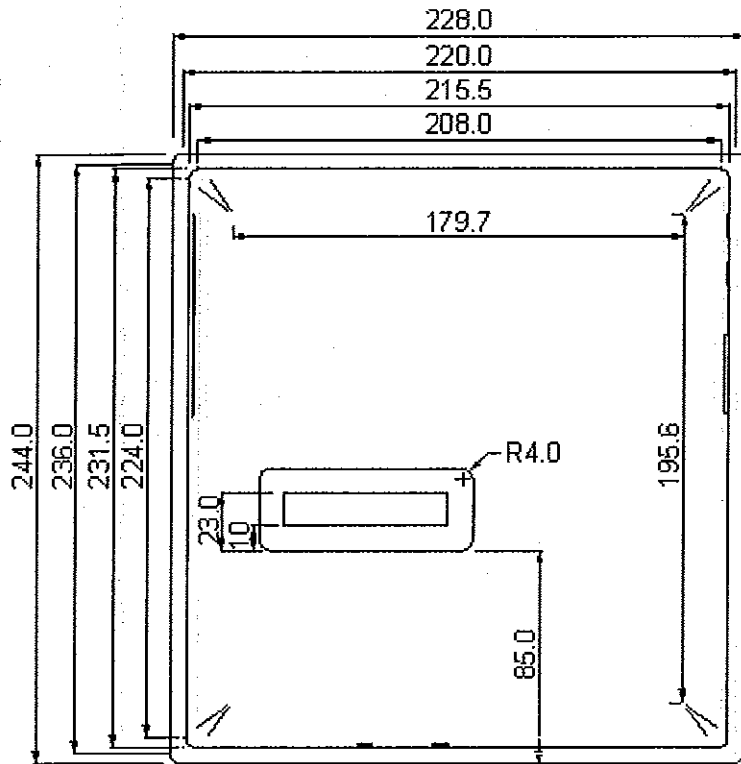
Figure I: Top view of the Vacuum Formed housing showing dimensions in mm.
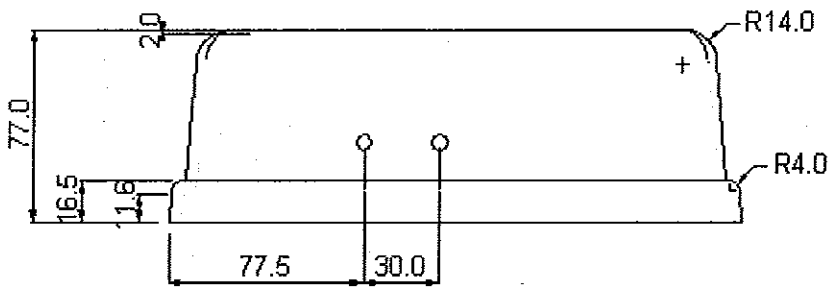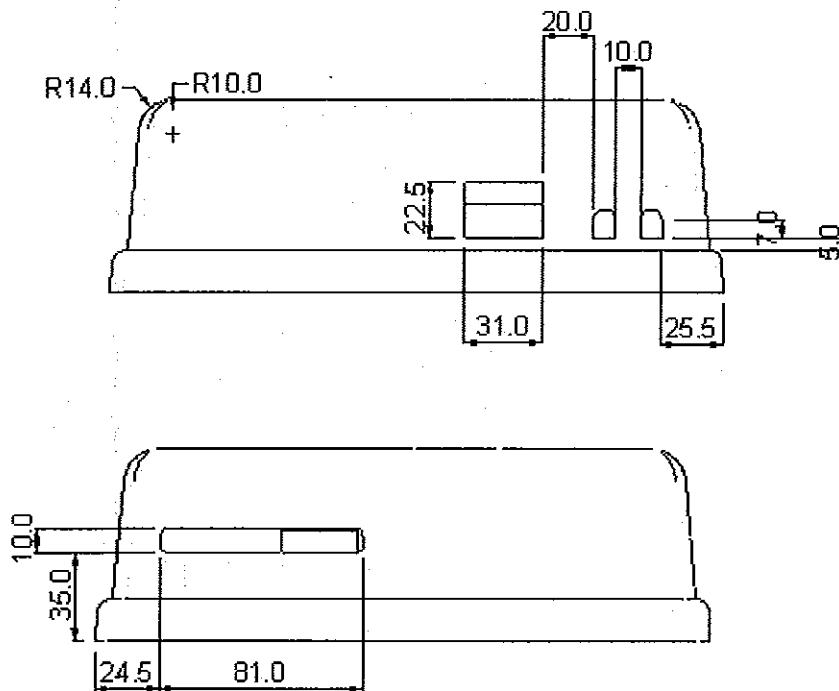

Figure J: Front view of the Vacuum Formed housing showing dimensions in mm. Wall taper = 5 degrees.

Figure K: The dimensions of the part and the locations of the cut-outs. This design is as small as the components would allow. The location of the cut outs is important as there is very little room to manoeuvre the components in the device. As there have only been a small number of these housings made the cut outs have thus far been done by hand. However if productivity were high this process would be automated and also carried out by Consort Case Company Ltd.

Components:

Pressure Transmitter:

This is a Model FC0332 differential pressure transmitter from Furness Controls. The pressure cell within the transmitter that reads the pressure is based on a unique reliable capacitive sensor. A microprocessor is used to control all functions of stability such as temperature correction and linearity. Another feature on the transducer is the 4.5" LCD display. This provides a digital indication of pressure in units of kilopascals (kPa).

The transducer has a pressure range of 20kPa above and below atmospheric pressure. There are two pneumatic outputs, one for positive pressure and the other for negative pressure.
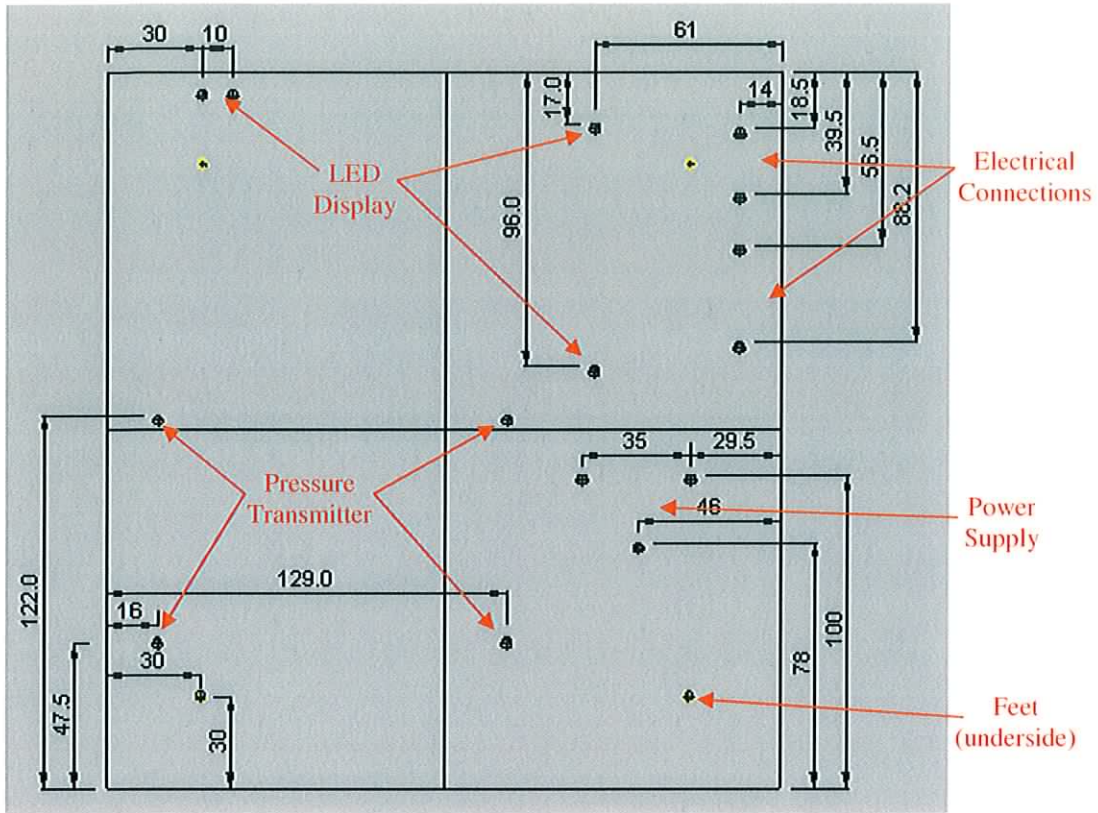
Figure L: The location of the holes for the brass inserts that hold the components in place on the base plate. Also shown (in yellow) are the holes for the feet. These are on the underside of the base plate. All holes are 4mm diameter and 8mm in depth.
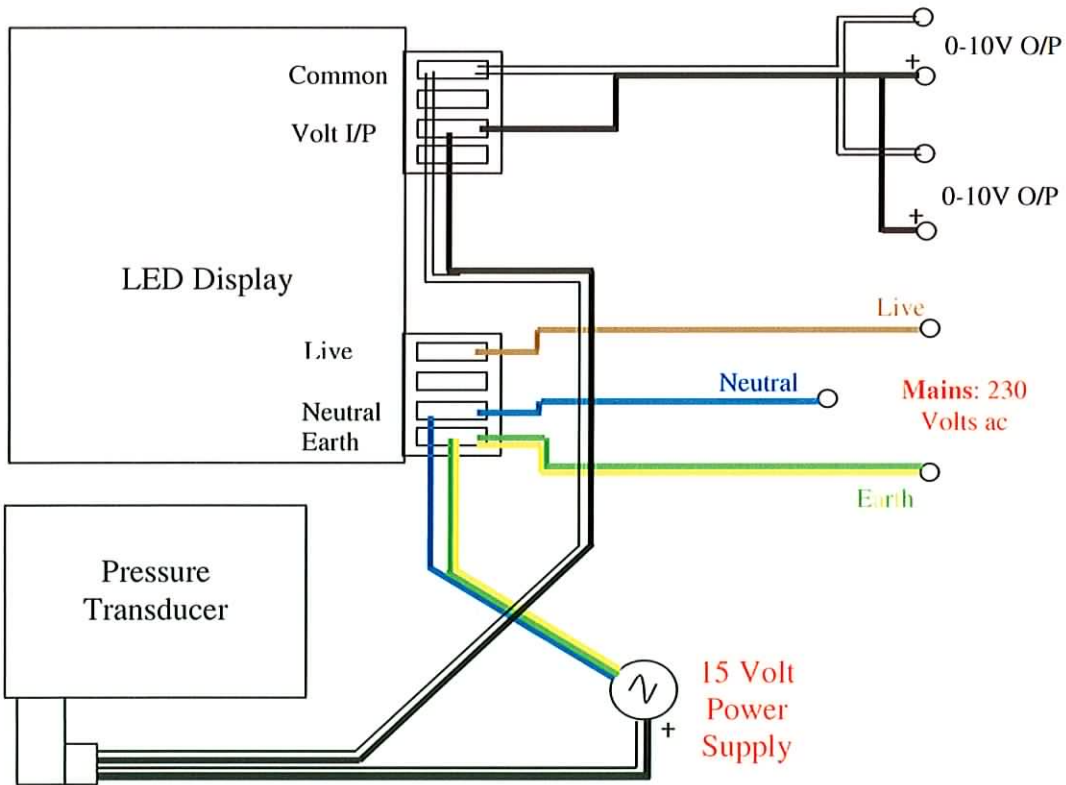

Figure M: Circuit diagram of the electrical connections within the device.

The software used with the device is Labview. LabVIEW has been used in this project for a number of different applications. It was chosen for the ease with which complex test and measurement applications can be set up. Firstly it provides a method of recording and viewing the breathing information of the patient. The information can be displayed as a waveform on screen and can simultaneously be stored as an Excel file.

LabVIEW is also used to form the software method of audio feedback. From the breathing information obtained it generates a sine wave whose frequency varies according to the information received. This is then played through the computers sound card and can be transferred to the patient through the sound system already in place in the MRI room.

LabVIEW can also be used as a testing rig for the bladder. LabVIEW enabled the testing of different sizes and types of bladders. It also provides the platform whereby leaks can be detected. The same VI that was used to monitor the patients breathing can be used to check for leaks. If the bladder is held under constant pressure then any leak will result in the LabVIEW programme showing a decreasing waveform. Small leaks can be detected by viewing the Excel files of data recorded over long periods of time.
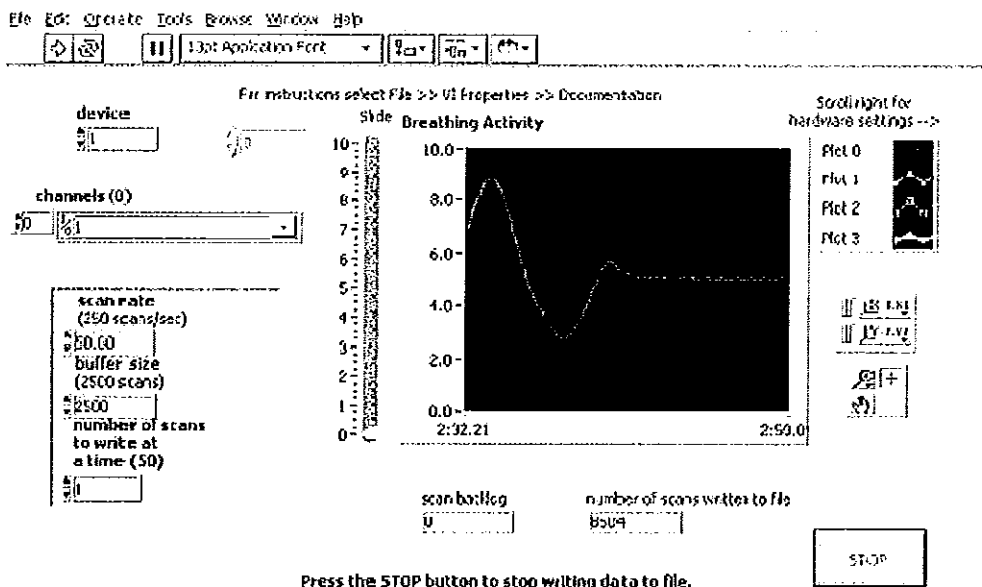
Figure N: User interface for the LabVIEW program that shows the breathing activity of the patient and stores the data for future analysis. The following values should be

183

assigned – scan rate: 3 scans/sec – buffer size: 2500 scans – number of scans to write at a time: 1. This will provide a smooth flowing waveform taking 3 samples a second. The user is given the choice of where to store the data obtained.
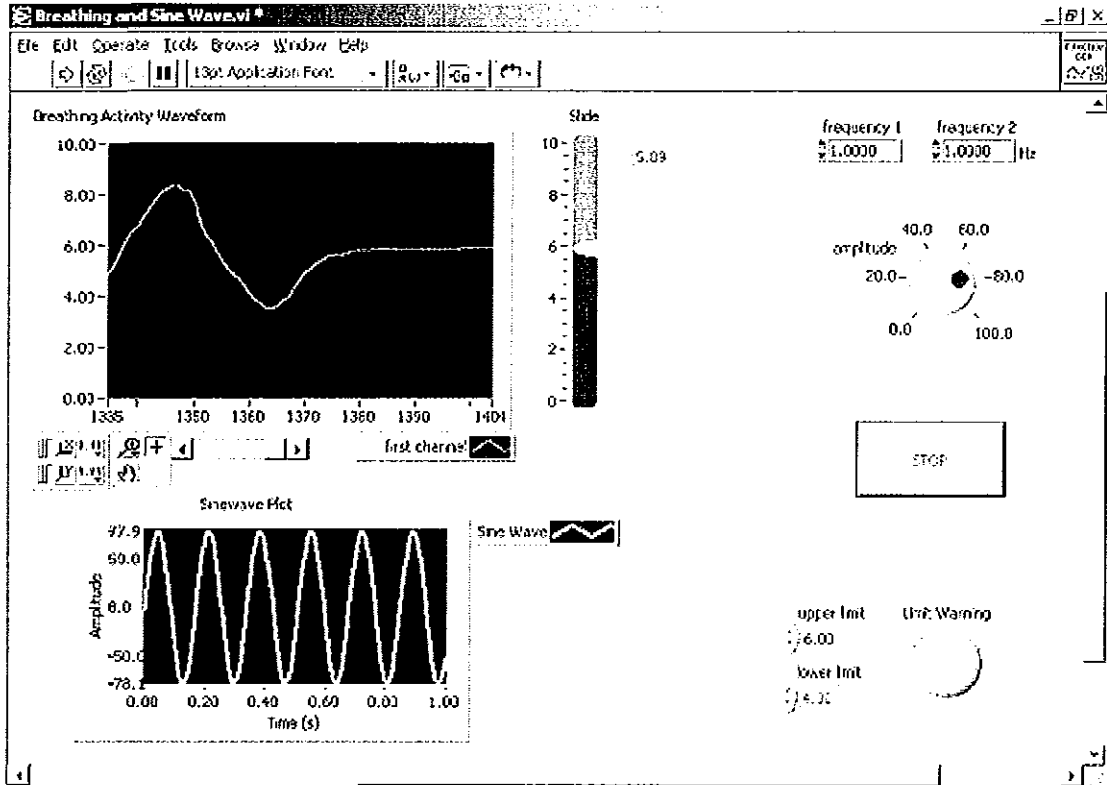
Figure O: User interface for the Labview program that creates the Audio Feedback signal while showing the breathing activity of the patient. The volume and frequency can be adjusted as required. For best results frequency 1 and 2 should be set to a value of 1. There is also a Limit Warning to assist the patient to hold their breath at a required frequency. The limits can be adjusted.

4.   This device is designed for use with MRI scanners but although they work in tandem they still work separately from each other

The fibre optic display and the bladder strap are within the scanner during scanning so tests were carried out to judge if the quality of the images produced were degraded by their presence. The signal to noise ratio (SNR) and image distortion are the points of interest. The following tests were carried out before and after the devices were placed in the scanner:

- SNR Measurement with Head Coil

  Pre Device Insertion: 1656

  Post Device Insertion: 1740

  % Difference: 3.2%

  Acceptable % Difference: 10%

- SNR Measurement with Phased Array Body Coil

  Pre Device Insertion: 88.3

  Post Device Insertion: 91.2

  % Difference: 3.3%

  Acceptable % Difference: 10%

- Geometric Linearity and Distortion Measurement

  Pre Device Insertion: Linear: 0.39%, transverse x – Gradient: 0.00%

  transverse y –   0.31%

  Post Device Insertion: Linear: 0.26%, transverse x – Gradient: 0.14%

  transverse y –   0.37%

  Acceptable: 1.00%

These tests show that the SNR values fall within acceptable limits and image linearity and distortion are extremely small and are also well within acceptable limits. This shows that although the devices work in tandem the breath monitor does not affect the operation of the scanner. As the electrical parts of the breath-monitoring device are outside the MRI room the scanner does not affect the operation of this device either. The device has been proven to work as shown by the clinical data retrieved from the field tests. Reference: Chapter 9.

## 5. Label and Description for Use

The following is a draft label to illustrate how the label may appear as specified in the essential requirements for labelling (Annex I - 93/42/EEC - 13.1).
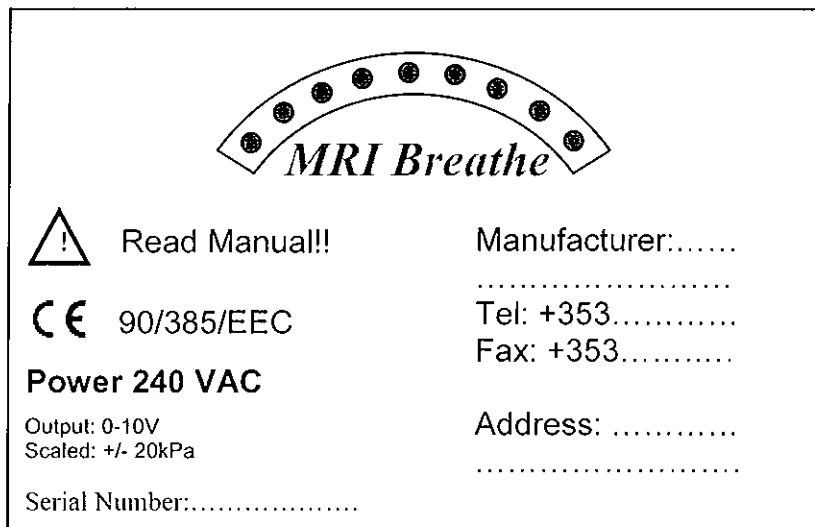
User Manual

Warnings / Precautions:

- Do not attach mains lead to the device while cover is removed.
- Only adjust connections with the power turned off.
- Install in a clean, dry environment.
- To clean the cover wipe with a soft damp cloth. Only dampen with water.
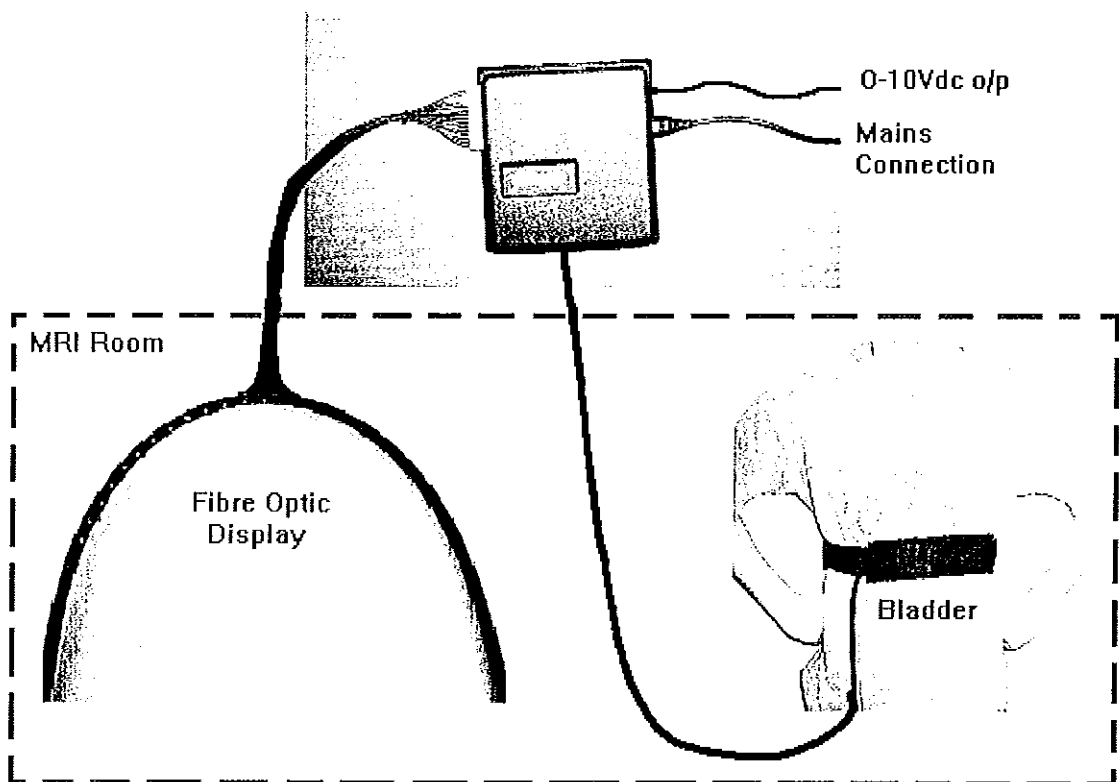
Connections

The Bladder, Fibre Optic Display and Electrical Connections should be connected to the core as shown above.

- Bladder: The bladder is connected to the main part of the device by 4mm/6mm inner/outer diameter tubing. This tubing is attached to a press-release pneumatic connector. The bladder should be in an unobstructed relaxed position before connection. Once connected the air in the bladder will be at

atmospheric pressure in this relaxed position. The pressure will increase once the bladder is squeezed.

- The Fibre Optic Display should be attached to the main part of the device by placing the plug through the housing and into the socket surrounding the LED display. The plug should then be secured using the attached screw.

- The mains connection for the device is via a mains kettle plug. This is attached to the corresponding socket on the main part of the device. An on/off switch on the mains lead allows the device to be turned on and off without removing the lead.

- The electrical output uses a 2.1mm dc plug and socket. This output can be connected to the computer for use with LabVIEW or to the sound feedback hardware device.

Instructions for Use:

- To turn the device on press the switch on the mains lead. A red light on the switch will show when the device is powered.

- The bladder should be placed in its belt and strapped around the lower thoracic region. The strap should be adjusted so that the display lights begin to show in a state of relaxation. The display lights should fluctuate on and off over a region close to the full display region during deep breathing. While breath holding the same number of lights should be constantly on.

- To record the breathing activity of the patient the Breathing Waveform.vi Labview program should be opened. This VI shows the breathing activity of the patient as a waveform. As the patient breaths the breathing waveform is generated and displayed simultaneously. Therefore the patient can be shown the waveform of their breathing activity as they breathe. The breathing activity information is also stored as a text file: DATA.txt. This information can later be viewed and analysed.

- Breathing and Sine Waveform.vi. This VI displays the breathing activity waveform in a similar way but uses different methods. The main differences between the two VI's are that this one does not save the breathing activity data but it does produce a sinusoidal waveform whose frequency varies with the breathing activity. This is the program used in the software method of audio

188

feedback. Some other features of this program are a limit warning whereby the patient can be asked to hold their breath between two points in the breath cycle. If they vary outside of these points a warning light shows and a warning buzzer is sounded. This helps to train patients to hold their breaths correctly and at specific points in the breath cycle if necessary.

- For the audio feedback signal or to record breathing activity data the ⬧ icon should be pressed when the corresponding Labview program is open. To end the program the STOP icon should be pressed.

Also included in the user manual will be the data sheets and manuals for the electrical components. These can be found in the appendices of this thesis. These will assist in the set up or recalibration of the device should any be required.

IRISH MEDICINES BOARD

Aidan McNally,
9 Pimlico,
Dublin 8

10th December 2003

Re: Classification of MRI Breath
**   Our reference no. CL-*129***

Dear Mr. McNally,

Further to your query regarding the MRI Breath classification, I would like to confirm that the classification of this product has been reviewed and is considered to be a Class I medical device.

We consider that as the device is an assistive device assisting in the diagnosis of MRI and is not used to diagnose, so the device does not fall under rule 10 of the MEDDEV 2.4/1 Revision 8. However, the device is an active device and Rule 12, all other active devices, will apply in this case.

This decision is based on the product information submitted by you as a Medical Device Classification query on the 5th of November 2003. The IMB reserves the right to review the above decision should new information come to light.

I hope this clarifies the situation for you.

Yours sincerely,

Maria Carleton
Medical Devices Department
Irish Medicines Board

Bord Leigheasra na hÉireann
Earlsfort Centre, Earisfort Terrace, Dublin 2   Tel· 353-1-676 4971 Fax 353-1-676 7836
Website: www.imb ie

Appendix D: LabVIEW Programs

Included in this section are the main LabVIEW programs used throughout the research. These include:

- The initial Breath.vi program – this vi generates a waveform representing the breathing activity of the patient and stores the data to a file.

- The Breathing and Sine Wave.vi program – this vi also generates a waveform representing the breathing activity. It also produces the sine waveform for audio feedback and allows limits to be placed to help the patient hold their breath correctly.

- Power Spectrum.vi – This vi allows the hardware and software frequency control systems to be compared. The audio signals are analysed to show the shape, frequency, and amplitude of the signal as well as the shape. The power spectrum of each signal can also be viewed.

- Finally there is the diagram for a piece of code that can be added to any of the above. This code allows the front panel to be saved into jpeg format.

For instructions select File >> VI Properties >> Documentation
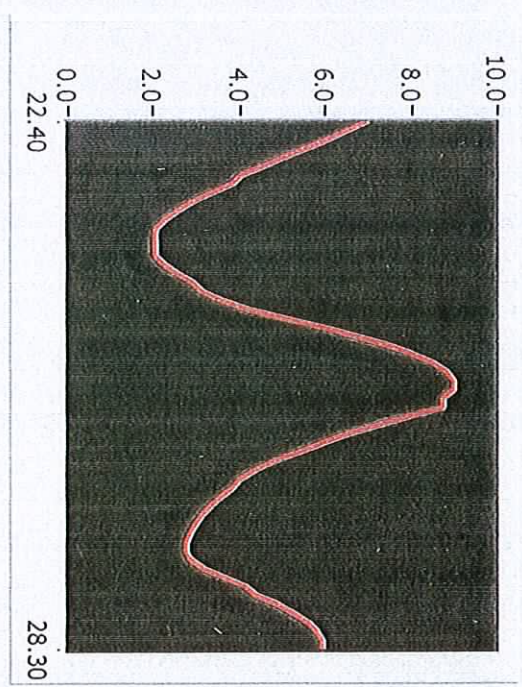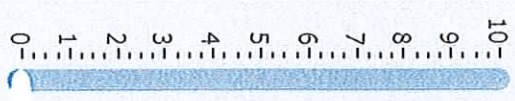
Scroll right for
hardware settings -->

device

channels (0)

Slide **Breathing Activity**

device: 1

channels: 1

0

10

scan rate
(250 scans/sec)
10.00

buffer size
(2500 scans)
2500

number of scans
to write at
a time (50)
1

5.94

0.00

0.00

0.00

10.0-
9-
8-
7-
6-
5-
4-
3-
2-
1-
0-

scan backlog
0

number of scans written to file
284

Press the STOP button to stop writing data to file.

STOP

Plot 0
Plot 1
Plot 2
Plot 3

10.0-
8.0-
6.0-
4.0-
2.0-
0.0-
22.40   28.30

hardware settings

input limits

0

high limit
0.00

low limit
0.00

interchannel delay (secs)
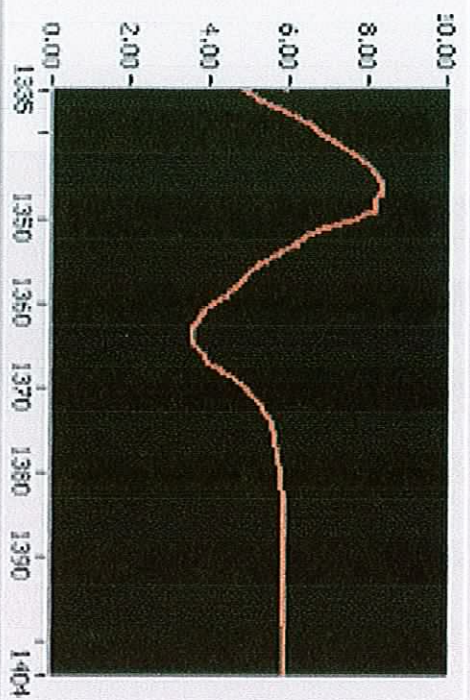(-1: hardware default)
-1.00

Select and open
file for data

Configure and start
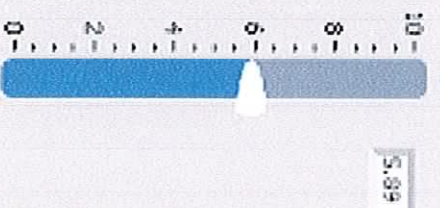the acquisition, then
write the scan rate to
the first line of the file.

Read the data, convert it to a spreadsheet string,
write it to the file, and plot it until an error occurs or
the stop button is pressed.
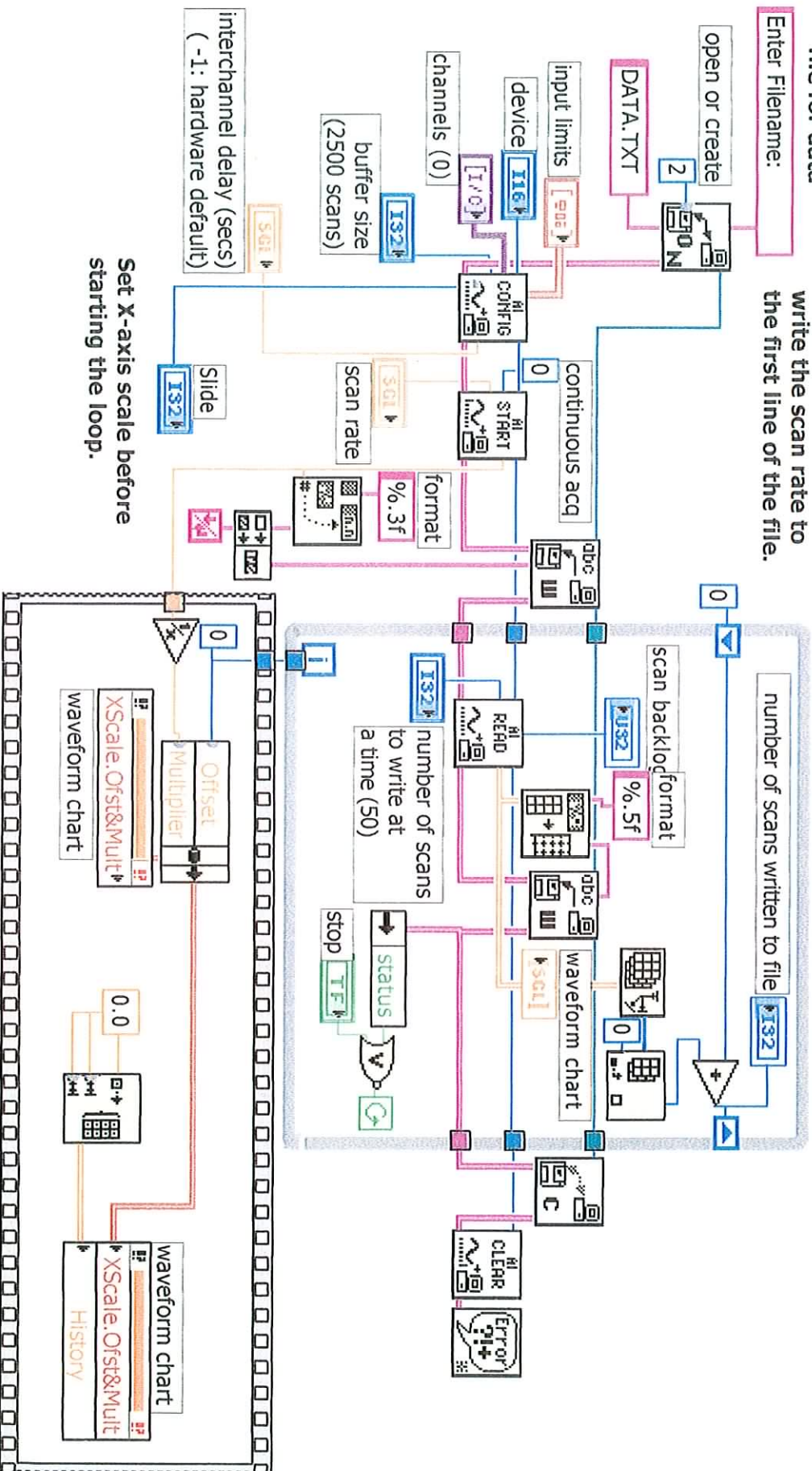
Enter Filename:

open or create

DATA.TXT

2

input limits

device

channels (0)

buffer size
(2500 scans)

interchannel delay (secs)
(-1: hardware default)

AI
CONFIG

AI
START

continuous acq

0

Slide

scan rate

format

%.3f

number of scans written to file

I32

scan backlog

format

%.5f

AI
READ

I32

number of scans
to write at
a time (50)

status

stop

waveform chart

Set X-axis scale before
starting the loop.

Offset

Multiplier

XScale.Ofst&Mult

waveform chart

0.0

AI
CLEAR

Error

XScale.Ofst&Mult

History

waveform chart
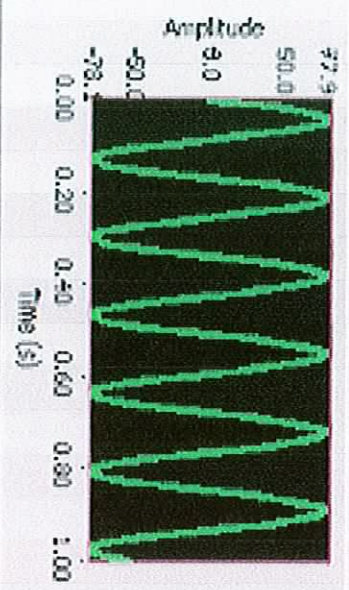
Block Diagram
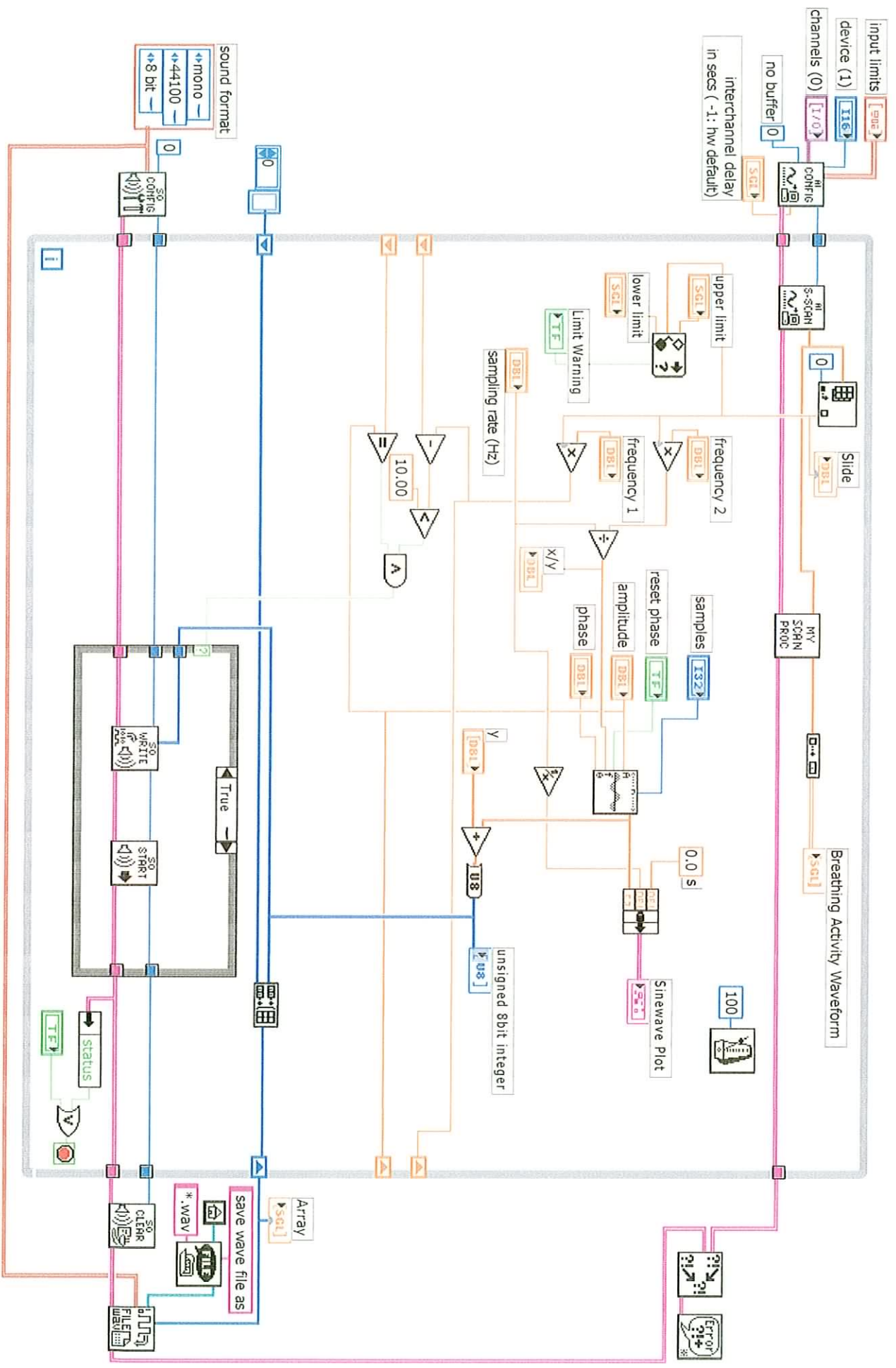
time waveform

Buffer size

8192

STOP

power spectrum
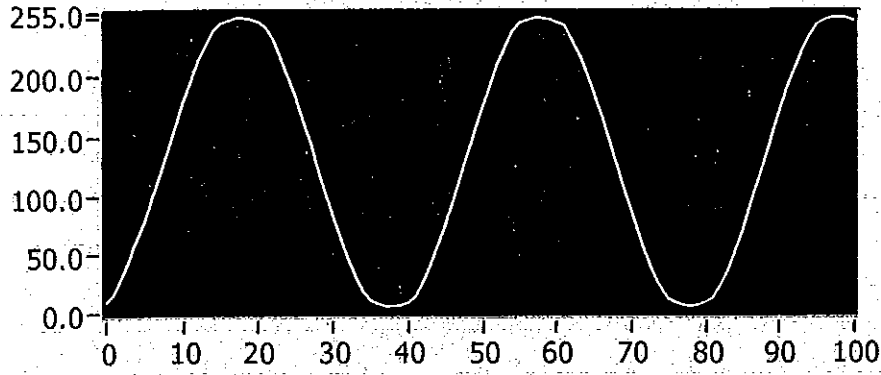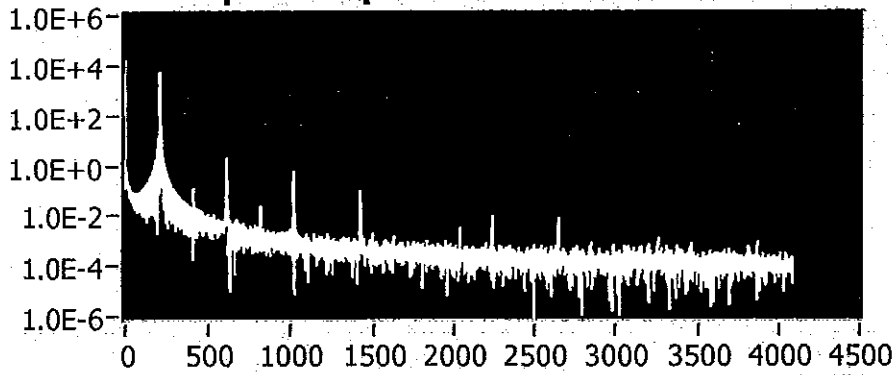

detected frequency

24.892E-3

detected amplitude

123.060

detected phase (deg)

-96.074

Array

0   0.02

0

sound input device
configuration

sound format

mono
44100
8 bit

Buffer size

device

U32

0

sampling rate

100

Computes auto
power spectrum

AutoPower
Spectrum

DBL

DBL

DBL

status

TF

Finds tone of highest
amplitude and returns
frequency, amplitude
& phase

AMP.
FREQ.

detected frequency

DBL

detected amplitude

DBL

detected phase (deg)

DBL

SI
CONFIG

SI
START

SI
READ

SI
CLEAR

error handling

Error

Output results to a txt file

Array

DBL

123
TXT

Program to retrieve the image seen on the front panel in jpeg format.

STOP
TF

i

stop program

STOP

commence
retrieval of
images
TF

Retrive Images
TF

?

sets the
number
of frames

Path

sets the file
name & path
where jpegs
are stored

Frames
I32

N

i

24

True

.jpg

Vimage

999
#

set image parameters

Get Panel Image
VI

visible area only

image depth

image

colors

bounds

JPEG
file

Writes a jpeg
file

Delay
U32

Allows number of
frames per second
to be set

RSNA 2002

Scientific Program

Search

Scientific Papers
  SESSION: Gastrointestinal (CT and MR of the Abdomen: New Technical Innovations)

Adjuvant Method to Control Respiration During Breath-hold Dependent Imaging

DATE: Wednesday, December 04 2002
START TIME: 11:51 AM
END TIME: 11:58 AM
LOCATION: Room E350

CODE: K05-971

PARTICIPANTS

PRESENTER

Ian Kelly MBBCh

Waterford

CO-AUTHOR

Aidan McNally

Gerry Woods PhD

INDEX TERMS

⊢ Bile ducts, MR
⊢ Images, quality
⊢ Magnetic resonance (MR), motion correction

Abstract:

Purpose: To develop and validate an adjuvant biofeedback device to improve breathing control in breath-hold dependent imaging.

Methods and Materials: A thoracic cage respiratory monitoring system based on a pneumatic pressure coil, differential pressure transducer, PC engine and laboratory analytical proprietary software (LabView National Instruments) was constructed. Patient biofeedback was via a LED incremental bargraph and screen spirographic display. Subjects were attached and their thoracic excursion calibrated (millipascals mPa). They were asked to suspend respiration in early expiration and maintain this for 20 seconds. They were then introduced to the graphic biofeedback device and trained for a period of 5 minutes to utilise in respiratory control. A second breathhold series was then performed. Graphs with and without the device were obtained and slopes calculated. The average difference and standard deviation in the slope of each pair were obtained and statistical paired t test applied.

Results: Subjects (n= 10) recruited for validation were medical students and residents. Average age 28 yrs. Thoracic wall motion sampling was 3 times per second for 20 seconds. The average difference in slope of the lines before and after the use of biofeedback was 0.0816 mPa, SD +/- 0.0395. n-1= 9, T statistic = 6.526. P< 0.0005

Conclusion: The use of an adjuvant biofeedback system should be considered in breathhold dependent imaging such as MRCP. A version of the above has been developed with varying pitch auditoty feedback which is MR compatible and easily applied to all MR systems.